Université de Montréal

Synthesis, Characterization and chromotropism Properties of Ni(II) Complexes Featuring Diphenyl(dipyrazolyl)methane

par

Natalie Baho

Département de Chimie

Faculté des Arts et des Sciences

Thèse présentée à la Faculté des études supérieures

en vue de l'obtention du grade de **Maîtriste en Science (M. Sc.)**

en chimie

Septembre 2007

Université de Montréal

Faculté des études supérieures

Cette thèse intitulée :

Synthesis, Characterization and Chromotropism Properties of Ni(II) Complexes Featuring Diphenyl(dipyrazolyl)methane

Présentée par :

Natalie Baho

a été évaluée par un jury composé des personnes suivantes :

André L. Beauchamp, président-rapporteur

Davit Zargarian, directeur de recherche

Garry S. Hanan, membre du jury

Résumé

Ce mémoire décrit la préparation et les propriétés d'une nouvelle série de complexes de Ni(II) avec le ligand diphényl(dipyrazolyl)méthane (dpdpm). Ces complexes ont été caractérisés au moyen de la diffraction des rayons X et des spectroscopies RMN, FTIR et UV-VIS-NIR.

Les espèces paramagnétiques dérivées de $Ni(NO_3)_2$ adoptent une géométrie octaédrique et montrent des propriétés intéressantes de chromotropisme. L'interconversion des complexes $[(dpdpm)Ni(\eta^2\text{-}NO_3)_2]$ (**2.1**, vert) et $[(dpdpm)Ni(\eta^1\text{-}NO_3)(CH_3CN)]NO_3$ (**2.2**, bleu) a été intensivement étudiée dans l'acétonitrile et à l'état solide en fonction de la température, de la concentration et de la pression de vapeur de CH_3CN.

Les complexes dérivés de $NiBr_2$ sont également paramagnétiques, à l'état solide et en solution, mais ils adoptent deux géométries différentes. Les complexes pentacoordonnés $[(dpdpm)Ni(\mu\text{-}Br)Br]_2$ (**3.1**), $[(dpdpm)NiBr_2(H_2O)]$ (**3.2a**) et $[(dpdpm)NiBr(H_2O)_2]Br$ (**3.2b**) montrent une faible interaction entre le Ni et un substituant phényle du ligand dpdpm. Ces interactions faibles remplissent le sixième site de coordination autour du centre de Ni, mais le phényle peut être remplacé aisément par une molécule de solvant, à l'état solide et en solution. De telles interactions Ni-solvant facilitent l'interconversion de ces composés dans diverses conditions et donnent lieu à des propriétés chromotropiques intéressantes. Une interconversion semblable a lieu également entre le complexe octaédrique $[(dpdpm)NiBr(H_2O)_2(CH_3CN)]Br$ (**3.3**) et **3.1**, quand on chauffe **3.3** et quand on expose **3.1** aux vapeurs de CH_3CN. Les complexes octaédriques $[(dpdpm)_2NiBr_2]$ (**3.4**) and $[(dpdpm)_2NiBr(H_2O)]Br$ (**3.5**) montrent également des propriétés chromotropiques à cause de l'interconversion entre **3.4**, **3.5** et **3.1**. Les propriétés solvato-, vapo-, et thermochromiques de cette famille de complexes ont été examinées par spectroscopie d'UV-VIS-NIR.

L'extraction de bromure du complexe $[(dpdpm)NiBr_2(H_2O)]$ (**3.2a**) avec l'hexafluorophosphate d'argent ($AgPF_6$) donne deux complexes, soit le composé multimétallique $[\{(dpdpm)(CH_3CN)NiBr_2\}(AgBr)]_2$ (**4.1**) et le complexe monométallique $[(dpdpm)NiBr(CH_3CN)_3]PF_6$ (**4.2**). Des méthodes plus directes ont été développées pour la préparation indépendante de ces complexes.

Nous avons brièvement étudié la chimie de coordination de sels de nickel et de palladium avec le ligand volumineux diphényl(3,5-dimethylpyrazolyl)méthane ($dpdpm^{Me2}$). Les réactions de ce ligand avec NiX_2 et $PdCl_2$ mènent à la dégradation du $dpdpm^{Me2}$ et donnent les adducts $[(Pz^{Me2})_2NiCl_2(H_2O)_2]$ (**5.12**), $[(Pz^{Me2})_2NiBr_2]$ (**5.13**) et $[(Pz^{Me2})_2PdCl_2]$ (**5.14**).

Des tentatives pour oxyder le centre Ni(II) dans le complexe $[(dpdpm)NiBr_2(H_2O)]$ (**3.2a**) avec $CuCl_2 \cdot 2H_2O$ et $[Cp_2Fe]PF_6$ donnent les nouveaux complexes $[(dpdpm)CuBr_2]$ (**5.15**) et $[(dpdpm)_2Ni(CH_3CN)_2][(FeBr_3)_2O]$ (**5.16**), respectivement. Ces résultats inattendus soulignent la labilité du complexe **3.2a** en solution et indiquent que la molécule d'eau de ce complexe pourrait jouer un rôle important dans ces transformations.

Mots-clés: Nickel, ligands bis(pyrazolyl)alkane, vapochromisme, solvatochromisme, thermochromisme, nitrate bidentate, nitrate monodentate, interactions Ag-Ag, interactions Ni-Br→Ag, dégradation du ligand bis(pyrazolyl)alkane.

Abstract

The present thesis describes the preparation and properties of a new series of Ni(II) complexes bearing the ligand diphenyl(dipyrazolyl)methane (dpdpm). These complexes were characterized by X-ray diffraction studies and NMR, FTIR, and UV-vis-NIR spectroscopy.

The paramagnetic species derived from $Ni(NO_3)_2$ adopt distorted octahedral geometry and show interesting chromotropism properties. The interconversion of the complexes $[(dpdpm)Ni(\eta^2\text{-}NO_3)_2]$ (**2.1**, green) and $[(dpdpm)Ni(\eta^1\text{-}NO_3)(CH_3CN)]NO_3$ (**2.2**, blue) has been extensively studied both in CH_3CN and in the solid state as a function of temperature, concentration, and vapor pressure of CH_3CN.

The complexes derived from $NiBr_2$ are also paramagnetic, both in the solid state and in solution, but they adopt two different geometries. The pentacoordinated complexes $[(dpdpm)Ni(\mu\text{-}Br)Br]_2$ (**3.1**), $[(dpdpm)NiBr_2(H_2O)]$ (**3.2a**), and $[(dpdpm)NiBr(H_2O)_2]Br$ (**3.2b**) display long-range interactions between a Ph substituent of the dpdpm ligand and the Ni center. These weak Ni-Ph interactions fill the sixth coordination site around the Ni center, but the Ph moiety can be replaced readily by solvent molecules, both in the solid state and in solution. Such Ni-solvent interactions facilitate the interconversion of these compounds under various conditions leading to interesting chromotropic properties. A similar interconversion also takes place between the octahedral complex $[(dpdpm)NiBr(H_2O)_2(CH_3CN)]Br$ (**3.3**) and the pentacoordianted species (**3.1**) when **3.3** is heated or **3.1** is exposed to CH_3CN vapors. The octahedral complexes $[(dpdpm)_2NiBr_2]$ (**3.4**) and $[(dpdpm)_2NiBr(H_2O)]Br$ (**3.5**) also show chromotropic properties due to the interconversion between **3.4**, **3.5** and **3.1**. The solvato-, vapo-, and thermochromic properties of this family of complexes have been probed by UV-vis-NIR spectroscopy.

Abstraction of a bromide from the complex $[(dpdpm)NiBr_2(H_2O)]$ (**3.2a**) with silver hexafluorophosphate ($AgPF_6$) results in two complexes, the multi-metallic compound $[\{(dpdpm)(CH_3CN)NiBr_2\}(AgBr)]_2$ (**4.1**) and the monometallic complex $[(dpdpm)NiBr(CH_3CN)_3]PF_6$ (**4.2**). More direct routes have been developed for the independent preparation of these complexes.

We have briefly studied the coordination chemistry of nickel and palladium salts with the bulky ligand diphenyl(3,5-dimethylpyrazolyl)methane ($dpdpm^{Me2}$). Reactions of this ligand with NiX_2 and $PdCl_2$ give the unexpected adducts $[(Pz^{Me2})_2NiCl_2(H_2O)_2]$ (**5.12**), $[(Pz^{Me2})_2NiBr_2]$ (**5.13**), and $[(Pz^{Me2})_2PdCl_2]$ (**5.14**) resulting from the degradation of $dpdpm^{Me2}$.

Attempts to oxidize Ni(II) in complex $[(dpdpm)NiBr_2(H_2O)]$ (**3.2a**) with $CuCl_2{\cdot}2H_2O$ and $[Cp_2Fe]PF_6$ resulted in the new complexes $[(dpdpm)CuBr_2]$ (**5.15**) and $[(dpdpm)_2Ni(CH_3CN)_2][(FeBr_3)_2O]$ (**5.16**), respectively. These unexpected results underline the lability of complex **3.2a** in solution and indicate that the water molecule of complex **3.2a** might play an important role in these transformations.

Keywords : Nickel, bis(pyrazolyl)alkane ligands, vapochromism, solvatochromism, thermochromism, bidentate nitrate, monodentate nitrate, Ag-Ag interactions, Ni-Br→Ag interactions, bis(pyrazolyl)alkane degradation.

Table of Contents

Résumé.....iii
Abstract.....v
Table of contents.....vii
List of tables.....ix
List of figures.....x
List of abbreviations..... xviii
Acknowledgements.....xvi

CHAPTER 1: Introduction.....1
1.1 Background.....1
1.1.1. Poly (pyrazolyl)alkane ligand.....4
1.1.2. Coordination complexes with bis(pyrazolyl)alkane ligands 7
1.1.3. Chromotropism.....9
1.1.4. The applications of N-hetrocycle nickel complexes in polymerization reactions.....15
1.2 Description of the thesis.....17
1.3 References.....18

CHAPTER 2: Syntheses, Structures, Spectroscopy, and Chromotropism of New Complexes Arising from the Reaction of Nickel(II) Nitrate with Diphenyl(dipyrazolyl)methane.....22
2.1 Abstract.....23
2.2 Introduction.....24
2.3 Experimental.....26
2.4 Results and Discussion.....31
2.5 Conclusion.....45
2.6 References.....47
2.7 Supporting Information 52

CHAPTER 3: Diphenyl(dipyrazolyl)methane Complexes of Ni: Syntheses, Structures Characterization, and Chromotropism of New $NiBr_2$ Derivatives 56

3.1 Abstract.....57

3.2 Introduction.....57

3.3 Results and Discussion.....59

3.4 Conclusion 80

3.5 Experimental 80

3.6 References.....86

CHAPTER 4: $[(L_2L'NiBr_2)(AgBr)]_2$: a Tetrametallic Ensemble Arising from Halophilicity of Silver.....91

4.1 Abstract.....92

4.2 Introduction.....92

4.3 Results and Discussion.....93

4.4 Concluding remarks.....99

4.5 Experimental.....99

4.6 Reference.....103

CHAPTER 5: Divers Results of Several Studies

5.1 Introduction.....106

5.2 New series of $NiCl_2$ and NiI_2 derivatives bearing dpdpm.....106

5.3 New series of transition metal derivatives with 3,5-dimethyl pyrazol (Pz^{Me2}) results from decomposition of diphenyl(3,5-dimethylpyrazolyl)methane ($dpdpm^{Me2}$).....115

5.4 Oxidations attempts for complex $[(dpdpm)NiBr_2(H_2O)]$ (**3.2a**) with $CuCl_2$ and $[Cp_2Fe]PF_6$.....123

5.5 Experimental.....128

5.6 References.....133

CHAPTER 6: Conclusion.....135

APPENDIX I.....I-1

APPENDIX II.....II-1

APPENDIX III.....III-1

APPENDIX IV.....IV-1

List of Tables

Table 2.1 Crystallographic data for complexes **2.1- 2.4**.....34

Table 2.2 Bond distances and angles for complexes **2.1-2.4**.....37

Table 2.3 Absorption energies, molar absorptivities and crystal-field parameters for spin-allowed bands of UV-Vis-NIR Spectra for complexes **2.1-2.4** in different solvents..... 42

Table 2.4 Crystal-field parameters for **2.1-2.4** and related compounds.....43

Table 3.1 Crystallographic data for **3.1a**, **3.2a**, **3.2b** and **3.3**.....63

Table 3.2 Crystallographic data for **3.4**, **3.5**.....64

Table 3.3 Selected structure parameters for complex **3.2a, 3.2b** and **3.3**.....67

Table 3.4 Selected structure parameters for complex **3.4** and **3.5**.....70

Table 4.1 Selected bond lengths (Å) and angles (degrees) for **4.1**.....96

Table 4.2 Selected bond distances (in Å) and angles (in degrees) for **4.2**.....98

Table 4.3 Crystallographic data for **4.1** and **4.2**.....102

Table 5.1 Crystallographic data for **5.6**, **5.7**, **5.8**, and **5.9**.....109

Table 5.2 Bond distances and angles for complexes for **5.6** and **5.7**.....111

Table 5.3 Bond distances and angles for complexes for **5.8**.....113

Table 5.4 Bond distances and angles for complexes for **5.9**.....114

Table 5.5. Crystallographic data for **5.10b**.....121

Table 5.6 Bond distances and angles for complexes for **5.10b**.....122

Table 5.7 Crystallographic data for **5.13** and **5.14**.....125

Table 5.8 Bond distances and angles for complexes for **5.13** and [(dpdpm)$CuCl_2$]...126

Table 5.9 Selected structure parameters for complex for **5.14**.....127

List of Figures

Figure 1.1 General structures of tris- and bis(pyrazolyl)alkane and tris- and bis (pyrazolyl) borate ligands.....1

Figure 1.2 Different examples of mixed ligand complexes.....2

Figure 1.3 A few examples of previously synthesized nickel complexes of bpm^{Me2} 3

Figure 1.4 General structure of bis(pyrazolyl)alkane ligands.....5

Figure 1.5 Schematic drawings of possible configurations for the six-membered ring C-N-N-M-N-N metallacycle 5

Figure 1.6 Schematic drawings of possible long-range interaction between the R substituent situated on the bridge carbon and the metallic center.....6

Figure 1.7 C-N bond break.....7

Figure 1.8 Few examples of different coordinated complexes 8

Figure 1.9 Structure of bapp **(a)** and dachdRa **(b)**.....10

Figure 1.10 Mixed-ligand complexes $[M(diam)(dike)]^+$.....12

Figure 1.11 Solvatochromism and termochromism of complex $[Ni(diam)(dike)]^+$.....13

Figure 1.12 Vapochromic salts of platinum (II).....14

Figure 1.13 Polymerization of ethylene and α–olifins by bulky α–diimine nickel and palladium complexes.....15

Figure 1.14 Organometalic complexes with pd, $[(dpdpm)PdMe_2]$ **(a)**, $[(bpp)PdMe_2]$ **(b)** and $[(bpp)Pd(allyl)]^+$ **(c)**.....16

Figure 2.1 ORTEP view of complex **2.1**. Thermal ellipsoids are shown at 30% probability.....35

Figure 2.2 ORTEP view of complex **2.2**. Thermal ellipsoids are shown at 30% probability.....35

Figure 2.3 ORTEP view of complex **2.3**. Thermal ellipsoids are shown at 30% probability.....36

Figure 2.4 ORTEP view of complex **2.4**. Thermal ellipsoids are shown at 30% probability.....36

Figure 2.5 The UV-Vis-NIR spectra of complex **2.1** in different solvents.....40

Figure 2.6 The UV-Vis-NIR spectra of complexes **2.1**, **2.2**, **2.3** and **2.4** in acetonitrile.....40

Figure 2.7 Shift in the absorption wavelength of the high-energy band in the UV-visible spectra of **2.1** as a function of solvent composition (CH_2Cl_2:CH_3CN).....44

Figure 2.5a The UV-Vis-NIR spectra of complex **2.2** in different solvents.....53

Figure 2.5b The UV-Vis-NIR spectra of complex **2.3** in different solvents.....54

Figure 2.5c The UV-Vis-NIR spectra of complex **2.4** in different solvents.....55

Figure 3.1 **O**RTEP view of complex **3.1**. Thermal ellipsoids are shown at 30% Probability.....65

Figure 3.2 ORTEP view of complex **3.2a**. Thermal ellipsoids are shown at 30% probability.....65

Figure 3.3 ORTEP view of complex **3.2b**. Thermal ellipsoids are shown at 30% pobability.....66

Figure 3.4 ORTEP view of complex **3.3**. Thermal ellipsoids are shown at 30% probability.....66

Figure 3.5 Different perspectives of the ORTEP diagrams for complexes **3.1**, **3.2a**, and **3.2b** showing the long-range Ni-C distances.....68

Figure 3.6 ORTEP view of complex **3.4**. Thermal ellipsoids are shown at 30% probability.....69

Figure 3.7 ORTEP view of complex **3.5**. Thermal ellipsoids are shown at 30% probability.....69

Figure 3.8 Room temperature UV-vis-NIR spectra of MeOH solutions of **3.1** (1.3 mM) and **3.2a** (2.1 mM)..... 73

Figure 3.9 Room temperature UV-vis-NIR spectra of CH_3CN solutions of **3.1** (1.3 mM) and **2a** (2.7 mM).....73

Figure 3.10 Room temperature UV-vis-NIR spectra of **3.2a** in CH_2Cl_2 (8.7 mM) and acetone (8.3 mM).....74

Figure 3.11 Variable temperature UV-vis-NIR spectra for a 6.5 mM solution of **3.2a** in acetone.....75

Figure 3.12 UV-vis-NIR spectra for solutions of **3.2a** (8.7 mM in CH_2Cl_2 and 6.5 mM in acetone) and acetone solutions of **3.4** (4.7 mM) and **3.5** (6.6mM).....76

Figure 3.13 Variable temperature UV-vis-NIR spectra for **3.4** in CH_2Cl_2 (4.7mM).....78

Figure 3.14 Variable temperature UV-vis-NIR spectra for **3.4** in MeOH (3.9 mM)..... 78

Figure 3.15 Variable temperature UV-vis-NIR spectra for **3.4** in CH_3CN (8.7 mM).... 79

Figure 3.16 Variable temperature UV-vis-NIR spectra for **3.5** in CH_2Cl_2 (6.6 mM).....79

Figure 4.1 ORTEP view of complex **4.1** showing the Ag-Br-Ag-Br moiety in the plane of the paper. Thermal ellipsoids are shown at 30% probability.....95

Figure 4.2 Partial view of the ORTEP diagram for complex **4.1** showing the boat configuration adopted by the dpdpm ligand without the carbon atoms of the pyrazolyl rings and the long-range Ni-Ph interactions.....96

Figure 4.3 ORTEP diagrams of complex **4.2**, with (left diagram) and without the carbon atoms of the pyrazolyl rings. Thermal ellipsoids are shown at 30% probability.....98

Figure 5.1 ORTEP view of complex **5.6**. Thermal ellipsoids are shown at 30% probability.....110

Figure 5.2 ORTEP view of complex **5.7**. Thermal ellipsoids are shown at 30% probability.....110

Figure 5.3 ORTEP view of complex **5.8**. Thermal ellipsoids are shown at 30% probability. 112

Figure 5.4 ORTEP view of complex **5.9**. Thermal ellipsoids are shown at 30% probability.....113

Figure 5.5 ORTEP view of complex **5.11** and **5.12**. Thermal ellipsoids are shown at 30%probability. 115

Figure 5.6 ORTEP view of complex **5.10b**. Thermal ellipsoids are shown at 30% probability 122

Figure 5.7 ORTEP view of complex **5.13**. Thermal ellipsoids are shown at 30% probability.....126

Figure 5.8 ORTEP view of complex **5.14**. Thermal ellipsoids are shown at 30% probability 127

List of abbreviations

BM	bohr magneton
bapp	1,4-bis-(3-aminopropyl)piperazine
dachda	1,4-diazacycloheptanediacetate
bpm^{Me2}	bis(3,5-dimethylpyrazolyl)methane
bpp	bis(pyrazolyl)propane
br	broad
δ	NMR chemical shift in ppm
d	doublet
dd	doublet of doublets
diam	*N*-alkylated diamine
DME	1,2-dimethoxyethane
dike	β-diketone
dpdpb	diphenyl(dipyrazolyl)borate
dpdpm	diphenyl(dipyrazolyl)methane
$dpdpm^{Me}$	diphenyl(3 or 5-dimethylpyrazolyl)methane
$dpdpm^{Me2}$	diphenyl(3,5-dimethylpyrazolyl)methane
$dpdpm^{tBu}$	diphenyl(3-tertbutylpyrazolyl)methane
equiv.	equivalent
ε	molar absorptivity [$M^{-1}cm^{-1}$]
IR	infrared
L	generalized neutral ligand
MeOH	methanol
EtOH	ethanol
ν	wave number (cm^{-1})
MeCN	acetonitrile
Me	methyl, CH_3
NMR	nuclear magnetic resonance
Ph	phenyl

PhCN	benzonitrile
PPh_3	triphenylphosphine
py	pyridine-2-yl
Pz	pyrazol
Pz^{Me2}	3,5-dimethyl pyrazol
R	alkyl group
s	singlet
λ	wave length (nm)
M	metal
mp	melting point
mim	N-methylimidazol-2-yl
t	triplet
t-Bu	tert-butyl, $C(CH_3)_3^-$
th	thienyl
tmen	*N*, *N*, *N'*, *N'* -tetramethylethylenediamine
Tp^-	tris(pyrazolyl)borate
Tpm^*	tris(3,5-dimethylpyrazolyl)methane
UV-vis	ultraviolet and visible
vs	very strong
w	weak

To Nariman Tarzibachi and Jean Baho

Acknowledgements

At the outset, my deepest gratitude for this thesis goes to my supervisor Davit Zargarian, for providing me the opportunity to be a member in his group and for his continuous encouragement during my master studies. His enjoyment of scientific research contributed greatly to establish the overall direction of my research. I thank him for his supervision, patience, and continued support.

I am grateful to Michel Simard and Francine Belanger-Gariépy for their kind assistance with X-ray crystallography, their patient and their deep explanation. I am grateful to Profs. Christian Reber, Garry Hanan, William Skene and their research groups for allowing me to use their UV-Vis-NIR instrument and their valuable help. More over, I would like to thank Sylvie Bilodeau and Phan Viet Minh Tan for their help with the NMR spectroscopy.

I would like to thank all collogues in Aile-A6 for their help in many aspects especially Valerica, Annie, Sylvain, Jason, Daniel and Yijing, I was lucky to work with you all. Thank you for your valuable discussions, help and the productive time we had together.

I wish to thanks my friends for helping me to get through the difficult times, and for their emotional support, camaraderie, entertainment, and caring they provided.

Very special thanks goes to my sister Roula and her husband Abe, thank you for being always there when I needed you, for your priceless advices, for your unlimited support and thanks my niece, my little Maria, for bringing enormous joy into my life.

Last, but not least, I would like to dedicate this thesis to my father and mother, who have done all they could and more to get me to this point. Thank you for your love, sacrifices, support and understanding. Thank you for everything.

Chapter 1: Introduction

1.1.Background

Poly(pyrazolyl)alkanes (Figure 1.1) constitute a family of air stable and flexible ligands that adopt variable hapticities and form non rigid metallacycle conformations, thereby, giving rise to many different structures. These multidentate ligands are isoelectronic and isosteric with the well-known poly(pyrazolyl)borates introduced in the late 1960s by S. Trofimenko.[1] Hence the neutral, so-called scorpionate poly(pyrazolyl)-alkanes are the analogues of the anionic poly(pyrazolyl)borates and are formally derived by replacing the apical $[BH]^-$ anionic moiety with the isoelectronic CR group.

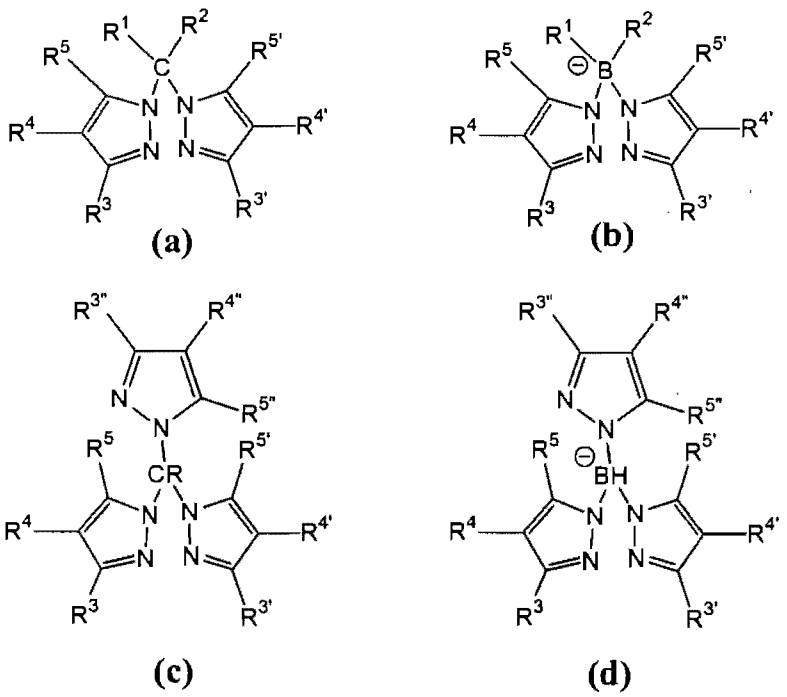

Figure 1.1. General structures of tris- and bis(pyrazolyl)alkane and tris- and bis(pyrazolyl)-borate ligands

The ease of synthesis of variously substituted pyrazol rings is the most interesting feature for the incorporation of pyrazolyl groups in the design of new pyrazolyl alkane or borate ligands. This feature allows a great deal of control over the electronic and steric properties of the metal complexes of these ligands.[2] Hence, there are many examples of

mixed ligands based on the combination of pyrazol rings with different ligand moieties like pyridine-2-yl (py), *N*-methylimidazol-2-yl (mim) and thienyl (th).[3] Some of these combinations have been studied extensively with Pt and usually form stable organometallic complexes such as **1a** and **2a** in Figure 1.2. A number of coordination complexes of nickel featuring such mixed ligands have also been reported including complex **1b** in Figure 1.2.

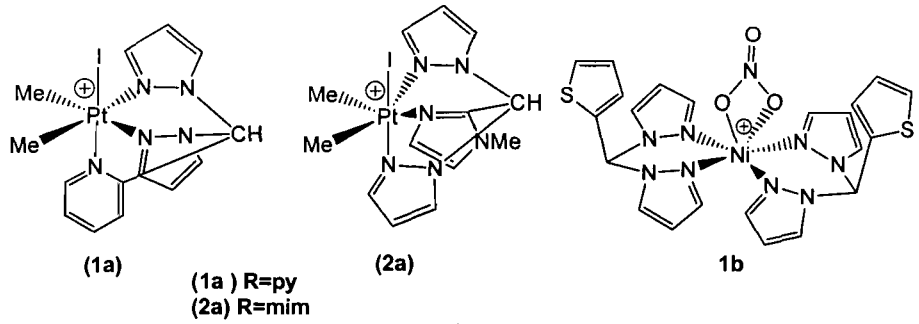

Figure 1.2. Different examples of mixed ligand complexes

The organometallic chemistry of complexes bearing anionic bis- or tris(pyrazolyl)borate ligands has been explored in much greater detail[4,5] in comparison to that of complexes bearing neutral, bis- or tris(pyrazolyl)alkane ligands. The latter ligands show richer coordination chemistry[6,7] and their complexes are believed to possess pharmacological activities. This is especially true for complexes of nickel, an essential element for bacteria, plants, animals, and humans and one that plays an important role in the catalytic activities of certain enzymes.[8]

Although no organonickel complex of the neutral poly(pyrazolyl)alkane ligands has been reported to date, we became interested in preparing the first examples of such complexes and studying their reactivities. This interest was strongly inspired by the breakthrough reports of Brookhart and coworkers in the late 1990's that showed that sterically crowded α-diimine Ni and Pd complexes have interesting catalytic activities in the production of high molecular weight polyolefins. This breakthrough has prompted many researchers to develop new ligands containing different N- heterocyclic ligands and explore the catalytic reactivities of their complexes with late transition metals.

Therefore, previous studies in our group have explored the preparation,[9] characterization[10] and spectroscopy[11] of a family of Ni(II) complexes $LNiX_2$ and $[LNiX]^+$

where L is a poly(pyrazol-1-yl)methane ligand, bis(pyrazolyl)propane (bpp), bis(3,5-dimethylpyrazolyl)methane (bpm^{Me2}) and tris(3,5-dimethylpyrazolyl)methane (tpm^{Me2}), where X is Cl, Br, I, NO_3, acetate, formate or phthalimide (Figure 1.3). UV-vis studies were carried out to study the solvato- and thermochromic properties of the complexes $[(bpm^{Me2})_2NiBr]Br$ and $[(bpm^{Me2})NiBr_2]$. These studies also showed that organometallic derivatives of these simple precursor complexes were inaccessible, because all attempts to alkylate these species were unsuccessful, probably because of the thermal instability of the resulting species or the deprotonation of the carbon bridge.

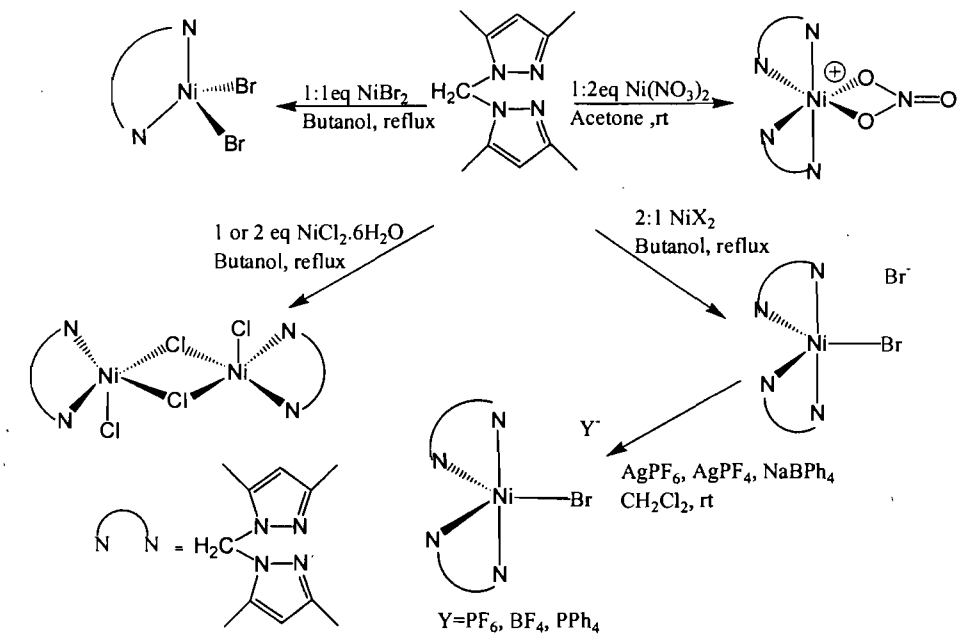

Figure 1.3. A few examples of previously synthesized nickel complexes of bpm^{Me2}

Hence, the broad objective of the present thesis is to expand the previous studies of our group in this area by exploring the synthesis, structural and photo-physical properties of new nickel complexes based on ligands not having any C-H moieties on the alkane bridge, namely diphenyl(dipyrazolyl)methane (dpdpm) and diphenyl(3,5-dimethylpyrazolyl)methane ($dpdpm^{Me2}$). We sought to: a) explore the influence of electronic and steric hindrance effects of these ligands on the geometry adopted by the resulting nickel complexes, and b) study the physical properties and different reactivities of the resulting complexes.

The remainder of this chapter will provide background information the preparation, structures, and physical properties of a few dpdpm complexes of different metals. A global introduction to the concept of chromotropism will also be presented, as well as a brief discussion on the importance of N-heterocyclic Nickel-Palladium complexes in the polymerization reactions. The main objectives of our work will be outlined in detail at the end of this chapter.

1.1.1 Poly(pyrazolyl)alkane ligands

In contrast to the extensively used poly(pyrazoly)borate metal fragments $[HB(Pz)_3MX_n]^+$ and $[HRB(Pz)_2MX_n]^+$, the analogous poly(pyrazolyl)alkane derivatives $[RC(Pz)_3MX_n]^+$ and $[R_2C(Pz)_2MX_n]^+$ have attracted comparatively less attention. Nevertheless, significant progress has been made recently in the chemistry of the poly(pyrazolyl)alkane metal complexes.[2-11]

Bis(pyrazolyl)alkane ligands form a broad and versatile class of neutral ligand, that form a variety of novel coordination compounds with various transition metals. This family of ligand is derived from two or more N-deprotonated pyrazole rings bound to a CR_2 bridge through one of the nitrogen atoms of the pyrazole ring. The ligands are primarily σ-donors that give four electrons to the metal centre. They are weaker σ-donors and poorer π-acceptors than imine or pyridine ligands such as 2,2'-bipyridine and 1,10-phenanthroline. The less robust M-N bonds in complexes of bis(pyrazolyl)alkane ligands are expected to result in more electrophilic and more reactive complexes. The versatility of these donor ligands stems from the possibility of tuning their electronic, steric, and coordinating properties by changing the nature of the groups attached to the bridge carbon atom, and by introducing various sterically bulky or electronically diverse pyrazole ring substituents. For example, the presence of electro-withdrawing substituents (CF_3) on the pyrazole ring reduces the donating ability of the ligand, [12] while methyl groups increase it (Figure 1.4).

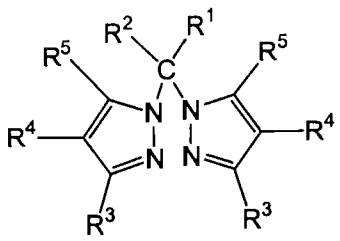

$R^{1,2}$ = H, Me, ^{t}Bu, Ph, Pz, py, mim, th.

$R^{3,4,5}$ = H, Me, ^{t}Bu, Ph, Br, Cl, CF_3.

Figure 1.4. General structure of bis(pyrazolyl)alkane ligands

One important aspect of bis(pyrazolyl)alkane ligands is that they promote the interaction of the metal center with two pyrazole rings in addition to a possible third interaction from R substituent situated on the methylene bridge. The latter interaction depends on the steric hindrance generated by the nature of the metallic center, and the conformation of the six-membered ring C-N-N-M-N-N metallacycle formed from the chelation of the metal (Figure 1.5).

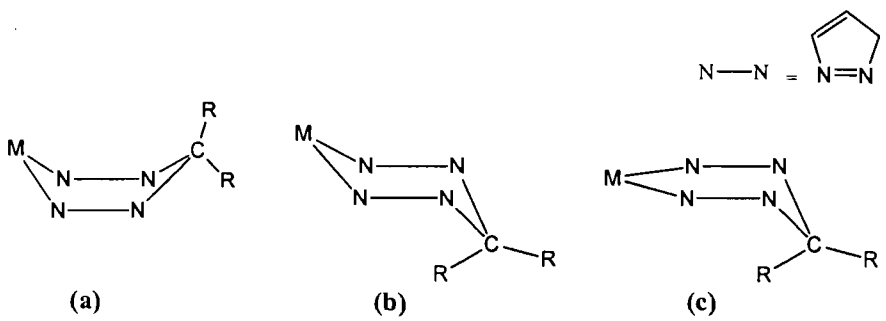

Figure 1.5. Schematic drawings of possible configurations for the six-membered ring C-N-N-M-N-N metallacycle

The six membered metallacycle usually forms a boat conformation (**a** in Figure 1.5) as in dihydrobis(3,5-dimethylpyrazolyl)borate(η^3-allyl)dicarbonylmolybdenum[13] for the four, five and hexacoordination complexes. For the chair conformation only one example has been reported, which is the dimeric [bis(cyclopentadienyltitanium)(μ–pyrazolato-

N,N')]$_2$[14] (**b** in Figure 1.5). The half chair conformation is usually present in hexacoordinated complexes (**c** in Figure 1.5). The boat conformations facilitate the additional interactions in the four or five coordination complexes due to the short distance generated between the metal and methyl protons,[15] (agostic interactions M...H-C **a** and **b** in Figure 1.6); alternatively, a long range interaction can be established between the metal and the π-electron cloud of the phenyl substituent (η^2- arene) [16] (**c** in Figure 1.6).

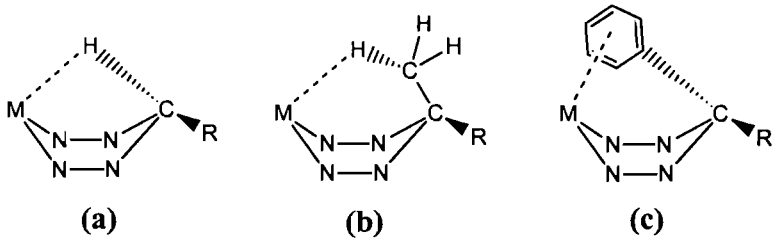

Figure 1.6. Schematic drawings of possible long-range interaction between the R substituent situated on the bridge carbon and the metallic center

Another important aspect of the chemistry of these scorpionate ligand, which is less well understood, is the cleavage of the boron-nitrogen bond in bis(pyrazolyl)borate complexes,[17] a similar carbon-nitrogen bond cleavage has been reported for the poly(pyrazolyl)alkane complexes with Pt,[18] Sn,[19] Cu,[20] Zn and V[21] metals. In the case of the platinum complex, for example, it was proposed that the cleavage of the ligand (bpp) might be initiated by agostic type Pt···H-C interactions. Analogous interactions were observed in analogues palladium complexes; interestingly, however, no cleavage was seen with these Pd complexes. On the other hand, the cleavage of the ligand (C-N bond rupture) occurs even when no agostic interaction is possible. For example, the reaction of $SnCl_4 \cdot 5H_2O$ with bis(3,4,5-trimethylpyrazol-1-yl)methane forms the adduct $[(Pz^{Me3})_2SnCl_4]$ containing individual pyrazole moieties (Figure 1.7); the cleavage of the ligand in this case was explained by the greater stability of the resulting adduct relative to the original ligand, perhaps owing to the greater steric bulk of the donor ligand.

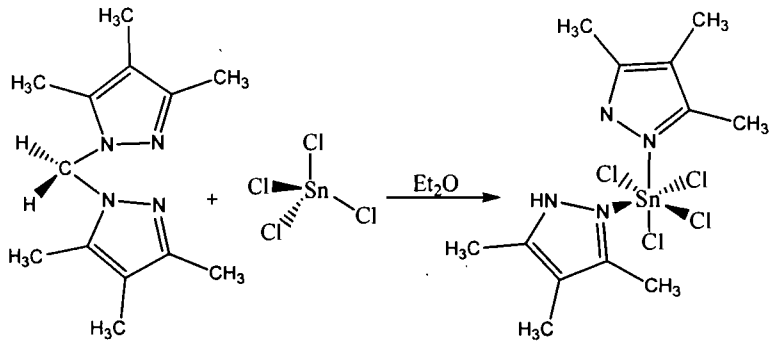

Figure 1.7. C-N bond break

In addition, several research groups have investigated the lability of this family of ligands by NMR in solution at different temperatures. Poly(pyrazolyl)methane or borate can undergo a chemical exchange through a boat-to-boat inversion; the substituents at 3, 4 and 5 positions of the pyrazol ring could play an important role on the speed of this exchange.[22,7c] These substituents can also have a major effect on the partial dissociation of this ligand from the metal, which is inferred from one broad peak in the NMR spectrum for the corresponding complex.[1e] At low temperature, this dissociation is slower and we can observe the ligand peaks for the inequivalent fragments.[4]

1.1.2. Coordination complexes with bis(pyrazolyl)alkane ligands

Several groups have investigated the coordination chemistry of bis(pyrazolyl)alkane ligands with transition and non-transition metals to generate several inorganic[23,8a] and organometallic complexes.[24] A number of reports have studied the interaction of dpdpm with Mo,[17] Pd,[7c] Ag[25] and Cu[26] metals, while its analogous bis(pyrazolyl)borate dpdpb has been studied with Sn, Co, and Pt metals.[18b,d,e] The geometries of these complexes vary from distorted square planar for four-coordinated complexes (i.e. **a** Figure 1.8), to octahedral geometry in the six-coordination complexes (**b** in Figure 1.8).

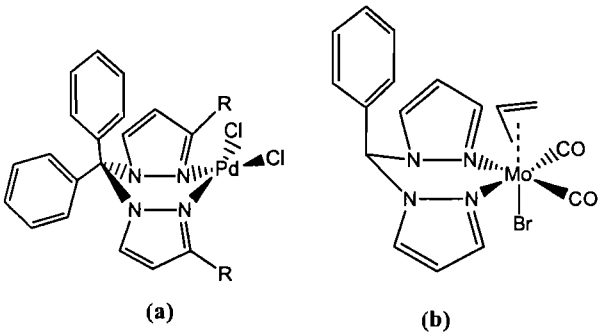

Figure 1.8. A few examples of different coordinated complexes

Curiously, a five-coordinated complex bearing the bis(pyrazolyl)alkanes or borate ligands can form distorted square pyramidal or trigonal bipyramidal geometry, that are very few.[27] For example, some of the known five coordinated complex are the complex [(dpdpm)Cu(η^2-NO_3)(η^1-NO_3)] with dpdpm ligand,[26] Reedijk's dimer[34] [Ni(bpm^{Me2})Cl_2]$_2$ (see Scheme 1.1), [V(bpm^{Me2})$_2$Cl]X (X = BPh_4^-, PF_6^-)[28] with bpm^{Me2} ligand, and [Cr(bpm)X][BPh_4] (X = Cl^-, Br^-)[29] with bis(pyrazolyl)methane ligand (bpm).

It is noteworthy that all of the known platinum complexes with dpdpm or dpdpb form either square planar or octahedral geometry around the metal center and no formation of a five-coordination complex or metal-phenyl interaction has been noted. In contrast, many five-coordinated complexes are formed with Cu and Sn. For example, (dpdpb)SnCl(CH_3)$_2$ is formed by reacting K(dpdpb) with (CH_3)$_2$$SnCl_2$ in CH_2Cl_2 (eq. 1). Similarly, the five-coordinate complex [($dpdpm^{Me}$)Cu(η^1-NO_3)(η^2-NO_3)] was obtained as a green solid by reacting diphenylbis(3-methylpyrazolyl)methane ($dpdpm^{Me}$) with Cu(NO_3)$_2$ for 2 h at room temperature in THF (eq. 2). A similar reaction with dpdpm in MeOH gave as a blue solid that was identified as the five-coordinate complex [(dpdpm)Cu(η^1-NO_3)$_2$(H_2O)] (eq. 3). On the other hand, reacting Cu(NO_3)$_2$ the ligand diphenylbis(3,5-methylpyrazolyl)methane ($dpdpm^{Me2}$) in MeOH led to the unexpected adduct Cu(Pz^{Me2})$_3$(NO_3)$_2$ that results from the degradation of the ligand (eq. 4).

$$K(dpdpb) + (CH_3)_2SnCl_2 \xrightarrow{CH_2Cl_2,\ 2\ h} (dpdpb)SnCl(CH_3)_2 \quad (1)$$

$$dpdpm^{Me} + Cu(NO_3)_2 \xrightarrow{THF,\ 2\ h} [(dpdpm^{Me})Cu(^{\eta 1}NO_3)(^{\eta 2}NO_3)] \quad (2)$$

$$dpdpm + Cu(NO_3)_2 \xrightarrow{MeOH,\ 2\ h} [(dpdpm)Cu(^{\eta 1}NO_3)_2(H_2O)] \quad (3)$$

$$dpdpm^{Me2} + Cu(NO_3)_2 \xrightarrow{MeOH,\ 12\ h} [Cu(Pz^{Me2})_3(NO_3)_2] \quad (4)$$

It appears, therefore, that the outcome of these reactions and the geometry of the resulting complexes are affected by various parameters such as the nature of the metal, the reaction conditions (humidity, solvent and the time of the reaction) and the steric bulk of the ligand.

1.1.3. Chromotropism

Chromotropism is known as the reversible colour changes of a compound by outside stimulations like heat, electricity, pressure, light, vapor and solvent. These stimuli affect the energy levels of the HOMO-LUMO orbitals leading to a transformation of the complex to different geometry and thereby to a colour change. Each of these physical and chemical stimulations has its own scientific label, namely thermochromism (heat), electrochromism (electricity), piezochromism (pressure), photochromism (light), vapochromism (vapor), and solvatochromism (solvent). The compounds that have these properties are used as sensors for detecting the surrounding chemical and physical outer stimulations. Some organic materials show chromotropic properties; some examples include 4',7-bis(dimethylamino)-4-phenylflavylium perchlorate in various sugar-gel matrices[30] and salicylideneanilines.[31]

Inorganic complexes of nickel(II) and copper(II)[32] are very commonly studied for their thermo- and solvatochromic properties. Interestingly, almost all known thermo- and solvatochromic Ni(II) complexes feature N-N donor ligands or mixed ligands bearing at least one N-N donor ligand. Particularly, excellent results have been reported for the thermochromism in solution with the cyclic diimine nickel complexes 1,4-bis-(3-aminopropyl)-piperazine (bapp) ligand (**a** in Figure 1.9), 1,4-diazacycloheptanediacetate (dachda) and its alkyl derivatives (dachdRa) (**b** in Figure 1.9). [33]

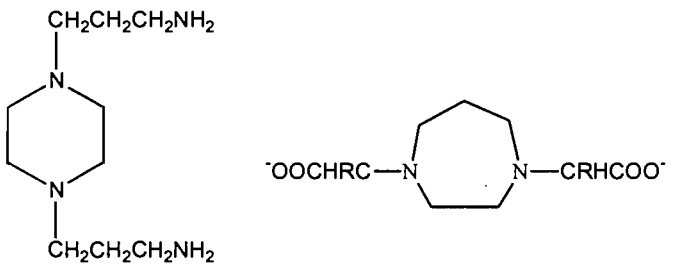

Figure 1.9. Structure of bapp **(a)** and dachdRa **(b)**

Complex $[Ni(bapp)]^{2+}$ has a square-planar geometry and orange colour in donor solvents such as DMF and acetonitrile, and interestingly keeps its geometry without solvent interaction. On the other hand, decreasing the temperature to -50 °C leads to the formation of a blue solution indicating the presence of octahedral geometry around the nickel center in $[Ni(bapp)(S)_2]$ (eq. 5).[34]

$$\underset{\text{blue-violet}\\\text{6-coordinated}}{[Ni(bapp)(S)_2]^{2+}} \underset{\text{cool}}{\overset{\text{heat}}{\rightleftharpoons}} \underset{\text{orange}\\\text{square-planar}}{[Ni(bapp)]^{2+}} + 2\,S \qquad (5)$$

Heating the solution of complex $[Ni(dachda)(H_2O)_2]$ results in a colour change from green to orange, which is due to changes in the geometry around the nickel center from octahedral to square-planar by the dissociation of one water molecule (dachda when R=H (eq. 6)). Whereas, heating a solid sample of complex $[Ni(dacdRa)(H_2O)]$ leads to the dissociation of one molecule of water and transforms the five-coordinated nickel complexes to square-planar (dacdRa when R= Me, Et, n-Pr. (eq. 7)).

$$\underset{\text{green (room temp.)}}{[Ni(dachda)(H_2O)_2]} \underset{\text{cool}}{\overset{\text{heat}}{\rightleftharpoons}} \underset{\text{orange (high temp.)}}{[Ni(dachda)]} + 2\,H_2O \qquad (6)$$

$$\underset{\text{5-coordinated}}{[Ni(dachdRa)(H_2O)]} \underset{\text{cool}}{\overset{\text{heat}}{\rightleftharpoons}} \underset{\text{square-planar}}{[Ni(dachdRa)]} + H_2O \qquad (7)$$

Another interesting example of a thermochromic solid is the complex $[Ni(bpm^{Me2})Cl_2]_2$, which was first synthesized and characterized by Reedjik[34] and represents an interesting case of thermochromism in both solid state and solution. This square-pyramidal complex undergoes a facile transition into a violet tetrahedral monomer $[Ni(dpm^{Me2})Cl_2]$ at high temperatures (Scheme 1.1). Since one of the Ni-(μ-Cl) bonds is significantly longer, an abrupt formation of the monomer takes place which produces a tetrahedral geometry weakening the remaining bridge and allowing the second nickel ion to rearrange. The uncommon behavior of this system is perhaps due to the difficulty in getting the two monomeric species at room temperature where they simultaneously reorient themselves to form the dimeric species.

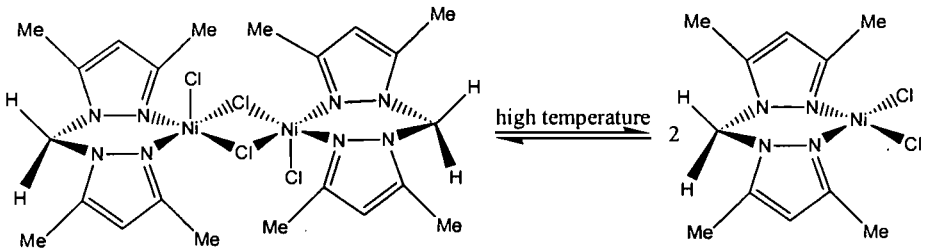

Scheme1.1. The five-coordinated complex $[Ni(bpm^{Me2})Cl_2]_2$ rearrangement at high temperature to form the four-coordinate $[Ni(bpm^{Me2})Cl_2]$ monomer

Similarly to thermochromism, solvatochromism is defined as a phenomenon of colour change in the solution due to the interaction of the solvent with the solute. Solvent interactions lead to changes in the geometry around the metallic centre that produce a change in the HOMO-LUMO gap and hence the colour change. These changes are visible to the naked eye, but can also be observed as red or blue shifts in UV-vis absorption spectra (positive and negative solvatochromism,* respectively). Solvatochromism can also be observed as: a) a pronounced change in the intensity of electronic absorption bands, or b) new emission bands accompanying a change in the polarity of the medium.

* Negative solvatochromism is called blue shift because the peaks shift to the high-energy field; While the positive solvatochromism which is called the red shift because of the shifting to the weak-energy field.

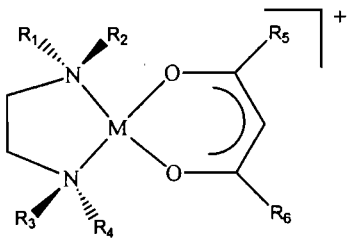

M = Ni, Cu

R1-4 = H, Me, Et

R5-6 = H, Me, ^{t}Bu, Ph, CF_3

Figure 1.10. Mixed-ligand complexes $[M(diam)(dike)]^+$

Solvatochromism of metal complex results from either a strong or weak interaction of the solvent molecules with the complex solute. We will discuss in this thesis the case of the most pronounced interaction, namely the strong interaction of solvent molecules with the metallic centre. Some mixed-ligand complexes such as complex $[M(diam)(dike)]^+$ (diam = *N*-alkylated diamine, dike = β–diketone) with copper(II) and nickel(II) ions exhibit a pronounced solvatochromism (Figure 1.10).

These square-planar geometry of Ni(II) and Cu(II)) complexes are maintained in weakly donating solvents (e.g. CH_2Cl_2), while increasing the solvent nucleophility (e.g. DMF and DMSO) results in the formation of octahedral species. The solvation of $[Ni(diam)(dike)]^+$, for example, proceeds in two steps. In the first step, the initial four-coordinated complex interacts with the first solvent molecule to give a five-coordinated intermediate complex. The geometry of this intermediate depends on the strength of the M-solvent interaction: less nucleophilic solvents lead to a small deformation giving a square-pyramidal geometry, whereas strongly nucleophilic solvents lead to trigonal-bipyramidal complexes. In the second step of the salvation, an octahedral geometry is formed around the nickel either with a *trans*- (typical of weak donor molecules) or a *cis*-species (characteristic for strong donor systems). In solvents of intermediate donor strength (e.g. acetone and higher alcohols), both square-planar and octahedral species are present.

Complete solvation of the nickel center will cause a change in the spin state from S = 0 (diamagnetic, square-planar geometry) to S = 1 (paramagnetic, octahedral geometry) (Figure 1.11), which will be reflected in an abrupt change in the UV-vis spectrum. Cu complexes, on the other hand, have continuous changes in the spectrum because no spin changes are involved.

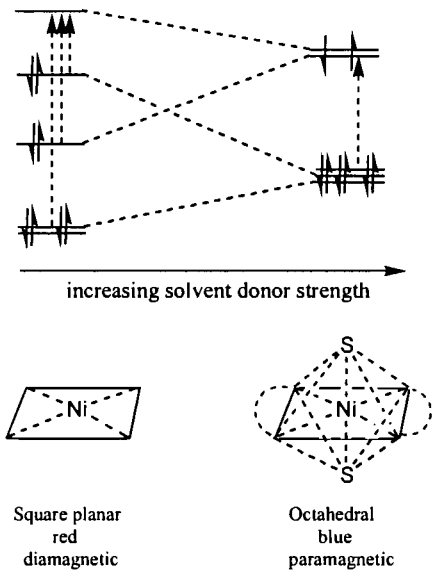

Figure 1.11. Solvatochromism and thermochromism of complex $[Ni(diam)(dike)]^+$

Vapochromism has found increasing interest over the past decade because of the need to develop sensitive sensors to detect chemical and biological analysts. In general, a solid is said to be vapochromic when its colour changes due to direct interaction with the vapors of organic solvents. This change should be reversible without decomposition of the solid. The cause of this phenomenon could be an interaction of the type solvent-metal, ligand-metal or metal-metal.

Recent development in vapochromic-Pt salts has shown promise in sensor developments. [35, 36] For example, the chloride salt of complex $[Pt(Me_2bzimpy)Cl]^+$ (Figure 1.12) changes its yellow colour to orange when a film of this compound is exposed to a vapor of MeOH, $CHCl_3$, CH_2Cl_2, ethanol or acetonitrile. In contrast, the PF_6^- salts of the analogous complex only responded to acetonitrile vapor, changing from yellow to violet within seconds.

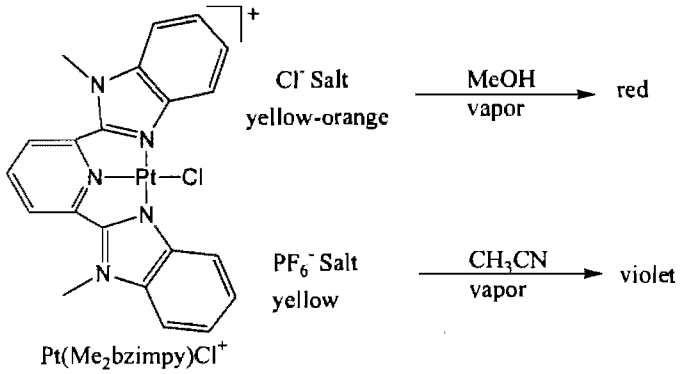

Figure 1.12. Vapochromic salts of platinum(II)

Apparently, what causes this change is the absorption of a molecule of solvent that increases the weak Pt···Pt interactions. We can characterize the vapochromism response by UV-visible absorption spectroscopy possibly resulting from a change in the orbital character of the lowest emissive state. A number of reports have concentrated on studying vapochromism of transition metals like Au,[37] but very few with Ni.[38]

In addition, several methods have been developed to characterize this phenomenon accurately. The best method is the X-ray crystal measurement for each colour change occurring in the crystal. We can also follow the colour changes by measuring IR spectra or UV-vis and luminescence[37,35c] spectra of the solid. Usually the method used for solid measurements involves making a thin film of the solid either with special polymers or spin-coated layers (thickness ~2 μm), or even by the slow evaporation of complex solute on glass or silicon. These very thin and smooth films of the vapochromic complexes will increase their sensitivity toward absorbing the vapor and eventually will detect faster any changes in the atmosphere that surrounds it more rapidly.

1.1.4. The applications of N-heterocycle nickel complexes in the polymerization reactions.

As was mentioned earlier, the interest in coordination chemistry of nickel complexes with nitrogen containing heterocycles has increased rapidly in the recent years.[39] Especially, following the revolutionary work of Brookhart on the development of palladium(II) and nickel(II) complexes, which proved that certain types of complexes are capable of polymerizing ethylene to high molecular weight polymers (Figure 1.13). The key to this discovery was the incorporation of bulky 2,6-disubstituted aryl rings into the α-diimine ligand. The bulky aryl rings are oriented perpendicular to the coordination plane, which forces the 2,6-aryl substituents to lie above and below the plane of the metal center. As a result, access to the axial sites of the metal is inhibited and associative ligand exchange and β-H elimination processes are retarded.[40] Hence, the use of these bulky N-N ligands promotes the generation of high molecular weight polymers.

In this thesis we are not going to discuss any polymerization reactivity of dpdpm complexes, but due to the important aspects of these issues, we are going to give a small resume on its application in poly(pyrazolyl)alkane complexes.

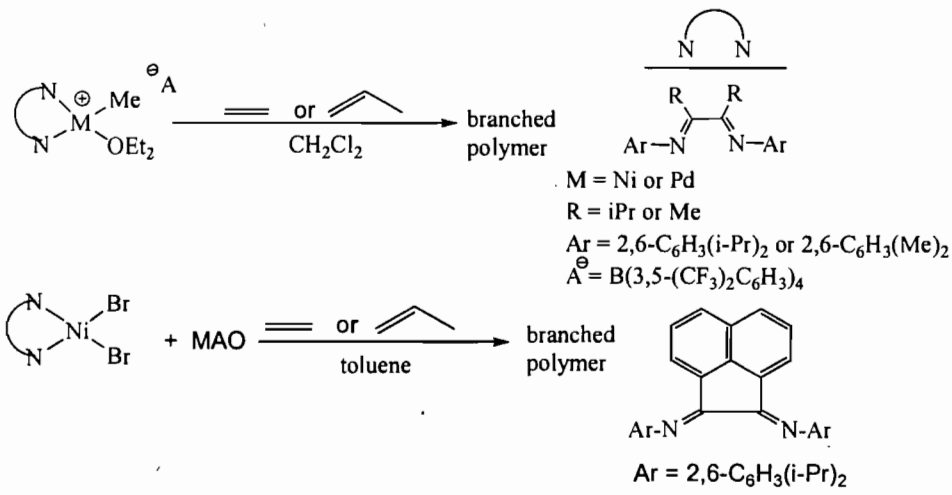

Figure 1.13. Polymerization of ethylene and α–olefins by bulky α–diimine nickel and palladium complexes

Several research groups have been exploring the possibility of using other bidentate ligands based on imines for promoting similar reactivities. Previous work in the Jordan

group focused on the chemistry of bis(pyrazolyl)methane Pd(II) alkyl ethylene complexes of the general formula $[(bpp)Pd(R)(H_2C{=}CH_2)]^+$.[7c] Canty, Trofimenko, and others have also prepared several types of Pd(II) bis(pyrazolyl)methane complexes, including $[(dpdpm)PdMe_2]$ (**a** in Figure 1.14), $[(bpp)PdMe_2]$ (**b** in Figure 1.14),[4] $[(bpm)PdMe_2]$ (bpm = bis(pyrazolyl)methane), and $[(bpp)Pd(allyl)]^+$ (**c** in Figure 1.14).[1e] However, the insertion in ethylene into the palladium methyl bond of $[(bpp)PdMe(H_2C{=}CH_2)]^+$ was observed to be slower than the corresponding insertions of $[(diimine)PdMe(H_2C{=}CH_2)]^+$ or $[(phen)PdMe(H_2C{=}CH_2)]^+$ complexes.

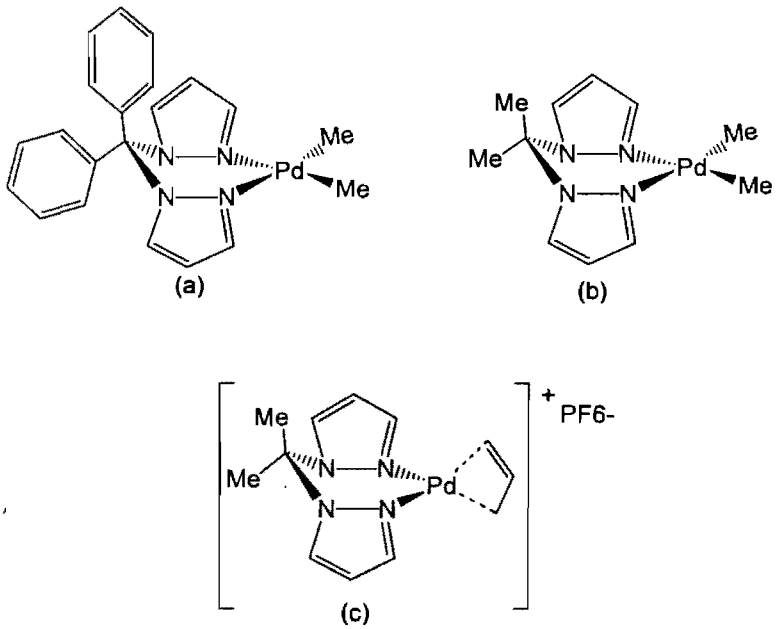

Figure 1.14. Organometallic complexes with Pd, $[(dpdpm)PdMe_2]$ (**a**), $[(bpp)PdMe_2]$ (**b**) and $[(bpp)Pd(allyl)]^+$ (**c**)

1.2. Description of the thesis

The main theme of this thesis is to study the interaction of Ni(II) salts with the ligand diphenyl(dipyrazolyl)methane (dpdpm) in order to prepare new complexes and study their properties. One important issue is to investigate the effect of the stoichiometry of the reactants on the resulting complexes. Another aspect is to study the influence of the two phenyl substituents situated on the bridge carbon over the resulting structure of the complexes. The conformational effect of the six-membered boat-metallacycle in the dpdpm-Ni fragment will also be examined to see if intramolecular η^2-arene or agostic (long range) Ni···H-C interactions are present. Finally, we will study the chromotropism of these complexes by spectroscopy.

During the course of our studies, we have synthesized and characterized four new nickel nitrate compounds with dpdpm ligand and studied the vapo-,solvate- and thermochromic properties for some complexes in solid and liquid state. This work has been published and will be described in Chapter 2. Chapter 3 reports the preparation, characterization and physical measurements on the thermo-, solvato- and vapochromic properties of a series of dpdpm complexes with $NiBr_2$. Similarly to the nitrate complexes, these complexes are sensitive to temperature, solvents, and humidity. This work has been published.

Chapter 4 focuses on studying the abstraction of the bromide from one of the complexes described in chapter 3, namely $[(dpdpm)NiBr_2(H_2O)]$. One of the resulting compounds is a multi-metallic five-coordinated species featuring Ag-Ag interaction. The second complex has an octahedral geometry bearing three molecules of CH_3CN, which makes this complex a good precursor for ligand exchange studies with other donor ligands.

Chapter 5 describes miscellaneous results that were not completed during the course of our studies, namely: a) studying the interaction of $NiCl_2 \cdot 6H_2O$ and NiI_2 with dpdpm, and the interaction of Ni(II) and Pd(II) salts with the ligand diphenyl(3,5-dipyrazolyl)methane ($dpdpm^{Me2}$); b) unsuccessful attempts to oxidize nickel(II) to nickel(III) by reacting $[(dpdpm)NiBr_2(H_2O)]$ with $CuCl_2 \cdot 2H_2O$ and $[Cp_2Fe]PF_6$. Finally, the last chapter presents a global conclusion.

1.3. References

(1) (a) Trofimenko, S. *J. Am. Chem.* Soc. **1966**, *88*, 1842. (b) Trofimenko, S. *J. Am. Chem.* Soc. **1967**, *89*, 3170. (c) Trofimenko, S. *J. Am. Chem.* Soc. **1967**, *89*, 6288. (d) Trofimenko, S. *J. Am. Chem.* Soc. **1969**, *91*, 588. (e) Trofimenko, S. *J. Am. Chem.* Soc. **1970**, *92*, 5118. (f) Trofimenko, S. *J. Am. Chem.* Soc. **1970**, *92*, 1499.

(2) For more reports on the synthesis of different poly(pyrazolyl)methane or borate ligands see: (a) Hill, M. S.; Mahon, M. F.; Mcginley, J. M. G.; Molloy, K. C. *Polyhedron* **2001**, *20*, 1995. (b) Reger, D. L.; Grattan, T. C.; Brown, K. J.; Little, C. A.; Lamba, J. J. S.; Rheingold, A. L.; Sommer, R. D. *J. Organomet. Chem.* **2000**, *607*, 120. (c) Juliá, S.; Sala, P.; Del Mazo, J.; Sancho, M.; Ochoa, C.; Elguero, J.; Fayet, J.-P.; Vertut, M.-C. *J. Heterocycylic Chem.* **1982**, *19*, 1141. (d) Goodman, M. S.; Bateman, M. A. *Tetrahedron letteres* **2001**, *42*, 5. (e) Reger, D. L.; Grattan, T. C. *Synthesis* **2003**, *3*, 350.

(3) For more report on the synthesis of different mixed complexes: (a) Canty, A. J.; Honeyman, R. T.; Skelton B. W.; White A. H. *J. Organomet. Chem.* **1992**, *424*, 381. (b) Byer, P. K.; Canty, A. J.; Honeyman, R. T.; Watson, A. A. *J. Organomet. Chem.* **1990**, *385*, 429. (c) Canty, A. J.; Honeyman, R. T. *J. Organomet. Chem.* **1990**, *387*, 247. (d) Astley, T.; Hitchman, M. A.; Skelton,W. B.; White, A. H. *Aust. J. Chem.* **1997**, *50*, 145.

(4) Byers, P. K.; Canty, A. J.; Honeyman, R. T. *Adv. Organomet. Chem.* **1992**, *34*, 1. (See in particular pp. 26 and 34.)

(5) Canty, A. J.; Andrew, S.; Skelton, B. W.; Traill, P. R.; White, A. H. *Organometallics* **1995**, *14*, 199.

(6) Byers, P. K.; Canty, A. J.; Skelton, B. W.; White, A. H. *Organometallics* **1990**, *9*, 826.

(7) For recent reports on organometallic complexes of Pd based on poly(pyrazolyl)alkane ligands see: (a) Sánchez, G.; Serrano, J. L.; Pérez, J.; Ramírez de Arellano, M. C. López, G.; Molins, E. *Inorg. Chim. Acta* **1999**, *295*, 136. (b) Arroyo, N.; Gomez-de La Tore, F.; Jalon, A. F.; Manzano, B. R.; Moreno-Lara. B.; Rodriguez, A. M. *J. Organomet. Chem.* **2000**, *603*, 174. (c) Tsuji, S.; Swenson, D. C.; Jordan, R. F. *Organometallics* **1999**, *18*, 4758.

(8) (a) Maier, R. J.; Benoit, S. L.; Seshadri, S. *BioMetals* **2007**, *20*, 655. (b) Walsh, C. T.; Orme-Johnson, W. H. *Biochemistry*, **1987**, *26*, 4901. (c) Evans, D. J. *Coord. Chem. Rev.*

2005, *249*, 1582. (d) Mahlert, F.; Bauer, C. ; Jaun, B. ;Thauer, R. K. ; Duin, E.C. *J. Biol. Inorg. Chem.* **2002**, *7*, 500.

(9) Michaud, A.; Fontaine, F.-G.; Zargarian, D. *Inorg. Chim. Acta* **2006**, *359*, 2592.

(10) (a) Michaud, A.; Fontaine, F.-G.; Zargarian, D. *Acta Crystallogr.* **2005**, E *61*, m784.

(b) Michaud, A.; Fontaine, F.-G.; Zargarian, D. *Acta Crystallogr.* **2005**, E *61*, m904.

(11) Nolet, M.-C.; Michaud, A.; Bain, C.; Zargarian, D.; Reber, C. *Photochem. Photobiology* **2006**, *82*, 57.

(12) Rodriguez, V.; Atheaux, I.; Donnadieu, B.; Sabo-Étienne, S.; Chaude, B. *Organometallics* **2000**, *19*, 2916.

(13) Kosky, C. A.; Ganis, P.; Avitabile, G. *Acta Crystallogr.* **1971**, *B 27*, 1859.

(14) Fieselmann, B. F.; Stucky, G. D. *Inorg. Chem.* **1978**, *17*, 2074.

(15) (a) Minghetti, G.; Cinellu, M. A.; Bandini, A. L.; Banditelli, G.; Demartin, F.; Manassero, M. *J. Organomet. Chem.* **1986**, *315*, 387. (b) Michaud, A. M. Sc. Dissertation, Université de Montréal, 2004.

(16) (a) Shiu, K.-B.; Yeh L.-Y.; Peng. S.-M.; Cheng, M.-C. *J. Organomet. Chem.* **1993**, *460*, 203. (b) Shiu, K.-B.; Chou, C.-C.; Wang, S.-L.; Wei, S.-C. *Organometallics* **1990**, *9*, 286.

(17) (a) Bieller, S.; Haghiri, A.; Bolte, M.; Bats, J. W.; Wagner, M.; Lerner, H.-W. *Inorg. Chim. Acta* **2006**, *359*, 1559. (b) Thomas, C. M.; Peters, J. C. *Organometallics* **2005**, *24*, 5858. (c) Santi, R.; Romano, A. M.; Sommazzi, A.; Grande, M.; Bianchini, C.; Mantovani, G. *J. Mol. Catal. A: Chem.* **2005**, *229*, 191. (d) Schneider, J. L.; Young, V. G.; Tolman, W. B. *Inorg. Chem.* **2001**, *40*, 165. (e) Dungan, C. H.; Maringgele, W.; Meller, A.; Niedenzu, K.; Nöth, H.; Serwatowska, J.; Serwatowski, J. *Inorg. Chem.* **1991**, *30*, 4799.

(18) Cinellu, M. A.; stoccoro, S.; Minghetti, G.; Bandini, A. L. Banditelli, G.; Bovio, B. *J. Organomet. Chem.* **1989**, *372*, 311.

(19) Pettinari, C.; Lorenzotti, A.; Sclavi, G.; Cingolani, A.; Rivarola, E.; Colapietro, M.; Cassetta, A. *J. Organomet. Chem.* **1995**, *496*, 69.

(20) Reger, D. L.; Gardinier, J. R.; Smith, M. D. *Inorg. Chem.* **2004**, *43*, 3825.

(21) Pettinari, C.; Cingolani, A.; Bovio, B. *Polyhedron* **1996**, *15*, 115.

(22) Arroyo, N.; Gómez-de La Torre, F.; Jalón, F. A.; Manzano, B. R.; Moreno-Lara, B.; Rodríguez. A. M. *J. Organomet. Chem.* **2000**, *603*, 174.

(23) For inorganic complexes see: (a) Otero, A.; Fernández-Baeza.j, Antiñolo, A.; Tejeda, J.; Lara-Sánchez, A. *Dalton Trans.* **2004**, 1499. (b) Mahon, M. F.; McGinley, J.; Molloy, K.C. *J. Inorg. Chim. Acta* **2003**, *355*, 368. (c) Pettinari, C.; Pettinari, R. *Coord. Chem. Rev.* **2005**, *249*, 663. (d) Pettinari, C.; Marchetti, F.; Cingolani, A.; Leonesi, D.; Colapietro, M.; Margadonna, S. *Polyhedron* **1998**, *17*, 4145.

(24) For organometalic complexes see: (a) Arroyo, N.; Gómez-de La Torre, F.; Jalón, F. A.; Manzano, B. R.; Moreno-Lara, B.; Rodríguez. A. M. *J. Organomet. Chem.* **2000**, *603*, 174. (b) Canty, A. J.; Honeyman, R. T.; Skelton, B. W.; White, A. H. *J. Organomet. Chem.* **1990**, *389*, 277.

(25) Reger, D. L.; Gardinier, J. R.; Smith, M. D. *Inorg. Chem.* **2004**, *43*, 3825.

(26) Shaw, J. L.; Cardon, T. B.; Lorigan, G. A.; Ziegler, C. J. *Eur. J. Inorg. Chem.* **2004**, 1073.

(27) For five coordinate complexes See: Pt with $[RB(Pz)_3]^-$ ligands see reference 4 in particular pp. 23.

(28) Mani, F. *Inorg. Chim. Acta* **1980**, *38*,97.

(29) Mani, F.; Morassi, R. *Inorg. Chim. Acta* **1979**, *36*, 63.

(30) Matsushima, R.; Okuda, H.; Aida, M.; Ogiue, A. *Bull. Chem. Soc. Jpn.* **2001**, *74*, 2295.

(31) Fujiwara, T.; Harada, J.; Ogawa, K. *J. Phys. Chem. B* **2004**, *108*, 4035.

(32) (a) Harlow, R. L.; Wells, W. J.; Watt, G. W.; Simonsen, S. H. *Inorg. Chem.* **1974**, *13*, 2106. (b) Fabbrizzi, L.; Micheloni, M.; Paoletti, P. *Inorg. Chem.* **1974**, *13*, 3019. (c) Bourdin, D.; Lavabre, D.; Beteille, J. P.; Levy, G.; Micheau, J. *Bull. Chem. Soc. Jpn* **1990**, *63*, 2985.

(33) (a) Fukuda, Y.; Murata, F.; El-Ayaan, U. *Monatsh. Chem.* **2001**, *132*, 1279. (b) Gibson, J. G.; McKenzie E.D. *J. Chem. Soc. A* **1971**, 1029.

(34) Jansen, J. C.; van Koningsveld, H.; Ooijen, J. A. C.; Reedijk, J. *Inorg. Chem.* **1980**, *19*, 170.

(35) (a) Grove, L. J.; Rennekamp, J. M.; Jude, H.; Connick, W.B. *J. Am. Chem. Soc.* **2004**, *126*, 1594. (b) Wadas, T. J.; Wang, Q.-M.; Kim, Y.-J.; Flaschenreim, C. *J. Am. Chem. Soc.* **2004**, *126*, 16841.

(36) Kato, M.; Omura, A.; Toshikawa, A.; Kishi, S.; Suginoto, Y. *Angew. Chem. Int. Ed.* **2002**, *41*, 17.

(37) Mansour, M. A.; Connick, W. B.; Lachicotte, R. J.; Gysling, H. J.; Eisenberg, R. *J. Am. Chem. Soc.* **1998**, *120*, 1329

38 Flamini, A.; Mattei, G.; Panusa, A. *J. Inclusion Phenom.* **1999**, *33*, 377.

(39) For few references for polymerization of ethylene and olefins by using Ni(II) and Pd(II) with N- hetrocyclic ligands: (a) Johnson, L. K.; Killian, C. M.; Brookhart, M. *J. Am. Chem. Soc.* **1995**, *117*, 6414. (b) Kunrath, F. A.; de Souza, R. F.; Casagrande, O. L.; Brooks, N. R.; Young, V. G. *Organometallics* **2003**, *22*, 4739. (c) Leatherman, M. D.; Svejda, S. A.; Johnson, L. K.; Brookhart, M. *J. Am. Chem. Soc.* **2003**, *125*, 3068. (d) Speiser, F.; Braunstein, P. *Organometallics* **2004**, *23*, 2633. (e) Svejda, S. A.; Brookhart, M. *Organometallics* **1999**, *18*, 65. (f) Svejda. S. A.; Johnson. L. K.; Brookhart, M. *J. Am. Chem. Soc.* **1999**, *121*, 10634. (g) Feldman. J.; McLain. S. J.; Parthasarathy, A.; Marshall, W. J.; Calabrese. J. C.; Arthur. S. D. *Organometallics* **1997**, *16*, 1514.

(40) (a) Mecking, S.; Johnson, L. K.; Wang, L.; Brookhart, M. *J. Am. Chem. Soc.* **1998**, *120*, 888. (b) Gates, D. P.; Svejda, S. A.; Onate, E.; Killian, C. M.; Johnson, L. K.; White, P. S.; Brookhart, M. *Macromolecules* **2000**, *33*, 2320.

Chapter 2: Syntheses, Structures, Spectroscopy, and Chromotropism of New Complexes Arising from the Reaction of Nickel(II) Nitrate with Diphenyl(dipyrazolyl)methane

Article 1

Syntheses, Structures, Spectroscopy, and Chromotropism of New Complexes Arising from the Reaction of Nickel(II) Nitrate with Diphenyl(dipyrazolyl)methane

Natalie Baho and Davit Zargarian*

Département de chimie, Université de Montréal,

Montréal, Québec, Canada H3C 3J7

Inorg. Chem. **2007**, *46*, 299

2.1 Abstract

The complexes [(dpdpm)Ni(η^2-NO_3)$_2$] (**2.1**), [(dpdpm)Ni(η^2-NO_3)(η^1-NO_3)(CH_3CN)] (**2.2**), [(dpdpm)$_2$Ni(η^1-NO_3)(H_2O)]NO_3 (**2.3**), and [(dpdpm)$_2$Ni(H_2O)$_2$][NO_3]$_2$ (**2.4**) (dpdpm = diphenyl(dipyrazolyl)methane, $Ph_2C(C_3N_2H_3)_2$), have been prepared and characterized by IR and UV-Vis-NIR spectroscopy and X-ray diffraction studies. X-ray studies have confirmed that complexes **2.1-2.4** all adopt variously distorted octahedral structures in the solid state, the largest distortions arising from the small bite-angle of the bidentate nitrate ligand in **2.1** and **2.2**. Magnetic moment measurements indicate that these solids are paramagnetic with two unpaired electrons. The solution ^{1}H NMR data show that the paramagnetism is maintained in solution. Absorption spectra of **2.1-2.4** show three main bands in the region of 350-1000 nm representing spin allowed (d-d) transitions from the ground state $^3A_{2g}$ to the excited states $^3T_{2g}$, $^3T_{1g}(^3F)$, and $^3T_{1g}(^3P)$. A weak shoulder was also detected at about 700-800 nm in most spectra, representing spin-forbidden transitions $^3A_{2g} \rightarrow {}^1E_g$. A comparison of the crystal field parameters 10Dq and B for **2.1-2.4** to the corresponding values for related complexes indicated that these parameters are fairly insensitive to structural variations within this family of complexes. The 10Dq/B ratios show greater variations, but no clear correlations are apparent between 10Dq/B and such structural features as the nature of ligator atoms (N:O ratio), the bonding mode of the nitrate ligand, or the overall charge. Complexes **2.1** (green) and **2.2** (blue) interconvert as a function of temperature (solutions and solid samples), concentration of CH_3CN (solutions), or CH_3CN vapor pressure (solid samples).

Keywords: Nickel, dipyrazolylmethane ligands, vapochromism, solvatochromism, thermochromism, bidentate nitrate, monodentate nitrate.

2.2 Introduction

Since Trofimenko's initial reports on poly(pyrazolyl)borates[1] and poly(pyrazolyl)alkanes,[2] these so-called scorpionate ligands have found wide applications in coordination, organometallic, and bioinorganic chemistry.[3] Perhaps the most important feature of these two classes of ligands is the ease with which their steric and electronic properties can be modified by simple synthetic modifications, thereby allowing a fine-tuning of ligand properties. The anionic bis- or tris(pyrazolyl)borates are the most commonly studied of the scorpionate ligands. This family of ligands has shown great versatility for stabilizing a wide range of coordination and organometallic complexes, in particular those possessing metals in their less common oxidation states (e.g., Pd(IV)[4,5] and Pt(IV)[5,6]). By comparison, the neutral bis- or tris(pyrazolyl)alkanes have had less impact in organometallic chemistry.[7] The paucity of organometallic compounds based on poly(pyrazolyl)alkane ligands is particularly evident in the case of nickel, for which no organometallic complex has been reported.[8]

We have explored the preparation and characterization of new nickel-poly(pyrazolyl)alkane complexes as precursors for new organometallic species.[9] In previous reports we have described the synthesis,[10] structural characterization,[11] and spectroscopy[12] of a series of complexes based on bpm^{Me2} and tpm^{Me2} ligands (bpm^{Me2} = bis(3,5-dimethylpyrazolyl)methane, tpm^{Me2} = tris(3,5-dimethylpyrazolyl)methane). All of these compounds are paramagnetic and some display continuous thermo-, solvato-, and vapochromic behaviour. These properties arise from the relatively facile changes in the coordination geometry of these compounds or from the substitution of one or more ligands by solvent molecules or coordinating anions. The observation of these phenomena in our complexes implies the existence of closely related structural derivatives of very comparable energies.

Thermochromic behavior has been observed with other Ni(II) complexes bearing bis(pyrazolyl)methane or ethylenediamine type ligands. For instance, dichloro(bis(3,5-dimethylpyrazolyl)methane)Ni^{II} undergoes a monomer-dimer equilibrium (in the solid state) as a function of temperature: the orange, chloro-bridged dimer is stable below 130 °C and adopts a square pyramidal geometry, while the deep purple monomer forms at higher

temperatures and adopts a pseudo-tetrahedral geometry around Ni.[1e,13] On the other hand, the complex [bis(*N,N*-diethylethylenediamine)Ni^{II}][NO_3]$_2$ and its Cu^{II} analogue undergo reversible coordination of the nitrate anions to convert the red square planar form to a purple octahedral species at high temperatures.[13,14]

Solvatochromism of Ni(II) species based on ethylenediamine type ligands has been studied intensively.[15] These studies have shown that the solvatochromism of these complexes is based, primarily, on the coordination of solvent molecules to the metal center in the initially square planar species; depending on the donor strength of the solvent or the steric bulk of the ligands, one or two solvent molecules can bind to give square pyramidal or octahedral solvato products, respectively. In some cases, the coordinating ability of certain anions can modulate the outcome of these interactions. Similarly, vapochromism arises from metal-ligand or metal-metal interactions, or more subtle changes in the compound lattice, when a complex is exposed to volatile organic compounds; this phenomenon leads to changes in the absorption or luminescence properties of the complex. Vapochromism has been studied extensively with a number of transition metal compounds, including those of platinum[16] and gold,[17] but very few studies have been reported with Ni(II) complexes. For instance, a recent report outlined the development of sensors based on the vapochromic properties of the complex bis(1,2,6,7-tetracyano-3,5-dihydro-3,5-diiminopyrrolizinido)nickel(II) dispersed inside spin coated poly(vinylbutyral) thin films.[18] To our knowledge, the vapochromic properties of Ni complexes based on bis(pyrazolyl)methane type ligands have not been explored.

As a follow-up to our earlier studies, we have prepared a new series of nickel complexes featuring the ligand dpdpm (dpdpm = diphenyl(dipyrazolyl)methane).[19] Solid state structural studies and UV-Vis-NIR spectroscopy have been employed to investigate structural changes in the first examples of this family of compounds as a function of temperature, different solvents, and type of anions used. Herein we report on the synthesis, structural characterization, and spectroscopy of complexes arising from the reaction of dpdpm with $Ni(NO_3)_2$. The relatively labile coordination of the nitrate anion has given access to compounds featuring η^{2-}, η^{1-}, and η^{0-} nitrate moieties. Thus, the nitrate ligand in the complex [(dpdpm)Ni(η^2–NO_3)$_2$], **2.1**, undergoes a hapticity change to give

[(dpdpm)Ni(η^1–NO_3)(η^2–NO_3)(CH_3CN)], **2.2**; these two compounds interconvert as a function of temperature (solutions and solid samples), acetonitrile concentration (solutions), or acetonitrile vapor pressure (solid samples).

2.3 Experimental

2.3.1. General.

All starting materials were purchased from Sigma-Aldrich and used as received. $Ni(NO_3)_2 \cdot 6H_2O$ was used without dehydration. The main ligand used in this study, diphenyl(dipyrazolyl)methane (dpdpm), was synthesized according to a published procedure.[13b] The NMR spectra were recorded on a Bruker Av400 (^1H at 400 MHz). The IR spectra were recorded between 4000 and 400 cm^{-1} using KBr pellets on a Perkin Elmer Spectrum One spectrophotometer using the Spectrum v.3.01.00 software. The UV-Vis-NIR spectra were recorded between 1300 and 250 nm with a 1 cm quartz cell on a Varian Cary 500i; baseline correction was applied prior to recording the spectra. The magnetic susceptibility measurements were carried out at room temperature using the Gouy method with a Johnson Matthey Magnetic Susceptibility Balance calibrated on $[HgCo(SCN)_4]$ samples. The elemental analyses (C, H, and N) were performed in duplicate by Laboratoire d'Analyse Élémentaire de l'Université de Montréal.

2.3.2. Syntheses

[(dpdpm)Ni(η^2-NO_3)$_2$] (2.1). Solid $Ni(NO_3)_2 \cdot 6H_2O$ (0.45 g, 1.67 mmol) was added to a stirred solution of dpdpm (0.50 g, 1.67 mmol) in CH_2Cl_2 (40 mL), and the reaction mixture was heated to reflux for 4 h. The final mixture was cooled to room temperature, filtered, and evaporated to give a dark turquoise-green solid. This was washed with hot hexane (2 × 40 mL) and extracted into CH_2Cl_2 to remove insoluble impurities. Removal of the solvent gave a turquoise-green solid (0.67 g, 83% yield). X-ray quality single crystals (emerald green) were obtained by diffusion of Et_2O into a concentrated CH_2Cl_2 solution. ^1H NMR ($CDCl_3$): δ 62.05 (br), 44.43 (br), 7.21 (br), 6.87 (br). IR (KBr): υ (cm^{-1}) 3430 (br), 3138 (m), 2506 (w), 1769 (m), 1522 (s), 1491 (vs), 1452 (s), 1434 (s), 1408 (s), 1384 (s), 1308 (s), 1278 (s), 1260 (m), 1217 (w), 1194 (w), 1165 (w), 1102 (s), 1087 (w), 1068 (s), 1016

(m), 1001 (w), 958 (w), 940 (w), 921 (w), 891 (w), 861 (w), 807 (w), 785 (m), 750 (s), 699 (s), 659 (s), 636 (w), 604 (w). m.p. 240°C. $\mu_{eff.}$ 3.22 BM. Anal. Calcd for $C_{19}H_{16}N_6O_6Ni$: C, 47.24; H, 3.34; N, 17.40. Found: C, 47.28; H, 3.40; N, 17.00.

[(dpdpm)Ni(η^1-NO_3)(CH_3CN)][NO_3] (2.2). To a solid sample of complex **2.1** (0.40 g, 0.83 mmol) was added a sufficiently small amount of CH_3CN (0.55 g, 13 mmol) to avoid complete dissolution of the solid. The color of the "wet" solid changed immediately from green to blue. Placing the "wet" blue solid and the residual blue solution under vacuum for a brief period (1-2 min) gave a blue solid (0.34 g, 78 % yield). X-ray quality crystals (blue) of the new product were grown by diffusion of Et_2O into a saturated CH_3CN solution. ^1H NMR (CD_3CN): δ 67.7 (br), 65.8 (br), 54.0 (br), 44.4 (br), 7.32 (br), 7.03 (br), 2.11 (br). (NB: The spectra of aged solutions also displayed broadened signals for free dppm, and the broad signal at 2.11 merged with the residual solvent peak.) IR (KBr): υ (cm^{-1}) 3401 (br), 3151 (m), 3064 (m), 2314 (w), 2288 (w), 1619 (m), 1492 (vs), 1450 (vs), 1435 (s), 1407 (s), 1384 (s), 1306 (vs), 1277 (s), 1220 (m), 1194 (m), 1171 (w), 1105 (m), 1085 (w), 1069 (s), 1018 (w), 1000 (m), 939 (m), 921 (m), 890 (m), 871 (m), 808 (m), 752 (vs), 698 (s), 658 (m), 636 (m), 605 (w). $\mu_{eff.}$ 3.86 BM. m.p. 238 °C. The elemental analysis of this compound was problematic because thorough evaporation of the sample resulted in an analysis identical to that of complex **2.1** (i.e., loss of coordinated CH_3CN). To minimize the loss of CH_3CN, a batch of crystals was heated <u>for a few seconds only</u> in a 100 °C oven prior to the analysis, which gave results consistent with the inclusion of one half molecule of Et_2O: Found: C, 49.16; H, 3.98; N, 17.53. (Calcd for $C_{21}H_{19}N_7O_6Ni$: C, 48.12; H, 3.65; N, 18.71. Calcd for $C_{21}H_{19}N_7O_6Ni$ + ½ ($C_4H_{10}O$): C, 49.23; H, 4.31; N, 17.47.)

[$(dpdpm)_2Ni(H_2O)$(η^1-NO_3)][NO_3] (2.3). Solid $Ni(NO_3)_2 \cdot 6H_2O$ (0.24 g, 0.83 mmol) was added to a stirred solution of dpdpm (0.50 g, 1.67 mmol) in CH_2Cl_2 (40 mL) and the reaction mixture was heated to reflux for 4 h. The final mixture was cooled to room temperature, filtered, and evaporated to give a royal blue solid. This was washed with hot hexane (2 × 40 mL) and extracted into CH_2Cl_2 to remove insoluble impurities. Removal of the solvent gave a royal blue solid (0.60 g, 91% yield). X-ray quality single crystals (navy

blue) were obtained by diffusion of Et_2O into a concentrated CH_2Cl_2 solution. ^1H NMR ($CDCl_3$): δ 68.4 (br), 62.4 (br), 44.0 (br), 37.5 (br), 8.0-7.0 (br), 6.9 (br), plus sharp signals due to free dpdpm at 7.69 (s), 7.55 (d, *J*= 3), 7.37 (psq, *J* = 8), 7.07 (d, *J* = 8), 6.30 (s). IR (KBr): υ (cm^{-1}) 3402 (br), 3135 (w), 3121 (m), 3059 (m), 3035 (m), 2926 (w), 2854 (w), 2427 (w), 1996 (w), 1748 (w), 1631 (m), 1517 (m), 1493 (m), 1448-1438 (s), 1384 (s), 1339 (m), 1326 (m), 1305-1293 (w), 1249 (w), 1219 (m), 1195 (m), 1168 (m), 1112 (s), 1087 (m), 1066 (s), 1038 (w), 1001 (w), 991 (w), 939 (w), 921 (w), 891 (w), 873 (w), 863 (w), 826 (w), 757-748 (vs), 700 (vs), 659 (w), 638 (m), 618 (w), 607 (w), 511 (w). μ_{eff} 3.36 BM. m.p. 145 °C. Anal. Calcd for $C_{38}H_{34}N_{10}O_7Ni$: C, 56.95; H, 4.28; N, 17.48. Found: C, 56.54; H, 4.26; N, 17.42.

[(dpdpm)$_2$Ni (H_2O)$_2$][NO_3]$_2$ (2.4). Solid $Ni(NO_3)_2 \cdot 6H_2O$ (0.24 g, 0.83 mmol) was added to a stirred solution of dpdpm (0.50 g, 1.67 mmol) in MeOH (40 mL) and the reaction mixture was refluxed for 18 h. The final mixture was cooled to room temperature, filtered, and evaporated to give a dark blue solid. This was washed with hot hexane (3 × 50 mL) and extracted into CH_2Cl_2 to remove insoluble impurities. Removal of the solvent gave a dark blue solid (0.56 g, 82% yield). X-ray quality single crystals (blue) were obtained by diffusion of Et_2O into a concentrated MeOH solution. ^1H NMR ($CDCl_3$): δ 65.7 (br), 52.7 (br), 45.3 (br), 49.0 (br), 7.7-6.5 (br), plus signals corresponding to free dpdpm. IR (KBr): υ (cm^{-1}) 3390 (br), 3164 (m), 3130 (m), 3120 (m), 3056 (m), 2418 (w), 1655 (m), 1518 (m), 1492 (m), 1449-1385 (vs), 1332-1306 (vs), 1251 (m), 1219 (m), 1189 (s), 1165 (m), 1109 (m), 1086 (m), 1063 (s), 1041 (m), 994 (w), 982 (w), 938 (w), 915 (w), 890 (w), 872 (w), 823 (w), 753 (vs), 698 (vs), 659 (w), 635 (m), 605 (w), 501 (w). μ_{eff} 3.17 BM. m.p. 195-205 °C. Anal. Calcd for $C_{38}H_{36}N_{10}O_8Ni$: C, 55.70; H, 4.43; N, 17.09. Found: C, 55.25; H, 4.35; N, 17.03.

2.3.3. Crystallographic studies. The crystal data for compound **2.1** were collected on an Enraf-Nonius CAD-4 four-circle diffractometer at 298(2) K. The diffraction data were collected with graphite-monochromated Cu Kα radiation; the cell parameters were refined

using CAD-4 software on 25 reflections, while NRC-2 and NRC-2A were used for the data reduction.[20] The crystal data for **2.2, 2.3,** and **2.4** were collected on a Bruker AXS SMART 6K diffractometer mounted with rotating anode Cu Kα radiation at 293(2) K (SMART[21] software). Cell refinement and data reduction were carried out using SAINT.[22] All structures were solved by direct methods using SHELXS97[23], and the refinements were done on F^2 by full-matrix least squares.[24] All non-hydrogen atoms were refined anisotropically. The positional parameters for H atoms in water molecules were refined isotropically, but all other hydrogens were constrained to the parent atom using a riding model.

The monodentate nitrate ligand of complex **2.2** showed some disorder in the positions of the O5 and O55 atoms; the occupancies of these atoms were initially refined and then fixed at 0.50. This structure also contained disordered Et_2O molecules, which were refined isotropically using a constrained model; disordered solvent molecules were then introduced over two positions and refined using ISOR restrained technique. The crystal structures of **2.3** and **2.4** are stabilized by intermolecular hydrogen bonds. The details on O-H···O distances are available from the detailed structure reports (Supporting Information at the end of this thesis). For the sake of clarity, the disordered Et_2O molecules in **2.2** and the counter ions in **2.3** and **2.4** have been removed from the ORTEP diagrams. All the details concerning the refinement of the crystal structures are listed in Table 2.1.

2.3.4. Testing the reversible chromotropic properties of complex 2.1.

Solvatochromic behaviour of complexes **2.1** and **2.2**. Dissolving ca. 15 mg of green complex **2.1** in ca. 1 mL of CH_2Cl_2 gave a green solution. Evaporating this solution to dryness gave back the green solid, which was dissolved in ca. 1 mL of CH_3CN to give a blue solution. Evaporation of CH_3CN to dryness gave back the original green solid. Re-dissolving the green solid in CH_3CN followed by evaporation resulted in the same colour changes.

In order to confirm that the observed colour changes correspond to the interconversion of complexes **2.1** and **2.2**, UV-Vis-NIR spectra were recorded for samples of **2.1** in CH_2Cl_2 and CH_3CN. The spectrum of the CH_3CN solution of **2.1** was identical to

that of complex **2.2** in CH_3CN. UV-Vis-NIR spectra were also recorded for CH_2Cl_2:CH_3CN mixtures of various proportions (ca. 6.5 mM). The narrowest absorptions in the spectra obtained for 100:0 and 0:100 samples (at 381 and 374 nm, respectively) were selected for monitoring the solvent-induced interconversion of the two complexes. The spectra for the 80:20, 60:40, 50:50, 40:60, and 20:80 samples showed an incremental shift in the peak maximum, as shown in Figure 2.6.

Reversible vapochromic behavior of complexes **2.1** and **2.2**. A small, uncapped vial containing 4 mg of complex **2.1** was placed inside a 25 mL round bottom flask containing ca. 3 mL of CH_3CN; care was taken to make sure that the solid and the solvent did not come in direct contact. The flask was then stoppered to allow a build-up of solvent vapour at room temperature. The turquoise-green colour of complex **2.1** changed to light blue in 8 min. At this point, the sample vial was taken out of the flask and placed in a 100 °C oven for one min, which caused the original turquoise-green colour of the sample to reappear; the sample did not show any visible sign of degradation. Exposing the green solid to CH_3CN vapours resulted once again in a green-to-blue colour change. Repeating this procedure five times on the same sample showed the same observations: samples of **2.1** obtained by heating **2.2** for only one min at 100 °C required between 5 and 10 min (the average over five trials being 7 min) of exposure to CH_3CN vapours to undergo the green-to-blue colour change in a convincing fashion.

Reversible thermochromic behaviour of complexes **2.1** and **2.2**. Dissolving a solid sample of turquoise-green **2.1** in CH_3CN (ca. 0.02 M) gave a blue solution at ambient temperature. Heating this solution to 65 °C resulted in a rapid colour change to the green colour of CH_2Cl_2 solutions of **2.1**. This colour could be maintained over 45 min of heating without decomposition. Cooling the green solution to 18 °C regenerated the initial blue colour of the sample. Repeating this heating-cooling cycle 10 times confirmed the reversible nature of this thermochromic behavior. Evaporation of the solution furnished the green complex **2.1** unchanged.

In a similar experiment, we recorded the variable temperature (264-360 K) UV-Vis-NIR spectra of a solution of **2.1** in CH_3CN and the thermochromic behaviour was

monitored by following the high-energy absorption peaks (ca. 370-380 nm). This experiment showed that higher temperatures result in an incremental shift in the band maximum of the monitored absorption, from ca. 370 nm (for **2.2**) to ca. 380 nm (for **2.1**).

2.4 Results and Discussion

2.4.1 Syntheses. The reaction of $Ni(NO_3)_2 \cdot 6H_2O$ with 1 equiv of dpdpm in CH_2Cl_2 under reflux over 4 h afforded a green solution, which was evaporated to give complex **2.1** as a turquoise-green solid (Scheme 2.1). The same result can be obtained from the room temperature reaction during 18 h. Washing the turquoise-green solid with hot hexane to remove any excess of unreacted ligand, followed by extraction into CH_2Cl_2 to eliminate unreacted $Ni(NO_3)_2 \cdot 6H_2O$, yielded an analytically pure product. Recrystallization from CH_2Cl_2/Et_2O gave emerald green crystals that were subjected to spectral analysis and X-ray diffraction studies (*vide infra*). Bis(η^2-NO_3) complexes of Ni similar to **2.1** have been reported.[25]

Scheme 2.1

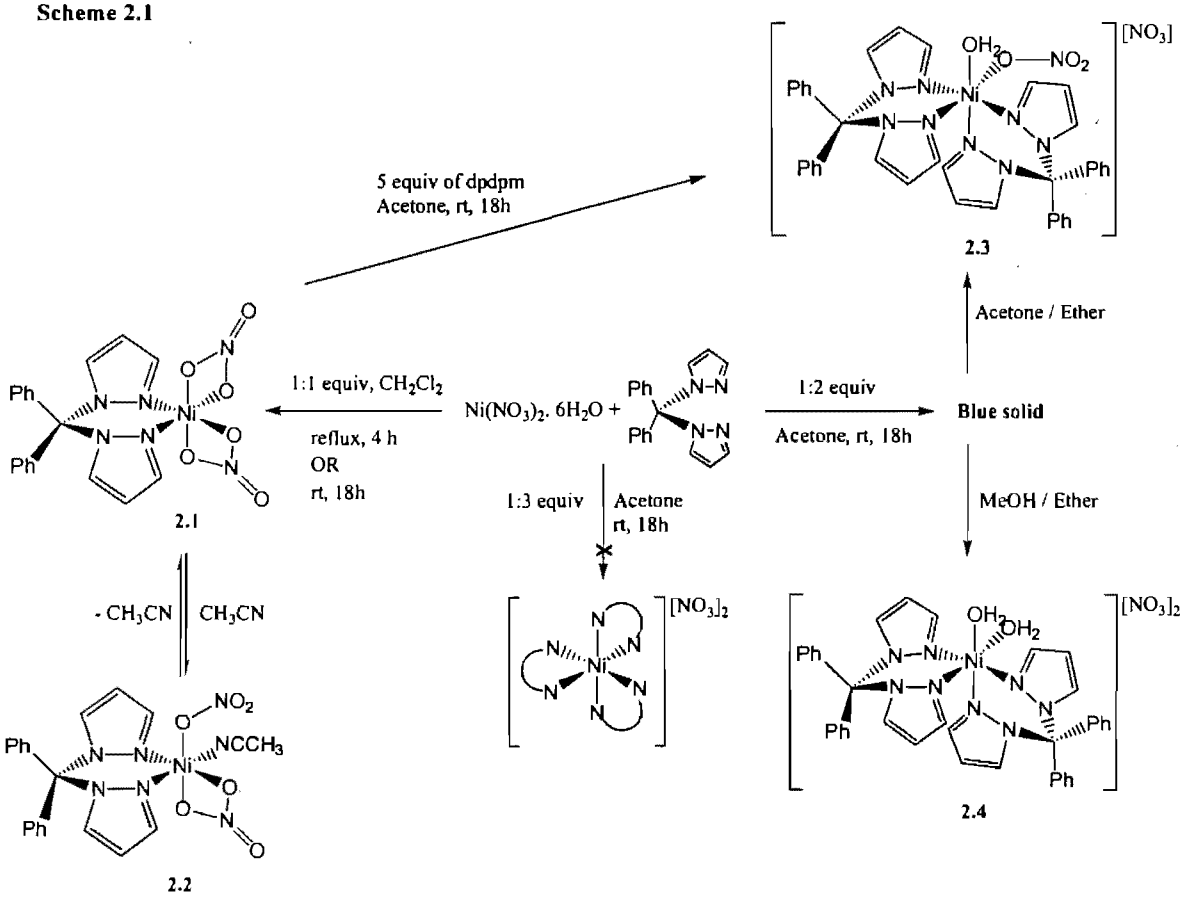

The analogous reaction of $Ni(NO_3)_2.6H_2O$ with 2 equiv of dpdpm gave, after work-up and purification, a blue solid. Contrary to our expectations, this product was neither $[(dpdpm)_2Ni(\eta^2\text{-}NO_3)][NO_3]$ nor $[(dpdpm)_2Ni(\eta^1\text{-}NO_3)_2]$. Indeed, the final outcome of the reaction depended on the solvent of recrystallization, producing $[(dpdpm)_2Ni(\eta^1\text{-}NO_3)(H_2O)]$, **2.3**, from acetone, or $[(dpdpm)_2Ni(H_2O)_2]$, **2.4**, from CH_2Cl_2, CH_3CN or MeOH. Complexes **2.3** and **2.4** were studied by spectroscopy and X-ray diffraction (*vide infra*).

The formation of **2.3** and **2.4** indicates that the nitrate ligand in these bis(dpdpm) species is very labile and can be displaced readily by residual water. In an effort to prevent the displacement of the nitrate ligands by water, the reaction of $Ni(NO_3)_2$ with 2 equiv of dpdpm was carried out in dry CH_2Cl_2 under an atmosphere of dry nitrogen. This reaction gave a lilac solid that proved to be very sensitive to water: exposure of this new product to

air for a few min converted it to complex **2.3**. We were unable to identify the lilac solid, but its facile hydration to **2.3** suggests it might be one of the anticipated precursors to **2.3**, i.e., $[(dpdpm)_2Ni(\eta^2\text{-}NO_3)][NO_3]$ or $[(dpdpm)_2Ni(\eta^1\text{-}NO_3)_2]$.[26]

A number of observations have indicated that all the ligands in **2.3** and **2.4** are fairly labile and can be displaced by coordinating solvents. Thus, the UV-Vis-NIR spectra of **2.3** and **2.4** displayed small but significant variations as a function of solvent (*vide infra*), while their NMR spectra in CD_3CN led to a gradual broadening of the original peaks and gave rise to signals for free dpdpm (*vide infra*). Unfortunately, however, we were unable to intercept and isolate any solvato derivatives of **2.3** or **2.4**. In contrast, complex **2.1** reacted readily with water, MeOH or CH_3CN to give blue solvato derivatives, and we succeeded in isolating and characterizing the acetonitrile derivative $[(dpdpm)Ni(\eta^2\text{-}NO_3)(\eta^1\text{-}NO_3)(CH3CN)]$, **2.2** (*vide infra*).

Finally, we were unable to prepare the homoleptic complex $[Ni(dpdpm)_3][NO_3]_2$ from the reaction of excess dpdpm (> 5 equiv) with $Ni(NO_3)_2$, **2.3**, or **2.4**, whereas reacting **2.1** with excess dpdpm gave **2.3** (Scheme 1). The precise reasons for our failure to prepare a tris(dpdpm) complex are not known, but we can rule out steric or enthalpic factors since we have observed the formation of $[Ni(dpdpm)_3]^{2+}$ from NiI_2.[27]

2.4.2 Crystal structures. Single crystals of **2.1**, **2.2**, **2.3** and **2.4** were obtained by vapour diffusion of Et_2O into solutions of these complexes in CH_2Cl_2, acetonitrile, methanol, and acetone, respectively. To ensure that the crystals retain their integrity throughout the data collection period, they were coated by either Paratone-N oil or epoxy glue and mounted rapidly. All four sets of diffraction data resulted in fairly accurate structures for the complexes studied, as reflected in the R_1 values of ca. 0.0444 (**2.1**), 0.0525 (**2.2**), 0.0506 (**2.3**), and 0.0325 (**2.4**). The crystal data and details of data collection are listed in Table 2.1, the principal geometric parameters are listed in Table 2.2, and ORTEP III[28] molecular structures are illustrated in Figures 2.1-2.4.

Table 2.1. Crystallographic data for complexes **2.1**-**2.4**

	2.1	**2.2**·(0.5 Et_2O)	**2.3**	**2.4**
Formula	$C_{19}H_{16}N_6O_6Ni$	$C_{21}H_{19}N_7O_6Ni$· 0.5 ($C_4H_{10}O$)	$C_{38}H_{34}N_{10}O_7Ni$	$C_{38}H_{36}N_{10}O_8Ni$
Mol wt	483.09	561.20	801.46	819.48
Cryst color	Green	Blue	Blue	Blue
Cryst dimens, mm	0.26×0.15×0.14	0.24 ×0.26×0.30	0.33 ×0.26×0.13	0.16 ×0.14 ×0.12
Symmetry	Monoclinic	Triclinic	Monoclinic	Monoclinic
Space group	$P2_1/n$	P-1	$P2_1/c$	$P2_1/c$
a, Å	8.400(2)	8.4150(2)	13.5458(8)	11.6537(2)
b, Å	14.861(5)	9.4669(2)	16.9361(9)	16.4081(3)
c, Å	17.029(6)	16.6064(3)	16.4455(9)	19.2521(3)
α, deg	90	76.1910(10)	90	90
β, deg	102.17(2)	85.0970(10)	104.175(3)	92.0130(10)
γ, deg	90	86.125(2)	90	90
Volume, $Å^3$	2078.0(11)	1278.47(5)	3657.9(4)	3679.02(11)
Z	4	2	4	4
D(calcd), g. cm^{-1}	1.544	1.458	1.455	1.479
Diffractometer	CAD-4	Bruker AXS SMART 2K	Bruker AXS SMART 2K	Bruker AXS SMART 2K
Temp, K	293(2)	200(2)	220(2)	200(2)
λ	1.5418	1.5418	1.5418	1.5418
μ, mm^{-1}	1.798	1.569	1.318	1.344
Scan type	ω scan	ω scan	ω scan	ω scan
F(000)	992	582	1664	1704
θ_{max}, deg	69.92	73.01	72.03	68.89
h,k,l range	$-10 \le h \le 10$ $-18 \le k \le 18$ $-20 \le l \le 20$	$-10 \le h \le 10$ $-11 \le k \le 11$ $-20 \le l \le 20$	$-16 \le h \le 15$ $-20 \le k \le 20$ $-19 \le l \le 20$	$-14 \le h \le 13$ $-18 \le k \le 19$ $-23 \le l \le 23$
Reflns observed ($I > 2\sigma(I)$)	3382	6433	6504	5518
Absorption Correction	Multi-scan SADABS	Multi-scan SADABS	Multi-scan SADABS	Multi-scan SADABS
T (min, max)	0.65, 0.79	0.76, 0.65	0.94,0.70	0.80, 0.85
$R\ [F^2>2\sigma(F^2)]$, $wR(F^2)$	0.0444, 0.1143	0.0525, 0.1296	0.0506, 0.1238	0.0325, 0.0924
GOF	1.042	1.041	1.052	1.036

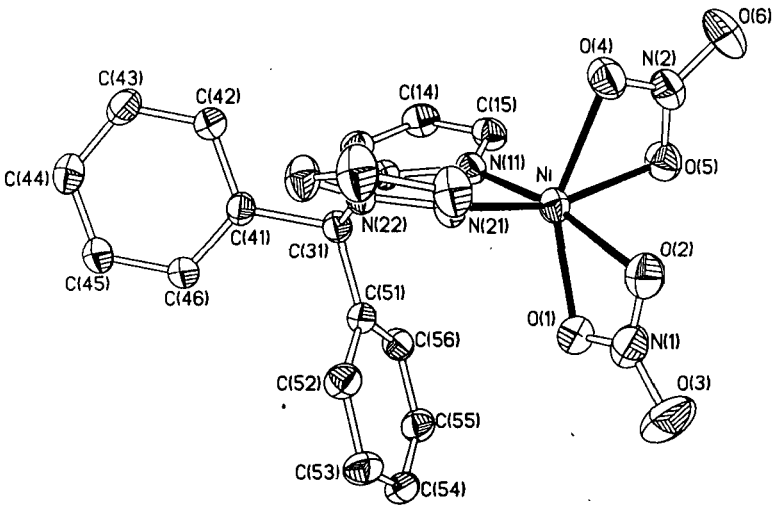

Figure 2.1. ORTEP view of complex **2.1**. Thermal ellipsoids are shown at 30% probability

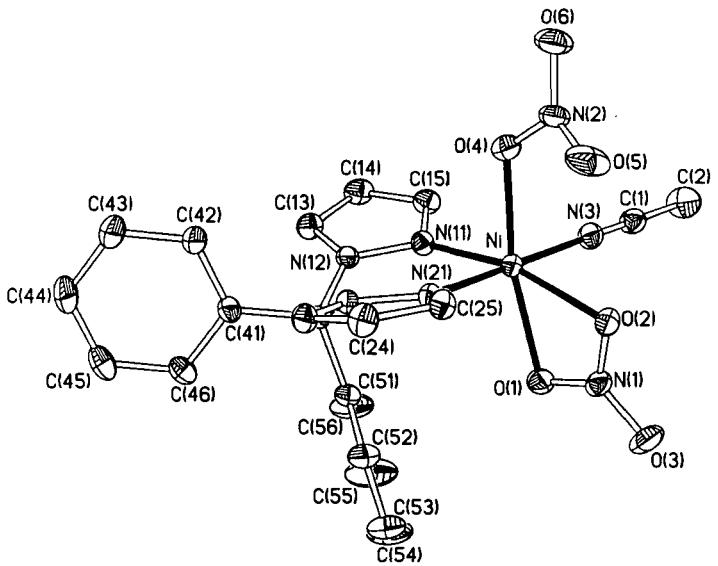

Figure 2.2. ORTEP view of complex **2.2**. Thermal ellipsoids are shown at 30% probability. Only one of the two positions (0.50 : 0.50) is shown for the disordered O5 atom. The disordered Et_2O molecule has been omitted for clarity

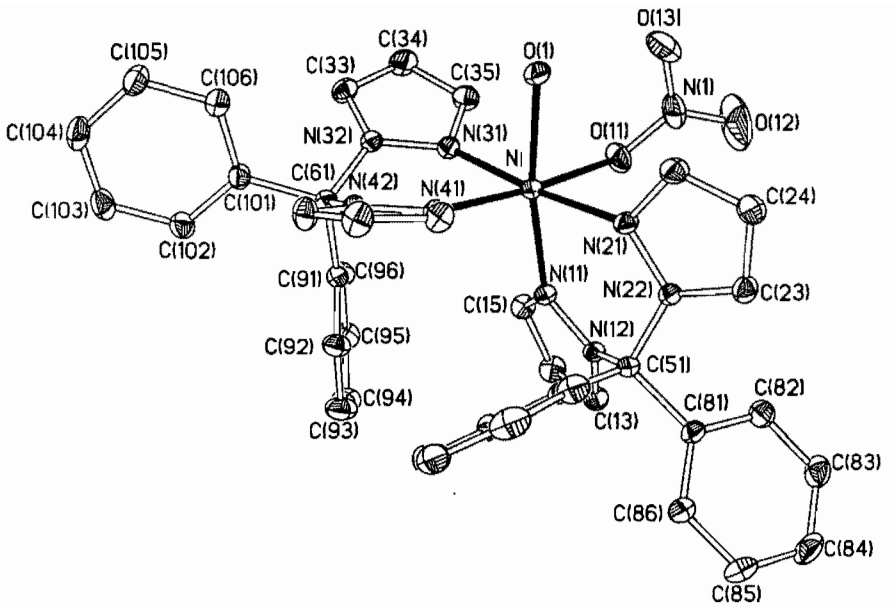

Figure 2. 3. ORTEP view of complex **2.3**. Thermal ellipsoids are shown at 30% probability. The NO_3^- counter ion has been omitted for clarity

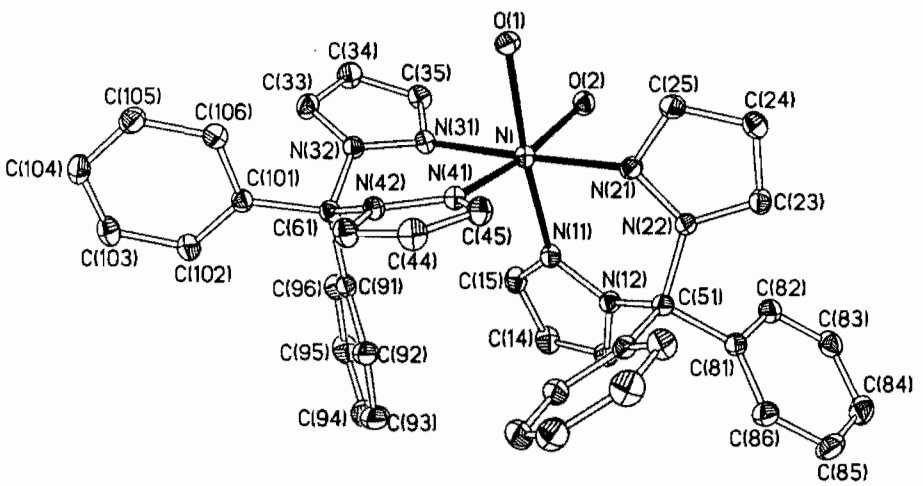

Figure 2.4. ORTEP view of complex **2.4**. Thermal ellipsoids are shown at 30% probability. The NO_3^- counter ions have been omitted for clarity

Table 2.2. Bond distances and angles for complexes **2.1-2.4**

	2.1	**2.2**		**2.3**	**2.4**
Ni-N(11)	2.027(2)	2.0284(16)	Ni-N(11)	2.0630(13)	2.0593(14)
Ni-N(21)	1.994(2)	2.0329(16)	Ni-N(21)	2.0841(14)	2.0806(14)
Ni-O(1)	2.080(2)	2.1293(15)	Ni-N(31)	2.0952(14)	2.0971(13)
Ni-O(2)	2.113(2)	2.1017(14)	Ni-N(41)	2.0567(14)	2.0686(13)
Ni-O(4)	2.081(2)	2.0591(16)	Ni-O(1)	2.0724(12)	2.1273(12)
Ni-O(5)	2.093(2)	-	Ni-X	2.1409(13)	2.0925(11)
Ni-N(3)	-	2.0650(18)	-	-	-
N(11)-Ni-N(21)	89.61(9)	88.81(7)	N(11)-Ni-N(21)	86.81(5)	86.24(5)
N(11)-Ni-O(1)	105.89(9)	103.30(7)	N(11)-Ni-N(31)	96.65(5)	94.68(5)
N(11)-Ni-O(2)	167.40(9)	164.25(7)	N(11)-Ni-N(41)	101.37(5)	99.46(5)
N(11)-Ni-O(4)	97.83(9)	86.80(7)	N(21)-Ni-N(31)	175.00(5)	177.85(5)
N(11)-Ni-O(5)	93.28(9)	-	N(21)-Ni-N(41)	97.31(6)	95.03(5)
N(21)-Ni-O(1)	102.42(9)	94.06(6)	N(31)-Ni-N(41)	85.58(5)	86.74(5)
N(21)-Ni-O(2)	91.91(9)	90.45(6)	N(11)-Ni-O(1)	170.79(5)	173.67(5)
N(21)-Ni-O(4)	97.75(9)	91.00(7)	N(11)-Ni-X	81.83(5)	88.25(5)
N(21)-Ni-O(5)	159.56(9)	-	N(21)-Ni-O(1)	87.66(5)	90.95(5)
O(1)-Ni-O(2)	61.58(9)	61.06(6)	N(21)-Ni-X	87.17(6)	86.91(5)
O(1)-Ni-O(4)	148.73(9)	168.78(6)	N(31)-Ni-O(1)	88.44(5)	87.94(5)
O(1)-Ni-O(5)	96.23(9)	-	N(31)-Ni-X	89.73(6)	91.18(5)
O(2)-Ni-O(4)	94.35(10)	108.95(6)	N(41)-Ni-O(1)	86.63(5)	86.43(5)
O(2)-Ni-O(5)	89.65(9)	-	N(41)-Ni-X	174.59(6)	172.15(5)
O(4)-Ni-O(5)	61.81(8)	-	O(1)-Ni-X	90.55(5)	85.93(5)
N(11)-Ni-N(3)	-	92.92(7)	-	-	-
N(21)-Ni-N(3)	-	178.21(7)	-	-	-
N(3)-Ni-O(1)	-	86.03(7)	-	-	-
N(3)-Ni-O(2)	-	88.03(7)	-	-	-
N(3)-Ni-O(4)	-	88.60(7)	-	-	-

All four complexes adopt variously distorted octahedral structures. The small bite angle of the bidentate nitrate ligands causes the largest distortions from ideal octahedral geometry in complexes **2.1** and **2.2**: *cis*-O-Ni-O angles are ca. 62°, while *trans*-O-Ni-O and *trans*-O-Ni-N angles are ca. 149-167°. Further distortions are introduced by the significantly different Ni-O bond distances in **2.1** (Ni-O1 ~ Ni-O4 < Ni-O5 < Ni-O2) and **2.2** (Ni-O4 < Ni-O2 < Ni-O1). By comparison, the bis(dpdpm) species **2.3** and **2.4** show somewhat less pronounced angular distortions because of the absence of a chelating nitrate

in these complexes and the fact that the two dpdpm ligands in these compounds adopt fairly regular *cis* and *trans* N-Ni-N angles (~86-102° and 175-178°).

Inspection of the Ni-$O_{nitrate}$ distances in the structures of **2.1** and **2.2** supports our previously proposed[10] trans influence orders of pyrazolyl > η^2-O_2NO and η^1-ONO_2 > η^2-O_2NO. For instance, Ni-O1, Ni-O4 < Ni-O2, Ni-O5 in **2.1**, and Ni-O4 < Ni-O1 in **2.2**. In addition, the pyrazolyl ligand also appears to have a somewhat greater trans influence than η^1-NO_3 and water: Ni-N21, Ni-N31> Ni-N11, Ni-N41 in **2.3**; Ni-N21, Ni-N31 > Ni-N11, Ni-N41 in **2.4**. On the other hand, since the difference between Ni-N11 and Ni-N41 in **2.3** is statistically insignificant ($\pm 3\sigma$), we conclude that water and η^1-NO_3 possess very similar trans influences. Finally, inspection of Ni-$N_{pyrazolyl}$ distances in the structure of **2.2** indicates that CH_3CN and η^2-NO_3 possess fairly similar trans influence values. Combining these observations gives the following *trans* influence order: pyrazolyl ~ H_2O ~ η^1-ONO_2 > NCMe ~ η^2-O_2NO.

2.4.3 Magnetic and spectroscopic studies. Magnetic susceptibility measurements using the Gouy method have established that μ_{eff} for complexes **2.1**, **2.3**, and **2.4** are between 3.1 and 3.4 BM, whereas that of complex **2.2** is 3.9 BM. These magnetic susceptibilities are somewhat higher than the corresponding values obtained for our previously reported bis- and tris-(pyrazolyl)methane complexes of nickel (2.8-3.3 BM);[10] nevertheless, all of these values are in the expected range for octahedral Ni(II) complexes,[29] and indicate the presence of two unpaired electrons.

The ^{1}H NMR spectra of these complexes display broad and, for the most part, featureless signals that serve primarily as fingerprints for identifying this family of complexes and provide little structural information. We believe that the broadness of the signals is caused primarily by the paramagnetism of the compounds, but this family of bis(pyrazolyl)alkane ligands can also undergo a dynamic exchange process involving the flip of the M-N-N-C-N-N ring between chair and boat conformations. Moreover, in the NMR spectra of complexes **2.4** and **2.2** the ligand peaks appear to be somewhat broader when the spectra are run in CD_3CN. Since the peak due to residual solvent signal

(CHD_2CN) is also fairly broadened, we suspect that these observations are due to a ligand exchange process whereby solvent molecules displace dpdpm ligand from the coordination sphere of the complexes. It should be added, however, that no dpdpm-free complexes have been obtained in the solid state.

The IR spectra of the complexes show a large number of absorptions. The very strong signals observed at 1491 and 1278 cm^{-1} in the IR spectrum of **2.1** are tentatively attributed to the η^2-NO_3 moiety. For comparison, the corresponding absorptions in the analogous complex $[(bpm^{Me2})_2Ni(\eta^2\text{-}NO_3)][NO_3]$ were found at 1480 and 1290 cm^{-1}.[10,30] The complexes bearing monodentate nitrate ligands give rise to sharp peaks at 1448-1438 and 1384 cm^{-1} (**2.3**) and at 1450-1435 and 1384 (**2.2**). Finally, the nitrate counter anions in **2.4** gave rise to absorptions at 1449-1385 and 1332-1306 cm^{-1}.

The different colours of the complexes under discussion (green for **2.1**, blue for **2.2**, **2.3**, and **2.4**) hinted at energetic differences in the electronic transitions for these d^8 complexes. Although Laporte rules stipulate that d-d transitions are forbidden in perfectly octahedral complexes, the geometrical distortions present in our compounds would be expected to facilitate weak d-d transitions. UV-vis spectroscopy was, therefore, used to delineate the differences in the electronic states of complexes **2.1**-**2.4**. Given the possibility of geometrical changes in solution upon solvent coordination, the UV-vis-NIR spectra were recorded in acetone, CH_2Cl_2, CH_3CN, and MeOH (Figure 2.5 for complex **2.1**, and Figures 2.5a-c in Supporting Information for complexes **2.2**-**2.4**).

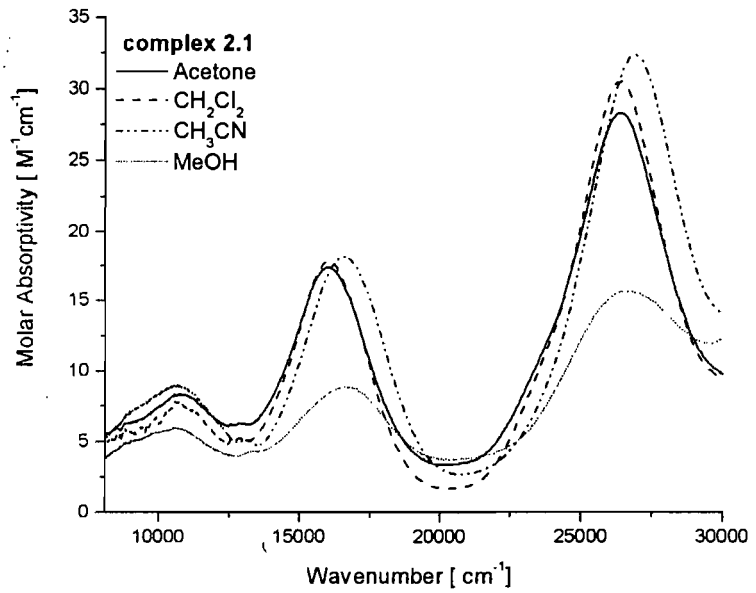

Figure 2.5. The UV-vis-NIR spectra of complex **2.1** in different solvents

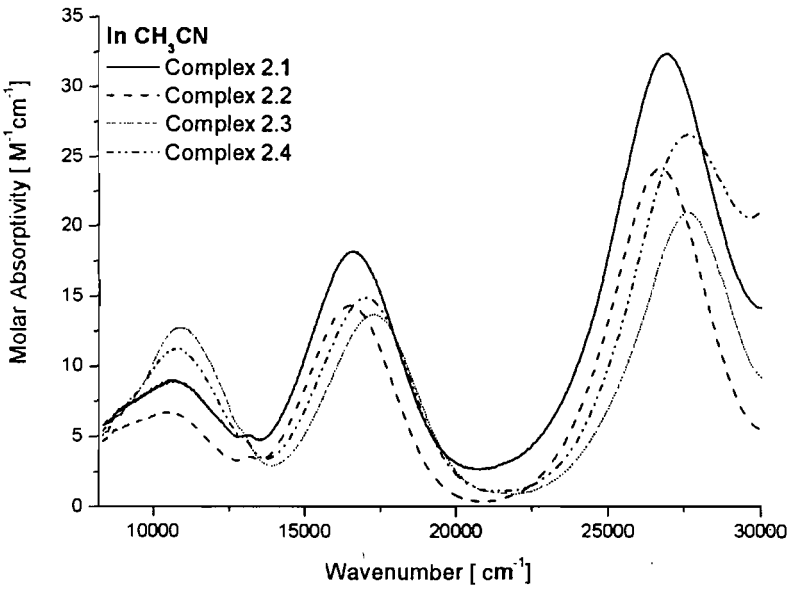

Figure 2.6. The UV-vis-NIR spectra of complexes **2.1**, **2.2**, **2.3** and **2.4** in acetonitrile

As expected for octahedral d^8 complexes,[31] complexes **2.1**-**2.4** displayed three main bands featuring low molar absorptivities at around 1000, 650, and 380 nm; a weak shoulder was also detected at about 700-800 nm in most spectra.[32] Table 2.3 lists the band maxima and molar absorptivities for all four complexes. All bands have been assigned from the Tanabe-Sugano diagram for octahedral complexes, as follows. The three main bands represent spin allowed (d-d) transitions from the ground state $^3A_{2g}$ to the $^3T_{2g}$, $^3T_{1g}(^3F)$, and $^3T_{1g}(^3P)$ excited states commonly observed for essentially octahedral nickel(II) complexes. Weak features due to spin forbidden transitions $^3A_{2g} \rightarrow {}^1Eg$ also occur at energies intermediate between the $^3A_{2g} \rightarrow {}^3T_{2g}$ and $^3A_{2g} \rightarrow {}^3T_{1g}(^3F)$ transitions.[33] The observation of this spin-forbidden transition is thought to be facilitated by the close proximity of $^3A_{2g} \rightarrow {}^3T_{2g}$ and $^3A_{2g} \rightarrow {}^1Eg$ transitions, which leads to a strong mixing through spin-orbit coupling and an increase of the intensity and bandwidth for the spin-forbidden transition.[12]

Qualitative analysis of the electronic spectra for these complexes in different solvents allows us to speculate on possible solvent-Ni interactions. For instance, the transition energies are quite similar in the acetone and CH_2Cl_2 spectra, but fairly different in the MeOH spectra, especially in the case of complexes **2.3** and **2.4** (Figures 2.5b and 2.5c in Supporting Information); these observations hint at possible MeOH-Ni interactions in these complexes. As mentioned earlier, however, no MeOH adducts have been isolated in the solid, implying that the aquo adducts crystallize more readily. Moreover, the similarity of the spectra recorded for acetone and CH_2Cl_2 samples of **2.1** (Figure 2.5) and **2.2** (Figure 2.5a in Supporting Information) suggests that the coordinated CH_3CN in complex **2.2** likely dissociates in these solvents, thus forming **2.1**.

The well-resolved bands for the three main transitions have allowed us to determine the 10Dq value and Racah parameter, B, for each complex based on the following equations:[34]

$$10Dq = E(^3A_{2g} \rightarrow {}^3T_{2g}) = \nu 1 \qquad (1)$$

$$15B = E(^3A_{2g} \rightarrow {}^3T_{1g}(^3F)) + E(^3A_{2g} \rightarrow {}^3T_{1g}(^3P)) - 3Dq = \nu 2 + \nu 3 - 3\nu 1 \qquad (2)$$

Table 2.3. Absorption energies, molar absorptivities and crystal-field parameters for spin-allowed bands of UV-Vis-NIR Spectra for complexes **2.1-2.4** in different solvents*

Complex	Solvent	E (cm^{-1}), ε ($M^{-1}.cm^{-1}$)					
		ν1= 10Dq	Eg	ν2	ν3	B (cm^{-1})	10Dq/B
2.1	Acetone	10784, 8	12946, 6	16043, 17	26395, 28	672	16.0
	CH_2Cl_2	10639, 8	12892, 5	16001, 18	26268, 30	690	15.4
	CH_3CN	10633, 9	13122, 5	16588, 18	26894, 32	772	13.8
	MeOH	10595, 6	13378, 4	16638, 9	26669, 16	767	13.8
2.2	Acetone	10786, 8	12743,6	16315, 12	26650, 18	707	15.2
	CH_2Cl_2	10685, 7	12781, 4	16075, 11	26593, 20	707	15.1
	CH_3CN	10537, 8	13205, 4	16483, 17	26706, 24	772	13.6
	MeOH	10391, 4	13360, 3	16531, 7	26355, 10	781	13.3
2.3	Acetone	10835, 15	12817, 8	16605, 20	26986, 32	739	14.7
	CH_2Cl_2	10820, 13	-	16803, 14	27122, 32	764	14.1
	CH_3CN	10883, 13	13839, 3	17249, 14	27625, 21	815	13.4
	MeOH	10485, 7	12921, 3	16805, 9	26776, 13	808	13.0
2.4	Acetone	10805, 11	13231, 6	16437, 18	26948, 33	731	14.8
	CH_2Cl_2	10779, 9	-	16643, 13	27097, 28	760	14.0
	CH_3CN	10744, 11	13989, 4	16998, 15	27610, 27	824	13.0
	MeOH	10614, 6	13280, 2	16770, 9	27210, 17	809	13.1

* The spectra were recorded at room temperature. 10Dq and B values were calculated from eq. (1) and (2) in the text.

All calculated values for 10Dq and B in various solvents are listed in Table 2.3. The 10Dq parameters (Δ) for **2.1-2.4** are remarkably similar for all four complexes (e.g., 10805-10870 cm^{-1} for spectra of acetone solutions). Interestingly, the largest 10Dq and B values are found in acetone spectra. In order to establish a possible correlation between structural features and crystal field parameters, we have compiled a list of these parameters for a range of octahedral Ni(II) complexes in Table 2.4.

Table 2.4. Crystal-field parameters for **2.1**-**2.4** and related compounds

Compound	N : O	10Dq (cm^{-1})	B (cm^{-1})	10Dq/B	Ref.
$[Ni(H_2O)_6]^{2+}$	0 : 6	8580	929	9.2	[32]
Complex **2.1**	2 : 4	10633	772	13.8	This work
Complex **2.2**	3 : 3	10537	772	13.6	This work
$(tpm^{Me2})Ni(\eta^2\text{-}NO_3)(\eta^1\text{-}NO_3)$	3 : 3	10300	837	12.3	[12]
$[(bpm^{Me2})_2Ni(\eta^2\text{-}NO_3)]^+$	4 : 2	10170	869	11.7	[12]
Complex **2.3**	4 : 2	10883	815	13.4	This work
Complex **2.4**	4 : 2	10744	824	13.0	This work
$[(bpm^{Me2})(tpm^{Me2})Ni(\eta^1\text{-}NO_3)]^+$	5 : 1	10420	891	11.7	[12]
$[Ni(tpm^{Me2})_2]^{2+}$	6 : 0	11670	786	14.8	[12]
$[Ni(pyrazol)_6]^{2+}$	6 : 0	10650	843	12.6	[35]
$[Ni(NH_3)_6]^{2+}$	6 : 0	10730	830	12.9	[32]
$[Ni(o\text{-phenanthroline})_3]^{2+}$	6 : 0	12690	710	17.9	[33]

* All spectra have been recorded for acetonitrile solutions.

Comparisons of this data reveals similarly uniform 10Dq values (within 500 cm^{-1}) for the analogous complexes of Ni bearing bpm^{Me2} and tpm^{Me2} ligands,[12] implying that within a family of closely related compounds the 10Dq value is fairly insensitive to structural variations such as the nature of ligator atoms (N: O ratio), the bonding mode of the nitrate ligand, and the overall charge. Indeed, the only complexes that give rise to significantly different 10Dq values are $[Ni(H_2O)_6]^{2+}$ and $[Ni(o\text{-phenanthroline})_3]^{2+}$. On the other hand, greater variations are observed in the 10Dq/B ratios for all the complexes (Table 2.4). Thus, the values of ca. 13-16 for complexes **2.1**-**2.4** are intermediate between the corresponding values reported for the homoleptic dicationic complexes $[NiL_6]^{2+}$ bearing strong-field ligands such as *o*-phenanthroline (17.9)[33] and weak-field ligands such as water (9.2).[36] Nevertheless, there appears to be no simple correlation between the 10Dq/B ratio and the structural parameters.

2.4.4 Solvato-, vapo-, and thermochromic properties of complexes 2.1 and 2.2. As mentioned earlier, dissolving **2.1** (green) in CH_3CN gave a blue species that was identified as the CH_3CN adduct **2.2** arising from the $\eta^2 \rightarrow \eta^1$ hapticity change of a nitrate ligand. A series of experiments established that the interconversion of **2.1** and **2.2** is reversible

(Scheme 2.2). Thus, evaporation of blue solutions obtained by dissolving **2.1** in CH_3CN gave back green samples of **2.1**, which produced blue solutions when redissolved in CH_3CN.

Scheme 2.2

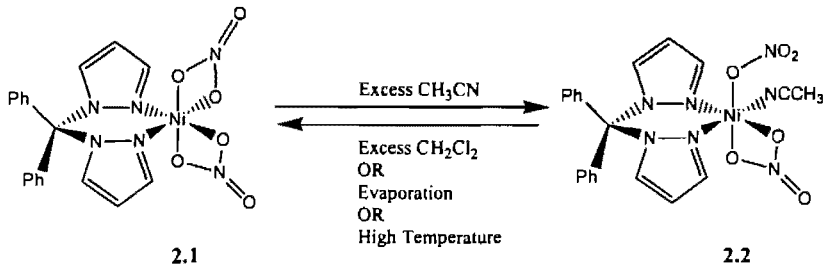

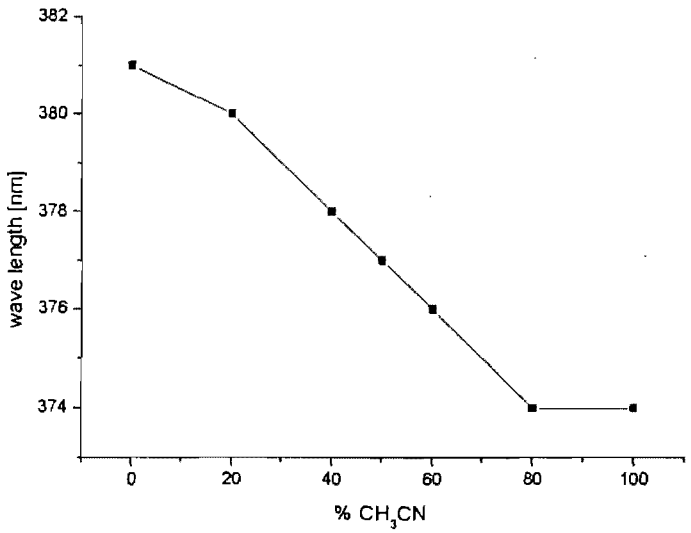

Figure 2.7. Shift in the absorption wavelength of the high-energy band in the UV-visible spectra of **2.1** as a function of solvent composition (CH_2Cl_2:CH_3CN)

This process could be repeated several times. UV-vis spectroscopy showed that the presence of greater proportions of CH_3CN in CH_2Cl_2 solutions of **2.1** resulted in an incremental blue-shift in the high-energy band maximum, from ca. 381 nm for **2.1** (100% CH_2Cl_2) to ca. 374 nm for **2.2** (80% CH_3CN), as shown in Figure 2.7. Similar green-to-blue colour changes were noted in CH_2Cl_2/MeOH and acetone/water mixtures, but the new

species arising from the interaction of MeOH and water with the Ni center in **2.1** have not been identified.

The temperature-dependence of the CH_3CN-induced $\eta^2 \rightarrow \eta^1$ hapticity change of one of the nitrate ligands in **2.1** was studied briefly, as follows. The blue solution obtained by dissolving a sample of **2.1** in CH_3CN was heated gradually to ca. 80 °C and its color was monitored. A gradual, blue-to-green color change was observed up to ca. 65 °C, at which point the green color was dominant. Further heating to ca. 80 °C resulted only deepened the green color, whereas allowing the solution to cool to room temperature re-established the original blue colour. Repeating this heating/cooling cycle 10 times showed that the heat-induced interconversion of **2.1** and **2.2** was reversible. On the other hand, variable temperature UV-Vis spectra of a CH_3CN solution of **2.1** confirmed that complexes **2.1** and **2.2** are in equilibrium, the major species being complex **2.2** below 0 °C (band maximum for ν_3 at 372 nm) and complex **2.1** above 70 °C (band maximum for ν_3 at 378 nm).

The observation that this CH_3CN-induced $\eta^2 \rightarrow \eta^1$ slippage of one of the nitrate ligands in **2.1** can take place in solutions raised the question of whether or not this process might take place by exposure of solid samples to CH_3CN vapor. Tests showed that green samples of **2.1** turned blue when exposed to CH_3CN vapour, while the resulting blue solid (or independently prepared samples of **2.2**) turned green when heated briefly (1-2 min at ca. 100 °C) or placed under vacuum. This reversible interconversion of **2.1** and **2.2** took place over several cycles without degradation.

2.5 Conclusion

The preparation and characterization of complexes **2.1**-**2.4** has allowed us to study the structural and spectroscopic properties of a new series of Ni(II) complexes bearing the dpdpm ligand. The solid state structures of these complexes are fairly similar to those of the analogous bpm^{Me2} complexes reported earlier,[10] implying that the different sterics of these two ligands have little or no influence over the structures adopted by their complexes. These closely related complexes also display fairly comparable UV-Vis-NIR spectra,

implying that the electronic structures of this family of complexes are not very sensitive to subtle structural differences.

The most intriguing aspect of the present study is the solvato-, thermo-, and vapochromism of complex **2.1**, which is caused by the reversible coordination of acetonitrile to the Ni center in **2.1** and the resulting conversion of one of the η^2-NO_3 to η^1-NO_3. That the formation of complex **2.1** is favoured at higher temperature is presumably due to entropic factors that tend to favour the chelation of the nitrate ligand and the dissociation of a molecule of acetonitrile. Future investigations will probe the vapo- and thermochromic properties of thin films produced from polymer matrices containing complex **2.1**.

Supporting Information

UV-Vis spectra of complexes **2.2**-**2.4** in different solvents (Figures 2.5a-c). This material is available free of charge via the Internet at http://pubs.acs.org. Crystallographic data for the structural analysis have been deposited with the Cambridge Crystallographic Data Centre, CCDC No. 614549 (**2.1**), 614551 (**2.2**), 614552 (**2.3**), 614550 (**2.4**). Copies of this information may be obtained free of charge from The Director, CCDC, 12 Union Road, Cambridge, CB2 1EZ, UK (fax: +44-1223-336-033; email: deposit@ccdc.cam.ac.uk or www: http://www.ccdc.cam.ac.uk).

Acknowledgments. The Natural Sciences and Engineering Research Council of Canada and Fonds Québécois de la Recherche sur la Nature et les Technologies are gratefully acknowledged for their financial support. We are grateful to Profs. G. Hanan and C. Reber and their research groups for their valuable help with the UV-Vis-NIR spectra.

2.6 References

(1) (a) Trofimenko, S. *J. Am. Chem.* Soc. **1966**, *88*, 1842-1844. (b) Trofimenko, S. *J. Am. Chem.* Soc. **1967**, *89*, 3170. (c) Trofimenko, S. *J. Am. Chem.* Soc. **1967**, *89*, 6288. (d) Trofimenko, S. *J. Am. Chem.* Soc. **1969**, *91*, 588. (e) Trofimenko, S. *J. Am. Chem.* Soc. **1970**, *92*, 5118.

(2) Trofimenko, S. *J. Am. Chem.* Soc. **1970**, *92*, 1499.

(3) For a few recent reviews on the development of the coordination chemistry of scorpionate ligands see: (a) Reger, D. L. *Com. Inorg. Chem.* **1999**, *21*, 1. (b) Sadimenko, A. P. *Adv. Hetero. Chem.* **2001**, *81*, 167. (c) Trofimenko, S. *Chem. Rev.* **1993**, *93*, 943. (d) Trofimenko, S. *Polyhedron* **2004**, *23*, 197. (e) Otero, A; Fernandez-Baeza, J.; Antinolo, A.; Tejeda, J.; Lara-Sanchez, A. *Dalton Trans.* **2004,** 1499. (f) Pettinari, C.; Pettinari, R. *Coord. Chem. Rev.* **2005,** *249*, 525. (g) *ibid.* 663.(h) Bigmore, H. R.; Lawrence, S. C.; Mountford, P.; Tredget, C. S. *Dalton Trans.* **2005**, 635.

(4) Byers, P. K.; Canty, A. J.; Honeyman, R. T. *Adv. Organomet. Chem.* **1992**, *34*, 1. (See in particular pp. 26 and 34.)

(5) Canty, A. J.; Andrew, S.; Skelton, B. W.; Traill, P. R.; White, A. H. *Organometallics* **1995**, *14*, 199.

(6) Reinartz, S.; Brookhart, M.; Templeton, J. L. *Organometallics* **2002**, *21*, 247.

(7) Byers, P. K.; Canty, A. J.; Skelton, B. W.; White, A. H. *Organometallics* **1990**, *9*, 826.

(8) For recent reports on organometallic complexes of Pd based on poly(pyrazolyl)alkane ligands see: (a) Sanchez, G.; Serrano, L. J.; Pérez, J.; Ramirez de Arellano, M. C.; Lopez, G.; Molins, E. *Inorg. Chem. Acta* **1999,** *295*, 136. (b) Arroyo, N.; Gomez-de La Tore, F.; Jalon, A. F.; Manzano, B. R.; Moreno-Lara. B.; Rodriguez., A. M. *J. Organomet. Chem.* **2000,** *603*, 174. (c) Tsuji, S.; Swenson, D. C.; Jordan, R. F. *Organomet.* **1999**, *18*, 4758.

(9) For representative reports on coordination complexes of Ni featuring poly(pyrazolyl)alkane ligands see: (a) Mahon, M. F.; McGinley, J.; Molloy, K. C.; *Inorg. Chim. Acta* **2003**, *355*, 368. (b) Wolfgang, K.; Berghahn, M.; Frank, W.; Reiss, G. J.; Schonherr, T.; Rheinwald, G.; Lang, H. *Eur. J. Inorg. Chem.* **2003,** *11*, 2059. (c) Pettinari, C.; Marchetti, F.; Cingolani, A.; Leonesi, D.; Colapietro, M.; Margadonna, S. *Polyhedron*

1998, *17*, 4145. (d) Mann, K. L.; Jeffery, J. C.; McCleverty, J. A.; Thornton, P.; Ward, M. D. *J. Chem. Soc., Dalton Trans.* **1998**, *1*, 89. (e) Pettinari, C.; Cingolani, A.; Bovio, B. *Polyhedron* **1996**, *15*, 115. (f) Astley, T.; Gulbis, J. M.; Hitchman M. A.; Tiekink, E. R. T. *J. Chem. Soc., Dalton Trans.* **1993**, 509. (g) Mesubi, M. A.; Omotowa, B. A. *Synth. React. Inorg. Metl-Org. Chem.* **1993,** *23*, 213. (h) Astley, T.; Canty, A. J.; Hitchman, M. A.; Rowbottom, G. L.; Skelton, B. W.; White, A. H. *J. Chem. Soc., Dalton Trans.* **1991**, 1981. (i) Reedijk, J.; Verbiest, J. *Trans. Met. Chem.* **1979**, *4*, 239. (j) Jansen, J.C.; Van Koningsveld, H.; Van Ooijen, J. A. C.; Reedijk, J. *Inorg. Chem.* **1980**, *19*, 170. (k) Reedijk, J.; Verbiest, J.; *Trans. Met. Chem.* **1978**, *3*, 51.

(10) Michaud, A.; Fontaine, F.-G.; Zargarian, D. *Inorg. Chim. Acta* **2006**, *359*, 2592.

(11) (a) Michaud, A.; Fontaine, F.-G.; Zargarian, D. *Acta Cryst.* **2005**, E *61*, m784. (b) Michaud, A.; Fontaine, F.-G.; Zargarian, D. *Acta Cryst.* **2005**, E *61*, m904.

(12) Nolet, M.-C.; Michaud, A.; Bain, C.; Zargarian, D.; Reber, C. *Photochem. Photobiology* **2006**, *82*, 57.

(13) Bloomquist, D. R.; Willet, R. D. *Coord. Chem. Rev.* **1982**, *47*, 125.

(14) Fabbrizzi, L.; Micheloni, M.; Paoletti, P. *Inorg. Chem.* **1974**, *13*, 3019.

(15) (a) Fukuda, Y.; Cho, M.; Sone, K. *Bull. Chem. Soc. Jpn* **1989**, *62*, 51. (b) Bourdin, D.; Lavabre, D.; Beteille, J.P.; Levy, G.; Micheau, J. *Bull. Chem. Soc. Jpn* **1990**, *63*, 2985. (c) Linert, W.; Gutmann, V. *Coord. Chem. Rev.* **1992**, *117*, 159. (d) Linert, W.; Fukuda, Y.; Camard, A. *Coord. Chem. Rev.* **2001**, *218*, 113. e) Berger, S. *Zeitschrift Phys. Chemie* **2002**, *216*, 1363.

(16) Wadas, T. J.; Wang, Q. M.; Kim, Y. J.; Fraschenreim, C.; Blanton, T. N.; Eisenberg, T. *J. Am. Chem. Soc.* **2004**, *126*, 16841.

(17) Lefebvre, J.; Batchelor, R. J.; Leznoff, D. B. *J. Am. Chem. Soc.* **2004**, *126*, 16117.

(18) Flamini, a.; Mattei, G.; Panusa, A. *J. Incl. Phenom.* **2004**, *33*, 377.

(19) Recent reports have described a number of dpdpm complexes of copper (a) and silver (b): (a) Shaw, L.J.; Cardon, T. B.; Lorigan, G. A.; Ziegler, C. J.; *Eur. J. Inorg. Chem.* **2004**, 1073. (b) Reger, L. D.; Gardinier, J. R.; Smith, M.D. *Inorg. Chem.* **2004**, *43*, 3825.

(20) (a) Ahmed, F. R.; Hall, S. R.; Pippy, M. E.; Huber, C. P. NRC Crystallographic Computer Programs for the IBM/360. Accession Nos. 133-147 in *J. Appl. Cryst.* **1973**, *6*, 309. (b) Bruker (1997). SHELXTL (1997). Release 5.10; The Complete Software Package for Single Crystal Structure Determination. Bruker AXS Inc., Madison, USA. (c) Enraf-Nonius (1989). CAD-4 Software. Version 5. Enraf-Nonius, Delft, The Netherlands. (d) LePage, Y. *J. Appl. Cryst.* **1987**, *20*, 264-269. (e) Nonius (1998). Collect Software, Nonius B.V., Delft, The Netherlands. (f) Sheldrick, G. M. (1986). SHELXS86. Program for Crystal Structure solution. University of Gottingen, Germany.(j) Sheldrick, G. M. (1997a). SHELXS97. Program for Crystal Structure solution. University of Gottingen, Germany. (h) Sheldrick, G. M. (1997b). SHELXL97. Program for crystal structure refinement. University of Gottingen, Germany. (g) Spek, A. L. (2000). PLATON, 2000 version; Molecular Geometry Program, University of Utrecht, Utrecht, Holland. (h) Gabe, E. J.; Le Page, Y.; Charlant, J. P.; Lee, F. L.; White, P. S. *J. Appl. Cryst.* **1989**, *22*, 384.

(21) SMART, (**2001**) Release 5.059; Bruker Molecular Analysis Research Tool; Bruker AXS Inc.: Madison, WI 53719-1173.

(22) SAINT, (**2003**) Release 6.06; Integration Software for Single Crystal Data; Bruker AXS Inc.: Madison, WI 53719-1173.

(23) Sheldrick, G. M. SHELXS, Program for the Solution of Crystal Structures; University of Goettingen: Germany, **1997**.

(24) (a) Bruker (1997). SHELXTL (1997). Release 5.10; The Complete Software Package for Single Crystal Structure Determination. Bruker AXS Inc., Madison, USA. (b) Bruker (1999a). SAINT (2003). Release 7.06. Integration Software for Single Crystal Data. Bruker AXS Inc., Madison, USA. (c) Bruker (1999b). SMART (2001) Release 5.625; Bruker Molecular Analysis Research Tool, Bruker AXS Inc., Madison, USA. (d) Sheldrick, G. M. (1996). SADABS, Bruker Area Detector Absorption Corrections. (e) Bruker AXS Inc., Madison, USA. f) Sheldrick, G. M. (1997a). SHELXS97. Program for Crystal Structure solution. University of Gottingen, Germany. (f) Sheldrick, G. M. (1997b). SHELXL97. Program for crystal structure refinement. University of Gottingen, Germany. (g) Spek, A.

L. (2000). PLATON, 2000 version; Molecular Geometry Program, University of Utrecht, Utrecht, Holland.

(25) (a) Głowiak, T.; Kurdziel, K. *J. Mol. Struct.* **2000**, *516*, 1. (b) Carr, P.; Piggott, B.; Tinton, H.J. *Acta Cryst., Sect. C: Cryst. Struct. Commun.* **1985**, *41*, 372. (c) Turpeinen, E. *Suom. Kemistil. B.* **1973**, *46*, 208. (d) Diamantopopoulou, E.; Zafiropoulos, T. F.; Perplepes, S. P.; Raptopoulou, C. P. Terzis. A. *Polyhedron* **1994**, *13*, 1593. (e) Claramunt, R. M; Domiano, P.; Elguero, J.; Lavandera, J. L. *Bull. Soc. Chim. Fr.* **1989**, 472.

(26) Two structurally related mono(η^2-NO_3) compounds have been reported recently: $[(bpm^{Me2})_2Ni(\eta^2\text{-}NO_3)][NO_3]$ (ref. 10) and $[(pz_2thCH)_2Ni(\eta^2\text{-}NO_3)][NO_3]$ (pz_2thCH= bis(pyrazolyl)(2-thienyl)methane; Astley, T.; Hitchman, M.A.; Skelton,W. B.; White, A. H. *Aust. J. Chem.* **1997**, *50*, 145.)

(27) The preparation and full characterization of this compound and related species arising from the reaction of nickel halides will be the subject of an upcoming report.

(28) Burnett, M. N.; Johnson, C. K. (**1996**). ORTEPIII - Oak Ridge Thermal Ellipsoid Plot Program for Crystal Structure Illustrations, Technical Report ORNL-6895. Oak Ridge National Laboratory, Tennessee, USA.

(29) Collinson, S. R.; Schröder, M. "Nickel: Inorganic & Coordination Chemistry", in *Encyclopedia of Inorganic Chemistry*; **2006**, Wiley InterScience, 2-nd edition, King, R. B. (Ed.), vol. VI.

(30) For a general discussion of NO_3 stretching frequencies see: Nakamoto, K. *Raman Spectra of Inorganic and Coordination Compounds. Part B: Applications in Coordination, Organometallic and Bioinorganic Chemistry*; Wiley, 5-th edition (1997), Ch. 8, pp. 87-88.

(31) Sacconi, L.; Mani, F.; Bencini, A. "Nickel" in *Comprehensive Coordination Chemistry*, Wilkinson, G.; Gilard, R.; McCleverty, J. (Editors) **1987** (Pergamon Press, Oxford), Vol. *5*, p. 58.

(32) Very similar "weak shoulders" have been observed in the absorption spectra of $[Ni(NH_3)_6]^{2+}$. For a discussion see: Triest, M.; Bussière, G.; Bélisle, H.; Reber, C. *J. Chem. Educ.* **2000**, *77*, 670. Available at:
http://jchemed.chem.wisc.edu/jcewww/articles/JCENi/ JCENi.html

(33) For a description of this phenomenon, including detailed analyses of these transitions based on Tanabe-Sugano diagrams and modern theoretical models, see : M.-C. Nolet, R. Beaulac, A.-M. Boulanger, C. Reber, *Struc. Bond.* **2004**, *107*, 145.

(34) (a) Reedijk, J.; Van Leeuwen, P. W. N. M., Groeneveld, W. L. *Recl. Trav. Chim. Pays-Bas* **1968**, *87*, 129. (b) König, E. *Struct. Bonding* **1971**, *9*, 175.

(35) Reimann, C. W. *J. Phys. Chem.* **1970**, *74*, 561.

(36) Bussière, G.; Reber, C. *J. Am. Chem. Soc.* **1998**, *120*, 6306.

2.7. Supporting Information

for

New Complexes Arising From The Reaction of Nickel (II) Nitrate With Diphenyl(dipyrazolyl)methane: Syntheses, Structures, and Spectroscopy

Natalie Baho and Davit Zargarian*

Département de chimie, Université de Montréal,

Montréal, Québec, Canada H3C 3J7

Contents:

- Figure 2.5a: The UV-Vis-NIR spectra of complex **2.2** in different solvents.
- Figure 2.5b: The UV-Vis-NIR spectra of complex **2.3** in different solvents.
- Figure 2.5c: The UV-Vis-NIR spectra of complex **2.4** in different solvents.

- **Figure 2.5a.** The UV-Vis-NIR spectra of complex **2.2** in different solvents

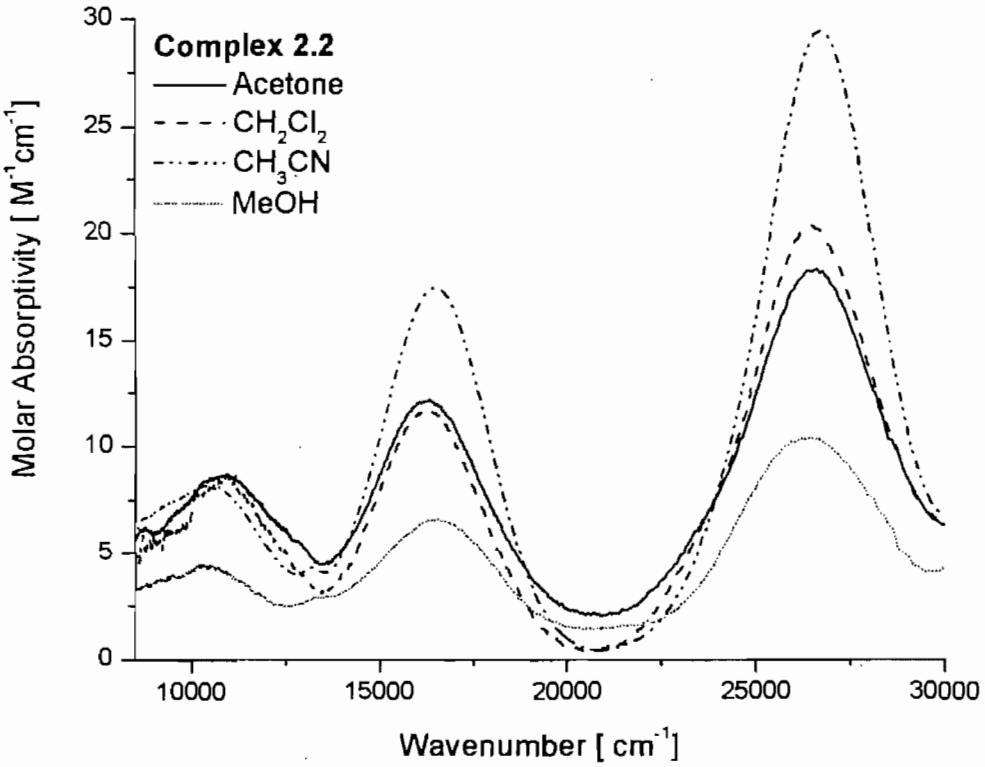

Figure 2.5b. The UV-Vis-NIR spectra of complex **2.3** in different solvents

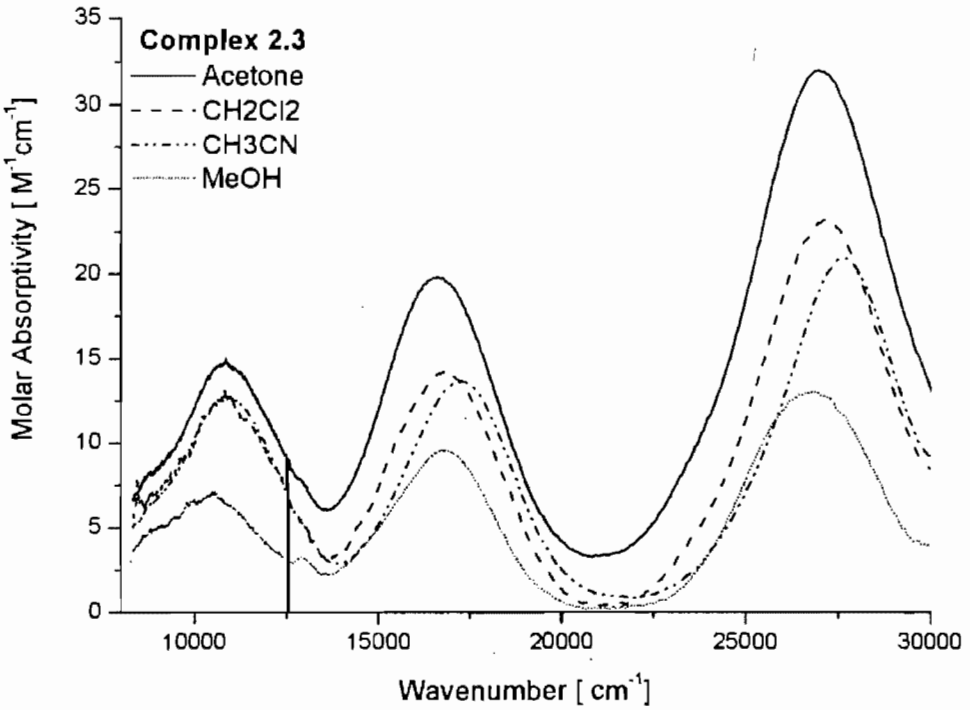

Figure 2.5c. The UV-Vis-NIR spectra of complex **2.4** in different solvents

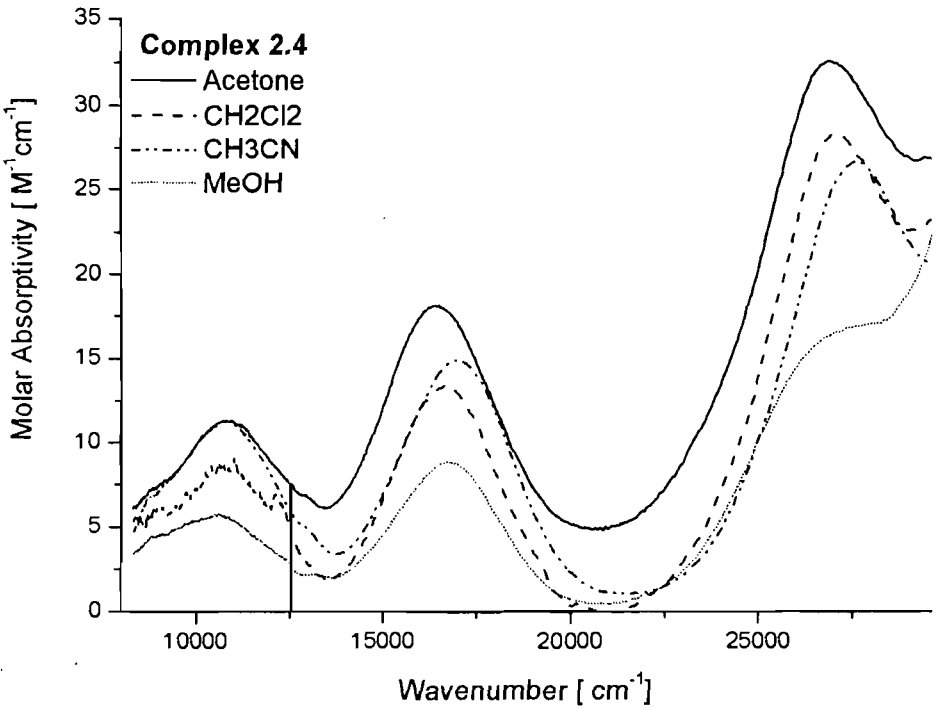

Chapter 3: Diphenyl(dipyrazolyl)methane Complexes of Ni: Syntheses, Structural Characterization, and Chromotropism of New $NiBr_2$ Derivatives

Article 2

Diphenyl(dipyrazolyl)methane Complexes of Ni: Syntheses, Structural Characterization, and Chromotropism of New $NiBr_2$ Derivatives

Natalie Baho and Davit Zargarian*

Département de chimie, Université de Montréal,

Montréal, Québec, Canada H3C 3J7

Inorg. Chem. **2007**, *46*, 7621

3. 1 Abstract

The reaction of $NiBr_2$ with the bidentate ligand diphenyl(dipyrazolyl)methane (dpdpm) gives the penta-coordinated complexes $[(dpdpm)Ni(\mu\text{-}Br)Br]_2$ (**3.1**), $[(dpdpm)NiBr_2(H_2O)]$ (**3.2a**), and $[(dpdpm)NiBr(H_2O)_2]Br$ (**3.2b**), or the octahedral complexes $[(dpdpm)NiBr(H_2O)_2(CH_3CN)]Br$ (**3.3**), $[(dpdpm)_2NiBr_2]$ (**3.4**), and $[(dpdpm)_2NiBr(H_2O)]Br$ (**3.5**). All of these complexes are paramagnetic, both in the solid state and in solution, and have been characterized by spectroscopic (IR, NMR, and UV-vis-NIR) and X-ray diffraction studies. The unoccupied coordination site in the penta-coordinated compounds allows long-range interactions, in the solid state, between the Ni center and a Ph substituent of the dpdpm ligand. These weak interactions are replaced by Ni-solvent interactions, both in the solid state and in solution, facilitating the interconversion of these compounds under various reaction conditions and leading to interesting solvato-, vapo-, and thermochromic properties. UV-vis-NIR spectroscopy has been used to study these phenomena. Absorption spectra for the room temperature methanol or acetonitrile solutions of the penta-coordinate or octahedral compounds show three main bands in the region of 350-1000 nm that represent spin allowed (d-d) transitions from the ground state $^3A_{2g}$ to the excited states $^3T_{2g}$, $^3T_{1g}(^3F)$, and $^3T_{1g}(^3P)$. A weak shoulder was also detected on the middle peak in most spectra (700-800 nm), representing the spin-forbidden $^3A_{2g} \rightarrow {}^1E_g$ transition. On the other hand, the spectra of high temperature CH_2Cl_2 or acetone solutions of all complexes show four main bands at ca. 490, 650-660, 860, and 1000 nm, in addition to a shoulder on the first or second band.

3.2 Introduction

Scorpionate-type poly(pyrazolyl)borate[1] and poly(pyrazolyl)alkane[2] ligands have found wide applications in coordination, organometallic, and bioinorganic chemistry.[3] The increasing interest in these ligands is due to their generally robust nature and the ease with which their steric and electronic properties can be modified via simple synthetic protocols, thereby allowing a fine-tuning of ligand properties.[4] The anionic bis- or tris(pyrazolyl)borates have been used in the preparation of a wide range of coordination and organometallic complexes, including species featuring metals in their less common oxidation states such as Pd(IV)[5,6] and Pt(IV).[5,7] In contrast, the neutral bis- and tris(pyrazolyl)alkanes appear to be less suitable for the preparation of complexes featuring strong-field co-ligands such as hydride, alkyls, aryls, etc.[8] As a result,

poly(pyrazolyl)alkanes have had less impact in organometallic chemistry, particularly in the case of late transition metals of the first row such as nickel for which no organometallic complex has been reported.[9,10]

Our interest in the chemistry of organonickel complexes[11] has prompted us to explore the structures and reactivities of nickel complexes based on poly(pyrazolyl)alkanes. Our initial studies focused on the reactions of $Ni(NO_3)_2$ with the ligands bis- and tris(3,5-dimethylpyrazolyl)methane (bpm^{Me2} and tpm^{Me2}),[12] bis(pyrazolyl)propane (bpp),[13] and diphenyl(dipyrazolyl)methane (dpdpm).[14] The complexes arising from these reactions are octahedral species featuring mono- and/or bidentate nitrate ligands. Our results to date show that these compounds cannot serve as suitable precursors for the preparation of organometallic species, but many of them exhibit interesting solvato-, vapo-, and thermochromic properties owing to the labile coordination of the nitrate ligand.[14] Indeed, literature reports show that several nickel complexes featuring polydentate amine or imine-type ligands display solvato- and thermochromic behavior arising from displacement of labile ligands by solvent molecules or counterions. In the case of coordination complexes, solvatochromism refers to changes in the electronic absorption spectra due to weak dipole interactions or hydrogen bonds with solvent molecules, or a strong and specific interaction between the solvent and the metal center.[15] Solvato- and thermochromism can also involve various types of structural isomerism such as monomer-dimer equilibria, some examples of which have been reported for $[Ni(L\text{-}L)Cl_2]_2$ wherein L-L is a bidentate, N-based ligand.[16]

As a continuation of our earlier studies,[12,13,14] we are investigating the structures and chromotropic properties of complexes arising from the reactions of other Nickel(II) salts with poly(pyrazolyl)alkane ligands. The present report describes the synthesis, structural characterization, and solvato-, vapo-, and thermochromic behavior of the $NiBr_2$ derivatives of dpdpm, namely: $[(dpdpm)Ni(\mu\text{-}Br)Br]_2$ (**3.1**), $[(dpdpm)NiBr_2(H_2O)]$ (**3.2a**), $[(dpdpm)NiBr(H_2O)_2]Br$ (**3.2b**), $[(dpdpm)NiBr(H_2O)_2(CH_3CN)]Br$ (**3.3**), $[(dpdpm)_2NiBr_2]$ (**3.4**), and $[(dpdpm)_2NiBr(H_2O)]Br$ (**3.5**). Complexes featuring the dpdpm ligand have been reported for Cu,[17] Mo,[18] Ag,[19] and Pd.[10c]

3.3 Results and Discussion

3.3.1 Synthesis of the complexes. The outcome of the reaction between $NiBr_2$ and dpdpm depends on a few parameters, including the metal:ligand ratio, the reaction temperature, the coordinating ability of the solvent, and the degree of residual moisture present in the reaction medium. Thus, refluxing a 1:1 mixture of $NiBr_2$ and dpdpm in dried and distilled acetone for 18 h gave a brown suspension, which was filtered to give a brown solid identified as the dimeric species **3.1** (crude yield 79%, Scheme 3.1).

Scheme 3.1

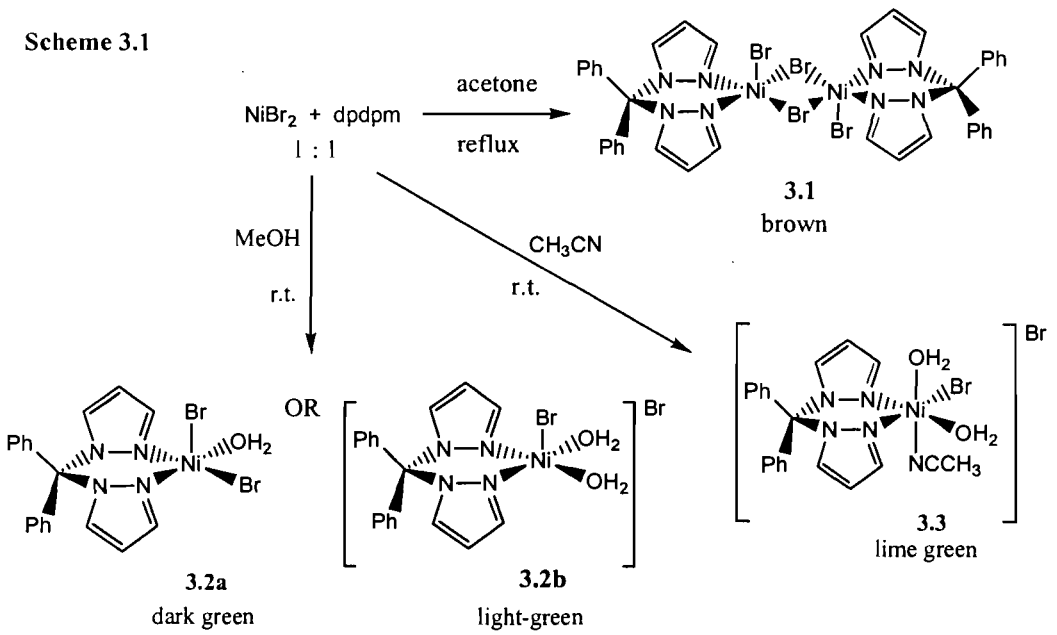

In contrast, carrying out the reaction in untreated MeOH at room temperature gave a dark green solid (crude yield 83%) that provided, after recrystallization from acetone/Et_2O, dark green crystals identified as the monomeric, mono(aquo) compound **3.2a**. Interestingly, recrystallizing the dark green solid from acetone/hexane gave light green crystals identified as the cationic bis(aquo) species **3.2b**. Finally, overnight stirring of a 1:1 mixture of $NiBr_2$ and dpdpm in acetonitrile at room temperature gave a dark green solution; removal of the solvent produced a dark green powder (crude yield 85%), which was recrystallized from acetonitrile/Et_2O to give lime green crystals of the octahedral species **3.3**.

Scheme 3.2

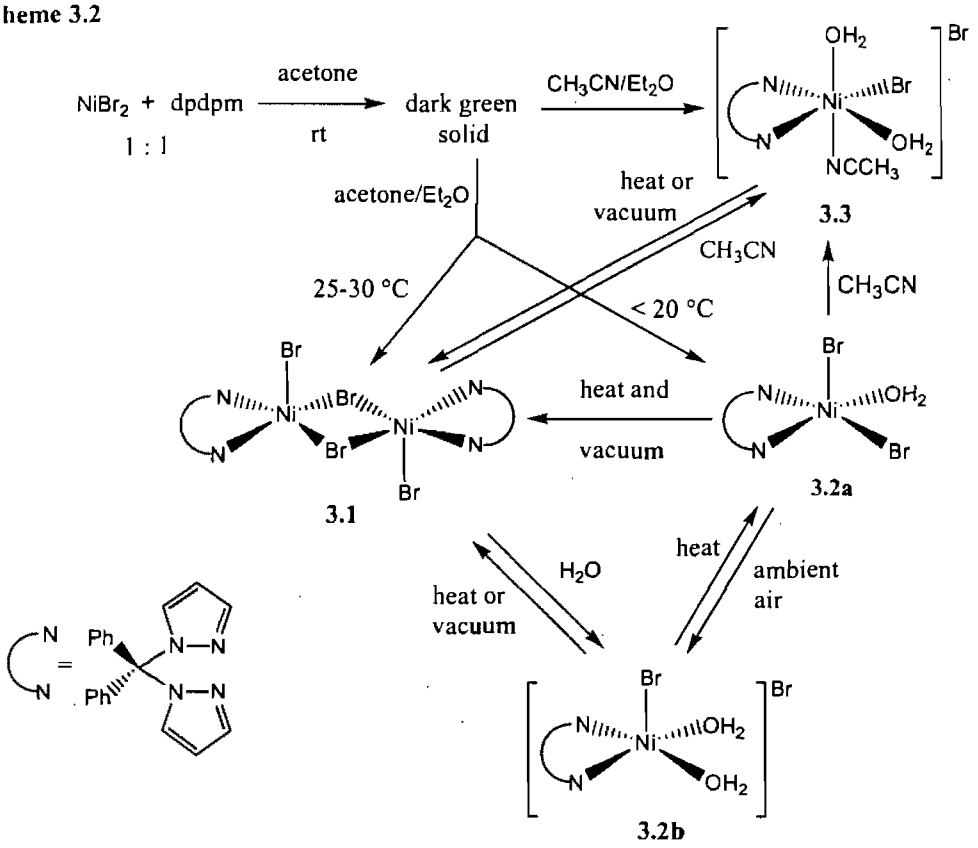

It is noteworthy that, under appropriate recrystallization conditions, all of the new products mentioned above can be derived from a common species obtained from the 1:1 reaction of $NiBr_2$ and dpdpm in acetone at room temperature, as shown in Scheme 2. Thus, allowing Et_2O vapors to diffuse into concentrated acetone solutions of the dark green solid at 25-30 °C and with minimum exposure to humid air gave brown crystals that were identified by X-ray diffraction studies as **3.1**. Alternatively, recrystallization from acetone/Et_2O solutions at lower temperatures (< 20 °C) resulted in the formation of dark green crystals that were identified by X-ray diffraction studies as the mono(aquo) compound **3.2a**. Recrystallization attempts at around 0 °C gave blue crystals, presumably an octahedral bis(aquo) adduct, but we were unable to characterize this compound because of the poor quality of the crystals obtained. Finally, recrystallization of the dark green solid from acetonitrile gave lime green crystals that were identified as **3.3**.

These mono(dpdpm) derivatives can also interconvert under various experimental conditions (Scheme 3.2). For instance, allowing brown crystals of **3.1** to stand overnight in the (green) mother liquor, unprotected from ambient atmosphere, turned them into light green crystals that were identified as **3.2b**. The latter compound was also obtained by

allowing the mono(aquo) species **3.2a** to stand in ambient atmosphere for two days or more, while dissolving **3.2a** in CH_3CN gave the octahedral species **3.3**. On the other hand, heating solid samples of **3.2b** or **3.3** to ca. 100 °C, or placing them under reduced pressure, converts these compounds to **3.1**. In the case of **3.2a**, both heating and reduced pressure were needed to convert this compound to **3.1**. As will be mentioned later, the interconversion of complexes **3.1**, **3.2a**, and **3.2b** can be affected by controlling the temperature of their acetone solutions, whereas dissolving complex **3.1** in CH_3CN generates complex **3.3** (*vide infra*).

Scheme 3

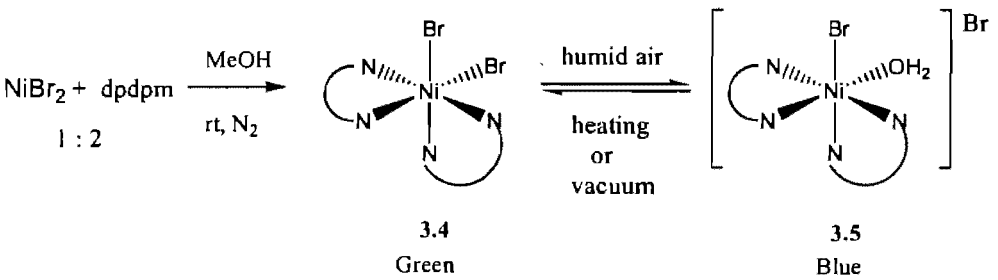

3.4 Green

3.5 Blue

Formation of the penta-coordinated compounds **3.1**, **3.2a**, and **3.2b** from the 1:1 reactions with $NiBr_2$ is in contrast to the exclusive formation of octahedral products from the 1:1 reactions of $Ni(NO_3)_2$ with dpdpm (*cf.* (dpdpm)Ni(η^2-NO_3)$_2$, (dpdpm)Ni(η^2-NO_3)(η^1-NO_3)(NCMe).[14] Using a 2:1 dpdpm : $NiBr_2$ ratio gave only octahedral species. Thus, stirring a methanol mixture of $NiBr_2$ and 2 equivalents of dpdpm, at room temperature and under nitrogen, produced a green mixture that was filtered and evaporated to give a green solid; recrystallization of this solid from CH_2Cl_2/Et_2O under a nitrogen atmosphere gave green crystals that were identified by X-ray diffraction studies as the complex **3.4** (Scheme 3). When complex **3.4** was exposed to humidity, both in the solid state and in solution, it hydrolyzed readily to its mono(aquo) derivative, the blue complex **3.5**. Moreover, heating solutions or solid samples of **3.5**, or placing them under vacuum, gave back the dibromo species **3.4**. Longer exposures of **3.4** to ambient humidity produced another blue compound that was insoluble and has not been identified.

3.3.2 Solid state structures. Suitable crystals of **3.1**, **3.2a**, **3.2b**, **3.3**, **3.4**, and **3.5** for X-ray diffraction studies were obtained by vapour diffusion of Et_2O or hexane into solutions of these complexes in acetone (**3.1**, **3.2a**, and **3.2b**), acetonitrile (**3.3**), and dichloromethane (**3.4** and **3.5**). All six sets of diffraction data resulted in fairly accurate structures for the complexes studied, as reflected in the R values of ca. 0.0289-0.0499. The ORTEP diagrams of these complexes are shown in Figures 3.1-3.6, crystallographic data are tabulated in Tables 3.1 and 3.2, and bond distances and angles are in Tables 3.3 and 3.4.

Table 3.1. Crystallographic data for **3.1**, **3.2a**, **3.2b**, and **3.3**

	3.1	**3.2a**	**3.2b.H_2O**	**3.3.CH_3CN**
Formula	$C_{38}H_{32}N_8Ni_2Br_4$	$C_{19}H_{18}N_4Ni\ Br_2O$	$C_{19}H_{20}N_4NiBr_2O_2.H_2O$	$C_{19}H_{20}N_4Br_2NiO_2.(C_2H_3N)$
Mol wt	1037.78	536.90	572.94	637.03
Cryst color, habit	Light brown	Green dark	Green	Green
Cryst dimens, mm	0.21×0.12×0.09	0.24×0.21×0.09	0.46×0.23×0.15	0.96×0.24×0.18
Symmetry	Triclinic	Monoclinic	Triclinic	Triclinic
Space group	P-1	$P2_1/n$	P-1	P-1
a, Å	8.9395(6)	9.8267(5)	10.012(10)	9.41210(10)
b, Å	9.1559(6)	14.4774(7)	10.8995(10)	10.3895(2)
c, Å	11.8205(8)	14.1184(7)	11.3825(10)	14.6092(2)
α, deg	84.166(3)	90	79.529(10)	81.2430(10)
β, deg	81.795(3)	93.890(2)	65.182(10)	79.5330(10)
γ, deg	84.779(3)	90	73.380(10)	66.8230(10)
Volume, $Å^3$	949.76(11)	2003.93(17)	1077.589(17)	1286.28(3)
Z	1	4	2	2
D(calcd), g cm^{-1}	1.814	1.780	1.766	1.645
Diffractometer	Bruker AXS SMART 2K	Bruker AXS SMART 2K	Bruker AXS SMART 2K	Bruker AXS SMART 2K
Temp, K	100(2)	100(2)	100(2)	100(2)
λ	1.5418	1.5418	1.5418	1.5418
μ, mm^{-1}	6.480	6.203	5.881	4.990
scan type	ω scan	ω scan	ω scan	ω scan
F(000)	512	1064	572	640
θ_{max}, deg	72.06	72.02	72.84	72.77
h,k,l	$-11 \le h \le 11$ $-10 \le k \le 11$ $-14 \le l \le 14$	$-12 \le h \le 12$ $-17 \le k \le 17$ $-17 \le l \le 17$	$-12 \le h \le 12$ $-13 \le k \le 12$ $-13 \le l \le 13$	$-11 \le h \le 11$ $-12 \le k \le 13$ $-17 \le l \le 18$
Reflns used ($I > 2\sigma(I)$)	3192	3833	4048	4743
Absorption Correction	multi-scan SADABS	multi-scan SADABS	multi-scan SADABS	multi-scan SADABS
T (min, max)	0.33,0.67	0.33,0.68	0.40,0.68	0.70,0.72
R [$F^2 > 2\sigma(F^2)$], *wR*(F^2, all)	0.0499, 0.1566	0.0327, 0.0837	0.0288, 0.0753	0.0303, 0.0763
GOF	1.127	1.071	1.102	1.071

Table 3.2. Crystallographic data for **3.4** and **3.5**

	3.4. $2CH_2Cl_2$	**3.5**
Formula	$C_{38}H_{32}N_8NiBr_2 \cdot 2(CH_2Cl_2)$	$C_{38}H_{34}Br_2N_8NiO$
Mol wt	989.06	837.26
Cryst color, habit	Green	Blue
Cryst dimens, mm	0.3×0.3×0.2	0.28×0.13×0.03
Symmetry	orthorhombic	Monoclinic
Space group	$P2_12_12_1$	$P2_1/n$
a, Å	12.8738(5)	13.0397(2)
b, Å	16.6019(7)	16.3398(2)
c, Å	19.5642(8)	16.8061(2)
α, deg	90	90
β, deg	90	107.6370(10)
γ, deg	90	90
Volume, $Å^3$	4181.4(3)	3412.49 (8)
Z	4	4
D(calcd), g cm^{-1}	1.571	1.630
Diffractometer	Bruker AXS SMART 2K	Bruker AXS SMART 2K
Temp, K	100(2)	100(2)
λ	1.5418	1.5418
μ, mm^{-1}	5.579	3.925
Scan type	ω scan	ω scan
F(000)	1992	1696
θ_{max}, deg	72.03	72.93
h,k,l	$-15 \le h \le 15$ $-20 \le k \le 20$ $-24 \le l \le 24$	$-16 \le h \le 16$ $-19 \le k \le 20$ $-20 \le l \le 20$
Reflns used ($I > 2\sigma(I)$)	8071	5030
Absorption Correction	multi-scan SADABS	multi-scan SADABS
T (min, max)	0.67,1.00	0.58,0.92
$R\ [F^2>2\sigma(F^2)]$, $wR(F^2$, all)	0.0357, 0.0759	0.0383, 0.0941
GOF	1.054	0.925

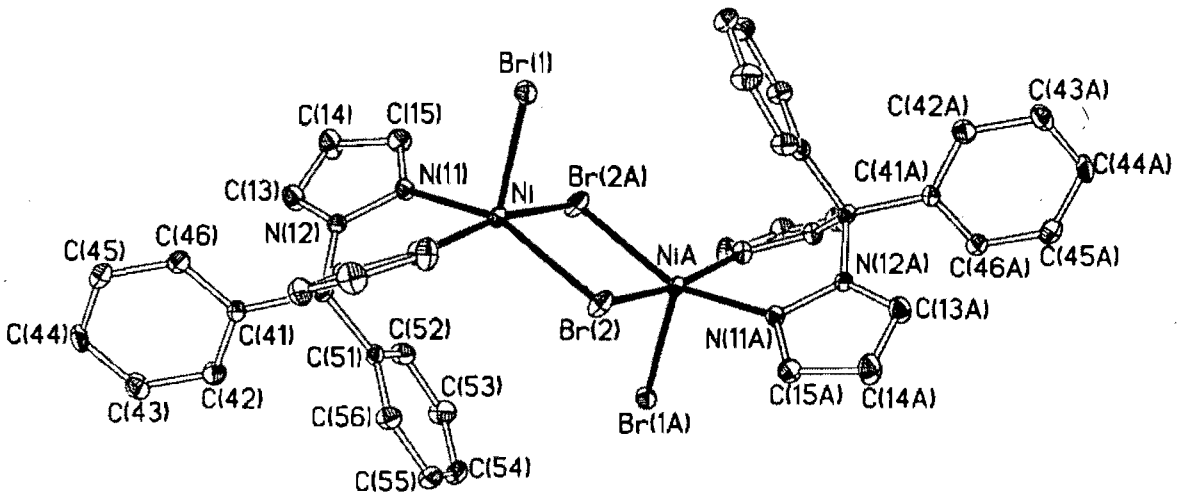

Figure 3.1. ORTEP view of complex **3.1**. Thermal ellipsoids are shown at 30% probability

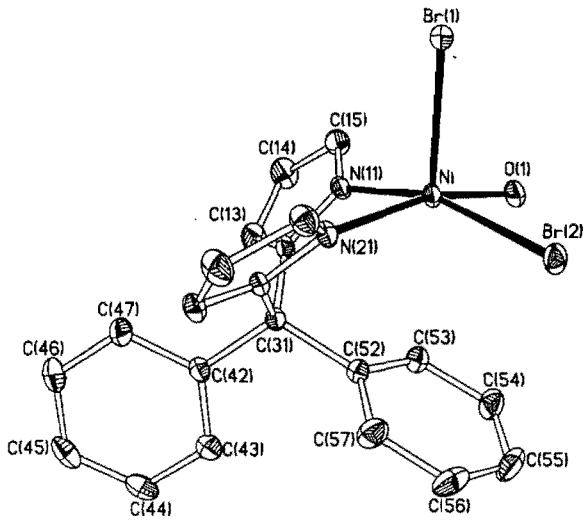

Figure 3.2. ORTEP view of complex **3.2a**. Thermal ellipsoids are shown at 30% probability

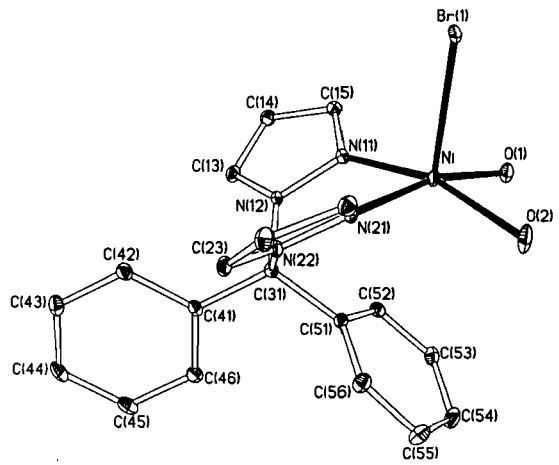

Figure 3.3. ORTEP view of complex **3.2b**. Thermal ellipsoids are shown at 30% probability. Br^- counter ion has been omitted for clarity

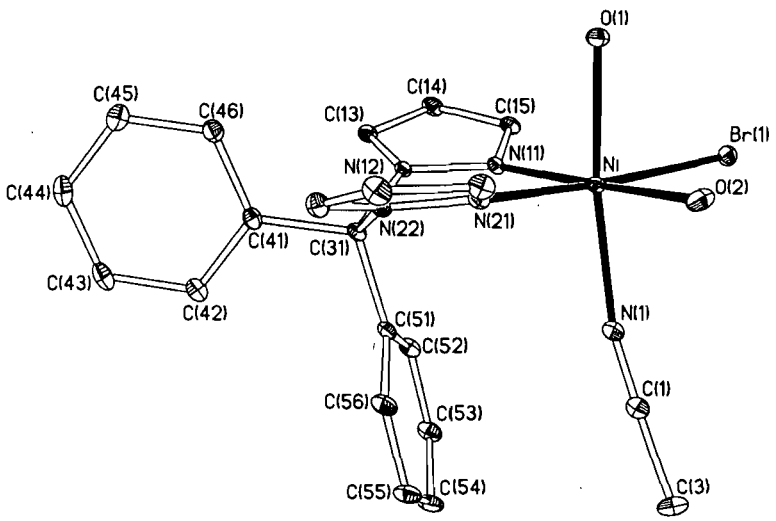

Figure 3.4. ORTEP view of complex **3.3**. Thermal ellipsoids are shown at 30% probability. Br^- counter ion has been omitted for clarity

Table 3.3. Selected structure parameters for complexes **3.1**, **3.2a**, **3.2b**, and **3.3**[a]

	3.1	**3.2a**	**3.2b**	**3.3**
Ni-Br(1)	2.4387(7)	2.4595(4)	2.4779(4)	2.5681(4)
Ni-Br(2)	2.4804(8)	2.4757(4)	-	-
Ni-Br(2A)	2.5433(8)	-	-	-
Ni-O(1)	-	2.0571(16)	2.0317(16)	2.0984(15)
Ni-O(2)	-	-	2.0077(17)	2.0640(15)
Ni-N(11)	2.047(4)	2.0546(19)	2.0254(18)	2.0766(17)
Ni-N(21)	2.064(4)	2.0420(19)	2.0316(19)	2.0857(17)
N(11)-Ni-Br(1)	100.63(9)	97.61(6)	96.58(5)	94.03(5)
N(11)-Ni-Br(2)	155.82(10)	161.93(6)	-	-
N(21)-Ni-Br(1)	93.62 (10)	100.06(5)	96.79(5)	175.49(5)
N(21)-Ni-Br(2)	92.36(10)	94.00(6)	-	-
N(11)-Ni-N(21)	85.44(14)	83.83(8)	87.87(7)	86.31(6)
N(11)-Ni- O(1)	-	85.67(7)	91.87(7)	89.05(6)
N(11)-Ni- O(2)	-	-	161.39(8)	174.83(7)
N(21)-Ni-O(1)	-	160.72(7)	165.91(7)	88.76(6)
N(21)-Ni- O(2)	-	-	89.75(8)	89.43(7)
N(11)-Ni- Br(2A)	90.29(10)	-	-	-
N(21)-Ni- Br(2A)	166.07 (10)	-	-	-
O(1)-Ni-Br(1)	-	97.33(5)	97.24(5)	86.75(4)
O(1)-Ni-Br(2)	-	90.98(5)	-	-
O(2)-Ni-Br(1)	-	-	102.02(7)	89.98(5)
O(1)-Ni-O(2)	-	-	86.00(7)	87.92(7)
Br(1)-Ni-Br(2)	103.55(3)	100.430(1)	-	-
Br(1)-Ni-Br(2A)	100.21(3)	-	-	-
Br(2)-Ni-Br(2A)	86.11(2)	-	-	-
Ni-Br2-Ni(A)	93.89(2)	-	-	-
Ni-N(1)	-	-	-	2.0957(17)
N(11)-Ni-N(1)	-	-	-	99.52 (7)
N(21)-Ni-N(1)	-	-	-	93.53(6)
N(1)-Ni-Br(1)	-	-	-	90.85(5)
N(1)-Ni-O(1)	-	-	-	171.25(7)
N(1)-Ni-O(2)	-	-	-	83.66(7)

[a]Bond lengths in Å and bond angles in deg.

Complex **3.1** possesses a crystallographically imposed center of symmetry. On the basis of the low value of the structural index τ in each complex,[20] the coordination geometry around the Ni centers in **3.1** (0.17), **3.2a** (0.02), and **3.2b** (0.08) can be characterized as lightly distorted square pyramidal. In comparison to **3.1**, the closely related dimeric species $[(bpp)Ni(\mu\text{-}Br)Br]_2$ displays a less distorted square pyramidal structure ($\tau \sim 0.04$),[13] whereas $[(bpm^*)Ni(\mu\text{-}Cl)Cl]_2$ shows a much greater distortion toward a trigonal bipyramidal geometry ($\tau \sim 0.50$).[9j,21] The differences in the overall geometry of the Ni

centers in these closely analogous penta-coordinated Ni(II) complexes based on bpm*, bpp, or dpdpm are caused by the differences in the ligand structures, i.e., the different substituents at the 3- and 5-positions of the pyrazolyl groups (H, Me) and the different CR_2 moieties bridging them (R = Ph, Me, H). It is also interesting to note that the axial site in all complexes adopting lightly distorted square pyramidal structures (**3.1**, **3.2a**, **3.2b**, and $[(bpp)Ni(\mu\text{-}Br)Br]_2$) is occupied by a Br atom, whereas in the compound $[(bpm^*)Ni(\mu\text{-}Cl)Cl]_2$ that shows major trigonal distortions the axial site is occupied by the pyrazolyl N. This may, of course, be related to the substantial difference in the relative sizes of Cl and Br atoms.[22]

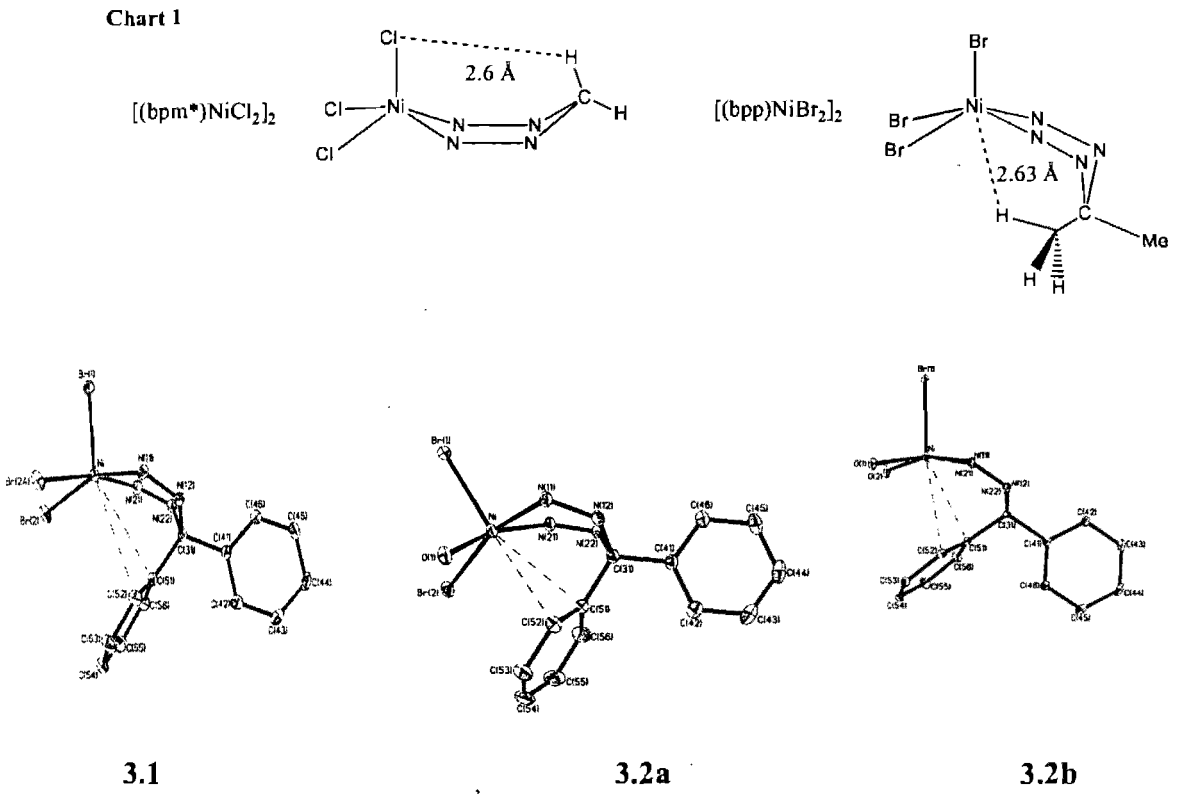

Figure 3.5. Different perspectives of the ORTEP diagrams for complexes **3.1**, **3.2a**, and **3.2b** showing the long-range Ni-C distances

The differences in the ligand architecture also give rise to a different conformation of the metallacycle formed by the chelating bis(pyrazole) moiety in the penta-coordinated species. Thus, the methylene moiety displays a Cl···H-C interaction in $[(bpm^{Me2})Ni(\mu\text{-}Cl)Cl]_2$ and an agostic type Ni···H-C interaction in $[(bpp)Ni(\mu\text{-}Br)Br]_2$ (Chart 1). The

bridging CR_2 moiety in our dpdpm compounds **3.1**, **3.2a**, and **3.2b** points toward the Ni center (Figure 3.5) to allow a long-range interaction between a C=C bond of a Ph substituent and the Ni center with the following Ni-C distances (in Å) : 3.34 and 3.63 in **3.1**; 3.04 and 3.13 in **3.2a**; 3.02 and 3.23 in **3.2b**. An examination of space-filling representations of the solid state structures of these complexes indicates that steric considerations alone can justify the longer Ni-Ph distances in the dimeric species **3.1**.[22]

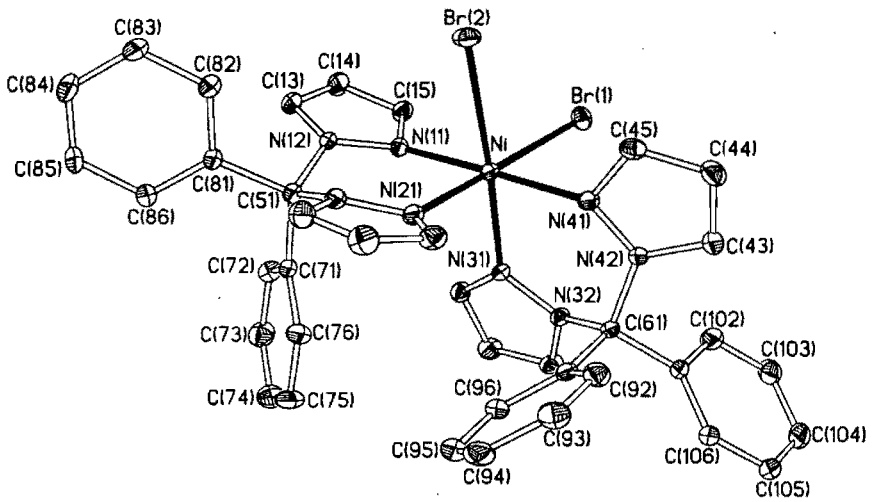

Figure 3.6. ORTEP view of complex **3.4**. Thermal ellipsoids are shown at 30% probability

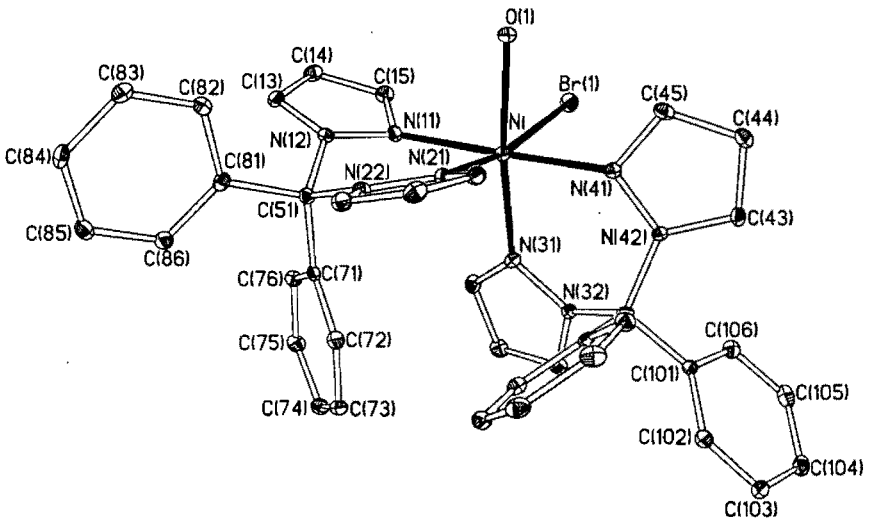

Figure 3.7. ORTEP view of complex **3.5**. Thermal ellipsoids are shown at 30% probability. Br^- counter ion has been omitted for clarity

Table 3.4. Selected structure parameters for complex **3.4** and **3.5**[a]

	3.4 (X2= Br2)	**3.5** (X2= O1)
Ni-Br(1)	2.5971 (4)	2.6146 (7)
Ni-X(2)	2.6476 (4)	2.106 (2)
Ni-N(11)	2.0740 (19)	2.116 (3)
Ni-N921)	2.0949 (19)	2.074 (3)
Ni-N(31)	2.1031 (17)	2.061 (3)
Ni-N(41)	2.0835 (18)	2.076 (3)
N(11)-Ni-N(21)	87.84 (7)	84.49 (11)
N(11)-Ni-N(31)	91.74 (7)	95.84 (11)
N(11)-Ni-N(41)	178.34 (7)	176.84 (11)
N(21)-Ni-N(31)	93.41 (7)	100.39 (11)
N(21)-Ni-N(41)	92.76 (7)	93.16 (11)
N(31)-Ni-N(41)	86.69 (7)	86.65 (11)
N(11)-Ni-Br(1)	94.94 (5)	94.26 (8)
N(21)-Ni-Br(1)	175.74 (6)	169.51 (8)
N(31)-Ni-Br(1)	89.73 (5)	90.10 (8)
N(41)-Ni-Br(1)	84.55 (5)	87.67 (8)
N(11)-Ni-X(2)	86.05 (5)	88.56 (10)
N(21)-Ni-X(2)	84.13 (5)	87.23 (10)
N(31)-Ni-X(2)	176.75 (5)	171.52 (11)
N(41)-Ni-X(2)	95.54 (5)	89.22 (10)
X(1)-Ni-X(2)	92.827 (13)	82.33 (7)

[a]Bond lengths in Å and bond angles in deg.

Complexes **3.3**, **3.4**, and **3.5** display slightly distorted octahedral geometries, the cis and trans bond angles ranging from 84-100° and 171-176° in **3.3**, 84-96° and 176-178° in 3.4, and 82-100° and 170-177° in **5** (Tables 3.3 and 3.4). An important structural difference between these octahedral species and the above-discussed penta-coordinated compounds is the conformation of the 6-membered ring formed by the coordination of the chelating dpdpm ligand to the Ni center. Evidently, the occupation of the 6-th coordination site around the Ni center in the octahedral compounds pushes the Ph substituents of dpdpm toward the equatorial plane, thereby changing the conformation of the Ni-N-N-C-N-N ring from a boat conformation observed in the penta-coordinated complexes to a half-chair conformation observed in **3.3**, **3.4**, and **3.5**. The different spatial disposition of the Ph substituents in the octahedral and penta-coordinated complexes can be quantified by comparing the angles between the equatorial coordination plane (defined by the ligating atoms N11, N21, Br/O/N, Br/O/N) and the chelation plane defined by the four N atoms of

the dpdpm ligand; these angles have the values of ca. 57° in **1**, 47° in **2a**, 38° in **2b**, 4° in **3.3**, 16° in **3.4**, and 1° in **3.5**.

Apart from the overall geometry of the new complexes and the conformation of the metallacycles, the Ni-element bond distances are informative about the relative stabilities of the various species and the relative trans influence of the ligands. For instance, the Ni-(μ-Br) distances in complex **3.1** are much longer than the axial Ni-Br distance (2.48 and 2.54 Å vs. 2.44 Å, ΔNi-Br > 50 e.s.d.). These weak Ni-(μ-Br) interactions explain why this dimer is susceptible to cleavage and transformation into monomeric derivatives **3.2a** and **3.2b** by hydrolysis. Fairly inequivalent distances were also found for the Ni-Br bonds in **3.2a** (axial < basal; ΔNi-Br ~ 40 e.s.d.) and the Ni-O bonds in **3.2b** (ΔNi-O ~ 14 e.s.d.). On the other hand, the two Ni-N distances in **3.1**, **3.2a**, and **3.2b** are fairly similar to each other (ΔNi-N ~ 4 e.s.d. in **3.1**, ~ 6 e.s.d. in **3.2a**, and ~ 3 e.s.d. in **3.2b**).

Finally, the Ni-N distances trans to Ni-OH_2 are somewhat shorter than the corresponding distances trans to Ni-Br in **3.2a** (2.042(2) vs. 2.055(2) Å), **3.3** (2.077(2) vs. 2.086(2) Å), and **3.5** (2.061(3) vs. 2.074(3) Å), implying that Br has a greater trans influence than H_2O. Moreover, in **3.4** the Ni-N_{av} distance trans to Br is somewhat longer than those trans from the pyrazolyl group (2.099(2) vs. 2.079(2) Å), implying a slightly greater trans influence for Br. Interestingly, the Ni-O distance trans to MeCN in **3.3** is longer than that trans to the pyrazolyl group (2.098(2) vs. 2.064(2) Å), implying a greater trans influence for MeCN. These observations lead to the following order of relative trans influence strengths in these compounds: CH_3CN ~ Br > H_2O ~ dpdpm. It should be noted, however, that the structural parameters for the octahedral species arising from the reactions of $Ni(NO_3)_2$ with dpdpm have implied a greater trans influence for the pyrazolyl group (dpdpm ~ H_2O ~ η^1-ONO_2 > CH_3CN ~ η^2-O_2NO).[14]

3.3.3 Magnetic measurements and spectroscopic studies. Magnetic susceptibility measurements using the Gouy method have established that all the dpdpm compounds investigated here are paramagnetic in the solid state. Thus, μ_{eff} for penta-coordinated complexes **3.1**, **3.2a**, and **3.2b** were found to be between 3.2 and 3.4 BM, whereas those of the hexa-coordinated complex **3.3-3.5** were ca. 3.3 BM. All of these values are in the expected range for square pyramidal or octahedral Ni(II) complexes having two unpaired electrons.[23]

That the paramagnetism of these compounds is maintained in solution is reflected in ^{1}H NMR spectra displaying broad and, for the most part, featureless signals that resonated as far upfield as -160 ppm and as far downfield as 70 ppm. The broadness of the NMR signals in bis(pyrazolyl)alkane complexes may also be caused by the dynamic exchange process involving the flipping of the M-N-N-C-N-N ring between chair and boat conformations. Moreover, the ^{1}H NMR spectra recorded in CD_3CN feature a fairly broadened residual solvent signal (at 1.94 ppm) in addition to somewhat broader signals due to the dpdpm ligand (at 6.69, 6.36, and 6.13 ppm). We suspect, therefore, that a ligand exchange process involving CD_3CN molecules and the dpdpm ligand might be taking place in solution, but no dpdpm-free complex or species with monodentate dpdpm has been obtained in the solid state. The IR spectra of the new complexes contain a large number of absorptions that serve primarily as fingerprints for this family of complexes.

3.3.4. Solvato- and thermochromism of the penta-coordinated species. The presence of an "unfilled" coordination site around the Ni center in the penta-coordinated complexes **3.1**, **3.2a**, and **3.2b** facilitates the interaction of these species with nucleophiles or coordinating counter ions. We have examined the interaction of these complexes with solvent molecules of varying nucleophilicities and found a number of interesting color changes that signal structural changes. Since temperature variations can also influence metal-ligand interactions and structural changes, we have also probed the influence of temperature on the optical properties of these compounds. Given the similarities of the UV-visible-NIR spectra for solutions of **3.2a** and **3.2b** in various solvents, we have focused the present discussion on the spectra for **3.1** and **3.2a** only.

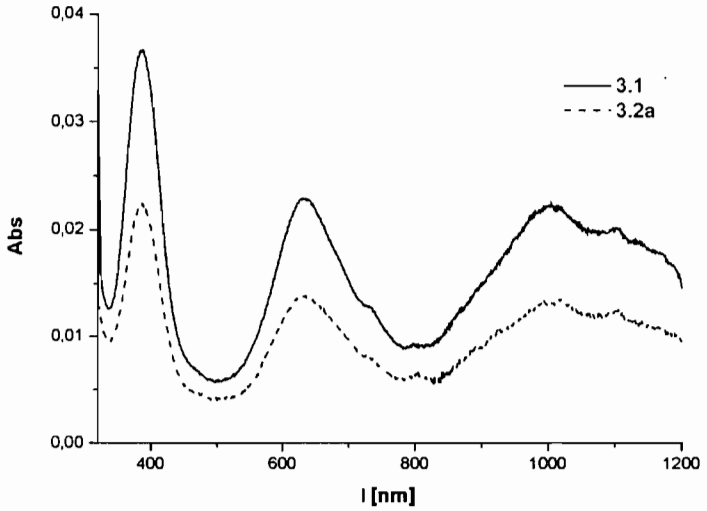

Figure 3.8. Room temperature UV-vis-NIR spectra of MeOH solutions of **3.1** (1.3 mM) and **3.2a** (2.1 mM)

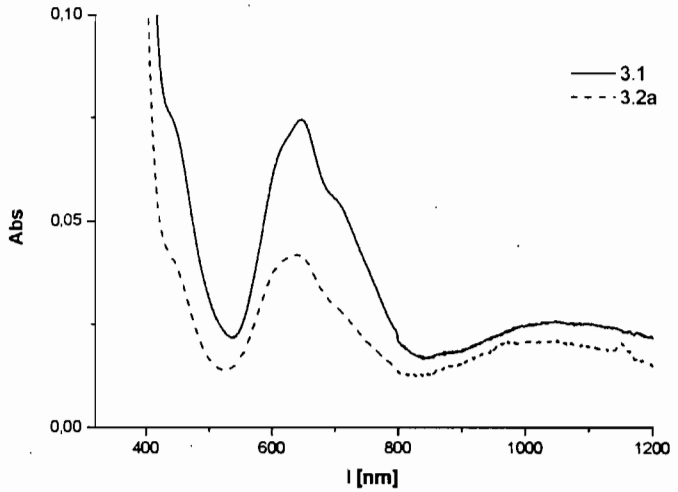

Figure 3.9. Room temperature UV-vis-NIR spectra of CH_3CN solutions of **3.1** (1.3 mM) and **3.2a** (2.7 mM)

Figures 3.8 and 3.9 show the UV-vis-NIR spectra of **3.1** and **3.2a** in MeOH (blue) and CH_3CN (lime-green), respectively. It is noteworthy that these spectra display the characteristic spectral pattern for octahedral Ni(II) compounds. Thus, all of these spectra contain the allowed d-d transitions $^3A_{2g} \rightarrow {}^3T_{2g}$, $^3A_{2g} \rightarrow {}^3T_{1g}(^3F)$, and $^3A_{2g} \rightarrow {}^3T_{1g}(^3P)$,[24]

although the bands of the CH_3CN spectra are more intense. Interestingly, the middle bands in these spectra ($^3A_{2g} \rightarrow {}^3T_{1g}$) have multiple maxima that arise from interactions between the allowed and non-allowed excited states, as described elsewhere.[25]

The pair wise similarities of the spectra obtained for MeOH and CH_3CN solutions of **3.1** and **3.2a** indicate that these compounds have similar structures in these solvents. Indeed, comparison of the CH_3CN spectra to that of complex **3.3** in this solvent shows that acetonitrile solutions of **3.1**, **3.2a**, and **3.3** contain the same species. We conclude, therefore, that interaction of the Ni center in **3.1** or **3.2a** with acetonitrile involves the coordination of CH_3CN and H_2O to form **3.3**. In the case of the species generated in MeOH solutions of **3.1** and **3.2a**, the absence of reliable structural information does not allow us to determine whether the resulting octahedral species is a simple MeOH or water adduct[26,27] or a compound arising from the displacement of Br by MeOH or water.[28]

Heating the MeOH solution of **3.1** produced a color change, going from light blue at room temperature to light green at ca. 60 °C, but the spectra recorded for these solutions do not show significant changes in the shapes of the bands or the energy maxima (<5-10 nm). These color changes are likely due to ligand exchange reactions that cause only minor modifications in the overall geometry of the complex.

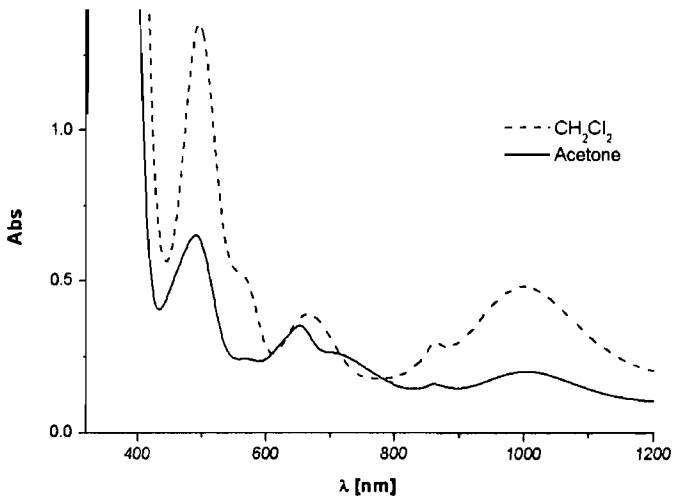

Figure 3.10. Room temperature UV-vis-NIR spectra of **3.2a** in CH_2Cl_2 (8.7 mM) and acetone (8.3 mM)

The electronic spectra of **3.2a** in CH_2Cl_2 and acetone (Figure 3.10) were quite different from those discussed above. For instance, the room temperature spectrum recorded for the acetone solution showed four main bands at 488, 650, 861, and 1006 nm; the band at 650 nm features a shoulder at 712 nm. The room temperature spectrum recorded in CH_2Cl_2 also shows four main peaks at 491, 662, 859, and 1002 nm; the band at 491 nm also shows a shoulder at 560 nm. These spectra are quite similar, their main difference being the position of the shoulder band. These observations indicate that CH_2Cl_2 and acetone solutions of **3.2a** do not contain octahedral species. Literature reports show that most penta-coordinated Ni(II) species display three or four bands of variable intensities.[29] On the other hand, computational studies have indicated that Ni(II) compounds surrounded by weak-field ligands arranged in a square pyramidal geometry (C_{4v} idealized symmetry, high-spin) should give rise to six spin-allowed transitions in the UV-visible region.[30] We propose that our observations are consistent with the maintenance of square pyramidal structure for **3.2a** in acetone and CH_2Cl_2 solutions, which is reasonable because both of these solvents have weaker coordinating abilities relative to MeOH and CH_3CN.

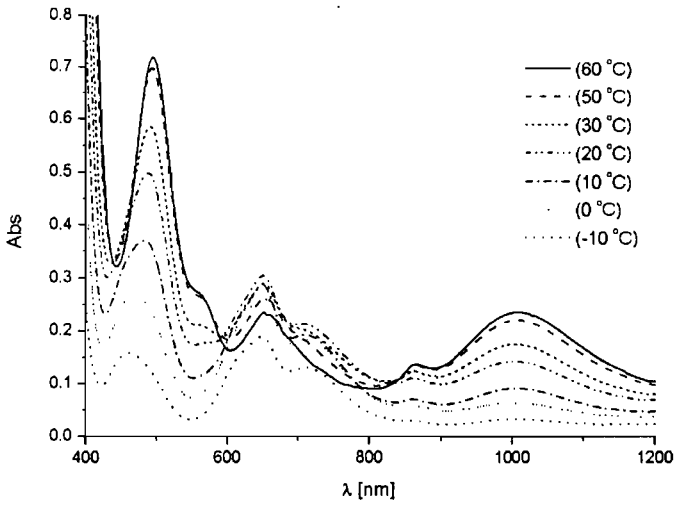

Figure 3.11. Variable temperature UV-vis-NIR spectra for a 6.5 mM solution of **3.2a** in acetone

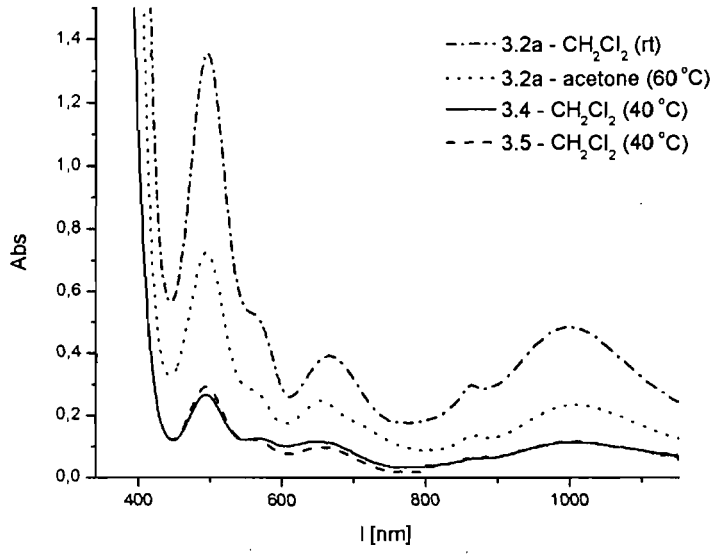

Figure 3.12. UV-vis-NIR spectra for solutions of **3.2a** (8.7 mM in CH_2Cl_2 and 6.5 mM in acetone) and acetone solutions of **3.4** (4.7 mM) and **3.5** (6.6mM)

The colors of the acetone and CH_2Cl_2 solutions of **3.2a** and their temperature-dependence also reveal an interesting interconversion between **3.2a** and **3.1**. Thus, the CH_2Cl_2 solution of **3.2a** is brown, very similar to the color of solid samples of **3.1**, while the room temperature acetone solution of **3.2a** is green. Varying the temperature of the acetone solution of **3.2a** caused a color variation from light green (< 30 °C) to dark green (30-40 °C) to brown (40-60 °C). Cooling the samples to 18 °C regenerated the light green colour of the solution, and repeating this heating-cooling cycle 8 times produced the same observations. The variable temperature spectra of an acetone solution of **3.2a** showed a continuous blue shift of the shoulder band from ca. 711 nm at -10 °C to ca. 555 nm at 60 °C (Figure 3.11). It is noteworthy that the high temperature acetone spectrum is virtually identical to the room temperature CH_2Cl_2 spectrum of **3.2a** (Figure 3.12), and both of these solutions have the same color as the solid samples of **3.1**. Since **3.1** can be prepared by dehydration of **3.2a** or **3.2b** (vide supra), these observations suggest that the continuous and reversible thermochromism of **3.2a** in acetone involves its conversion to **3.1** at high temperatures. Conversion of complex **3.2a** to **3.1** can also occur at room temperature in concentrated CH_2Cl_2 solutions. Unfortunately, the insufficient solubility of **3.1** in CH_2Cl_2

and acetone prevented us from recording the spectra of **3.1** in these solvents, which would allow us to confirm the conversion of **3.1** to **3.2a**.

Finally, we have briefly studied the effect of solvent vapor on the penta-coordinated species **3.2a** and **3.2b**. These studies showed that **3.2b** is readily converted to **3.1** in the presence of solvent vapors, whereas **3.2a** did not register important changes. Thus, exposing a small light green crystal of **3.2b** to the vapors of benzene, Et_2O, or toluene turned the crystals to brown in less than 2 min. Visual inspection indicated that the sample had lost its crystallinity; however, exposing this brown sample to humidity changed it back to green in a very slow process (many days).

3.3.5. Solvato- and thermochromism of the octahedral species 3.4 and 3.5.

In order to determine whether the coordinatively saturated Ni centers in our octahedral species can undergo similar solvato- and thermochromic changes, we examined (visually and by spectroscopy) the colors of the solutions of the bis(dpdpm) compounds **3.4** and **3.5**. Since complex **3.4** (green) is readily converted to **3.5** (blue) in the presence of humidity, both in solution and solid state, the thermo- and solvatochromism tests were carried out using dried and distilled solvents and with freshly grown crystals of these complexes.

Complexes **3.4** and **3.5** give variously colored solutions in different solvents; in addition, some of these solutions changed color as a function of temperature. Thus, CH_2Cl_2 solutions of **3.4** are dark green at room temperature and pink at 40 °C. The MeOH solution of **3.4** turns from turquoise blue at 20 °C to light green at 60 °C. The CH_3CN solutions of **3.4** are light green at room temperature or below, becoming dark green at higher temperatures. Room temperature solutions of complex **3.5** were light blue in both CH_2Cl_2 and MeOH, but green in CH_3CN. Increasing the temperature turned the CH_2Cl_2 solution from blue to pink at 40 °C, whereas the MeOH and CH_3CN solutions did not change color upon heating.

The UV-Vis-NIR spectra of various solutions prepared from crystals of **3.4** and **3.5** were recorded to monitor spectral changes as a function of solvent and temperature. Figures 3.13, 3.14, and 3.15 show the variable temperature spectra of **3.4** in CH_2Cl_2, MeOH, and CH_3CN, respectively. Figure 3.16 shows the variable temperature spectra recorded for CH_2Cl_2 solution of **3.5** (6.6 mM); the MeOH and CH_3CN spectra were very similar to those of complex **3.4**. The spectra taken at 20 °C for MeOH and CH_3CN solutions of complex **3.4** show the expected pattern for octahedral species, implying that **3.4** generates fairly similar

species in these relatively nucleophilic solvents. Varying the temperature of the MeOH solutions from -10 °C to 60 °C caused a red-shift of the 586 nm band (to 599 nm, Figure 3.14), whereas the corresponding band in the CH_3CN spectra (Figure 3.15) showed a blue-shift (591 to 577 nm) in addition to the emergence of a new shoulder band at 575 nm.

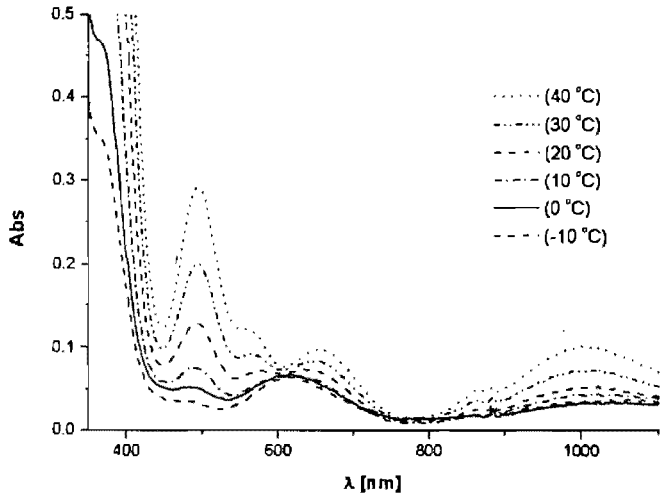

Figure 3.13. Variable temperature UV-vis-NIR spectra for **3.4** in CH_2Cl_2 (4.7mM)

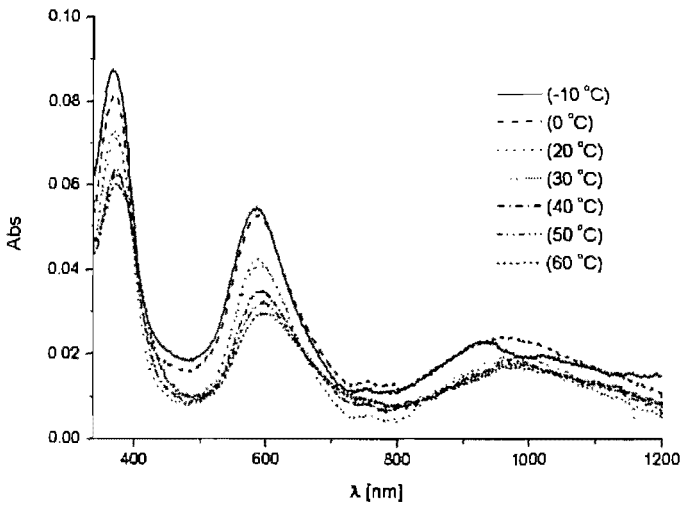

Figure 3.14. Variable temperature UV-vis-NIR spectra for **3.4** in MeOH (3.9 mM)

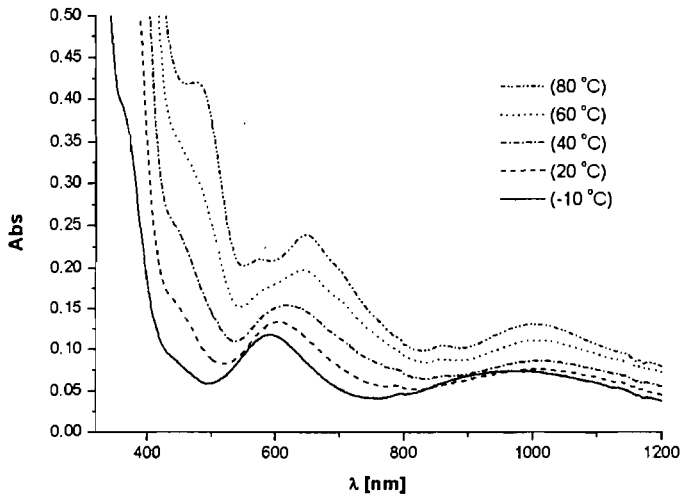

Figure 3.15. Variable temperature UV-vis-NIR spectra for **3.4** in CH_3CN (8.7 mM)

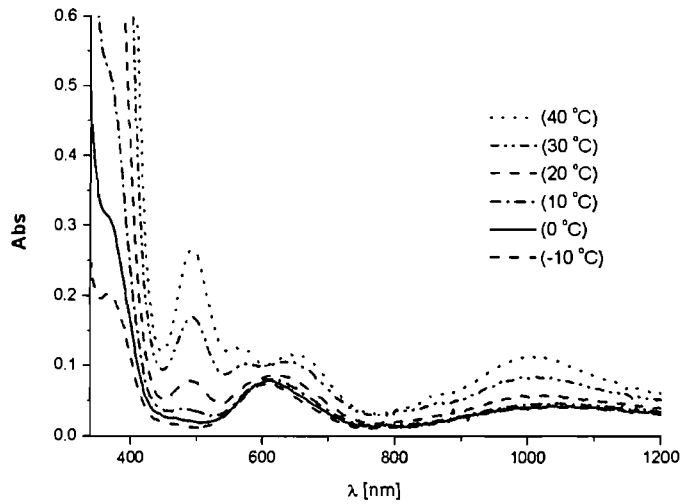

Figure 3.16. Variable temperature UV-vis-NIR spectra for **3.5** in CH_2Cl_2 (6.6 mM)

The variable temperature spectra of **3.4** and **3.5** in CH_2Cl_2 (Figures 3.13 and 3.16) registered major changes over a much narrower range of temperature (-10 °C to +40 °C), implying that significant changes take place in the overall structure of these complexes. It is interesting to note the striking similarity between the -10 and 40 °C spectra of **3.4** and **3.5**. Furthermore, as was mentioned above, at 40 °C the spectral features are reminiscent of those observed for CH_2Cl_2 solution of complex **3.2a** at room temperature and those of the

acetone solution at high temperatures. Based on these observations, we propose that heating CH_2Cl_2 solutions of the octahedral, bis(dpdpm) complexes **3.4** and **3.5** leads to the dissociation of a dpdpm ligand to form mono(dpdpm) species. The similarity between the colors of these solutions and the solid sample of **3.1** points to the possible formation of the dimeric structure of **3.1** at high temperature solutions of **3.4** and **3.5**.

3.4 Conclusion

$NiBr_2$ forms penta-coordinated complexes when it is reacted with one equivalent of dpdpm in weakly coordinating solvents. This is in contrast to the exclusive formation of octahedral species from the reaction of $Ni(NO_3)_3$ under similar conditions. The unusual geometry of the $NiBr_2$ derivatives appears to be stabilized, in the solid state, by long-range Ni-Ph interactions. In contrast, reactions using a 1:2 Ni:dpdpm ratio give octahedral species with both nitrate and bromide derivatives.

A common aspect of all Ni-dpdpm complexes prepared to date is the lability of all Ni-ligand bonds. This is perhaps the reason why these compounds are not suitable precursors for organometallic derivatives. It is worth noting, however, that the facile dissociation of Br^- or NO_3^- bestows interesting solvato-, vapo-, and thermochromic properties to these compounds. The results of our studies encourage us to explore the potential of these complexes in detecting solvent vapors or anions.

3.5 Experimental

3.5.1 General.

The main ligand used in this study, diphenyl(dipyrazolyl)methane (dpdpm), was synthesized according to a published procedure.[19] Anhydrous $NiBr_2$ was purchased from Sigma-Aldrich, stored in a drybox, and used without further dehydration. Where necessary, the synthetic manipulations were carried in dry and oxygen- free solvents under an atmosphere of ultra high purity nitrogen using standard Schlenk techniques and a drybox. The elemental analyses (C, H, and N) were performed in duplicate by Laboratoire d'Analyse Élémentaire de l'Université de Montréal. The ^1H NMR spectra were recorded on a Bruker Av400 (at 400 MHz). The IR spectra were recorded between 4000 and 400 cm^{-1} using KBr pellets on a Perkin Elmer Spectrum One spectrophotometer using the Spectrum v.3.01.00 software. The UV-vis-NIR spectra were recorded between 1300 and 250 nm with a 1 cm quartz cell on a Varian Cary 500i; the variable temperature spectra were recorded on

a Cary 500 spectrophotometer. The magnetic susceptibility measurements were carried out at room temperature using the Gouy method with a Johnson Matthey Magnetic Susceptibility Balance, using $HgCo(NCS)_4$ as standard.

3.5.2 Syntheses.

[(dpdpm)Ni(μ-Br)Br]$_2$ (3.1). A solution of dpdpm (1.00 g, 3.33 mmol) in distilled acetone (25 mL) was added to a stirred suspension of $NiBr_2$ (0.75 g, 3.34 mmol) in distilled acetone (25 mL). The reaction mixture was heated to reflux for 18 h, cooled to room temperature, filtered, and the remaining solid was washed with Et_2O (3×20 mL) to give an orange-brown powder (1.30 g, 79 % crude yield). X-ray quality single crystals (brown) were obtained by slow diffusion of Et_2O into a concentrated acetone solution kept at room temperature. m. p. 260°C. $\mu_{eff.}$ 3.55 BM. Anal. Calc. for $[C_{19}H_{16}N_4NiBr_2]_2$: C, 43.98; H, 3.11; N, 10.80. Found: C, 43.58; H, 2.99; N, 10.78%. ^{1}H NMR (CD_3OD): δ 59.55 (br), 40.47 (br), 7.58 (br), 7.47-7.44 (br), 7.34 (br), 7.37 (br), 7.18 (br), 6.72 (br), 2.14 (s), -141.07 (br), -160.34 (br). IR (KBr) : υ (cm^{-1}) 3604 (s), 3392 (br), 3158 (m), 3118 (m), 3058 (m), 1631 (m), 1517 (m), 1491 (s), 1450 (s), 1437 (s), 1408 (s), 1385 (s), 1330 (m), 1313 (vs), 1253 (s), 1222 (s), 1199 (s), 1171 (m), 1098 (s), 1080 (s), 1074 (s), 999 (m), 940 (w), 924 (w), 918 (m), 891 (m), 870 (m), 853 (m), 776 (s), 754 (vs), 704 (s), 692 (s), 656 (s), 637 (s), 614 (w), 605 (w), 497 (w).

[(dpdpm)NiBr$_2$(H$_2$O)] (3.2a). A solution of dpdpm (0.50 g, 1.66 mmol) in methanol (30 mL) was added to a stirred suspension of $NiBr_2$ (0.36 g, 1.66 mmol) in (30 mL) methanol. The reaction mixture was stirred for 20 h at room temperature, filtered to remove unreacted $NiBr_2$, and evaporated to give a dark green powder (2.99 g, 83% crude yield). X-ray quality single crystals (dark green) were obtained by slow diffusion of Et_2O into a concentrated acetone solution kept at room temperature. m.p. 234°C. $\mu_{eff.}$ 3.21 BM. Anal. Calc. for: $C_{19}H_{18}N_4ONiBr_2$: C, 42.51; H, 3.38; N, 10.44. Found: C, 42.96; H, 3.35; N, 10.28 %.^{1}H NMR ($CDCl_3$): δ 69.86 (br), 50.42 (br), 37.94 (br), 6.62 (br), 5.65 (br), 4.45 (br), 3.92 (br), 3.12 (br), 2.2 (br), 1.47 (br) 1.30 (br) 0.09 (br) -130.7 (br) -150.34 (br), -163.01 (br). IR (KBr): υ (cm^{-1}) 3323 (br), 3150-3033 (w), 1631 (vs), 1516 (w), 1491 (m), 1451 (s), 1434 (m), 1406 (s), 1385(m), 1332 (m), 1314 (s), 1254 (m), 1226 (m), 1198 (s), 1171 (m), 1091

(w), 1080 (w), 1070 (vs), 999 (m), 942 (w), 923 (m), 890 (m),867 (m), 847 (w), 771 (vs), 775 (s), 699 (s), 657 (m), 638(m), 605 (m), 578 (w), 502 (w).

[(dpdpm)NiBr(H_2O)$_2$]Br (3.2b). The procedure used for the synthesis of **2a** was followed. X-ray quality single crystals (light green) were obtained by slow diffusion of hexane into a concentrated acetone solution kept at room temperature. m.p.> 260°C. $\mu_{eff.}$ 3.22 BM. Anal. Calc. for $C_{19}H_{20}N_4O_2Ni\ Br_2$: C, 41.13; H, 3.63; N, 10.10. Found: C, 40.63; H, 3.43; N, 9.83 %. ^{1}H NMR (CD_3OD): δ 60.81 (br), 39.05 (br), 7.28 (br), 7.12 (br), 6.72 (br), -140.55 (br), -162 (br). IR (KBr): υ (cm^{-1}) 3395 (br), 3344 (br), 3127-3056 (w), 1631 (s), 1516 (m), 1491 (m), 1450 (s), 1437 (m), 1414 (s), 1385 (m), 1336 (m), 1318 (s), 1257 (m), 1223 (w), 1214 (m), 1198 (m), 1185 (w), 1174 (w), 1104 (m), 1086 (m), 1069 (vs), 1001 (m), 942 (w), 922 (m), 891 (m), 870 (w), 843 (w), 780 (s), 757 (w), 749 (vs), 702 (s), 567 (w), 642 (w), 611 (w), 600 (w), 537 (w), 511 (w).

[(dpdpm)NiBr(H_2O)$_2$(CH_3CN)]Br (3.3). A solution of dpdpm (2.00 g, 6.66 mmol) in acetonitrile (30 mL) was added to a stirred suspension of $NiBr_2$ (1.46 g, 6.70 mmol) in acetonitrile (30 mL). The reaction mixture was stirred for 20 h at room temperature, filtered, and the filtrate was evaporated to give a green solid (3.35 g, 85% crude yield). X-ray quality single crystals of **3** (green) were obtained by slow diffusion of hexane into a concentrated solution of acetonitrile kept at room temperature. m. p. 229°C. $\mu_{eff.}$ 3.33 BM. Anal. Calc. for $C_{21}H_{23}N_5O_2NiBr_2.CH_3CN$: C, 43.37; H, 4.11; N 13.19. Found: C, 42.99; H, 4.07; N, 12.91%. ^{1}H NMR (CD_3CN): δ 70.97 (br), 61.54 (br), 43.75 (br), 39.20 (br), 7.51-7.43, 6.53 (br), 5.70 (br), 5.51 (br), -129.97, -140.22 (br), -157.02 (br), -161.82 (br). IR(KBr): υ (cm^{-1}) 3605 (s), 3392 (br), 2368- 2241 (w), 1644 (br), 1515 (m), 1491 (s), 1450 (s), 1438 (s), 1410 (s), 1384 (s), 1332 (w), 1309 (vs), 1252 (m), 1218 (s), 1193 (s), 1166 (m), 1109 (s), 1078 (m), 1067 (vs), 1031 (w), 1000 (m), 940 (w), 918 (m), 892 (m), 874 (m), 858 (w), 784 (s), 764 (vs), 754 (vs), 704 (s), 568 (w), 658 (w), 636 (m), 614 (w),724 (w), 604 (m), 504 (m).

[(dpdpm)$_2$$NiBr_2$] (3.4) and **[(dpdpm)$_2$NiBr($H_2O$)]Br (3.5).** A solution of dpdpm (0.50 g, 1.66 mmol) in distilled hot methanol (20 mL) was added to a stirred suspension of $NiBr_2$ (0.18 g, 0.82 mmol) in distilled methanol (15 mL). The reaction mixture was stirred for 20

h at room temperature under nitrogen, filtered, and the filtrate evaporated to give a green solid (0.56 g, 81% crude yield). X-ray quality single crystals of **4** (green) were obtained by slow diffusion of Et_2O into a concentrated (green) solution of CH_2Cl_2 kept at room temperature and under nitrogen. Alternatively, repeating this same recrystallization procedure but with the solution exposed to air gave blue crystals of **5**. The latter were also obtained by exposing the green crystals of **4** to ambient atmosphere overnight.

3.4: m. p. 120°C. $\mu_{eff.}$ 3.26 BM. Anal. Calc. for $C_{38}H_{34}N_8$ Ni $Br_2.CH_2Cl_2$: C, 51.81; H, 3.79; N, 12.39. Found: C, 51.60; H, 3.26; N, 12.25%. ^{1}H NMR ($CDCl_3$): δ 60.33 (br), 38.75 (br), 7.18 (br), -141.05 (br), -162.17 (br). IR(cm^{-1}) : v (cm^{-1}) 3430 (br), 3146 (m), 3110 (m), 3098 (m), 3062 (m), 2962 (m), 2925 (m), 2855 (m), 2377 (w), 1629 (br), 1513 (m), 1491 (s), 1450 (s), 1433 (s), 1404 (m), 1382 (m), 1303 (s), 1272 (w), 1250 (w), 1222 (m), 1189 (s), 1161 (m), 1106 (s), 1085 (m), 1066 (vs), 1000 (w), 979 (w), 938 (m), 915 (m), 889 (m), 872 (w), 788 (w), 754 (vs), 725 (s), 699 (s), 669 (w) 658 (m), 634 (m), 605 (w).

3.5: m. p. 120°C. $\mu_{eff.}$ 3.01 BM Anal. Calc. for $C_{38}H_{34}N_8$ O_1 Ni Br_2: C, 54.51; H, 4.09; N, 13.38. Found: C, 54.51; H, 3.97; N, 13.52%. ^{1}H NMR ($CDCl_3$): δ 60.39 (br), 37.79 (br), 7.46 (br), 6.68 (br) -162.99 (br). IR (KBr): v (cm^{-1}) 3512 (s), 3431 (br), 3104 (m), 3052 (s), 2918 (m), 2850 (m), 2375 (w), 2361 (w), 2347 (w), 2019 (w), 1820 (w), 1763 (w), 1603 (br), 1522 (m), 1516 (m), 1491 (s), 1449 (s), 1435 (s), 1411 (m), 1384 (m), 1332 (m), 1305 (s), 1250 (m), 1220 (s), 1193 (s), 1187 (s), 1167 (m), 1108 (s), 1087 (m), 1064 (vs), 1000 (w), 990 (w), 980 (w), 938 (w), 918 (m), 914 (m), 890 (m), 873 (m), 856 (w), 762 (vs), 752 (vs), 700 (s), 683 (w), 657 (m), 636 (m), 618 (w), 604 (w).

3.5.3 Crystallographic studies.

All diffraction data sets were collected on a Bruker AXS SMART 2K diffractometer mounted with Cu Kα radiation at 100(2) K (SMART software).[31] Cell refinement and data reduction were carried out using SAINT.[32] All structures were solved by direct methods using SHELXS97,[33] and the refinements were done on F^2 by full-matrix least squares.[34] All non-hydrogen atoms were refined anisotropically. The positional parameters for H atoms in water molecules were refined isotropically, but all other hydrogens were constrained to the parent atom using a riding model.

The crystal structures of **3.2a, 3.2b, 3.3** and **3.5** are stabilized by intermolecular hydrogen bonds. The details on O-H···O distances are available from the detailed structure

reports (supporting information). The structure of complex **3.4** contained two disordered solvent molecules of CH_2Cl_2 which were refined isotropically using a constrained model. Disordered solvent molecules were then introduced over two positions and refined using ISOR restrained technique. For the sake of clarity, molecules of solvents (in **3.2b**, **3.3** and **3.4**) and the counter ions (in **3.2b, 3.3,** and **3.5**) have been removed from the ORTEP III[35] diagrams.

All details concerning the refinement of the crystal structures are listed in Tables 3.1 and 3.2. The relevant bond distance and angles are tabulated in tables 3.3, 3.4, 3.5.

3.5.4 Testing the reversible solvato-, vapo-, and thermochromic behaviors of complexes 3.1, 3.2a, 3.4, and 3.5. Dissolving solutions of **3.2a** (8.2-9.8 mM) gave different colors depending on the solvent and the temperature of the solution. At room temperature, **3.2a** is dark olive in acetone, forest-green in CH_3CN, and light blue in MeOH; the color of the CH_2Cl_2 solutions were concentration-dependant, giving light pink in dilute solutions and brown in concentrated solutions. Evaporation of all these solutions regenerated the green solid **3.2a**. Moreover, evaporation of concentrated acetone solutions with heating led to the precipitation of a brownish solid identified as **3.1**. The UV-Vis-NIR spectra of these solutions were recorded and are presented in Figures 3.8-3.11. The thermochromism of the complexes was studied by recording the variable temperature UV-Vis-NIR spectra (-10 to 60 °C). The spectral features are discussed in the Results and Discussion section.

The UV-Vis-NIR spectra for solutions of complexes **3.4** and **3.5** were recorded to monitor any spectral changes as a function of solvent and temperature. Figures 13-15 show the variable temperature spectra of **3.4** in CH_2Cl_2 (4.7 mM), MeOH (3.9 mM), and CH_3CN (8.7 mM). The sensitivity of complex **3.4** to humidity required that its spectra be recorded using crystals of **3.4** that had been kept in a Dry box or in a desiccator containing $CaCl_2$ in order to minimize any direct contact with humidity. The variable temperature spectra recorded for a 6.6 mM CH_2Cl_2 solution of **3.5** are shown in Figure 3.16. The thermochromism of **3.4** and **5** is discussed in the Results and Discussion section.

The vapochromic behavior of **3.1** and **3.2b** was studied briefly, as follows. A crystal of **3.2b** was fixed onto a glass fibre attached to the inside of the cap for a 5 mL drum vial. The cap was then placed on top of the vial containing 0.2 mL of a given solvent (benzene, Et_2O, or toluene). Exposure of the crystal to the solvent vapor caused a color change from green to brown in less than 2 min. Visual inspection of the transformed crystal showed that

it was no longer crystalline. Exposing this solid to ambient humidity brought back the initial green color over a few days.

Supporting Information

Crystallographic data for the structural analysis have been deposited with the Cambridge Crystallographic Data Centre, CCDC No. 633340 (**3.1**), 633341 (**3.2a**), 633342 (**3.2b**), 633343 (**3.3**), 633344 (**3.5**), and 633345 (**3.4**). Copies of this information may be obtained free of charge from The Director, CCDC, 12 Union Road, Cambridge, CB2 1EZ, UK (fax: +44-1223-336-033; email: deposit@ccdc.cam.ac.uk or www: http://www.ccdc.cam.ac.uk).

Acknowledgments

The Natural Sciences and Engineering Research Council of Canada and Fonds Québécois de la Recherche sur la Nature et les Technologies are gratefully acknowledged for their financial support. The authors are grateful to Profs. C. Reber, G. Hanan and W. Skene for access to their Cary spectrometers, and for valuable discussions.

3.6 Reference

(1) (a) Trofimenko, S.; Calabrese, J. C.; Thompson, S. J. *Inorg. Chem.* **1987**, *26,* 1507. (b) Trofimenko, S.; *J. A. Chem. Soc.*, **1970**, *92*, 5118. (c) Trofimenko, S.; Calabrese, J. C.; Domaille, P. J.; Thompson, J. S. *Inorg. Chem.* **1989**, *28*, 1091. (d) Paulo, A.; Correia, J. D. G.; Santos, I. *Rev. Inorg. Chem.* **1998**, *5*, 57. (e) Uehara, K.; Hikichi, S.; Akita, M. *J. Chem. Soc., Dalton Trans.*, **2002**, 3529. (f) Santi, R.; Romano, A. M.; Sommazzi, A.; Grande, M.; Bianchini, C.; Mantovani, G. *J. Mol. Catal. A : Chem.* **2005**, *229*, 191. (g) Shirasawa, N.; Nguyet, T.-T.; Hikichi, S.; Moro-oka, Y.; Akita, M. *Organometallics* **2001**, *20*, 3582. (h) Kisala, J.; Ciunik, Z.; Drabent, K.; Ruman, T.; Wolowiec, S. *Polyhedron* **2003**, *22*, 1645. (i) Rheingold, A. L.; Haggerty, B. S.; Liable-Sands, L. M.; Trofimenko, S. *Inorg. Chem.* **1999**, *38*, 6306. (j) Malbosc, F.; Chauby, V.; Serra-Le Berre, C.; Etienne, M.; Daran, J.; Kalck, P. *Eur. J. Inorg. Chem.* **2001**, 2689.

(2) Trofimenko, S. *J. Am. Chem.* Soc. **1970**, *92*, 1499.

(3) For a few recent reports and reviews on the development of the coordination chemistry of scorpionate ligands see: (a) Tang, T.; Wang, Z.; Xu, Y.; Wang, J.; Wang, H.; Yao, X. *Polyhedron* **1999**, *18*, 2383. (b) Sánchez, G.; Serrano, L. J.; Pérez, J.; Ramírez de Arellano, M. C.; López, G.; Molins, E. *Inorg. Chim. Acta* **1999**, *295*, 136. (c) Seymore, S. B.; Brown, S. N. *Inorg. Chem. 2000, 39*, 325. (d) Tang, L.-F.; Wang, Z.; Jia, W.-L.; Xu, Y.-M.; Wang, J.-T. *Polyhedron* **2002**, *19*, 381. (e) Burzlaff, N.; Hegelmann, I.; Weibert, B. *J. Organomet. Chem.* **2001**, *626*, 16. (f) Mattini, D.; Pellei, M.; Pettinari, C.; Skelton, B.W.; White, A. H. *Inorg. Chim. Acta* **2002**, *333*, 72. (g) Wang, Z.-H.; Tang, L.-F.; Jia, W.-L.; Wang, J.-T.; Wang, H.-G. *Polyhedron* **2002,** *21*, 873. (h) Kläui, W.; Berghahn, M.; Frank, W.; Reiß, G. J.; Schönherr, T.; Rheinwald, G.; Lang, H. *Eur. J. Inorg. Chem.* **2003**, 2059. (i) Mahon, M. F.; McGinley, J.; Molloy, K. C. *Inorg. Chim. Acta* **2003**, *355*, 368. (j) Otero, A.; Fernandez-Baeza. J.; Antinolo, A.; Tejeda, J.; Lara-Sánchez, A. *Dalton Trans.* **2004**, 1499. (k) Pettinari, C.; Pettinari, R. *Coord. Chem. Rev.* **2005**, *249*, 663. (l) Tredget, C. S.; Lawrence, S. C.; Ward. B. D.; Howe, R. G.; Cowley, A.R.; Mountford, P. *Organometallics* **2005**, *24*, 3136. (m) Montoya, V.; Pons, J.; Solans, X.; Font-bardia, M.; Ros, J. *Inorg. Chim. Acta* **2005**, *358*, 2312. (n) Pettinari, C.; Pettinari, R. *Coord. Chem. Rev.* **2005**, *249*, 525.

(4)(a) Hill, M. S.; Mahon, M. F.; Mcginley, J. M. G.; Molloy, K. C. *Polyhedron*, **2001**, *20*, 1995. (b) Reger, D. L.; Grattan, T. C.; Brown, K. J.; Little, C. A.; Lamba, J. J. S.; Rheingold, A. L.; Sommer, R. D. *J. Organomet. Chem.* **2000**, *607*, 120.

(5) Byers, P. K.; Canty, A. J.; Honeyman, R. T. *Adv. Organomet. Chem.* **1992**, *34*, 1. (See in particular pp. 26 and 34.)

(6) Canty, A. J.; Andrew, S.; Skelton, B. W.; Traill, P. R.; White, A. H. *Organometallics* **1995**, *14*, 199.

(7) Reinartz, S.; Brookhart, M.; Templeton, J. L. *Organometallics* **2002**, *21*, 247.

(8) Byers, P. K.; Canty, A. J.; Skelton, B. W.; White, A. H. *Organometallics* **1990**, *9*, 826.

(9) For representative reports on coordination complexes of Ni featuring poly(pyrazolyl)alkane ligands see: (a) Mahon, M. F.; McGinley, J.; Molloy, K. C.; *Inorg. Chim. Acta* **2003**, *355*, 368. (b) Wolfgang, K.; Berghahn, M.; Frank, W.; Reiss, G. J.; Schonherr, T.; Rheinwald, G.; Lang, H. *Eur. J. Inorg. Chem.* **2003**, *11*, 2059. (c) Pettinari, C.; Marchetti, F.; Cingolani, A.; Leonesi, D.; Colapietro, M.; Margadonna, S. *Polyhedron* **1998**, *17*, 4145. (d) Mann, K. L.; Jeffery, J. C.; McCleverty, J. A.; Thornton, P.; Ward, M. D. *J. Chem. Soc., Dalton Trans.* **1998**, *1*, 89. (e) Pettinari, C.; Cingolani, A.; Bovio, B. *Polyhedron* **1996**, *15*, 115. (f) Astley, T.; Gulbis, J. M.; Hitchman M. A.; Tiekink, E. R. T. *J. Chem. Soc., Dalton Trans.* **1993**, 509. (g) Mesubi, M. A.; Omotowa, B. A. *Synth. React. Inorg. Metal-Org. Chem.* **1993**, *23*, 213. (h) Astley, T.; Canty, A. J.; Hitchman, M. A.; Rowbottom, G. L.; Skelton, B. W.; White, A. H. *J. Chem. Soc., Dalton Trans.* **1991**, 1981. (i) Reedijk, J.; Verbiest, J. *Trans. Met. Chem.* **1979**, *4*, 239. (j) Jansen, J. C.; Van Koningsveld, H.; Van Ooijen, J. A. C.; Reedijk, J. *Inorg. Chem.* **1980**, *19*, 170. (k) Reedijk, J.; Verbiest, J. *Trans. Met. Chem.* **1978**, *3*, 51.

(10) For recent reports on organometallic complexes of Pd based on poly(pyrazolyl)alkane ligands see: (a) Sanchez, G.; Serrano, L. J.; Pérez, J.; Ramirez de Arellano, M. C.; Lopez, G.; Molins, E. *Inorg. Chim. Acta* **1999**, *295*, 136. (b) Arroyo, N.; Gomez-de La Tore, F.; Jalon, A. F.; Manzano, B. R.; Moreno-Lara. B.; Rodriguez., A. M. *J. Organomet. Chem.* **2000**, *603*, 174. (c) Tsuji, S.; Swenson, D. C.; Jordan, R. F. *Organometallics* **1999**, *18*, 4758.

(11) (a) Castonguay, A.; Sui-Seng, C.; Zargarian, D.; Beauchamp, A. L. *Organometallics* **2006**, *25*, 602. (b) Groux, L. F.; Bélanger-Garlépy, F.; Zargarian, D. *Can. J. Chem.* **2005**, *83*, 634. (c) Gareau, D.; Sui-Seng, C.; Groux, L. F.; Brisse, F.; Zargarian, D.

Organometallics **2005**, *24*, 4003. (d) Chen, Y.; Sui-Seng, C.; Zargarian, D. *Angew. Chemie, Int. Ed. Engl.* **2005**, *44*, 7721. (e) Boucher, S.; Zargarian, D. *Can. J. Chem.* **2005**, *84*, 233. (f) Chen, Y.; Sui-Seng, C.; Boucher, S.; Zargarian, D. *Organometallics* **2005**, *24*, 149. (g) Fontaine, F.-G.; Zargarian, D. *J. Am. Chem. Soc.* **2004**, *126*, 8786. (h) Groux, L. F.; Zargarian, D. *Organometallics* **2003**, *22*, 4759. (i) Fontaine, F.-G.; Nguyen, R.-V.; Zargarian, D. *Can. J. Chem.* **2003**, *81*, 1299. (j) Groux, L. F.; Zargarian, D. *Organometallics* **2003**, *22*, 3124. (k) Groux, L. F.; Zargarian, D.; Simon, L. C.; Soares, J. B. P. *J. Mol. Catal. A* **2003**, *19*, 51. (l) Rivera, E.; Wang, R.; Zhu, X. X.; Zargarian, D.; Giasson, R. *J. Molec. Catal. A* **2003**, *204-205*, 325. (m) Zargarian, D. *Coord. Chem. Rev.* **2002**, *233-234*, 157. (n) Wang, R.; Groux, L. F.; Zargarian, D. *Organometallics* **2002**, *21*, 5531. (o) Wang, R.; Groux, L. F.; Zargarian, D. *J. Organomet. Chem.* **2002**, *660*, 98. (p) Fontaine, F.-G.; Zargarian, D. *Organometallics* **2002**, *21*, 401. (q) Dubois, M.-A.; Wang, R.; Zargarian, D.; Tian, J.; Vollmerhaus, R.; Li, Z.; Collins, S. *Organometallics* **2001**, *20*, 663. (r) Groux, L. F.; Zargarian, D. *Organometallics* **2001**, *20*, 3811. (s) Groux, L. F.; Zargarian, D. *Organometallics* **2001**, *20*, 3811. (t) Fontaine, F.-G.; Dubois, M.-A.; Zargarian, D. *Organometallics* **2001**, *20*, 5156. (u) Wang, R.; Bélanger-Gariépy, F.; Zargarian, D. *Organometallics* **1999**, *18*, 5548. (v) Fontaine, F.-G.; Kadkhodazadeh, T.; Zargarian, D. *Chem. Commun.* **1998**, 1253. (w) Vollmerhaus, R.; Bélanger-Gariépy, F. ; Zargarian, D. *Organometallics* **1997**, *16*, 4762. (x) Huber, T. A.; Bayrakdarian, M.; Dion, S.; Dubuc, I.; Bélanger-Gariépy, F.; Zargarian, D. *Organometallics* **1997**, *16*, 5811. (y) Bayrakdarian, M.; Davis, M. J.; Reber, C.; Zargarian, D. *Can. J. Chem.* **1996**, *74*, 2194. (z) Huber, T. A.; Bélanger-Gariépy, F.; Zargarian, D. *Organometallics* **1995**, *14*, 4997.

(12) (a) Michaud, A.; Fontaine, F.-G.; Zargarian, D. *Inorg. Chim. Acta* **2006**, *359*, 2592. (b) Nolet, M.-C.; Michaud, A.; Bain, C.; Zargarian, D.; Reber, C. *Photochem. Photobiology* **2006**, *82*, 57. (c) Michaud, A.; Fontaine, F.-G.; Zargarian, D. *Acta Crystallogr.* **2005**, E *61*, m784. (b) Michaud, A.; Fontaine, F.-G.; Zargarian, D. *Acta Crystallogr.* **2005**, E *61*, m904.

(13) Michaud, A. M. Sc. Desertation, Université de Montréal, 2004.

(14) Baho, N.; Zargarian, D. *Inorg. Chem.* **2007**, *46*, 299.

(15) For a detailed discussion of these and similar phenomena see: (a) Morassi, R.; Bertini, I.; Sacconi, L. *Coord. Chem. Rev.*, **1973**, *11*, 343. (b) Reichardt, C. *Angew. Chem., Int. Ed. Engl.* **1965**, *4*, 29.

(16)(a) Bloomquist, D. R.; Willett, R. D. *Coord. Chem. Rev.* **1982**, *47*, 125. (b) Fabbrizzi, L.; Micheloni, M.; Paoletti, P. *Inorg. Chem.* **1974**, *13*, 1974.

(17) Shaw, J. L.; Cardon, T. B.; Lorigan, G. A.; Ziegler, C. J. *Eur. J. Inorg. Chem.* **2004**, 1073.

(18) Shiu, K.-B.; Yeh L.-Y.; Peng. S.-M.; Cheng, M.-C. *J. Organomet. Chem.* **1993**, *460*, 203.

(19) Reger, L. D.; Gardinier, J. R.; Smith, M. D. *Inorg. Chem.* **2004**, *43*, 3825.

(20) Addison, A. W.; Rao, T. N.; Reedijk, J; van Rijn, J.; Verschoor, G. C. *J. Chem. Soc., Dalton Trans.* **1984**, 1349. The structural index τ is determined from the equation $\tau = (\beta - \alpha)/60$, wherein β and α are, respectively, the largest basal angles ($\beta > \alpha$). The τ values for perfectly square pyramidal and trigonal bipyramidal structures are 0 and 1, respectively.

(21) A number of other dinickel species with similar structural motifs have also been reported, including $[(dab)NiBr_2]_2$ (dab = N,N'-di-*tert*-butyldiazabutadiene; $\tau \sim 0.12$; Jameson, G. B.; Oswald, H. R.; Beer, H. R. *J. Am. Chem. Soc.* **1984**, *106*, 1669) and $[(dmp)NiBr_2]_2$ (dmp = Bis(2,9-dimethyl-1,10-phenanthroline; $\tau \sim 0.40$; Butcher, R. J.; Sinn, E. *Inorg. Chem.* **1977**, *16*, 2334).

(22) The authors thank one of the reviewers of the manuscript for this suggestion.

(23) Collinson, S. R.; Schröder, M. Nickel: Inorganic and Coordination Chemistry. In *Encyclopedia of Inorganic Chemistry*. 2nd ed.; King, R. B., Ed.; Wiley InterScience: Vol. VI.

(24) (a) Landry-Hum, J.; Bussière, G.; Daniel, C.; Reber, C. *Inorg. Chem.* **2001**, *40*, 2595. (b) Bussière, G.; Beaulac, R.; Cardinal-David, B.; Reber, C. *Coord. Chem. Rev.* **2001**, *219-221*, 509.

(25) Very similar "weak shoulders" have been observed in the absorption spectra of many octahedral Ni(II) complexes, including $[Ni(NH_3)_6]^{2+}$. For a discussion of this phenomenon, including detailed analyses of these transitions based on Tanabe-Sugano diagrams and modern theoretical models, see : (a) Bussière, G.; Reber, C. *J. Am. Chem. Soc.* **1998**, *120*, 6306. (b) Triest, M.; Bussière, G.; Bélisle, H.; Reber, C. *J. Chem. Ed.* **2000**, *77*, 670. Available at: http://jchemed.chem.wisc.edu/jcewww/articles/JCENi/JCENi.html. (c) Bussière, G.; Reber, C.; Neuhauser, D.; Walter, D. A.; Zink J. I. *J. Phys. Chem. A.* **2003**, *107*, 1258. (d) Nolet, M.-C.; Beaulac, R.; Boulanger, A.-M.; Reber, C. *Struc. Bond.* **2004**,

107, 145. (e) González, e.; Rodrigue-Witchel, A.; Reber, C. *Coord. Chem. Rev.* **2007**, *251*, 351.

(26) For a few recent reports on a variety of Ni(II) complexes of (N-N) donor ligands containing coordinated MeOH see: (a) Sun, Y.-J; Cheng, P.; Yan, S.-P; Jiang, Z.-H; Liao, D.-Z; Shen, P.-W. *Inorg. Chem. Comm.*, **2000**, *3*, 289. (b) Dorta, R.; Shimon, L. J. W.; Rozenberg, H.; Ben-David, Y.; Milstein, D. *Inorg. Chem.* **2003**, *42*, 3160. (c) Casabó, J.; Pons, J.; Siddiqi, K. S.; Teixidor, F.; Molins, E.; Miravitlles, C. *J. Chem. Soc., Dalton Trans.* **1989**, 1401. (d) Makowska-Crzyska, M. M.; Szajna, E.; Shipley, C.; Arif, A. M.; Mitchell, M. H.; Halfen, J. A.; Berreau, L. M. *Inorg. Chem.* **2003**, *42*, 7472.

(27) Examples of penta- and hexa-coordinated Ni(II) complexes with a coordinated water molecule: (a) Adams, H.; Clunas, S.; Fenton, D. E. *Acta Crystallogr.* **2004**, *E60*, m338. (b) Matecka, M.; Rybarczyk-Pirek, A.; Olszak, T. A.; Malinowska, K.; Ochocki, J. *Acta Crystallogr.* **2001**. *C57*, 513. (d) Bazzicalupi, C.; Bencini, A.; Duce, C.; Fornasari, P.; Giorgi, C.; Paoletti, P.; Pardini, R.; Tinè, M. R.; Valtancoli, B. Dalton *Trans.* **2004**, 463.

(28) It should be recalled, however, that the only crystals obtained from blue solutions of **2a** in MeOH are those of light-green **2b**, implying that the octahedral species present in these solutions is a more soluble, presumably neutral compound such as $[(dpdpm)NiBr_2(OH_2)(L)]$ (L = H_2O or MeOH).

(29) (a) Larue, B.; Tran, L.-T.; Luneau, D.; Reber, C. *Can. J. Chem.* **2003**, *81*, 1168. (b) Sacconi, L.; Nannelli, P.; Nardi, N.; Campigli, U. *Inorg. Chem.* **1965**, *4*, 943.

(30) Ciampolini, M. *Inorg. Chem.* **1966**, *5*, 35.

(31) SMART (**2001**). Release 5.625. Bruker Molecular Analysis Research Tool; Bruker AXS Inc., Madison, WI.

(32) SAINT (**2003**). Release 7.06. Integration Software for Single Crystal Data. Bruker AXS Inc., Madison, WI.

(33) Sheldrick, G. M. SHELXS, Program for the Solution of Crystal Structures. University of Goettingen. Germany, 1997.

(34) (a) Bruker (1997). SHELXTL (1997). Release 5.10; The Complete Software Package for Single Crystal Structure Determination. Bruker AXS Inc., Madison, USA. (b) Bruker (1999a). SAINT (2003). Release 7.06. Integration Software for Single Crystal Data. Bruker AXS Inc., Madison, USA. (c) Bruker (1999b). SMART (2001) Release 5.625; Bruker

Molecular Analysis Research Tool, Bruker AXS Inc., Madison, USA. (d) Sheldrick, G. M. (1996). SADABS, Bruker Area Detector Absorption Corrections. (e) Bruker AXS Inc., Madison, USA. (f) Sheldrick, G. M. (1997a). SHELXS97. Program for Crystal Structure solution. University of Gottingen, Germany. (g) Sheldrick, G. M. (1997b). SHELXL97. Program for crystal structure refinement. University of Gottingen, Germany. (h) Spek, A. L. (2000). PLATON, 2000 version; Molecular Geometry Program, University of Utrecht, Utrecht, Holland.

(35) Burnett, M. N.; Johnson, C. K. (1996). ORTEPIII - Oak Ridge Thermal Ellipsoid Plot Program for Crystal Structure Illustrations, Technical Report ORNL-6895. Oak Ridge National Laboratory, TN.

Chapter 4: $[(L_2L'NiBr_2)(AgBr)]_2$: a Tetrametallic Ensemble Arising from Halophilicity of Silver

4.1 Introduction

Organonickel complexes have played a central role in the discovery and development of olefin oligo- and polymerization processes over the past few decades. More recently, a variety of nickel complexes featuring imine-type ligands have exhibited high catalytic activities in the preparation of a range of polyolefins. The active intermediates in most of these polymerization processes are believed to be the cationic species $[(imine)_2Ni(P)(olefin)]^+$ (P = H, alkyl, or the growing polymer chain) that are generated in-situ from the neutral halide precursors $(imine)_2NiX_2$. One notable example of the latter is the family of chelating α–diimine compounds $(\kappa^N,\kappa^{N'}\text{-ArN=CR-CR=NAr})NiX_2$ that are used in the Versipol® process.[1] Closely related Ni compounds bearing ligands based on pyridinylimine units are also used for olefin polymerization or co-polymerization processes.[2] Alternatively, some oligomerization precatalysts are based on cationic nickel compounds featuring labile ligands only. For instance, $[Ni(NCMe)_6]^{2+}$ catalyzes the oligomerization of propylene[3] and n-butenes[4] in the presence of organochloroaluminate ionic liquids.

The above considerations and our long-standing interest in the reactivities of organonickel complexes[5] prompted us to investigate the chemistry of nickel compounds featuring both imine-type chelating ligands and labile donors such as H_2O, CH_3CN, etc. We elected to focus our studies on poly(pyrazolyl)alkane ligands for many reasons, including the similarities of these ligands to the α–diimine and pyridinylimine chelates mentioned above, the possibility of accessing a wide array of poly(pyrazolyl)alkanes via simple synthetic protocols,[6] and the relatively underdeveloped coordination chemistry of nickel complexes featuring this family of ligands.[7] We have thus developed synthetic routes to a series of new bis- and tris(pyrazolyl)alkane-Ni complexes and studied their structural and spectroscopic features.[8] Most of the compounds studied to date are paramagnetic species displaying non-rigid and variable coordination geometries (octahedral, tetrahedral, or square pyramidal). Although we have not succeeded in isolating organometallic derivatives

of our compounds, recent literature reports indicate that nickel halide adducts of certain poly(pyrazolyl)alkanes can generate organonickel species that are efficient catalysts for olefin oligomerization reactions.[9]

The synthesis, solid state structure, and photophysical properties of the compound (dpdpm)$NiBr_2(H_2O)$ (**3.2a**, dpdpm = diphenyl(dipyrazolyl)methane) were reported recently. [10] We surmised that abstraction of a Br^- from **3.2a** should furnish $[(dpdpm)NiBr(H_2O)]^+$ that might display interesting catalytic reactivities under appropriate conditions owing to its similarity to the species $[(imine)_2Ni(P)(olefin)]^+$ discussed above. The present report describes the unexpected formation of $[\{(dpdpm)(NCMe)NiBr_2\}(AgBr)]_2$, **4.1,** and $[(dpdpm)NiBr(NCMe)_3]^+$, **4.2**, that were obtained by abstraction of bromide from **3.2a**.

4.2 Results and Discussion

The aquo complex **3.2a** was reacted with $AgPF_6$ to abstract one of its bromide ligands and form the target cationic complex $[(dpdpm)NiBr(H_2O)]^+$. Stirring a deep-red CH_2Cl_2 solution of **3.2a** (0.01 M) and $AgPF_6$ (Ni : Ag = 1:1) at room temperature resulted in a color change to yellow-green and the precipitation of a beige solid. Filtration of the reaction mixture and evaporation of the filtrate gave a light green solid. After numerous unsuccessful attempts to grow single crystals of this new compound in non-coordinating solvents, we undertook recrystallization from Et_2O/CH_3CN. Light green single crystals of the neutral compound **4.1** were obtained from cold solutions (ca. -30 °C), whereas room temperature solutions gave light blue single crystals of the cationic tris(acetonitrile) complex **4.2** (Scheme 4.1).

Formation of the tris(acetonitrile) cationic complex **4.2** can be rationalized by the general tendency of Ni(II) coordination compounds for attaining octahedral geometries, especially in the presence of strongly donor solvents such as acetonitrile. In contrast, the formation of **4.1**, which does not involve bromide abstraction from **4.1**, was unexpected. The incorporation of acetonitrile in the structures of these compounds indicated that their formation might be more efficient if the bromide abstraction reaction were conducted in this solvent. Thus, dropwise addition of a dark green acetonitrile solution of **3.2a** (0.03 M) to a stirring suspension of $AgPF_6$ in acetonitrile (Ni : Ag = 1:1) resulted in an instantaneous color change to sky blue and the concomitant formation of an off-white precipitate. Interestingly, this precipitate (presumably AgBr) turned pale green upon standing in the

reaction mixture for a few minutes. Filtration of the mixture and evaporation of the filtrate gave a light green solid that was recrystallized as above from Et_2O/CH_3CN to give complex **4.1** (19% yield) and complex **4.2** (35% yield).

Scheme 4.1

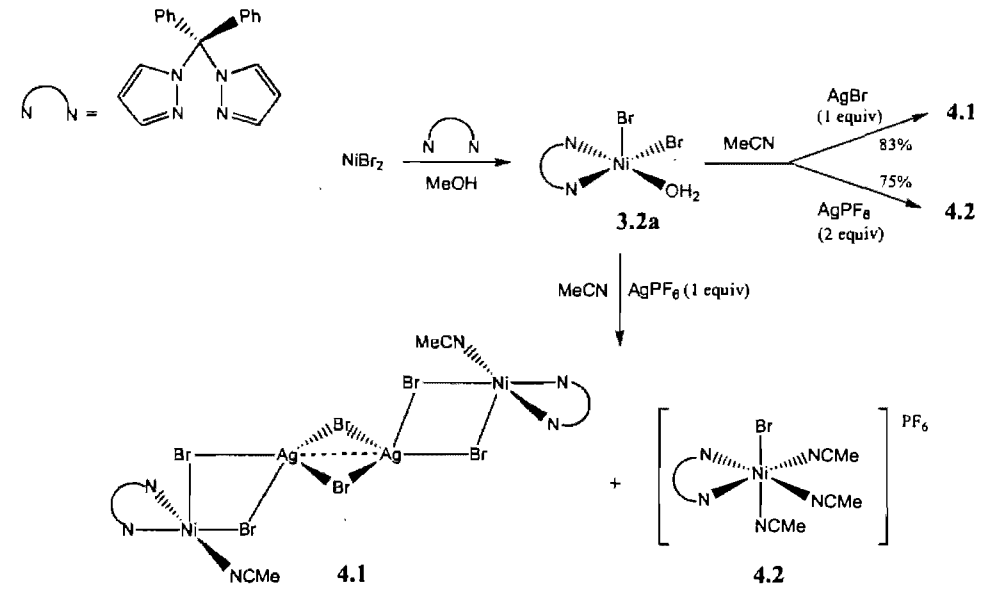

Complex **4.1** was also obtained in 83% isolated yield by stirring an equimolar mixture of **4.1** and AgBr in acetonitrile for 3 h (Scheme 4.1); this observation confirms that the unexpected formation of this tetrametallic species in the reaction of **3.2a** with $AgPF_6$ arises via the reaction of in-situ generated AgBr with unreacted **3.2a**. Consistent with this proposal, formation of **4.1** was suppressed completely when we reacted **3.2a** with 2 equivalents of $AgPF_6$, giving analytically pure **4.2** in 75% yield. Attempts to abstract both Br^- ligands of **3.2a** in reactions with 3 or more equivalents of $AgPF_6$ gave a reddish solid which remains unidentified, because it recrystallization did not yield single crystals.

Complex **4.1** is fairly insoluble, but soxhlet extraction over 2-3 days allowed us to prepare fairly concentrated solutions of acetonitrile from which analytically pure samples were obtained at low temperatures. Complex **4.2**, on the other hand, is freely soluble in acetonitrile; pure samples of this compound can be precipitated by allowing Et_2O vapors to diffuse into fairly concentrated acetonitrile solutions at room temperature. The different solubilities of **4.1** and **4.2** in acetonitrile facilitate the purification of reaction mixtures by repeated extractions.

Solid state structures of 4.1 and 4.2. Single crystals of **4.1** and **4.2** were subjected to X-ray diffraction studies. The collected diffraction data resulted in fairly accurate structures for these complexes, as reflected in the R_I values of ca. 0.0546 and 0.0399, respectively. All the details concerning the refinement of the crystals structure are listed in the supporting information at the end of this thesis (Appendix IV). The ORTEP diagrams for **4.1** and **4.2** are shown in Figures 4.1-4.3, and the bond distances and angles are given in Tables 4.1 and 4.2. All details concerning the refinement of the crystal structures are listed in Tables 4.3.

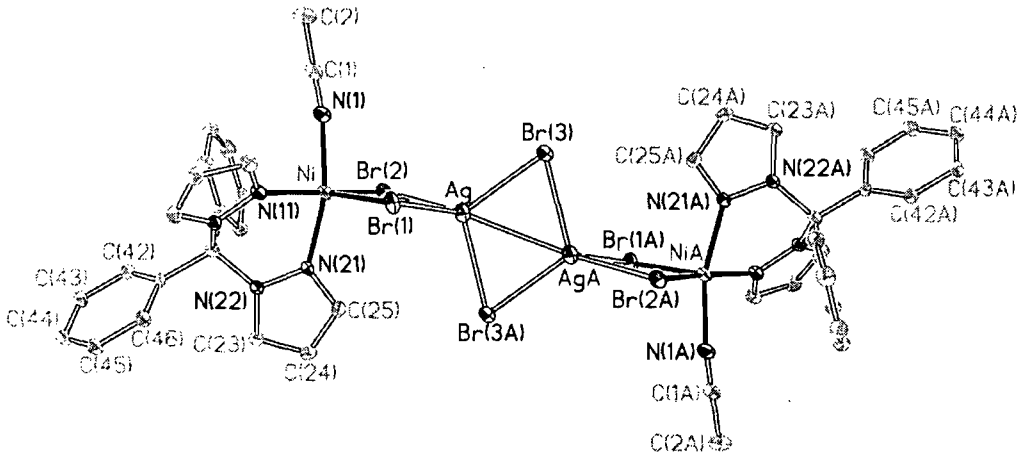

Figure 4.1. ORTEP view of complex **4.1** showing the Ag-Br-Ag-Br moiety in the plane of the paper. Thermal ellipsoids are shown at 30% probability.

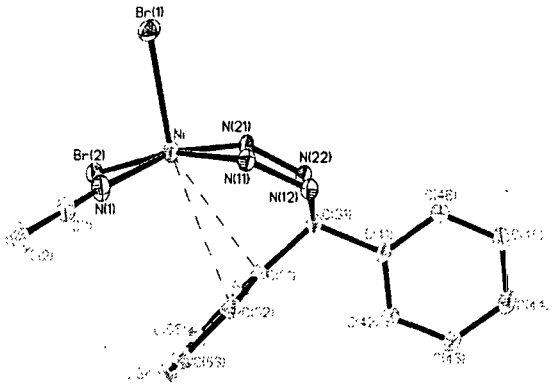

Figure 4.2. Partial view of the ORTEP diagram for complex **4.1** showing the boat configuration adopted by the dpdpm ligand without the carbon atoms of the pyrazolyl rings and the long-range Ni-Ph interactions

Table 4.1. Selected bond lengths (Å) and angles (degrees) for **4.1**

[{(dpdpm)(CH_3CN)$NiBr_2$}($AgBr$)]$_2$			
Ni-N(11)	2.050 (3)	Br(1)-Ag-Br(3A)	105.507 (1)
Ni-N(21)	2.036 (3)	Br(2)-Ag-Br(3)	120.049 (1)
Ni-N(1)	2.033 (4)	Br(2)-Ag-Ag(A)	141.64 (2)
Ni-Br(1)	2.4713 (8)	Br(2)-Ag-Br(3A)	111.657 (1)
Ni-Br(2)	2.4975 (8)	Br(3)-Ag- Ag(A)	57.923 (14)
Ag-Br(1)	2.7371 (5)	Br(3)-Ag-Br(3A)	112.858 (1)
Ag-Br(2)	2.7188 (6)	Br(3A)-Ag-Ag(A)	54.935 (15)
Ag-Br(3)	2.6465 (5)	N1-Ni-N(21)	163.79 (14)
Ag-Br(3A)	2.7397 (6)	N1-Ni-N(11)	86.37 (14)
AgA-Br(3)	2.7397 (6)	N1-Ni-Br(1)	96.03 (11)
AgA-Ag	2.9794 (7)	N1-Ni-Br(2)	91.93 (11)
Ag-Br(1)-Ni	85.67 (2)	N11-Ni-Br(1)	94.67 (10)
Ag-Br(2)-Ni	85.55 (2)	N11-Ni-Br(2)	165.49 (10)
Ag-Br(3)-Ag(A)	67.142 (15)	N21-Ni-Br(1)	98.44 (10)
Br(1)-Ag-Br(2)	88.345 (16)	N21-Ni-Br(2)	92.77 (9)
Br(1)-Ag-Br(3)	115.312 (1)	N21-Ni-N(11)	85.21 (13)
Br(1)-Ag-Ag(A)	128.73 (2)	Br(1)-Ni-Br(2)	99.84(3)

A = -x+1,-y+1,-z

The molecular structure of complex **4.1** consists of two pentacoordinated Ni(II) moieties connected to an Ag_2Br_2 core through bridging bromides. Inspection of the main

structural parameters shows a great resemblance between the Ni moieties in **4.1** and in **3.2a**. For instance, the nickel centers in both **4.1** and **3.2a** adopt a slightly distorted square pyramidal geometry reflected in *trans* angles of ca. 161-165° (N-Ni-N, N-Ni-Br, and N-Ni-O) and *cis* angles of 84-100°.[11] The low values of the τ index for **3.2a** (0.02) and **4.1** (0.03) are also very typical of other square pyramidal structures.[12] In both compounds, the Br occupies the axial position, presumably because of its greater trans influence compared to H_2O/CH_3CN. As expected, $Ni\text{-}Br_{axial}$ is somewhat shorter than $Ni\text{-}Br_{basal}$ in both compounds (2.47 vs 2.50 Å in **4.1**; 2.46 vs 2.48 Å in **3.2a**). The somewhat longer Ni-Br distances in **4.1** are presumably due to the bridging interactions with the Ag core.

Another common structural feature present in **3.2a** and **4.1** is the virtually identical boat configuration adopted by the metallacycle Ni-N-N-C-N-N; this configuration facilitates long-range interactions between the Ni centers and C=C bonds of the Ph substituents in both complexes (Ni···C = 3.06 and 3.42 Å in **4.1** vs. 3.04 and 3.13 Å in **3.2a**). It is significant to note that CH_3CN displaces the water ligand in **4.1** but not the intramolecular Ni-Ph interactions that fill the sixth coordination site around the Ni center.

The overall geometry of the silver center in each $AgBr_4$ moiety of **4.1** is nearly tetrahedral, as reflected in a) four Br-Ag-Br angles of 105°-115° that are close to ideal tetrahedral values, b) three fairly symmetrical Ag-Br distances of ca. 2.74 Å, and c) the nearly perpendicular (88.12°) planes defined by Ni-Br(1)-Ag-Br(2) and the Ag_2Br_2 core. The main distortions from ideal tetrahedral geometry include two Br-Ag-Br angles of 88° and 120°, and the shorter Ag-Br bond distance of 2.65 Å. Although the tetra-coordinated Ag centers should, in principle, be electronically saturated, the relatively short Ag-Ag distance of 2.979 Å indicates that there is a significant argentophilic interaction in complex **4.1**.

Chart 1

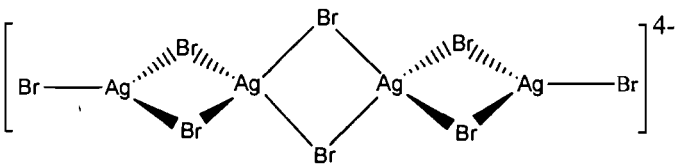

For comparison, much longer Ag-Ag distances have been reported for the tetra-coordinated Ag centers in the bromoargentate anion $[Br\{Ag(\mu\text{–}Br)_2\}_3AgBr]^{4-}$ (3.595 Å)[13] and the bromo(cyano)argentate anion $[Ag_5(CN)Br_6]^{2-}$ (3.190-3.591 Å, Chart 1). [14]

Compounds featuring multiple units of tetrahedral silver halides are relatively rare, but they are attracting increased attention because of their optical properties. For instance, solid state samples of $[Ag_5(CN)Br_6]^{2-}$ show a purple emission band at 390 nm upon photoexcitation at 307 nm (lifetime of 7.0 ps); the Ag-Ag interactions are believed to have an important influence on this emission.

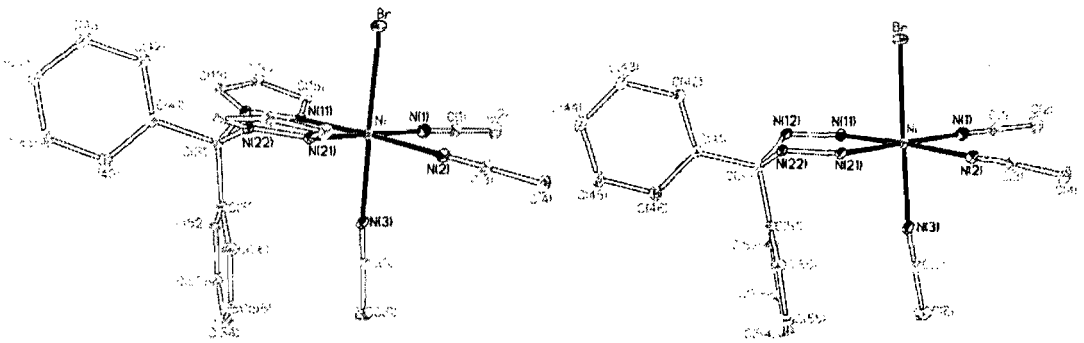

Figure 4.3. ORTEP diagrams of complex **4.2**, with (left diagram) and without the carbon atoms of the pyrazolyl rings. Thermal ellipsoids are shown at 30% probability.

Table 4.2. Selected bond distances (in Å) and angles (in degrees) for **4.2**

[(dpdpm) $NiBr(CH_3CN)_3]PF_6$			
Ni-N(11)	2.050(3)	N(21)-Ni-N(2)	90.96(11)
Ni-N(21)	2.055(3)	N(21)-Ni-N(3)	96.04(11)
Ni-N(1)	2.070(3)	N(1)-Ni-N(2)	87.32(12)
Ni-N(2)	2.085(3)	N(1)-Ni-N(3)	84.89(11)
Ni-N(3)	2.151(3)	N(2)-Ni-N(3)	87.90(11)
Ni-Br	2.5458(6)	Br-Ni- N(11)	89.04 (8)
N(11-Ni-N(21)	88.35(11)	Br-Ni- N(21)	87.87(7)
N(11)-Ni-N(1)	93.40(11)	Br-Ni- N(1)	91.24(8)
N(11)-Ni-N(2)	177.59(11)	Br-Ni- N(2)	93.24(8)
N(11)-Ni-N(3)	89.88(11)	Br-Ni- N(3)	175.92(8)

The coordination geometry around the nickel center in complex **4.2** (Figure 4.3) is slightly distorted octahedral, with *cis* and *trans* bond angles ranging from 88 to 93° and 176 to 178° (Table 4.2). The occupation of the sixth coordination site by a molecule of acetonitrile results in the displacement of the Ni-Ph interactions, which in turn changes the conformation of the six-membered chelate ring from a boat configuration to a half-chair

conformation. This is reflected in the small angle between the coordination planes N11-N12-N22-N21 and N11-N21-N2-N1 (2.27°) and the nearly parallel orientations of the Ni-N3 and C31-C51 vectors. Inspection of the five Ni-N bond distances in **4.2** indicate that the trans influences of the three different ligands follow the order Br > NCMe ~ dpdpm. Complex **4.2** is isostructural to the complex $[(\kappa^N,\kappa^N,\kappa^N\text{-HBpz}_3)\text{Ni(NCMe)}_3][OSO_2CF_3]$;[15] the fairly long Ni-N_{NCMe} distances in this cationic complex (2.12-2.13 Å) indicate that the anionic tris(pyrazolyl)borate ligand has a greater trans influence than the neutral bis(pyrazolyl)alkane ligand dpdpm.

4.3 Concluding remarks

The results described in this chapter reinforce the lability of complex **3.2a** implying that we can not predict the results of this kind of reactions. The label behavior of this penta-coordinated complex **3.2a** is due to several aspects; first the penta-coordinations geometry and the empty axial position, the label H_2O molecules can be considered as an active aspects. The lability of the acetonitrile ligand makes these cationic complexes potentially interesting precursors for preparing other Ni compounds or as pre-catalysts.

4.4 Experimental

4.4.1 General.

All manipulations were performed under an inert atmosphere of N_2 using standard schlenk techniques and drybox. Unless otherwise indicated, dry, oxygen-free solvents were employed throughout. The main ligand used in this study, diphenyl(dipyrazolyl)methane (dpdpm), was synthesized according to a published procedure,[13b] and complex $[(\text{dpdpm})NiBr_2(H_2O)]$ (**3.2a**) has been prepared according to the procedure in chapter 3. The NMR spectra were recorded on a Bruker Av400 (^{1}H at 400 MHz). The IR spectra were recorded between 4000 and 400 cm^{-1} using KBr pellets on a Perkin Elmer Spectrum One spectrophotometer using the Spectrum v.3.01.00 software. The UV-Vis-NIR spectra were recorded between 1300 and 250 nm with a 1 cm quartz cell on a Varian Cary 500i; baseline correction was applied prior to recording the spectra. The magnetic susceptibility measurements were carried out at room temperature using the Gouy method with a Johnson Matthey Magnetic Susceptibility Balance calibrated on $[HgCo(SCN)_4]$ samples. The

elemental analyses (C, H, and N) were performed in duplicate by Laboratoire d'Analyse Élémentaire de l'Université de Montréal.

4.4.2 Syntheses.

[{(dpdpm)(CH_3CN)$NiBr_2$}(AgBr)]$_2$ (4.1). A solution of **3.2a** (0.2 g, 0.37 mmol) in acetonitrile (15 mL) was added to a suspension of AgBr (0.065 g, 0.35 mmol) in acetonitrile (15 mL). A green light solid precipitated immediately. The mixture was filtered after 3 h of stirring at room temperature and the solid was washed with a minimum of acetonitrile (0.24 g, 86% crude yield). Crystals suitable for X-ray analysis were obtained by slow diffusion of ether into an acetonitrile solution of the compound kept at -30 °C. IR (KBr): υ (cm^{-1}) 3375 (br), 3156 (m), 3112 (w), 3086 (m), 2979 (m), 2915 (m), 2319 (s), 2291 (s), 1825 (w), 1623 (m), 1508 (m), 1489 (m), 1450 (s), 1436 (m), 1411 (s), 1385 (m), 1334 (w), 1316 (vs), 1256 (m), 1225 (m), 1211 (s), 1199 (m), 1187 (w), 1173 (w), 1101 (s), 1085 (s), 1063 (vs), 994 (m), 943 (m), 923 (m), 891 (m), 868 (m), 856 (w), 840 (w), 774 (s), 764 (s), 746 (vs), 700 (s), 657 (w), 642 (w), 609 (w), 511 (w). mp. 248 °C. $\mu_{eff.}$ 3.33 BM. Anal. Calc. for $C_{42}H_{42}Ag_2Br_6N_{10}Ni_2$: C, 33.73; H, 2.56; N 9.37. Found: C, 33.42; H, 2.52; N, 9.33 %.

[(dpdpm)NiBr(CH_3CN)$_3$]PF_6.CH_3CN (4.2). A solution of **3.2a** (0.2 g, 0.35 mmol) in acetonitrile (15 mL) was added to a suspension of $AgPF_6$ (0.18 g, 0.7 mmol) in acetonitrile (20 mL). The mixture was stirred for 15 min at room temperature and filtered to separate the precipitate (off-white) and the blue filtrate. Evaporation of the filtrate gave a blue solid (0.19g, 75% crude yield), which was recrystallized by slow diffusion of ether into an acetonitrile solution kept at room temperature to give crystals suitable for X-ray analysis. ^{1}H NMR (CD_3CN): δ 7.94 (br), 7.83 (br), 7.71(br), 7.61 (br), 7.43 (br), 6.94. IR (KBr): υ (cm^{-1}) 3375 (br), 3156 (m), 3112 (w), 3086 (m), 2979 (m), 2915 (m), 2317 (s), 2288 (s), 1634 (m), 1515 (m), 1490 (s), 1450 (s), 1436 (s), 1408 (s), 1383 (m), 1307 (vs), 1250 (m), 1222 (m), 1191 (s), 1169 (m), 1140 (w), 1107 (m), 1070 (s), 1085 (w), 1001 (w), 842 (vs), 754 (s), 700 (s), 659 (m), 637 (m), 603 (w), 559 (s). UV-Vis (CH_3CN): (λ (nm), ε $(mol/L)^{-1}(cm)^{-1}$): (336, 52.02), (582, 7.87), (735, 2.49), (952, 6.13). mp. 115 °C. Anal. Calc. for $C_{25}H_{25}$ N_7PF_6BrNi: C, 42.47; H, 3.56; N, 13.87. Found: C, 42.39; H, 3.54; N, 14.01%.

4.4.3 Crystallographic studies. All diffraction data sets were collected on a Bruker AXS SMART 2K diffractometer mounted with Cu Kα radiation at 173(2) and 100(2) K (SMART software).[16] Cell refinement and data reduction were carried out using SAINT.[17] All structures were solved by direct methods using SHELXS97,[18] and the refinements were done on F^2 by full-matrix least squares. [19] All non-hydrogen atoms were refined anisotropically. The structure of complex **4.2** contained one disordered solvent molecules of CH_3CN located on inversion centre that were refined isotropically using a constrained model. For the sake of clarity, the solvent molecule and the counter ions in **4.2** have been removed from the ORTEP III[20] diagram. The refinements of the crystal structures are listed in Tables 4.3.

Table 4.3. Crystallographic data for **4.1** and **4.2**

	4.1	**4.2**
Formula	$C_{42}H_{38}Ag_2Br_6N_{10}Ni_2$	$C_{26}H_{26.5}BrF_6N_{7.5}NiP$
Mol wt	1495.44	727.64
Cryst color, habit	Green	Blue
Cryst dimens, mm	0.49×0.32×0.14	0.44×0.22×0.22
Symmetry	Monoclinic	Triclinic
Space group	P^21/c	P-1
a, Å	11.7221(3)	11.1097(2)
b, Å	9.8588(3)	11.2849(2)
c, Å	20.4022(6)	12.0911(2)
α, deg	90	90.264(10)
β, deg	96.518(2)	94.231(10)
γ, deg	90	94.817(10)
Volume, $Å^3$	2342.56(12)	1506.32(5)
Z	2	2
D(calcd), g cm^{-1}	2.120	1.604
Diffractometer	Bruker AXS SMART 2K	Bruker AXS SMART 2K
Temp, K	173(2)	100(2)
λ	1.5418	1.5418
μ, mm^{-1}	13.852	3.596
Scan type	ω scan	ω scan
F(000)	1440	734
θ_{max}, deg	72.92	72.80
h,k,l	$-14 \le h \le 14$ $-11 \le k \le 12$ $-21 \le l \le 24$	$-13 \le h \le 13$ $-12 \le k \le 13$ $-14 \le l \le 14$
Reflns used ($I > 2\sigma(I)$)	3959	5382
Absorption	multi-scan	multi-scan
Correction	SADABS	SADABS
T (min, max)	0.09, 0.33	0.38, 0.59
R [$F^2>2\sigma(F^2)$],	0.0399,	0.0546,
wR(F^2, all)	0.1047	0.1652
GOF	1.000	1.052

4.5 Reference

(1) (a) Johnson, L. K.; Killian, C. M.; Brookhart, M. *J. Am. Chem. Soc.* **1995**, *117*, 6414. (b) Ittle, S. D.; Johnson, L. K.; Brookhart, M. *Chem. Rev.* **2000**, *100*, 1169. (c) Liu, H.-R.; Gomes, P. T.; Costa, S. I.; Duarte, M. T.; Branquinho, R.; Fernandes, A. C.; Chien, J. C. W.; Singh, R. P.; Marques, M. M. *J. Organomet. Chem.* **2005**, *690*, 1314.

(2) (a) Laine, T. V.; Piironen, U.; Lappalainen, K.; Klinga, M.; Aitola, E.; Leskelä, M. *J. Organomet. Chem.* **2000**, *606*, 112. (b) Suzuki, H.; Matsumura, S.-I.; Satoh, Y.; Sogoh, K.; Yasuda, H. *React. Funct. Polym.* **2004**, *59*, 253.

(3) de Souza, R. F.; Leal, B. C.; de Souza, M. O.; Thiele , D. *J. Mol. Catal. A Chem.* **2007**, *272*, 6.

(4) Chauvin, Y.; Olivier, H.; Wyrvalski, S. N.; Simon,L. C.; de Souza, R. F. *J. Catal.* **1997**, *165*, 275.

(5) (a) (b) Gareau, D.; Sui-Seng, C.; Groux, L. F.; Brisse, F.; Zargarian, D. *Organometallics* **2005**, *24*, 4003. (c) Chen, Y.; Sui-Seng, C.; Zargarian, D. *Angew. Chemie, Int. Ed. Engl.* **2005**, *44*, 7721. (d) Boucher, S.; Zargarian, D. *Can. J. Chem.* **2005**, *84*, 233. (e) Chen, Y.; Sui-Seng, C.; Boucher, S.; Zargarian, D. *Organometallics* **2005**, *24*, 149. (f) Fontaine, F.-G.; Zargarian, D. *J. Am. Chem. Soc.* **2004**, *126*, 8786. (g) Groux, L. F.; Zargarian, D. *Organometallics* **2003**, *22*, 4759. (h) Fontaine, F.-G.; Nguyen, R.-V.; Zargarian, D. *Can. J. Chem.* **2003**, *81*, 1299. (i) Groux, L. F.; Zargarian, D. *Organometallics* **2003**, *22*, 3124. (j) Groux, L. F.; Zargarian, D.; Simon, L. C.; Soares, J. B. P. *J. Mol. Catal. A* **2003**, *19*, 51. (k) Rivera, E.; Wang, R.; Zhu, X. X.; Zargarian, D.; Giasson, R. *J. Molec. Catal. A* **2003**, *204-205*, 325. (l) Zargarian, D. *Coord. Chem. Rev.* **2002**, *233-234*, 157. (m) Wang, R.; Groux, L. F.; Zargarian, D. *J. Organomet. Chem.* **2002**, *660*, 98. (n) Fontaine, F.-G.; Zargarian, D. *Organometallics* **2002**, *21*, 401. (o) Dubois, M.-A.; Wang, R.; Zargarian, D.; Tian, J.; Vollmerhaus, R.; Li, Z.; Collins, S. *Organometallics* **2001**, *20*, 663. (p) Groux, L. F.; Zargarian, D. *Organometallics* **2001**, *20*, 3811. (q) Groux, L. F.; Zargarian, D. *Organometallics* **2001**, *20*, 3811. (r) Fontaine, F.-G.; Dubois, M.-A.; Zargarian, D. *Organometallics* **2001**, *20*, 5156. (s) Wang, R.; Bélanger-Gariépy, F.; Zargarian, D. *Organometallics* **1999**, *18*, 5548. (t) Fontaine, F.-G.; Kadkhodazadeh, T.; Zargarian, D. *Chem. Commun.* **1998**, 1253. (u) Vollmerhaus, R.; Bélanger-Gariépy, F.; Zargarian, D. *Organometallics* **1997**, *16*, 4762. (v) Huber, T. A.; Bayrakdarian, M.; Dion, S.; Dubuc, I.; Bélanger-Gariépy, F.; Zargarian, D. *Organometallics* **1997**, *16*, 5811. (w)

Bayrakdarian, M.; Davis, M. J.; Reber, C.; Zargarian, D. *Can. J. Chem.* **1996**, *74*, 2194. (x) Huber, T. A.; Bélanger-Gariépy, F.; Zargarian, D. *Organometallics* **1995**, *14*, 4997.

(6) (a) Trofimenko, S. *J. Am. Chem.* Soc. **1970**, *92*, 1499. (b) Hill, M. S.; Mahon, M. F.; Mcginley, J. M. G.; Molloy, K. C. *Polyhedron*, **2001**, *20*, 1995. (c) Reger, D. L.; Grattan, T. C.; Brown, K. J.; Little, C. A.; Lamba, J. J. S.; Rheingold, A. L.; Sommer, R. D. *J. Organomet. Chem.* **2000**, *607*, 120.

(7) For representative reports on coordination complexes of Ni featuring poly(pyrazolyl)alkane ligands see: (a) Mahon, M. F.; McGinley, J.; Molloy, K. C.; *Inorg. Chim. Acta* **2003**, *355*, 368. (b) Wolfgang, K.; Berghahn, M.; Frank, W.; Reiss, G. J.; Schonherr, T.; Rheinwald, G.; Lang, H. *Eur. J. Inorg. Chem.* **2003,** *11*, 2059. (c) Pettinari, C.; Marchetti, F.; Cingolani, A.; Leonesi, D.; Colapietro, M.; Margadonna, S. *Polyhedron* **1998,** *17*, 4145. (d) Mann, K. L.; Jeffery, J. C.; McCleverty, J. A.; Thornton, P.; Ward, M. D. *J. Chem. Soc., Dalton Trans.* **1998**, *1*, 89. (e) Pettinari, C.; Cingolani, A.; Bovio, B. *Polyhedron* **1996**, *15*, 115. (f) Astley, T.; Gulbis, J. M.; Hitchman M. A.; Tiekink, E. R. T. *J. Chem. Soc., Dalton Trans.* **1993**, 509. (g) Mesubi, M. A.; Omotowa, B. A. *Synth. React. Inorg. Metal-Org. Chem.* **1993,** *23*, 213. (h) Astley, T.; Canty, A. J.; Hitchman, M. A.; Rowbottom, G. L.; Skelton, B. W.; White, A. H. *J. Chem. Soc., Dalton Trans.* **1991**, 1981. (i) Reedijk, J.; Verbiest, J. *Trans. Met. Chem.* **1979**, *4*, 239. (j) Jansen, J. C.; Van Koningsveld, H.; Van Ooijen, J. A. C.; Reedijk, J. *Inorg. Chem.* **1980**, *19*, 170. (k) Reedijk, J.; Verbiest, J. *Trans. Met. Chem.* **1978**, *3*, 51.

(8) (a) Baho, N.; Zargarian, D. *Inorg. Chem.* **2007**, *46*, 299. (b) Michaud, A.; Fontaine, F.-G.; Zargarian, D. *Inorg. Chim. Acta* **2006**, *359*, 2592. (c) Nolet, M.-C.; Michaud, A.; Bain, C.; Zargarian, D.; Reber, C. *Photochem. Photobiology* **2006**, *82*, 57. (d) Michaud, A.; Fontaine, F.-G.; Zargarian, D. *Acta Crystallogr.* **2005**, E *61*, m784. (e) Michaud, A.; Fontaine, F.-G.; Zargarian, D. *Acta Crystallogr.* **2005**, E *61*, m904.

(9) See for example: Ajellal, N.; Kuhn, M. C. A.; Boff, A. D. G.; Hörner, M.; Thomas, C. M.; Carpentier, J.-F.; Casagrande, Jr., O. L. *Organometallics* **2006**, *25*, 1213.

(10) Baho, N.; Zargarian, D. *Inorg. Chem.* **2007**,46.

(11) Note that most typical square pyramidal complexes possess two trans angles of 160-170° and at least four cis angles of 90-100°, whereas trigonal bipyramidal complexes

display one trans angle of ca. 180° and three cis angles of ca. 120°: Jansen, J. C.; van Koningsveld, H.; van Ooijen, J. A. C.; Reedijk, J. *Inorg. Chem.* **1980**, *19*, 170.

(12) The strcutural index τ is determined from $(\beta - \alpha)/60$, wherein β and α are, respectively, the largest basal angles (β>α); ideal τ values for perfectly square pyramidal and trigonal bipyramidal structures are 0 and 1, respectively: Addison, A. W.; Rao, T. N.; Reedijk, J;. van Rijn, J.; Verschoor, G. C. *J. Chem. Soc., Dalton Trans.* **1984**, 1349.

(13) Helgesson, G.; Jager, S. *Inorg. Chem.* **1991**, *30*, 2574.

(14) Liu, X.; Guo, G.-C.; Fu. M.-L.; Chen, W.-T.; Zhang, Z.-J.;Huang, J.-S. *Dalton Trans.* **2006**, 884.

(15) (a) Uehara, K.; Hikichi, S.; Akita, M. *J.Chem. Soc., Dalton Trans.* **2002**, 3529. (b) Riiba, E.; Simanko.W.; Mereiter, K.; Schmid. R.; Kirchner, K. *Inorg.Chem.***2000**, *39*, 382.

(16) SMART (**2001**). Release 5.625. Bruker Molecular Analysis Research Tool; Bruker AXS Inc., Madison, WI.

(17) SAINT (**2003**). Release 7.06. Integration Software for Single Crystal Data. Bruker AXS Inc., Madison, WI.

(18) Sheldrick, G. M. SHELXS, Program for the Solution of Crystal Structures. University of Goettingen. Germany, 1997.

(19) (a) Bruker (1997). SHELXTL (1997). Release 5.10; The Complete Software Package for Single Crystal Structure Determination. Bruker AXS Inc., Madison, USA. (b) Bruker (1999a). SAINT (2003). Release 7.06. Integration Software for Single Crystal Data. Bruker AXS Inc., Madison, USA. (c) Bruker (1999b). SMART (2001) Release 5.625; Bruker Molecular Analysis Research Tool, Bruker AXS Inc., Madison, USA. (d) Sheldrick, G. M. (1996). SADABS, Bruker Area Detector Absorption Corrections. (e) Bruker AXS Inc., Madison, USA. (f) Sheldrick, G. M. (1997a). SHELXS97. Program for Crystal Structure solution. University of Gottingen, Germany. (g) Sheldrick, G. M. (1997b). SHELXL97. Program for crystal structure refinement. University of Gottingen, Germany. (h) Spek, A. L. (2000). PLATON, 2000 version; Molecular Geometry Program, University of Utrecht, Utrecht, Holland.

(20) Burnett, M. N.; Johnson, C. K. (1996). ORTEPIII - Oak Ridge Thermal Ellipsoid Plot Program for Crystal Structure Illustrations, Technical Report ORNL-6895. Oak Ridge National Laboratory, TN.

Chapter 5: Diverse Results of Several Studies

5.1. Introduction

We observed in the previous chapters that the anion has an important influence on the outcome of the reaction. For this reason we were interested in studying the influence of Cl^- and I^- anions on the reaction results. The beginning of this chapter will present the results that were obtained during our attempts to prepare the dpdpm derivatives of $NiCl_2 \cdot 6H_2O$ and NiI_2 salts. These reactions gave the pentacoordinated complexes, $[(dpdpm)Ni(\mu\text{-}Cl)Cl]_2$ (**5.6**) and $[(dpdpm)NiCl(H_2O)_2]Cl$ (**5.7**), and the octahedral complexes $[(dpdpm)_3Ni][I_3]_2$ (**5.8**) and $[(Pz)_6Ni][I]_2$ (**5.9**). In preliminary studies aimed to explore the influence of hindered ligands on the preparation of nickel pyrazolyl complexes, we have examined the reaction of the methyl substituted dpdpm derivative diphenyl(3,5-dipyrazolyl)methane ($dpdpm^{Me2}$) with $NiCl_2 \cdot 6H_2O$ and $NiBr_2$. These reactions generate unexpected new adducts $[(Pz^{Me2})_2NiCl_2(H_2O)_2]$ (**5.10**) and $[(Pz^{Me2})_2NiBr_2]$ (**5.11**), which result from N-C bond cleavage. To establish whether the N-C cleavage is limited to nickel we examined the analogous reaction with $(PhCN)_2PdCl_2$ that gave complex $[(Pz^{Me2})_2PdCl_2]$ (**5.12**). We will also present our attempts to oxidize the complex $[(dpdpm)NiBr_2(H_2O)]$ (**2a**) with $CuCl_2 \cdot 2H_2O$ and $[Cp_2Fe][PF_6]$ that resulted in the unexpected adducts $(dpdpm)CuBr_2$ (**5.13**) and $[(dpdpm)_2Ni(CH_3CN)_2][(FeBr_3)_2O]$ (**5.14**), respectively. All these complexes are paramagnetic (except the palladium complex), both in the solid state and in solution, and most of them have been characterized by IR, NMR, and X-ray diffraction studies.

5.2. New series of $NiCl_2$ and NiI_2 derivatives bearing dpdpm

The nickel complexes were synthesized by a reaction of either nickel(II) chloride or nickel(II) iodide with dpdpm in a number of organic solvents. In most cases, the final product remained soluble throughout the reaction and was isolated by recrystallization from an appropriate solvent. X-ray quality crystals were obtained for all the reactions with little farther purification.

5.2.1 Synthesis

Stirring a 1:1 mixture of $NiCl_2$ and dpdpm in acetone for 18 h gave a brown precipitate, which was filtered to give a brown solid (79% crude yield) identified as the dimeric species **5.6** (Scheme 5.1). Allowing the brown crystals of **5.6** to stand overnight in the (green) mother liquor, unprotected from ambient atmosphere, turned them into light green crystals that were identified as the cationic bis(aquo) species, complex **5.7**.

Scheme 5.1

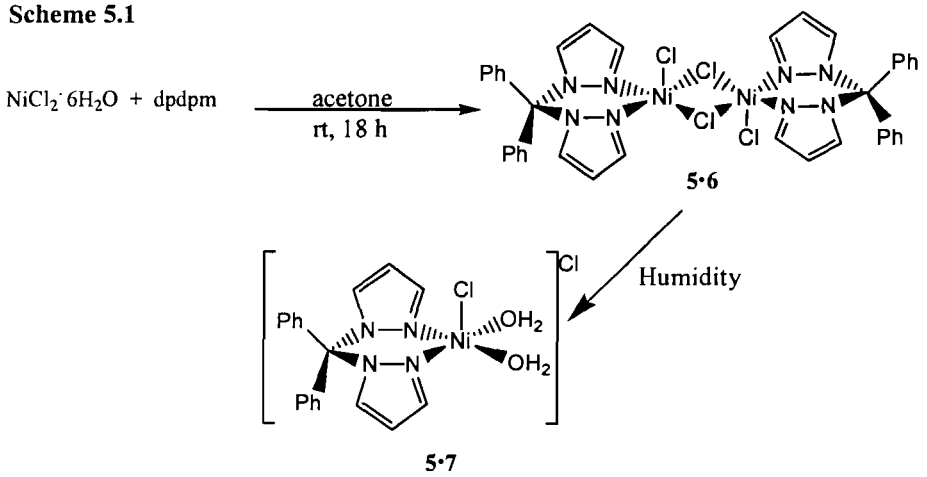

Refluxing an ethanol mixture of NiI_2 with one equiv. of dpdpm for 15 h gave a yellow solution, which was evaporated to give a dark brown solid. Contrary to our expectations, the crystallization of this solid from CH_2Cl_2/ether produced large brown needles, that were neither $[(dpdpm)Ni(\mu\text{-}I)I]_2$ nor $[(dpdpm)NiI_2]$. Indeed, the final outcome of the reaction gave the unpredicted compound **5.8** $[(dpdpm)_3Ni][I_3]_2$ (Scheme 5.2).

Scheme 5.2

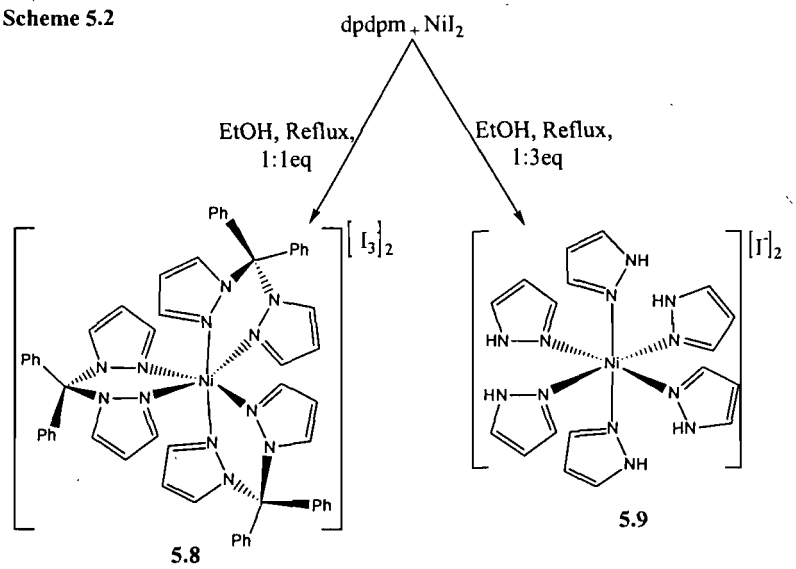

The analogous reaction of NiI_2 with 3 equiv. of dpdpm resulted in a yellow solution that gave a yellow solid after the evaporation of the solute. Crystallization of this solid from CH_2Cl_2/ether produced a few yellow crystals in addition to the colorless crystals of free dpdpm. X-ray analysis showed that these yellow crystals were complex **5.9**. Interestingly, a similar yellow solid was also obtained when this reaction was conducted in benzene and under nitrogen (room temperature, 3 d); we presume that this solid is complex **5.9**, but this possibility has not been confirmed. The purification of this complex proved difficulties due to its solubility in most organic solvents.

5.2.2 Crystallography

Single crystals of **5.6**, **5.7**, **5.8**, and **5.9** were obtained by vapour diffusion of Et_2O or hexane into solutions of these complexes in acetone for **5.6** and **5.7** or dichloromethane for **5.8** and **5.9**. All four sets of diffraction data resulted in fairly accurate structures for the studied complexes, as reflected in the R values of ca. 0.0312 (**5.6**), 0.0521 (**5.7**), 0.0520 (**5.8**), and 0.0207 (**5.9**). All the details concerning the refinement of the crystals structure are listed in the supporting information at the end of this thesis (Appendix IV). The crystallographic data are tabulated in Tables 5.1, the ORTEP diagrams of these complexes are shown in Figures 5.1-5.4, and while bond distances and angles are tabulated in Tables 5.2- 5.4.

Table 5.1. Crystallographic data for **5.6**, **5.7**, **5.8**, and **5.9**

	5.6	**5.7**	**5.8**	**5.9**
Formula	$C_{38}H_{32}Cl_4N_8Ni_2$	$C_{19}H_{22}N_4NiCl_2O_2.H_2O$	$C_{228}H_{192}N_{48}Ni_4I_{24}.(C_{12}H_{30}O_3).(C_{10}H_{10}Cl_{10})$	$C_{18}H_{24}N_{12}NiI_2$
mol wt	859.94	484.02	7531.73	721.00
Cryst color	orange	green	dark brown	yellow
Cryst dimens, mm	0.18×0.11×0.06	0.32×0.23×0.07	0.24×0.18×0.06	0.2 ×0.09 ×0.08
Symmetry	Triclinic	Triclinic	Monoclinic	Hexagonal
Space group	P-1	P-1	P21/n	P-3
a, Å	8.87110(10)	9.9327(2)	12.5268(4)	9.84900(10)
b, Å	9.0951(2)	10.8080(2)	26.8473(7)	9.84900(10)
c, Å	11.4915(2)	11.1787(2)	20.4728(7)	7.4921(2)
α, deg	84.3600(10)	80.5560(10)	90	90
β, deg	80.8950(10)	63.7130(10)	103.382(2)	90
γ, deg	84.4220(10)	74.5640(10)	90	120
Volume, $Å^3$	907.91(3)	1035.67(3)	6698.3(4)	629.388(19)
Z	1	2	1	1
D(calcd), g cm^{-1}	1.573	1.552	1.867	1.902
Diffractometer	Bruker AXS SMART 2K	Bruker AXS SMART 2K	Bruker AXS SMART 2K	Bruker AXS SMART 2K
Temp, K	100(2)	100(2)	100(2)	200(2)
λ	1.5418	1.5418	1.5418	1.5418
μ, mm^{-1}	4.329	3.972	23.433	20.634
Scan type	ω scan	ω scan	ω scan	ω scan
F(000)	440	500	3616	350
θ_{max}, (deg)	72.91	72.87	72.92	68.11
h,k,l range	$-10 \le h \le 10$ $-11 \le k \le 11$ $-13 \le l \le 14$	$-11 \le h \le 9$ $-13 \le k \le 13$ $-13 \le l \le 13$	$-15 \le h \le 15$ $-32 \le k \le 32$ $-23 \le l \le 25$	$-11 \le h \le 11$ $-11 \le k \le 11$ $-8 \le l \le 8$
Reflns used ($I > 2\sigma(I)$)	3034	3774	9506	772
Absorption Correction	Multi-scan SADABS	Multi-scan SADABS	Multi-scan SADABS	Multi-scan SADABS
T (min, max)	0.52, 0.71	0.53, 0.81	0.11, 0.43	0.24, 0.37
R [$F^2>2\sigma(F^2)$], $wR(F^2)$	0.0312, 0.0884	0.0521, 0.1622	0.0520, 0.1355	0.0207, 0.0567
GOF	1.072	1.100	1.00	1.109

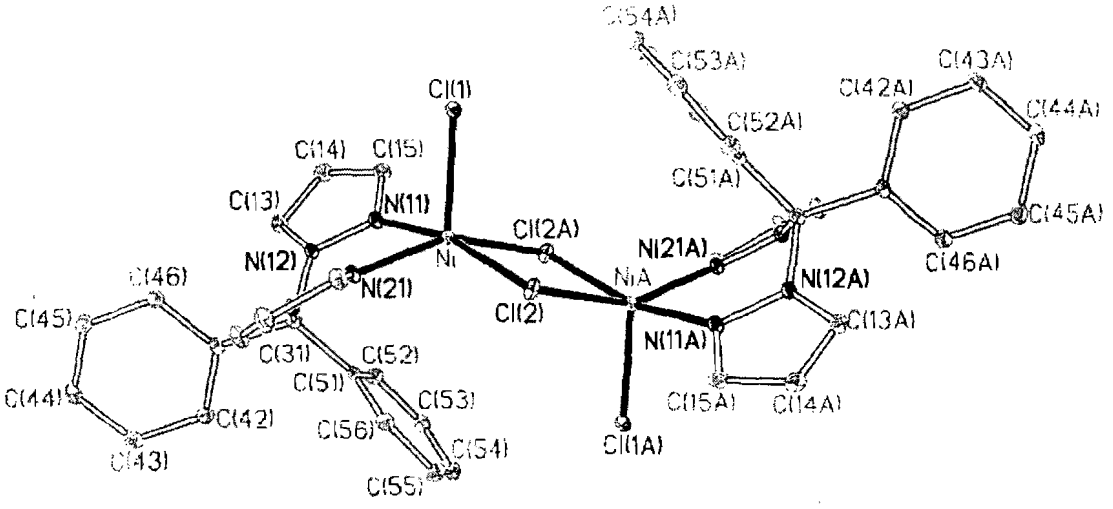

Figure 5.1. ORTEP view of complex **5.6**. Thermal ellipsoids are shown at 30% probability. The molecule lies on a crystallographic inversion center

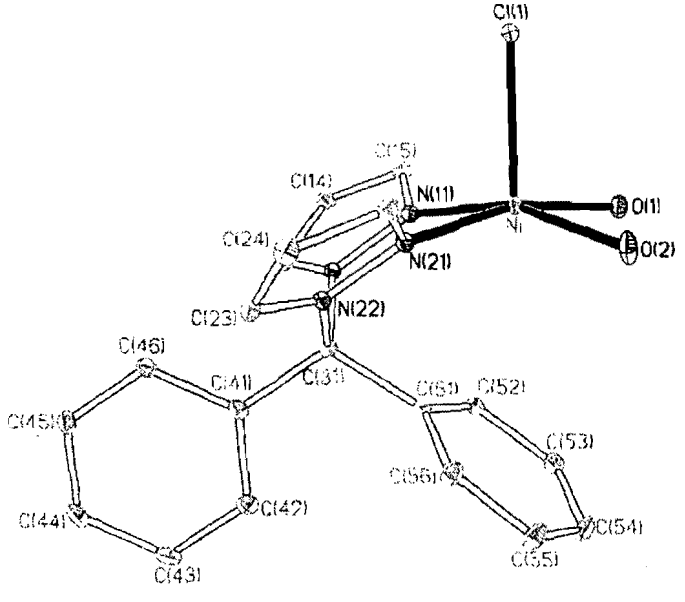

Figure 5.2. ORTEP view of complex **5.7**. Thermal ellipsoids are shown at 30% probability. Cl^- counter ion and solvent molecule have been omitted for clarity

Table 5.2. Bond distances and angles for complexes for **5.6** and **5.7**[a]

	5.6	**5.7**
Ni-Cl(1)	2.2999(5)	2.3352(7)
Ni-Cl(2)	2.3989(5)	-
Ni-Cl(2A)	2.3456(5)	-
Ni-O(1)	-	2.030(2)
Ni-O(2)	-	2.011(2)
Ni-N(11)	2.0560(16)	2.019(2)
Ni-N(21)	2.0530(16)	2.030(2)
N(11)-Ni-Cl(1)	92.90(5)	97.03(6)
N(11)-Ni-Cl(2)	167.19(5)	-
N(21)-Ni-Cl(1)	103.19(5)	96.59(7)
N(21)-Ni-Cl(2)	90.21(5)	-
N(11)-Ni-N(21)	85.53(6)	87.72(9)
N(11)-Ni- O(1)	-	92.34(9)
N(11)-Ni- O(2)	-	161.17(10)
N(21)-Ni-O(1)	-	166.13(9)
N(21)-Ni- O(2)	-	89.43(9)
N(11)-Ni- Cl(2A)	92.75(5)	-
N(21)-Ni- Cl(2A)	153.64(5)	-
O(1)-Ni-Cl(1)	-	97.17(6)
O(2)-Ni-Cl(1)	-	101.78(7)
O(1)-Ni-O(2)	-	86.05(9)
Cl(1)-Ni-Cl(2)	99.84(2)	-
Cl(1)-Ni-Cl(2A)	103.17(2)	-
Cl(2)-Ni-Cl(2A)	85.701(19)	-
Ni-Cl(2)-Ni(A)	94.299(18)	

[a]Bond lengths in Å and bond angles in deg

A = -x+1,-y+1,-z+1

Complex **5.6** and **5.7** are iso-structural to their analogous structures with bromide (complex **3.1** $[(dpdpm)Ni(\mu\text{-}Br)Br]_2$ and **3.2b** $[(dpdpm)NiBr(H_2O)_2]Br$). Similarly to complex **3.1,** complex **5.6** possesses a crystallographically imposed center of symmetry, and the coordination around the nickel centre is characterized as a lightly distorted square pyramidal geometry in both **5.6** and **5.7** complexes. The value of the structural index τ^1 for complex **5.7** is exactly the same as the corresponding values for complex **3.2b** (0.08), while complex **5.8** has ($\tau = 0.23$) which is closer to complex **3.1** (0.17). In comparison to complexes **5.6** and **5.7**, the complex $[(bpm^{Me2})Ni(\mu\text{-}Cl)Cl]_2$[2] shows a much greater distortion toward trigonal bipyramidal geometry ($\tau \sim 0.50$). Moreover, the angle between the coordination planes N11-N12-N22-N21 and ClA/O1-N11-N21-Cl2/O2 for complex **5.6** is smaller than the analogous angle for complex **3.1** (21° vs 57°), also the corresponding

angle for complex **5.7** is closer to its analogous complex **3.2b** ((36° vs 38°) in chapter 3. These results show that complex **5.6** shows a slight distortion toward trigonal bipyramidal geometry compared to complex **3.1**, while complex **5.7** and **5.2b** adopt the same square pyramidal geometry.

The bridging CR_2 moiety in these complexes **5.6** and **5.7** points toward the Ni center to allow a long-range interaction between a C=C bond of a phenyl substituent and the Ni center with the following Ni-C distances (in Å) 3.37 and 3.59 in **5.6**; 3.05 and 3.28 in **5.7**. Also, it is not clear whether the shorter Ni-C distances found in the monomeric aquo complex **7** are due to the diminished electronic donation from the water molecules or the greater steric repulsion in the dimeric complex **5.6**. Apart from the overall geometry of the new complexes and the conformation of the metallacycles, the Ni-element bond distances are informative about the relative stabilities of the various species and the relative *trans* influence of the ligands. The Ni-(μ-Cl) distances in complex **5.6** are much longer than the axial Ni-Cl distance (2.35 and 2.40 Å vs 2.30 Å, ΔNi-Cl > 91 e.s.d.). These weak Ni-(μ-Cl) interactions explain why this dimer is susceptible to cleavage and transformation into monomeric derivatives **5.6** by hydrolysis (in solution and solid state).

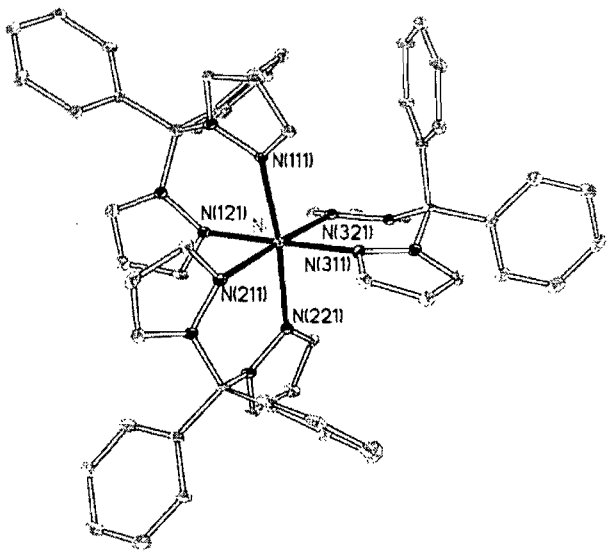

Figure 5.3. ORTEP view of complex **5.8**. Thermal ellipsoids are shown at 30% probability. I_3^- counter ion and solvent molecules have been omitted for clarity

Table 5.2. Bond distances and angles for complexes **5.8**[a]

5.8			
Ni-N(111)	2.068(5)	N(121)-Ni-N(311)	178.7(2)
Ni-N(121)	2.125(6)	N(121)-Ni-N(321)	92.3(2)
Ni-N(211)	2.145(6)	N(211)-Ni-N(221)	85.8(2)
Ni-N(221)	2.126(6)	N(211)-Ni-N(311)	94.8(2)
Ni-N(311)	2.103(6)	N(211)-Ni-N(321)	175.9(2)
Ni-N(321)	2.089(6)	N(221)-Ni-N(311)	91.0(2)
N(111)-Ni-N(121)	86.7(2)	N(221)-Ni-N(321)	90.3(2)
N(111)-Ni-N(211)	88.7(2)	N(311)-Ni-N(321)	86.4(2)
N(111)-Ni-N(221)	173.5(2)	I(1)-I(4)	2.8887(8)
N(111)-Ni-N(311)	93.0(2)	I(1)-I(5)	2.9629(8)
N(111)-Ni-N(321)	95.2(2)	I(2)-I(3)	2.8953(8)
N(121)-Ni-N(211)	86.5(2)	I(2)-I(6)	2.9470(8)
N(121)-Ni-N(221)	89.4(2)	I(4)-I1-I(5)	177.48(2)
		I(3)-I2-I(6)	175.61(2)

[a]Bond lengths in Å and bond angles in deg

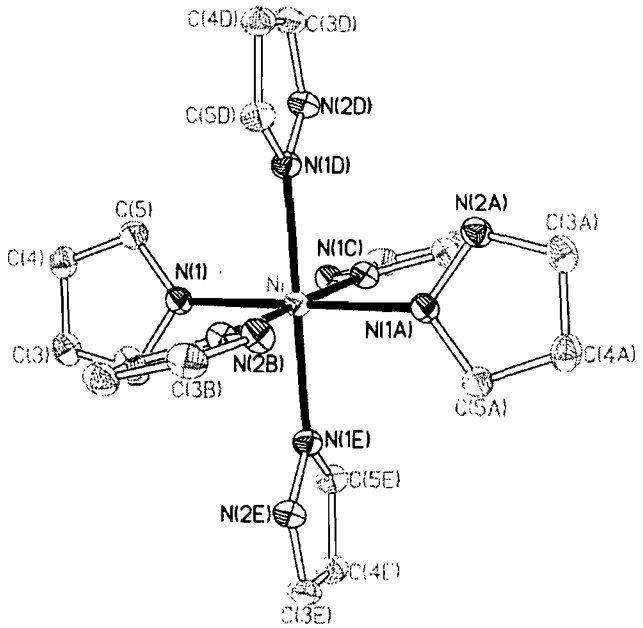

Figure 5.4. ORTEP view of complex **5.9**. Thermal ellipsoids are shown at 30% probability. I^- counter ions have been omitted for clarity. The nickel atom is on crystallographic 3-folder axes

Table 5.3. Bond distances and angles for complexes **5.9**[a]

	5.9
Ni-N(1)	2.068(5)
Ni-N(1A)	2.068(5)
Ni-N(1B)	2.068(5)
Ni-N(1C)	2.068(5)
Ni-N(1D)	2.068(5)
Ni-N(1E)	2.068(5)
N(1)-Ni-N(1A)	180
N(1)-Ni-N(1B)	89.41(8)
N(1)-Ni-N(1C)	90.59(8)
N(1)-Ni-N(1D)	89.41(8)
N(1)-Ni-N(1E)	90.59(8)
N(1D)-Ni-N(1E)	180
N(1C)-Ni-N(1B)	180

[a]Bond lengths in Å and bond angles in deg

1A = -x,-y,-z 1B = x-y,x,-z 1C = -x+y,-x,z

1D = -y,x-y,z 1E = y,-x+y,-z

Complex **5.8** (Figure 5.3) displays slightly distorted octahedral geometry around the nickel center, the *cis* and *trans* bond angles are ranging from 86 to 95° and 174 to 179°. The geometry around the nickel centre for complex **5.9** (Figure 5.4) is essentially undistorted octahedral with the *cis*-angles spanning between 89-91° and the *trans*-angles are 180° by symmetry (Table 5.3). The six-membered metallacycle formed by the chelation of dpdpm to the Ni center in **5.8** adopts a half-chair conformation, in contrast to the observation of a boat conformation in the penta-coordinated chloro and bromo complexes. The angle formed between the coordination plane N121-N211-N311-N321 and the plane formed by the pyrazole nitrogens in complex **5.8** (N311-N312-N322-N321) is 13.2°, which is closer to the corresponding angle in complex **3.4** (16°) and much greater than the corresponding angles in **3.3** (4°) and **3.5** (1°).

5.3. New series of transition metal derivatives with 3,5-dimethyl pyrazol results from decomposition of diphenyl(3,5-dimethylpyrazolyl)methane (dpdpm^{Me2})

Our interest in the chemistry of poly(pyrazolyl)alkanes has prompted us to explore the coordination chemistry of nickel with the hindered ligand dpdpm^{Me2}, which is bearing two methyl groups on the pyrazol rings in the positions 3 and 5. Recrystallization of the yellow solid obtained from the 1:1 reactions of dpdpm^{Me2} with either $(DME)_2NiCl_2$ or $NiCl_2 \cdot 6H_2O$ gave the unexpected compound $[(Pz^{Me2})_2NiCl_2(H_2O)_2]$ (**5.10b**) arising from the fragmentation of dpdpm^{Me2}. Similaral observations were made in the reactions of dpdpm^{Me2} with $NiBr_2$ and $(PhCN)_2PdCl_2$, giving $[(Pz^{Me2})_2NiBr_2]$ (**5.11**) and $[(Pz^{Me2})_2PdCl_2]$ (**5.14**), respectively. The preparation and structures of complexes **5.11**[3] and **5.12**[4] (Figure 5.5) will not be discussed further because these are known complexes, but the different cell parameters for these complexes are given in appendix IV. Complex **5.10** has not been reported previously and its synthesis and structure will, therefore, be discussed later.

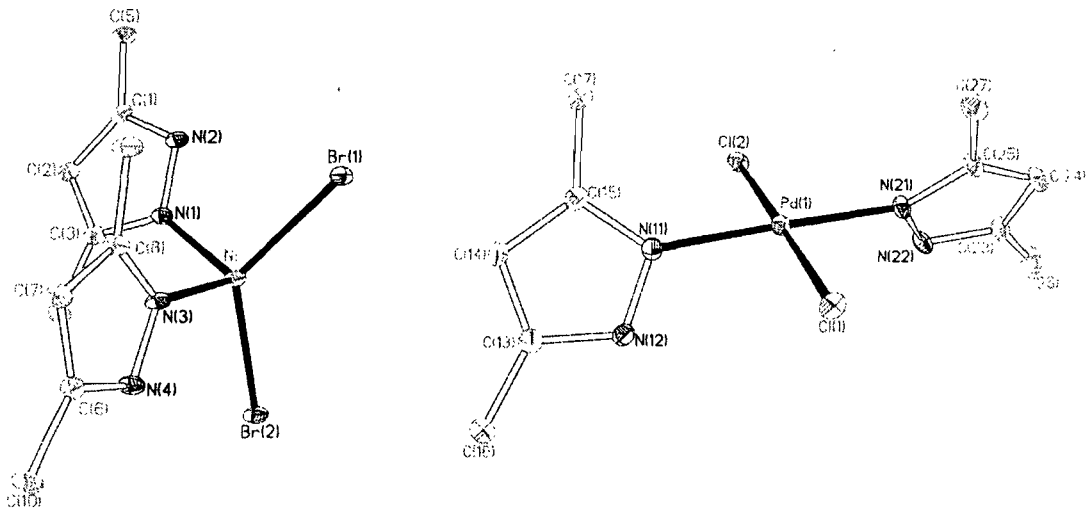

Figure 5.5. ORTEP view of complex **5.11** and **5.12**. Thermal ellipsoids are shown at 30% probability

5.3.1 Formation of complexes

The complexes **5.10b**, **5.11** and **5.12** were prepared as outlined in Scheme 5.3. The reaction of $(DME)_2NiCl_2$ with 1 equiv. of dpdpm^{Me2} in CH_2Cl_2 at room temperature over 45 min afforded a yellow suspension, which was precipitated by adding an excess of hexane. Filtration gave a yellow solid that was washed with hexane and recrystallized from acetone/hexane to give light green crystals of complex **5.10b**. This complex could also be

prepared by refluxing $NiCl_2 \cdot 6H_2O$ in BuOH with $dpdpm^{Me2}$ (1.4:1.0) or Pz^{Me2} (1:2). Both reactions gave a dark violet solution while hot, but turned to green upon cooling (presumably because of hydrolysis). Filtration and evaporation of the green filtrate gave a yellow solid (**5.10a**) that was washed with Et_2O to remove any excess of unreacted ligand. Recrystallization from ethanol/Et_2O gave light green crystals of complex **5.10b**, which was characterized by X-ray diffraction. We were unable to identify the yellow solid **5.10a** due to its weak solubility in common solvents and sensitivity toward moisture. Thus, exposing yellow samples of **5.10a** to ambient atmosphere over days leads to the formation of a green solid, which re-forms the initial yellow solid when heated at 100 °C for one minute. We propose that the yellow solid **5.10a** undergoes a hydrolysis process that leads to the formation of complex **5.10b**

Scheme 5.3

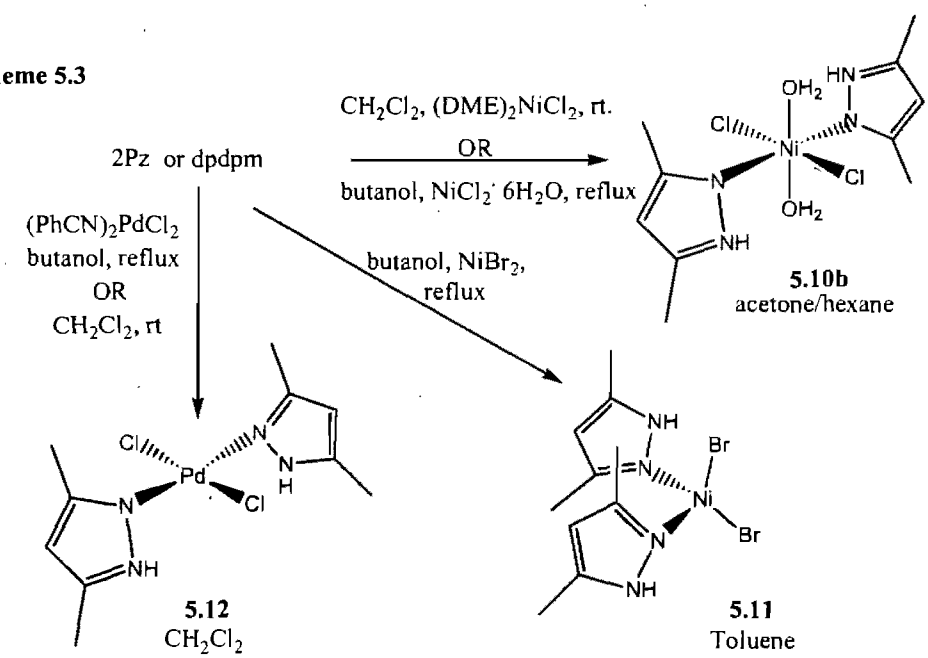

Refluxing a BuOH suspension of $NiBr_2$ and $dpdpm^{Me2}$ (1:1) gave a dark blue solution after 30 min. The resulting mixture was filtered and the filtrate was evaporated to give a dark blue solid, which was recrystalized from toluene to give complex **5.11** in 71% crude yield. Similarly, the 1:1 reaction of $(PhCN)_2PdCl_2$ with $dpdpm^{Me2}$ in CH_2Cl_2 (room temperature, 3 h) gave a yellow solution from which orange crystals of complex **5.12** were obtained. It is worth noting that Jordan's group has used the ligands dpdpm and $dpdpm^{tBu}$

(dpdpm^{tBu} = diphenyl(3-t-butylpyrazolyl)methane) to synthesize complexes [(dpdpm)$PdCl_2$] and (dpdpm^{tBu})$PdCl_2$, with no ligand fragmentation being observed.[5] The main difference in the experimental conditions used by this group is that their crystallization was done at -50 °C.

Complex **5.10a** has shown an interesting vapo-solvato and thermochromic properties that we have studied briefly. The yellow solid shows vapochromic properties since it could change its color to green **5.10b** after leaving it in a humid place, and it could be converted to the original yellow **5.10a** by placing the sample in a 100 °C oven for one minute without any visible degradation of the solid (Scheme 5.4).

Scheme 5.4

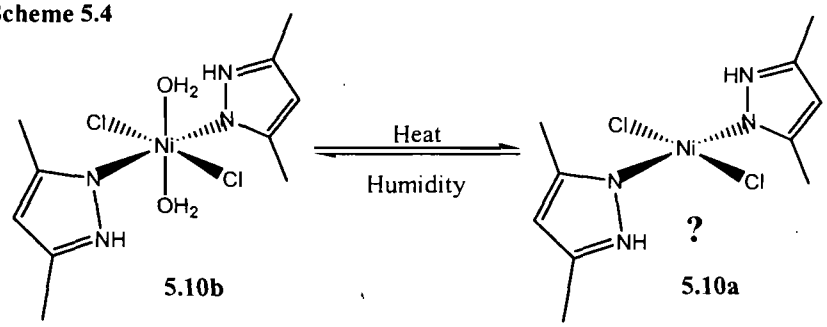

5.10b **5.10a**

Complex **5.10a** displays vapo-, solvate-, and thermochromic behavior. Thus, solid samples of this complex are readily converted to green or blue in the presence of MeOH or DMF vapors, respectively, but no significant color change was observed with acetone vapor. Solutions of complex **5.10a** are dark violet in acetone or ethyl acetate, light green in MeOH, dark blue in CH_3CN, and blue in DMF. Varying the temperature of the butanol solutions of **5.10a** caused a color variation from light green (< 30 °C) to dark green (30-40 °C) to yellow (40-70 °C); further heating resulted in darkening of the solution until it became deep violet at 100 °C. Cooling the samples to 18 °C regenerated the light green color of the solution, and repeating this heating-cooling cycle 3 times produced the same observations.

The complexes **5.10**, **5.11** and **5.12** are the result of the degradation of dpdpm^{Me2}. Although this degradation seemed unusual to us in the beginning, we have found out recently that the cleavage of a B-N or C-N bond has been reported in poly(pyrazolyl)borate[6] and poly(pyrazolyl)alkane chemistry. The cleavage can indeed occur in the presence of certain metal species such as a hydrolytic cleavage of C(sp^3)-N

bond was observed when the reaction between $VOCl_2$ and bpp (bis(pyrazolyl)propane) was carried out under reflux in MeOH and the resulting adduct $[(Pz)_2VOCl_2]$[7] has been obtained as a major product. This phenomenon has been observed with Sn and Zn[7] salts for the same ligand under mild reaction conditions. On the other hand, bpp and bpm^{Me2} can coordinate without any degradation to several metal salts (Mn,[8] Co,[8] Ni,[8,9] Cu,[10] Zn,[11] Cd,[8] Sn,[7] Pd[12]) under different reaction conditions. For example, no ligand break-up was observed in the preparation of the following complexes: $[(bpp)MMe_2]$ (M = Pd, Pt), [(bpp)PdClMe],[12] $[(bpm)PtCl_2]$, and $[(bpm^{Me2})PtCl_2]$ (bpm = (bis(pyrazolyl)methane); bpm^{Me2}= (bis(3,5-dimethylpyrazolyl)methane).

Minghetti et al. have proposed that the fragmentation of bpp in reaction with $PtCl_2$, $(RCN)_2PtCl_2$ or $K_2[PtCl_4]$ (*cis*- or *trans*-$Pt(Pz)_2Cl_2$) might be initiated by strong agostic-type interactions between Pt and one of the protons on the $C(CH_3)_2$ bridge.[13] The same authors have observed such C-H···M interactions in the structure of $[(bpp)PdCl_2]$; interestingly, however, this compound does not lead to the break-up of the ligand. Moreover, ligand fragmentation happens even when there is no possible agostic interaction. For example, the reaction of $SnCl_4 \cdot 5H_2O$ with bis(3,4,5-trimethylpyrazolyl)methane gives the adduct $[(Pz^{Me3})_2SnCl_4]$[14] (Figure 1.7 in Chapter 1). This cleavage was explained by the greater stability of the resulting adduct compared to the original ligand and perhaps owing to the greater steric bulk of the donor ligand. It is noteworthy that the presence of an intramolecular coordination with a weakly bound η^2-arene in complex $[(dpdpm^{Me2})Mo(CO)_3]$, $[(PhHC(3,5\text{-}Me_2Pz)_2)Mo(CO)_3]$ and $[(PhHC(3,5\text{-}Me_2Pz)_2)Mo(CO)_3]$ seems to stabilize the coordination of these complexes and no decomposition of the ligand was observed.[15]

There are several examples of different degradation processes with dpdpb. For example the formation of a new heterocycle was resulted from losing one pyrazolyl from each dpdpb and that was fallowed with a cycloaddition of CH_3CN to the B-pyrazolyl unit to give a new adduct (Scheme 5.5).[16]

Scheme 5.5

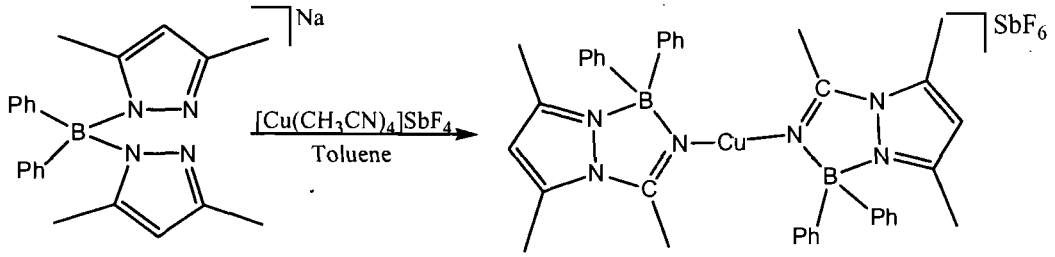

Another example of ligand degradation has shown that reacting complex $[NBu_4][(dpdpb)PtMe_2]$ with $[NN^{i\text{-}}Pr_2Et][BPh_4]$ at room temperature and in mesitylene (C_9H_{12}) gave complex $[(dpdpb)Pt(CH_2C_6H_3(CH_3)_2(Pz)]$ as a major product isolated in 50% yield. Therefore, the formation of this complex is accompanied by undesired borate ligand degradation. This B-N cleavage was due to the C-H activation of a sp^3-hybridized C-H bond position (Scheme 5.6). [17]

Scheme 5.6

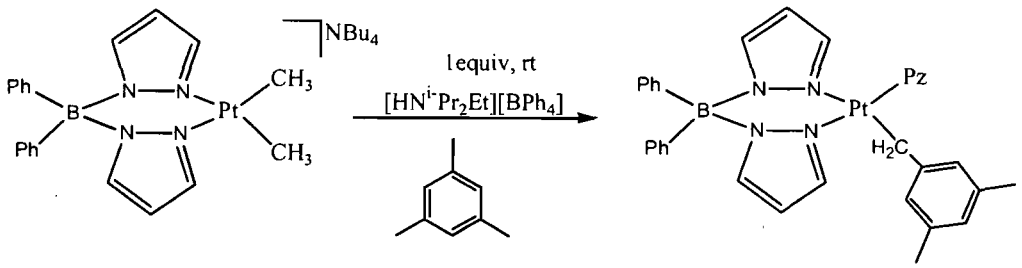

Evidently, in this system the benzylic C-H activation also occurred when the reaction was carried out in the presence of a donor solvent such as CH_3CN, THF, and pyridine, Although this activation was not observed with pentane, methylcyclohexane, or other nonaromatic hydrocarbons even at high temperatures, which indicates that this sp^3-hybridized C-H bond is operative only for more reactive benzylic C-H bonds.

On the other hand, we have found only one published report that discusses this kind of decomposition with $dpdpm^{Me2}$ that shows the same chemistry like ours. For example, the reaction of 1 equiv. of $Cu(NO_3)_2$ with 1 equiv. of $dpdpm^{Me2}$ in MeOH and for 12 h afford complex $[(Pz^{Me2})_3Cu(NO_3)]$ for 63% crude yield (Scheme 5.7). [18]

Schem 5.7

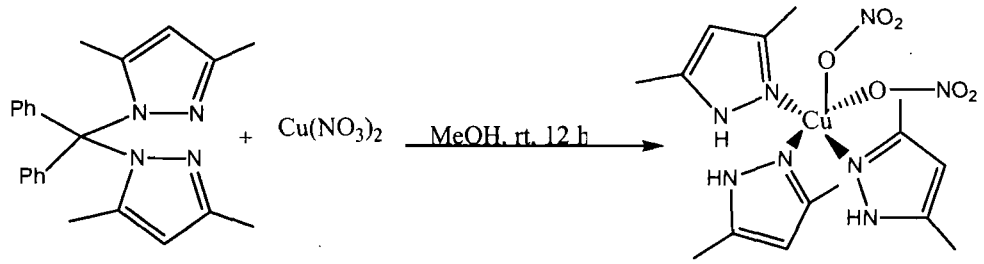

But interestingly, we can get the complex [(dpdm^{Me})Cu(η^1-NO_3)($\eta^2$$NO_3$)] from the 1:1 reaction of dpdpm^{Me} with $Cu(NO_3)_2$ in less polar and less humid solvent such as THF for 2 h. Hence, under this reaction conditions the methyl group on the position 5 of the pyrazole ring does not influence the stability of the ligand. Meanwhile, mixing a less hindered ligand such as dpdpm with $Cu(NO_3)_2$ in polar solvent like MeOH for 2 h and at rt gives [(dpdpm)Cu(η^1-NO_3)$_2$(H_2O)] complex.

In conclusion, at present we are not sure why the ligand is falling apart under certain reactions conditions. There are many factors that can play an important role in the stability of the resulting complexes. Thus, in addition to the choice of the metal salts, the hindered ligand, the possible agostic or intramolecular interaction and the reactions conditions, it seems that the humidity also favors a hydrolysis reaction and that may lead to the degradation process of the ligand. As mentioned above, the outcome of the reaction depends in some cases on whether the reaction was made in a humid environment or even in humid solvents like MeOH, acetone and Butanol, or heated to a high temperature for a long time. Furthermore, new studies have shown that some palladium(II) pyrazolyl complexes such as [(Pz)$_2$$PdCl_2$], [(Pz^{Me2})$_2$$PdCl_2$], [(Pz)$_2$Pd(SCN)$_2$] and [(Pz^{Me2})$_2$Pd(SCN)$_2$] undergo thermal decomposition studied by thermogravimetry (TG) and differential thermal analysis (DTA). The thermal stability of these complexes varies in the following order: Pz^{Me2}>Pz and Cl>SCN.[19] Finally, some unpublished new studies have shown that some ligands like diphenyl(5-^{t}Bu-pyrazolyl)methane (dpdpm^{tBu}) decompose under a nitrogen atmosphere and before reacting it with any metal salts.[20]

5.3.2 Crystallography

Suitable crystals of **5.10b** for X-ray diffraction studies were obtained by vapour diffusion of hexane into concentrated solutions of this complex in acetone. The set of

diffraction data resulted in fairly accurate structures for the studied complex, as reflected in the R value of ca. 0.0655 (**5.10b**). All the details concerning the refinement of the crystals structure are listed in the supporting information at the end of this thesis (Appendix IV). The crystallographic data are tabulated in Tables 5.5, the ORTEP diagram is shown in Figure 5.6, and while bond distances and angles are tabulated in Table 5.6.

Table 5.5. Crystallographic data for **5.10b**

	5.10b
Formula	$C_{10}H_{20}N_4\ NiClO_2$
mol wt	357.91
Cryst color	Green
Cryst dimens, mm	0.44×0.27×0.11
Symmetry	Monoclinic
Space group	P21/c
a, Å	10.794(5)
b, Å	9.312(3)
c, Å	7.849(2)
α, deg	90
β, deg	92.26(3)
γ, deg	90
Volume, Å^3	788.3(5)
Z	2
D(calcd), g cm^{-1}	1.508
Diffractometer	Bruker AXS SMART 2K
Temp, K	100(2)
λ	1.5418
μ, mm^{-1}	4.935
Scan type	ω scan
F(000)	372
θ_{max}, (deg)	69.93
h,k,l range	-13 ≤*h* ≤13 -11 ≤*k* ≤11 -13 ≤*l* ≤13
Reflns used ($I > 2\sigma(I)$)	1409
Absorption correction	multi-scan SADABS
T (min, max)	0.24, 0.61
$R\ [F^2>2\sigma(F^2)]$, $wR(F^2)$	0.0655,0.1833
GOF	1.135

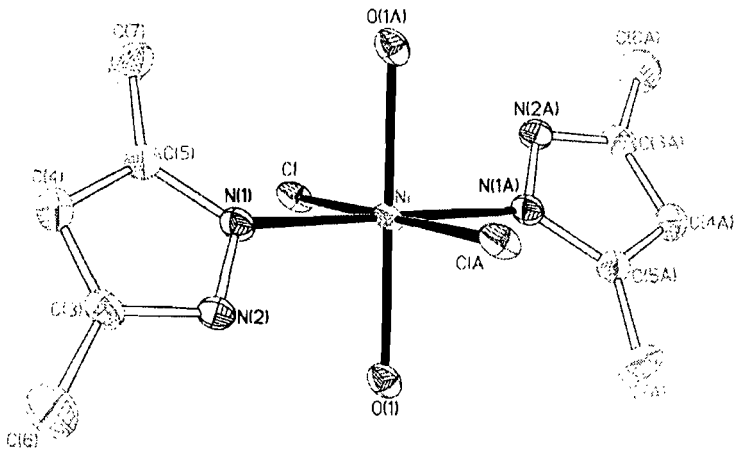

Figure 5.6. ORTEP view of complex **5.10b**. Thermal ellipsoids are shown at 30% probability. The molecule lies on a crystallographic inversion center

Table 5.6. Bond distances and angles for complexes for **5.10b**[a]

5.10b			
Ni-N(1)	2.102(3)	N(1A)-Ni-Cl(1A)	90.44(4)
Ni-O(1)	2.108(2)	N(1A)-Ni-O(1)	89.24(9)
Ni-Cl	2.4239(10)	N(1A)-Ni-O(1A)	90.76(9)
N(1)-Ni- N(1A)	180	O(1)-Ni- O(1A)	180
N(1)-Ni-O(1)	90.76(9)	O(1)-Ni-Cl	88.71(3)
N(1)-Ni-O(1A)	82.24(9)	O(1)-Ni-Cl(1A)	91.29(3)
N(1)-Ni-Cl	90.44(4)	O(1A)-Ni-Cl	91.29(3)
N(1)-Ni-Cl(1A)	89.56(4)	O(1A)-Ni-Cl(A)	88.71(3)
N(1A)-Ni-Cl	89.56(4)	Cl(1)-Ni- Cl(1A)	180

[a]Bond lengths in Å and bond angles in deg

A = -x+1,-y+1,-z+1

Complex **5.10b** (Figure 5.6) displays undistorted octahedral geometry around the nickel centre, the *cis* and *trans* angles are between 82-91° and 180° (Table 5.4). The Ni atom occupies a crystallographic inversion centre and only a half of the molecule is symmetry independent.

5.4. Oxidation attempts for complex [(dpdpm)$NiBr_2(H_2O)$] (3.2a) with $CuCl_2$ and $[Cp_2Fe]PF_6$

Recently in our group, we were able to isolate and characterize new nickel(III) complexes baring (POC_{sp}^3OP)$NiBr_2$ pincer ligand by reacting the pincer adduct (POC_{sp}^3OP)NiBr with $CuBr_2$ salts in hexane and acetone solution.[21] In our case, the pentacoordinated complex **3.2a** has a Ni-L_{axial} bond that involves some degree of repulsion because the dz^2 orbital is fully populated. We wondered how the stability of this compound would be affected if one electron was removed. Otherwise, what would happen if this complex is converted to octahedral Ni(III). To explore this issue, we studied the reaction of complex **3.2a** [(dpdpm)$NiBr_2(H_2O)$] with $CuCl_2 \cdot 2H_2O$, $CuBr_2$ and $[Cp_2Fe]PF_6$, expecting to get the octahedral and the cationic square pyramidal Ni(III) complexes.

5.4.1 Synthesis

Stirring a 1:1 mixture of $CuCl_2 \cdot 2H_2O$ and complex **3.2a** in distilled CH_2Cl_2 solution gave a light solid within a black solution in 30 min. The solution was filtered to give a pale yellow solid and black filtrate. The evaporation of the black filtrate gives a black solid (79% crude yield). The crystallization of this solid from CH_2Cl_2/ether gave black crystals. Curiously, the X-ray analysis showed it to be the monomeric compound **13** (Figure 5.7). The analogous reaction with $CuBr_2$ produced a black-blue solid that was crystallized from CH_2Cl_2/ether it gave black crystals. Unfortunately due to the weak quality of these crystals no farther X-ray studies were made. Also, the elemental analysis of the resulting black crystals did not match any reasonable formula.

The complications arising from the use of CuX_2 as oxidant promote us to use another oxidant. Refluxing a mixture of **3.2a** and $[Cp_2Fe]PF_6$ (1:1) in CH_2Cl_2/acetone for 1.5 h followed by filtration and the evaporation of the filtrate gave a brown solid which was crystallized from CH_3CN/ether to give yellow crystals that were identified as complex **5.14** (Figure 5.8). Indeed, the unexpected final outcome of the reaction depend on the solvent of recrystalization, which was the CH_3CN that produced the dianion $[(dpdpm)_2Ni(CH_3CN)_2][(FeBr_3)_2O]$ complex **5.14**. Several unsuccessful attempts were made to crystallize this solid from different solvents.

These results convinced us to abandon the objective of preparing Ni(III) species. But it is noteworthy to mention that this four-coordinate μ-oxo-diiron species is well known due to the possible use of this ion as a precursor in the preparation of synthetic

analogues enzymes.[22] The initial discovery[23] of the dinuclear oxo-bridged anion $[(FeCl_3)_2O]^{2-}$ that contains tetrahedral iron(III) has been isolated with variety of cations such as tetramethylammonium,[24] tetraethylammonium,[25] tetraphenylphoshonium,[26] ferrocenium[27] and $[(Ph_3P)_2CSe]^{2+}$.[28] The preparation of analogous complexes with bromo-species as their benzyltriphenylphosphonium[29] and ferrocenium[30] salts has been reported. The preparation of the ferrocenium salts could be done successfully in two steps and the presence of the constant pressure of oxygen led to the formation of the desired complex.

1- The formation of Fe(III)

$$FeBr_2 \longrightarrow FeBr_2^+ + 1e^-$$

$$1/2[Br_2 + 2e^- \longrightarrow 2Br^-]$$

$$FeBr_2 + 1/2Br_2 \xrightarrow{Et_2O} FeBr_3 \qquad (1)$$

2- Agitating the mixture of $FeBr_3$ with $FeCp_2$ for 9 h under steam of oxygen

$$FeCp_2 + FeBr_3 \xrightarrow{O_2,\ 9\ h} [FeCp_2]_2[(FeBr_3)_2O] \qquad (2)$$

In our case the formation of complex **5.14** is still a mystery since we do not have the desired structure for this reaction. But it looks as if a ligand exchange with nickel is happening, while H_2O and Br^- prefer to coordinate to Fe. Also the reaction and the crystallization were done under normal atmosphere that probably forces the formation of Br_3Fe-O-$FeBr_3$ species. This reaction has not been probed any further.

5.4.2 Crystallography

Suitable crystals of **5.13** and **5.14** for X-ray diffraction studies were obtained by vapour diffusion of Et_2O into concentrated solutions of these complexes in dichloromethane (**5.13**) and acetonitrile (**5.14**). The two sets of diffraction data resulted in fairly accurate structures for the complexes studied, as reflected in the R values of ca. 0.0483 (**5.13**) and 0.0457 (**5.14**). All the details concerning the refinement of the crystals structure are listed in the supporting information at the end of this thesis (Appendix IV). The crystallographic data are tabulated in Tables 5.7, the ORTEP diagrams of these complexes are shown in Figures 5.7-5.8, bond distances and angles are tabulated in Tables 5.8 and 5.9 for **5.13** and **5.14**, respectively.

Table 5.7. Crystallographic data for **5.13** and **5.14**

	5.13	**5.14**
Formula	$C_{19}H_{16}Br_2N_4Cu$	$C_{42}H_{38}Br_6Fe_2N_{10}NiO$
mol wt	523.72	1348.69
Cryst color	black	golden-yellow
Cryst dimens, mm	0.22×0.16×0.16	0.314×0.08×0.02
Symmetry	Triclinic	Monoclinic
Space group	P-1	C2/c
a, Å	7.55720(10)	23.9391(5)
b, Å	9.1562(2)	13.9637(3)
c, Å	14.4575(2)	14.9828(3)
α, deg	99.1930(10)	90
β, deg	106.7060(10)	106.9500(10)
γ, deg	90.2830(10)	90
Volume, Å^3	944.49(3)	4790.86(17)
Z	2	4
D(calcd), g cm^{-1}	1.842	1.870
Diffractometer	Bruker AXS SMART 2K	Bruker AXS SMART 2K
Temp, K	150(2)	148(2)
λ	1.5418	1.5418
μ, mm^{-1}	6.666	11.471
Scan type	ω scan	ω scan
F(000)	514	2632
θ_{max}, (deg)	68.25	68.66
h,k,l range	$-8 \le h \le 8$ $-10 \le k \le 11$ $-17 \le l \le 17$	$-28 \le h \le 28$ $-15 \le k \le 13$ $-17 \le l \le 18$
Reflns used (I >2σ(I))	3289	3095
Absorption Correction	Multi-scan SADABS	Multi-scan SADABS
T (min, max)	0.33, 0.50	0.67, 1.00
R [$F^2>2\sigma(F^2)$], *wR*(F^2)	0.0483,0.1390	0.0457,0.1250
GOF	1.042	0.979

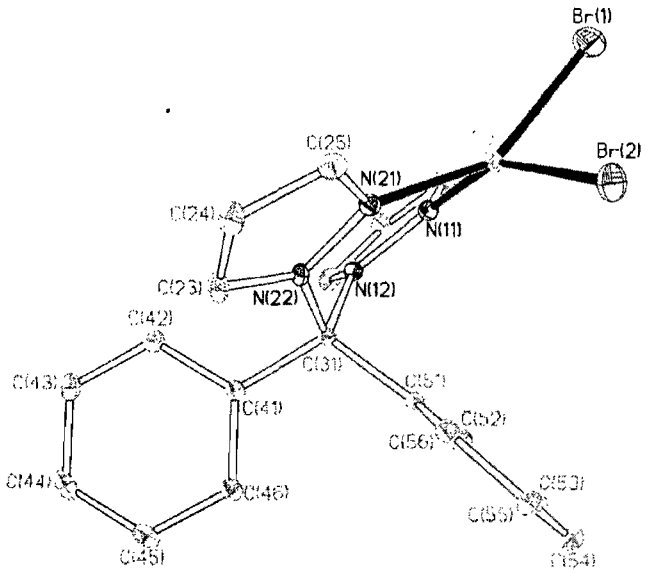

Figure 5.7. ORTEP view of complex **5.13**. Thermal ellipsoids are shown at 30% probability

Table 5. 5. Bond distances and angles for complexes for **5.13** and [(dpdpm)$CuCl_2$][a]

	[(dpdpm)$CuBr_2$] (**5.13**)	[(dpdpm)$CuCl_2$]
Cu-N(11)	2.006(4)	2.011(4)
Cu-N(21)	1.967(4)	1.961(4)
Cu-X(1)	2.3167(8)	2.2071(15)
Cu-X(2)	2.3488(8)	2.2388(16)
N(11)-Cu-X(1)	97.32(10)	95.66(12)
N(11)-Cu-X(2)	152.11(11)	153.99(12)
N(21)-Cu-X(1)	151.55(11)	153.42(13)
N(21)-Cu-X(20	91.71(10)	91.36(12)
N(21)-Cu-N(11)	88.71(15)	88.72(16)
X(1)-Cu-X(2)	95.49(3)	95.82(6)

[a]Bond lengths in Å and bond angles in deg

At first glance the structure of complex **5.13** appeared to be tetrahedral. However, inspection of bond angles indicates that it is twisted square planar geometry because the cis angles are within 88° and 97°, much closer to square planar than tetrahedral. In addition, the value of the angle between the plane of Br1-Cu-Br2 and the plane of N11-Cu-N21 is ca. 39°, which is somewhat closer to what would be expected in a square planar geometry 0° than in a tetrahedral 90°. The average Cu-N and Cu-Br bond lengths are 1.98 Å and 2.33 Å,

respectively. These lengths are in close agreement with those reported for similar complex [(dpdpm)$CuCl_2$] which is considered isostructural to **5.13**.

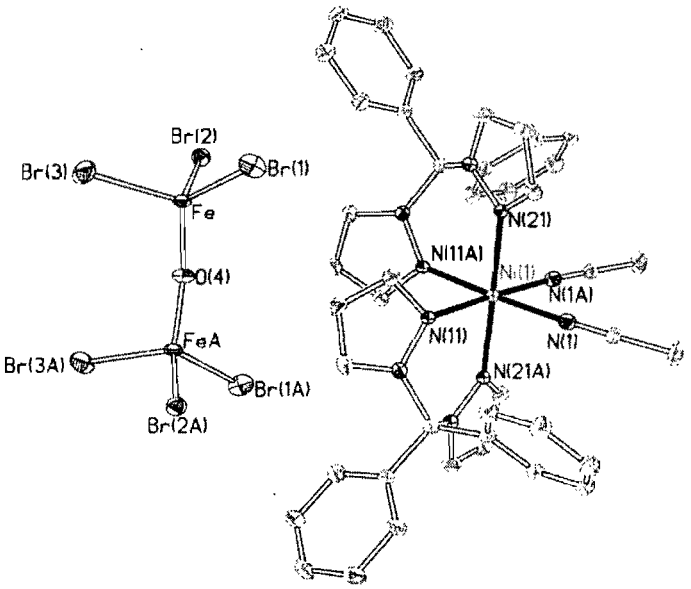

Figure 5.8. ORTEP view of complex **5.14**. Thermal ellipsoids are shown at 30% probability

Table 5.6. Bond distances and angles for complexes for **5.14**[a]

5.14			
Ni(1)-N(11)	2.093(4)	N(1A)-Ni(1)-N(11A)	95.40(16)
Ni(1)-N(21)	2.079(4)	N(21A)-Ni(1)-N(1A)	90.27(16)
Ni(1)-N(1)	2.092(4)	N(21A)-Ni(1)-N(11A)	92.74(15)
Br(1)-Fe	2.3390(11)	N(21)-Ni(1)-N(11A)	86.95(15)
Br(2)-Fe	2.3695(10)	N(21)-Ni(1)-N(1)	90.27(16)
Br(3)-Fe	2.3743(10)	N(1)-Ni(1)-N(1A)	84.6(2)
Fe-O(4)	1.7541(9)	N(21A)-Ni(1)-N(1)	90.03(16)
N(11)-Ni(1)-N(21)	92.74(15)	O(4)-Fe-Br(1)	112.75(15)
N(11)-Ni(1)-N(11A)	84.8(2)	O(4)-Fe-Br(2)	110.94(5)
N(11)-Ni(1)- N(21A)	86.95(15)	O(4)-Fe-Br(3)	108.47(18)
N(11)-Ni(1)-N(1)	95.40(16)	Br(1)-Fe-Br(2)	108.35(4)
N(11)-Ni(1)-N(1A)	177.22(15)	Br(1)-Fe-Br(3)	107.38(4)
N(21A)-Ni(1)-N(21)	179.6(2)	Br(2)-Fe-Br(3)	108.83(4)
N(1)-Ni(1)-N(11A)	177.22(15)	Fe-O-Fe	171.52(4)
N(21)-Ni(1)-N(1A)	90.03(16)		

[a]Bond lengths in Å and bond angles in deg

A = -x+1,y,-z+1/2

Complex **5.14** (Figure 5.8) displays slightly distorted octahedral geometry around the nickel centre. The *cis* and *trans* bond angles are ranging from 85-95° and 177-180°. The Ni atom is on crystallographic 2-fold axes bisecting N11-Ni-N11A and N1-Ni-N1A. As mentioned in chapter 3, the formation of an octahedral species changes the conformation of the six-membered metallacycle from a boat configuration to a half-chair conformation due to the Ph substituent of dpdpm, which is pushed toward the equatorial plane and is oriented parallel to Ni-$NCCH_3$, exactly the same as in complex 3.3, [(dpdpm)NiBr$(H_2O)_2(CH_3CN)$]Br. The angle formed between the coordination plane N21-N22-N12A-N11A and the plane formed by the pyrazole nitrogens in complex **5.14** N11A-N21-N1-N21A is nearly coplanar (angles of 5.5° in **5.14**, 4° in **3.3**). Moreover, in **5.8** the distance Ni-N_{av} 2.109(6) Å is somewhat longer than those in complexes **5.9** (2.068(5) Å) and **5.14** (2.088(4) Å). These observations lead to the following order for Ni-$N_{average}$ bond length for the three complexes: **5.8** > **5.14** > **5.9**. The slightly longer Ni-N bond distance in **5.8** is due to the steric hindrance generated from the phenyl rings of the three dpdpm ligands while for complex **5.9** yields in the least encumbered steric environment as compared to the other complexes and hence has the smallest Ni-N bond length.

5.5 Experimental

5.5.1 General. Literature procedures were used for the synthesis of diphenyl(dipyrazolyl)methane (dpdpm) and diphenyl(3,5-dimethylpyrazolyl)methane ($dpdpm^{Me2}$),[15] $(PhCN)_2PdCl_2$ and $(DME)_2NiCl_2$. Anhydrous $NiCl_2$ and NiI_2 were purchased from Sigma-Aldrich, stored in a Dry box, and used without further dehydration, while in some cases $NiCl_2 \cdot 6H_2O$ was used without further dehydration. Where necessary, the synthetic manipulations were carried out in dry and oxygen free solvents under an atmosphere of ultra high purity nitrogen using standard Schlenk techniques and a Dry box. The elemental analyses (C, H, and N) were performed in duplicate by Laboratoire d'Analyse Élémentaire de l'Université de Montréal. The ^1H NMR spectra were recorded on a Bruker Av400 (at 400 MHz). The IR spectra were recorded between 4000 and 400 cm^{-1} using KBr pellets on a Perkin Elmer Spectrum one spectrophotometer using the Spectrum v.3.01.00 software. The magnetic susceptibility measurements were carried out at room temperature using the Gouy method with a Johnson Matthey Magnetic Susceptibility Balance, using $HgCo(NCS)_4$ as standard.

5.5.2 Syntheses.

[(dpdpm)Ni(μ-Cl)Cl]$_2$ (5.6). A solution of dpdpm (0.50 g, 1.66 mmol) in acetone (25 mL) was added to a stirred suspension of $NiCl_2 \cdot 6H_2O$ (0.40 g, 1.66 mmol) in acetone (25 mL). The reaction mixture was stirred for 5 h at room temperature and filtered to give an orange solid (0.62 g, 86% crude yield). X-ray quality single crystals (dark orange) were obtained by slow diffusion of Et_2O into a concentrated acetone solution kept at room temperature. m.p. >260°C. $\mu_{eff.}$ 3.4 BM. Anal.Calc.For $[C_{19}H_{16}N_4NiCl_2]_2 \cdot 1/2\ Et_2O$: C, 54.01; H, 4.53; N, 12.00. Found: C, 53.58; H, 4.61; N, 11.39. ^{1}H NMR (CD_3OD): δ 60.44 (br), 38.75 (br), 7.11- 6.47 (br) 4.79 (br), 1.95 (br), 1.81 (br), -124 (br), -140.48 (br), -162.21. IR (KBr): υ (cm^{-1}) 3626 (s), 3402 (br), 1700 (m), 1527(m), 1518 (m), 1491 (m), 1449 (s), 1438 (s), 1408(m), 1384 (m), 1308 (vs), 1251 (m), 1220(s), 1190 (m), 1167 (m), 1108 (s), 1069 (vs), 1000 (w), 941 (w), 921 (w), 891 (w), 874 (w), 783 (m), 753 (s), 702 (s), 657 (w), 638 (sw), 604 (w).

[(dpdpm)NiCl(H_2O)$_2$]Cl (5.7). The procedure used for the synthesis complex 6 was followed. X-ray quality single crystals (light green) were obtained by slow diffusion of hexane into a concentrated acetone solution kept at room temperature. m.p. >260°C. μ_{eff} 3.4 BM. Anal.Calc. For $C_{19}H_{20}N_4Ni\ Cl_2O_2 \cdot H_2O$: C, 47.15; H, 4.58; N, 11.58. Found: C, 46.96; H, 4.49; N, 11.52%. ^{1}H NMR (CD_3OD): δ 60.60 (br), 48.72 (br), 38.96 (br), 7.48 (br), 7.35 (br), 7.21 (br), 7.05 (br), 6.68 (br), 6.26 (s), 4.83 (br), -124.11 (s), -140 (br), -161.96 (br). IR (KBr): υ (cm^{-1}) 3340 (br), 3163-3064 (br), 1631 (m), 1516 (m), 1491 (m), 1450 (s), 1437 (m), 1414 (s), 1385 (m), 1336 (m), 1318 (vs), 1257 (m), 1223 (w), 1214 (s), 1198 (m), 1188 (w), 1174 (w), 1104 (m), 1086 (m), 1069 (vs), 1001 (m), 943 (m), 922 (m), 891 (m), 870 (m), 843 (m), 780 (vs), 749 (vs), 702 (vs), 657 (m), 642 (m), 611 (m), 603 (m), 537 (w), 511 (w).

[(dpdpm)$_3$Ni][I_3^-]$_2$ (5.8). A solution of dpdpm (0.20 g, 0.66 mmol) in ethanol (20 mL) was added to a stirred solution of NiI_2 (0.21 g, 0.66 mmol) in ethanol (20 mL). The resultant mixture was heated to reflux for 15 h, cooled to room temperature, filtered, and evaporated to give a dark red-brown solid (0.28 g, 73% crude yield). X-ray quality single crystals (dark brown) were obtained by slow diffusion of ether into the CH_2Cl_2 solution, kept at room

temperature. m. p. 160°C. μ_{eff} 4.9 BM. For $C_{57}H_{48}N_{12}NiI_6$: C, 39.78; H, 2.81; N, 9.77. Found: C, 39.54; H, 2.50; N, 9.61%. ^{1}H NMR ($CDCl_3$): δ 7.69 (s), 7.55 (s), 7.37-7.35 (br), 7.08 (br), 6.30 (s), 1.19 (br). IR (KBr): υ (cm^{-1}) 3411 (br), 1628 (m), 1520 (w), 1492 (w), 1450(s), 1437 (s), 1407 (s), 1384 (m), 1305 (s), 1250 (m), 1222 (s), 1190 (s), 1169 (m), 1108 (s), 1069 (s), 1000 (w), 939 (w), 920 (w), 891 (w), 873 (w), 754 (vs), 700 (s), 659 (w), 638 (m).

[(Pz^{Me2})$_2$$NiCl_2$($H_2O$)$_2$] (5.10b). Method *I.* $dpdpm^{Me2}$ (0.0356 g, 0.10 mmol) disolved in CH_2Cl_2 (~2 mL) was added to $(DME)_2NiCl_2$ (0.22 g, 0.10 mmol) in CH_2Cl_2 (~4 mL) and stirred for 45 min at room temperature. Adding hexane (~3 mL) to the final suspension followed by filtration gave a yellow solid, which was washed with excess of hexane to give a yellow solid of **5.10a** (0.025 g, 78% crude yield). X-ray quality single crystals (light green 10b) were obtained by diffusion of hexane into a concentrated acetone solution. IR (for **5.10a**) (KBr) : v (cm^{-1}) 3314 (vs), 3254 (br), 3114 (w), 2931 (m), 1577 (vs), 1498 (w), 1468 (m), 1412 (m), 1381 (m), 1307 (s), 1273 (s), 1229 (w), 1180 (s), 1150 (m), 1047 (s), 1030 (s), 785 (m), 764 (s), 681 (w), 661 (m), 647 (s), 611 (w), 578 (s).

Method *II.* A hot solution of $dpdpm^{Me2}$ (0.30 g, 0.84 mmol) in butanol (20 mL) was added to a stirred hot solution of $NiCl_2.6H_2O$ (0.28 g, 1.15 mmol) in butanol (25 mL). The reaction mixture was heated to reflux for 30 min, cooled to room temperature, filtered, and the filtrate was evaporated to give a yellow solid (0.26 g, 96% crude yield). X-ray quality single crystals of **5.10b** (light green) were obtained by slow diffusion of toluene into a concentrated solution of acetone kept at room temperature.

Method *III.* A solution of Pz^{Me2} (1.15 g, 0.012 mmol) in butanol (25 mL) was added to a stirred hot solution of $NiCl_2{\cdot}6H_2O$ (1.48 g, 6.2 mmol) in butanol (25 mL). The reaction mixture was heated to reflux for 30 min, cooled to room temperature, filtered, and the remaining solid was washed with Et_2O (3×20 mL) to give a yellow powder (1.009 g, 45 % crude yield). The evaporation of the green filtrate gave a yellow powder, which was washed with Et_2O (3×20 mL) to give (0.70 g, 31% crude solid).

[(Pz^{Me2})$_2$NiBr$_2$] (5.11). Method *I.* A hot solution of $dpdpm^{Me2}$ (0.182 g, 0.51 mmol) in butanol (12 mL) was added to a stirred hot solution of $NiBr_2$ (0.112 g, 0.51 mmol) in butanol (12 mL). The reaction mixture was heated to reflux for 30 min, cooled to room temperature, filtered, and the filtrate was evaporated to give a blue solid. Recrystallization of the solid from 20 mL toluene yield X-ray quality blue dark crystals (0.15 g, 71%).

Method *II*. A solution of Pz^{Me2} (0.30 g, 3.12 mmol) in CH_2Cl_2 (25 mL) was added to a stirred suspension of NiBr (0.70 g, 3.20 mmol) in CH_2Cl_2 (25 mL). The reaction mixture was heated to reflux for 1.5 h cooled to room temperature, filtered to remove unreacted $NiBr_2$, and evaporated to give a dark blue powder (0.60 g, 94% crude yield). X-ray quality single crystals (dark blue) were obtained by slow diffusion of Et_2O into a concentrated acetone solution kept at room temperature.

[(Pz^{Me2})$_2$PdCl$_2$] (5.12). $dpdpm^{Me2}$ (0.046 g, 1.30 mmol) solved in CH_2Cl_2 (~6 mL) was added to $(PhCN)_2PdCl_2$ (0.05 g, 1.3 mmol) in CH_2Cl_2 (~3 mL) and stirred for 3 h at room temperature. The resulting mixture was filtered and the yellow filtrate was evaporated to give orange solid (0.029 g, 81% crude yield). X-ray quality single crystals (orange) were obtained by slow diffusion of Et_2O into a concentrated CH_2Cl_2 solution kept at room temperature.

[(dpdpm)CuBr$_2$] (5.13). Solid $CuCl_2.2H_2O$ (0.078 g, 0.46 mmol) was added directly to stirred solution of complex **3.2a** [(dpdpm)$NiBr_2(H_2O)$] (0.26 g, 0.47 mmol) in distilled CH_2Cl_2 (20 mL). The reaction mixture was stirred for 30 min at room temperature, filtered, and the filtrate evaporated to give a black solid (0.19 g, 80% crude yield). X-ray quality single crystals were obtained by diffusion of diethyl ether into a concentrated solution of CH_2Cl_2. m.p. 199°C. μ_{eff} 3.32 BM. Anal.Calc.for $C_{19}H_{16}N_4CuBr_2$: C, 43.57; H, 3.08; N 10.70. Found: C, 43.98; H, 2.97; N, 10.77%. ^{1}H NMR ($CDCl_3$): δ 8.10 (br), 7.93 (br), 6.96 (br), 0.88 (br). IR (KBr): ν (cm^{-1}) 3437 (br), 3168 (w), 3139 (w), 3124 (m), 3047 (w), 2963 (w), 2924 (w), 2374 (w), 1619 (br), 1508 (m), 1492 (s), 1451 (s), 1439 (s), 1405 (w), 1384 (s), 1314 (vs), 1256 (m), 1237 (m), 1216 (m), 1196 (m), 1173 (m) 1160 (w), 1105 (s), 1085 (s), 1065 (vs), 1001 (m), 988 (w), 940 (m), 921 (m), 892 (m), 867 (w), 765 (m), 755 (vs), 698 (vs), 683 (w), 668 (w), 656 (w), 633 (w), 606 (w).

$[(dpdpm)_2Ni(CH_3CN)_2][(FeBr_3)_2O]$ (5.14). A solution of the complex **3.2a** $[(dpdpm)NiBr_2(H_20)]$ (0.20 g, 0.36 mmol) in CH_2Cl_2 (25 mL) was added to a stirred suspension of $[Cp_2Fe]PF_6$ (0.11 g, 0.33 mmol) in acetone (30 mL). The reaction mixture was heated to reflux for 90 min, cooled to room temperature, filtered, and evaporated to give a brown powder (0.20 g, 95% crude yield). X-ray quality single crystals (yellow) were obtained by slow diffusion of Et_2O into a concentrated CH_3CN solution kept at room temperature. μ_{eff} 3.3 BM. IR (KBr) : v (cm^{-1}) 3437 (br), 3157 (w), 3117 (w), 2929 (w), 2343 (w), 2314 (w), 2924 (w), 2286 (w), 1631 (br), 1488 (s), 1449 (s), 1435 (s), 1405 (m), 1382 (m), 1326 (w), 1303 (vs), 1245 (w), 1218 (m), 1192 (m), 1161 (m), 1105 (s), 1068 (vs), 1001 (w), 938 (w), 920 (w), 887 (s), 871 (vs), 861 (s), 779 (s), 755 (vs), 697 (s), 654 (w), 636 (w), 602 (w).

5.6 Reference

(1) Addison, A. W.; Rao, T. N.; Reedijk, J.; van Rijn, J.; Verschoor, G. C. *J. Chem. Soc., Dalton Trans.* **1984**, 1349. The strcutural index τ is determined from the equation $\tau = (\beta - \alpha)/60$, wherein β and α are, respectively, the largest basal angles ($\beta > \alpha$). The τ values for perfectly square pyramidal and trigonal bipyramidal structures are 0 and 1, respectively.

(2) Jansen, J. C.; Van Koningsveld, H.; Van Ooijen, J. A. C.; Reedijk, J. *Inorg. Chem.* **1980**, *19*, 170.

(3) Nelana, F. S.; Darkwa, J.; Guzei, I. A.; Mapolie, S. F. *J. Organomet. Chem.* **2004**, *689*, 1835.

(4) Cheng, C.-H.; Lian, J.-S.; Wu, Y.-S.; Wang, S.-L. *Acta Crystallogr.* **1990**, *C46*, 208.

(5) Tsuji, S.; Swenson, D. C.; Jordan, R. F. *Organometallics* **1999**, *18*, 4758.

(6) (a) Bieller, S.; Haghiri, A.; Bolte, M.; Bats, J. W.; Wagner, M.; Lerner, H.-W. *Inorg. Chem. Acta* **2006**, *359*, 1559. (b) Santi, R.; Romano, A. M.; Sommazzi, A.; Grande, M.; Bianchini, C.; Mantovani, G. *J. Mol. Catal. A: Chem.* **2005**, *229*, 191.

(7) Pettinari, C.; Cingolani, A.; Bovio, B. *Polyhedron* **1996**, *15*, 115.

(8) With dpm^{Me2} ligand : Verbiest, J.; Van Ooijen, J. A. C.; Reedijk, J. *J. Inorg. Nucl. Chem.* **1980**, *42*, 971.

(9) With bpp ligand : Mesubi, M. A.; Ekemenzie, P. I. *Trans. Met. Chem.*, **1984**, *9*, 91.

(10) With bpp ligand : Mesubi, M.A. *J. Coord. Chem.* **1984**, *13*,179.

(11) With dpm^{Me2} ligand : Reedijk, J.; Verbiest J. *Trans. Met. Chem.* **1979**, *4*,239.

(12) With bpp ligand : (a) Minghetti, G. ; Cinellu, M.A. ; Bandini, A.L. ; Banditelli, G. ; De Martin, F. ; Manassero, M. *J. Organomet. Chem.* **1986**, *315*, 387. (b) Juanes, O. ; de Mendoza, J. ; Rodriguez-Ubis, J.C. *J. Organomet. Chem.* **1989**, *363*, 393.

(13) Minghetti, G.; Cinellu, M. A.; Bandini, A. L.; Banditelli, G.; Demartin, F.; Manassero, M. *J. Organomet. Chem.* **1986**, *315*, 387.

(14) Dungan, C. H.; Maringgele, W.; Meller, A.; Niedenzu, K.; Nöth, H.; Serwatowska, J.; Serwatowski, J. *Inorg. Chem.* **1991**, *30*, 4799.

(15) Shiu, K.-B.; Yeh L.-Y.; Peng. S.-M.; Cheng, M.-C. *J. Organomet. Chem.* **1993**, *460*, 203.

(16) Schneider, J. L.; Young, V. G.; Tolman, W. B. *Inorg. Chem.* **2001**, *40*, 165.

(17) Thomas, C. M.; Peters, J. C. *Organometallics* **2005**, *24*, 5858.

(18) Shaw, J. L.; Cardon, T. B.; Lorigan, G. A.; Ziegler, C. J. *Eur. J. Inorg. Chem.* **2004**, 1073.

(19) Netto, A. V. G.; Santana, A. M.; Mauro, A. E.; Frem, R. C. G.; de Almeida, E. T.; Crespi, M. S.; Zorel, H. E. *J. Therm. Anal. Calorimetry.* **2005**, *79*, 339.

(20) Shaw, J. L. PhD. Desertation, University of university of Georgia, 2004.

(21) Pandarus, V.; Zargarian, D. *Chem. Commun.*, **2007**, 978.

(22) Vincent, J. B.; Olivier-Lilley, G. L.; Averill, B. A. *Chem. Rev.* **1990**, *90*, 1447.

(23) Drew, M. G. B.; McKee, V.; Nelson, S. M.; *J. Chem. Soc., Dalton Trans.* **1978**, 80.

(24) Neuse, E. W.; Merim, M. G. *Transition Met.Chem.* **1984**, *9*, 205.

(25) Simon, E. D.; Holm, R. H. *Inorg. Chem.* **1983**, *22*, 3809.

(26) Dehnicke, K.; Prinz, H.; Massa, W.; Pebler, J.; Schmidt, Z. *Anorg. Allg. Chem.* **1983**, *499*, 20.

(27) (a) Bullen, G. J.; Howlin, B. J.; Silver, J.; Fitzsimmons, B. W.;Sayer, I.; Larkworthy, L. F. J. *Chem. Soc., Dalton Trans.* **1986**, 1937. (b) Carty, P.; Clare, K. C.; Creighton, E.; Metcalfe, E.; Raper, E. S.; Dawes, H. M. *Inorg. Chim. Acta* **1986**, *112*, 113.

(28) Schmidbauer, H.; Zybill, C. E.; Neugebauer, D.; *Angew. Chem., Int. Ed. Engl.* **1983**, *22*, 156.

(29) Petridis, D.; Terzis, A. *Inorg. Chim. Acta* **1986**, *118*, 129.

(30) Evans, P. J. M.; Fitzsimmons, B. W.; Marshall, W. G.; Golder, A. J.; Larkworthy,L. F.; Povey, D. C.; Smith, G. W. *J. Chem. Soc. Dalton Trans.* **1992**, 1065.

Chapter 6: Conclusion

Previous studies in our group have shown that bis(pyrazoly)alkane ligands bpp and bpm^{Me2} form complexes of different geometries with nickel halides and nitrate, all depending on the nature of the reactants and their stochiometry. For instance, bpp and bpm^{Me2} ligands always form octahedral species with nickel nitrate, regardless of the stochiometry of the reactants, while with nickel halides they form tetrahedral, trigonal bi-pyramidal and square pyramidal complexes depending on the stoichiometry of the reactants. Alkylation studies have been explored for bpm^{Me2} and bpp complexes, but no compound was isolated due to its thermal instability. This instability is due mainly to the deprotonation of the bridging moiety in these ligands. To test the validity of this scenario, we decided to use phenyl-substituted ligands. Another potential advantage of the phenyl substituent is the steric protection of the metal center in the envisaged reactivities in ethylene polymerization. Also, the phenyl substituents might have interesting influence on the thermo-, solvato-, and vapochromic properties of the complexes.

During the course of our studies, new dpdpm nickel complexes have been prepared and their structural and spectroscopic properties have been studied. Similarly to bpp and bpm^{Me2} ligands, dpdpm always forms octahedral species with nickel nitrate regardless of the stoichiometry of the reactants and the solvent used. We conclude that the different steric properties of these bis(pyrazolyl)alkane ligands have a little or no influence over the structures adopted by their complexes. The most important factor determining the geometry seems to be the nature of the anion (e.g. NO_3^-). The most interesting aspect of these complexes is the solvato-, thermo-, and vapochromism of complex $[(dpdpm)Ni(\eta^2\text{-}NO_3)_2]$ (**2.1**). We believe that these physical properties arise from the reversible coordination of acetonitrile to the Ni center in **2.1** to form complex $[(dpdpm)Ni(\eta^2\text{-}NO_3)(\eta^1\text{-}NO_3)(CH_3CN)]$ (**2.2**). Interestingly, complex **2.1** is regenerated at higher temperatures presumably due to entropic factors that tend to favour the chelation of the nitrate ligand and the dissociation of a molecule of acetonitrile. Comparing the nitrate complexes obtained in this thesis with previous reported bis(pyrazolyl)alkane complexes of nickel shows that dpdpm nitrate complexes have more pronounced solvato-, vapo-, and thermochromic properties.

The reaction of dpdpm with nickel bromide gave complexes of trigonal bi-pyramidal, square pyramidal and octahedral geometries depending on the stoichiometry of the reactants, the nature of the solvent, the humidity and the temperature of the reaction. This is in contrast to the exclusive formation of octahedral species from the reaction of $Ni(NO_3)_2$ under similar conditions. The formation of penta-corrdinate complexes is somewhat unusual; one possible reason for the possible prevalence of these complexes is the long-range Ni-Ph interaction that appears to stabilize the solid state structure.

A common aspect of all $NiBr_2$ derivatives prepared to date is the lability of all Ni-ligand bonds. Thus, we have observed that the dissociation of Br^- is very facile, which makes possible the observation of solvato-, vapo-, and thermochromic properties for these compounds. UV-Vis studies of complexes **3.1**, **3.2a** and **3.2b** revealed an interesting interconversion at different temperatures (shown in Scheme 6.1). Since **3.1** can be prepared by dehydration of **3.2a** or **3.2b** these observations suggest that the continuous and reversible thermochromism of **2a** in acetone involves its conversion to **3.1** at high temperatures and probably **2b** at low temperature.

Scheme 6.1

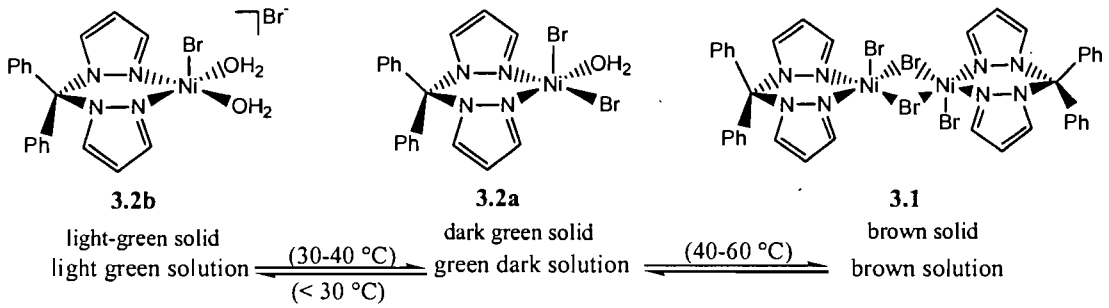

Thus, complex **3.2a** turns light green in acetone below 30 °C, presumably converting to complex **3.2b**. Increasing the temperature to 30-40 °C gives a dark green solution due to regenerating complex **3.2a**. Further heating to 40-60 °C gives a brown solution probably due to formation of complex **3.1**. Interestingly, the electronic spectrum of complex **3.2a** in CH_2Cl_2 at room temperature is almost identical to the spectra of complex **3.2a** in acetone at high temperature, implying complex **3.2a** in CH_2Cl_2 is converted to complex **3.1** in weakly coordinating solvents such as CH_2Cl_2 and hot acetone.

The solvatochromic properties of these complexes were evident from the UV-Vis spectra of **3.2a** in CH_2Cl_2. The electronic spectra of **3.2a** in CH_2Cl_2 and acetone show four

main bands with a shoulder; we proposed that in CH_2Cl_2 and acetone solution complex **3.2a** maintains its square pyramidal structure, which is reasonable because both of these solvents have weak coordinatination. On the other hand, the electronic spectra of complex **3.2a** in MeOH and CH_3CN show three main bands that indicate that complex **3.2a** in these solutions adopts a hexa-coordinated geometry due to the insertion of a molecule of solvent or water in the empty axial position. The formation of a coordinating octahedral species in these nucleophelic solvents is consistent with the observation of negligible thermochromic behavior in these solvents.

The bis(dpdpm) complexes **3.4** and **3.5** showed remarkable solvatochromism properties. This is most evident from the electronic spectra of the complexes in CH_2Cl_2 solutions, which registered major changes over a narrow range of temperature s (-10 °C to +40 °C). Interestingly, the spectra of both complexes are very similar at -10 and 40 °C, but not for intermediate temperatures. More over, the spectra features of both complexes at 40 °C were similar to those observed for complex **3.2a** in CH_2Cl_2 at rt. and at high temperatures in acetone solutions. Based on these observations, we propose that heating CH_2Cl_2 solutions of the octahedral bis(dpdpm) complexes **3.4** and **3.5** leads to the dissociation of a dpdpm ligand to form mono(dpdpm) species. The similarity between the colors of these solutions and the solid sample of complex **3.1** points to the possible formation of the dimeric structure of complex **3.1** at high temperature (Scheme 6.2).

Scheme 6.2

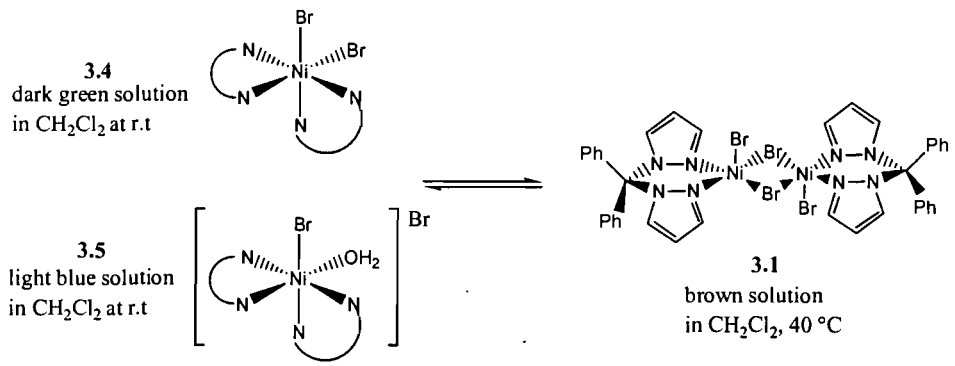

The vapochromism was very briefly studied for the complexes **3.1**, **3.2a**, **3.2b**, **3.4** and **3.5.** These complexes are very sensitive to humidity, and interconverted as a function of the amount of water in the atmosphere. For example, solid samples of complex **3.1**

(brown) turned to green after exposure to humidity, while complex **3.2a** (dark green) turned to light green and then light blue when kept in a humid environment for an extended period. In addition, complex **3.2b** (light green) readily converted to **3.1** (brown) in the presence of solvent vapors (benzene, Et_2O, or toluene), whereas **3.2a** did not record any important changes; however, the reversed reaction was much slower. Similarly, exposing complex **3.4** (green) to humid air convert it to **3.5** (blue), both in solution and solid state. In this case, however, the reversed reaction tooke place only if the sample was not exposed to humidity for extended periods.

The above observations demonstrate that Ni-complexes of dpdpm feature quite labile Ni-ligand bonds. To our disappointment these compounds did not prove suitable precursors for organometallic complexes. For example, several attempts to alkylate complex $[(dpdpm)_2Ni(Br)_2]$ with CH_3MgCl and CH_3Li were unsuccessful, and resulted in the eventual decomposition of the complex. Furthermore, attempts to prepare cationic derivatives of **3.2a** led to the unexpected formation of $[\{(dpdpm)(CH_3CN)NiBr_2\}(AgBr)]_2$ (**4.1**) and $[(dpdpm)\ NiBr(CH_3CN)_3]PF_6$ (**4.2**) complexes. Finally, our attempts to oxidize nickel(II) in complex **3.2a** by $CuCl_2{\cdot}2H_2O$ and $[Cp_2Fe]PF_6$ were unsuccessful and also produced unexpected complexes. In conclusion, we did not pursue our studies in this area.

In addition to the lability of these complexes, we also found that dpdpm was itself unstable under certain conditions. For example, the refluxing reaction of NiI_2 with dpdpm in EtOH gave complex $[(dpdpm)_3Ni][I_3]_2$ (**5.10**) and $[(Pz)_6Ni]I_2$ (**5.11**). The latter is presumably formed by the degradation of dpdpm. Interestingly, we have observed a similar behavior with the $dpdpm^{Me2}$ ligand. The reactions of nickel and palladium salts with this ligand led to the formation of the unexpected adducts $[(Pz^{Me2})_2NiCl_2(H_2O)_2]$ (**5.12**), $[(Pz^{Me2})_2NiBr_2]$ (**5.13**) and $[(Pz^{Me2})_2PdCl_2]$ (**5.14**). We do not know what is the real reason for the degradation of the ligand, but as mentioned previously, it looks as if the outcome of the reaction depends on several parameters, including the reaction condititions (the nature of the reactants, the metal/ligand ratio, the solvent used, temperature and time of the reaction); the coordinating ability of the solvent; the degree of residual moisture present in the reaction medium and the steric hindrance of the ligand.

6.1 Future work

Several interesting experiments could be done to develop, complete and continue the studies described in this thesis. It will be interesting to probe the vapo- and thermochromic properties of thin films produced from polymer matrices containing complexes $[(dpdpm)Ni(\eta^2\text{-}NO_3)_2]$, $[(dpdpm)Ni(Br)_2]_2$, $[(dpdpm)Ni(Br)_2(H_2O)]$ and $[(dpdpm)_2Ni(Br)_2]$. It would be interesting to form a polymer based on complex **3.1** $[(dpdpm)Ni(Br)_2]_2$ by using ligand $[C(Pz)_4]$ (Scheme 6.3).

Scheme 6.3

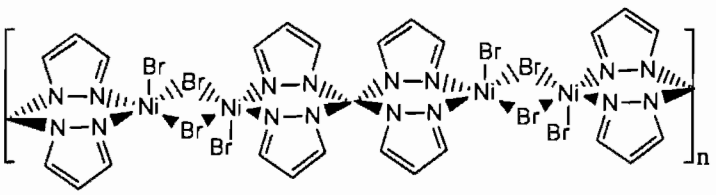

Article 1

Syntheses, Structure, Spectroscopy, and Chromotropism of New Complexes Arising from the Reaction of Nickel(II) Nitrate with Diphenyl(dipyrazolyl)methane

Supplementary material

Table I-1 Atomic coordinates and equivalent isotropic displacement parameters ($Å^2 \times 10^3$) for [(dpdpm)Ni(η^2-NO_3)$_2$] (**2.1**).

Table I-2 Hydrogen coordinates ($\times 10^4$) and isotropic displacement parameters ($Å^2 \times 10^3$) for [(dpdpm)Ni(η^2-NO_3)$_2$] (**2.1**).

Table I-3 Anisotropic displacement parameters ($Å^2 \times 10^3$) for [(dpdpm)Ni(η^2-NO_3)$_2$] (**2.1**).

Table I-4 Bond length [Å] and angles [°] for [(dpdpm)Ni(η^2-NO_3)$_2$] (**2.1**).

Table I-5 Torsion angles [°] for [(dpdpm)Ni(η^2-NO_3)$_2$] (**2.1**).

Table I-6 Atomic coordinates and equivalent isotropic displacement parameters ($Å^2 \times 10^3$) for [(dpdpm)Ni(η^1-NO_3)(CH_3CN)][NO_3] (**2.2**).

Table I-7 Hydrogen coordinates ($\times 10^4$) and isotropic displacement parameters ($Å^2 \times 10^3$) for [(dpdpm)Ni(η^1-NO_3)(CH_3CN)][NO_3] (**2.2**).

Table I-8 Anisotropic displacement ($Å^2 \times 10^3$) for [(dpdpm)Ni(η^1-NO_3)(CH_3CN)][NO_3] (**2.2**).

Table I-9 Bond length [Å] and angles [°] for [(dpdpm)Ni(η^1-NO_3)(CH_3CN)][NO_3] (**2.2**).

Table I-10 Torsion angles [°] for [(dpdpm)Ni(η^1-NO_3)(CH_3CN)][NO_3] (**2.2**).

Table I-11 Atomic coordinates and equivalent isotropic displacement parameters ($Å^2 \times 10^3$) for [(dpdpm)$_2$Ni(H_2O)(η^1-NO_3)][NO_3] (**2.3**).

Table I-12 Hydrogen coordinates ($\times 10^4$) and isotropic displacement parameters ($Å^2 \times 10^3$) for $[(dpdpm)_2Ni(H_2O)(\eta^1\text{-}NO_3)][NO_3]$ (**2.3**).

Table I-13 Anisotropic displacement parameters ($Å^2 \times 10^3$) for $[(dpdpm)_2Ni(H_2O)(\eta^1\text{-}NO_3)][NO_3]$ (**2.3**).

Table I-14 Bond length [Å] and angles [°] for $[(dpdpm)_2Ni(H_2O)(\eta^1\text{-}NO_3)][NO_3]$ (**2.3**).

Table I-15 Bond lengths [Å] and angles [°] related to the hydrogen bonding for $[(dpdpm)_2Ni(H_2O)(\eta^1\text{-}NO_3)][NO_3]$ (**2.3**).

Table I-16 Atomic coordinates and equivalent isotropic displacement parameters ($Å^2 \times 10^3$) for $[(dpdpm)_2Ni(H_2O)_2][NO_3]_2$ (**2.4**).

Table I-17 Hydrogen coordinates ($\times 10^4$) and isotropic displacement parameters ($Å^2 \times 10^3$) for $[(dpdpm)_2Ni(H_2O)_2][NO_3]_2$ (**2.4**).

Table I-18 Anisotropic displacement parameters ($Å^2 \times 10^3$) for $[(dpdpm)_2Ni(H_2O)_2][NO_3]_2$ (**2.4**).

Table I-19 Bond length [Å] and angles [°] for $[(dpdpm)_2Ni\ (H_2O)_2][NO_3]_2$ (**2.4**).

Table I-20 Torsion angles [°] for $[(dpdpm)_2Ni(H_2O)_2][NO_3]_2$ (**2.4**).

Table I-21 Bond lengths [Å] and angles [°] related to the hydrogen bonding for $[(dpdpm)_2Ni(H_2O)_2][NO_3]_2$ (**2.4**).

Table I-1. Atomic coordinates (x 10^4) and equivalent isotropic displacement parameters ($Å^2$ x 10^3) for [(dpdpm)Ni(η2-NO3)2] (**2.1**).

U_{eq} is defined as one third of the trace of the orthogonalized Uij tensor.

	x	y	z	U_{eq}
Ni	1941(1)	3212(1)	1493(1)	44(1)
O(1)	3371(3)	4361(1)	1757(1)	60(1)
O(2)	2090(3)	4107(2)	547(1)	67(1)
O(3)	3570(4)	5316(2)	814(2)	101(1)
O(4)	1207(2)	2121(2)	737(1)	63(1)
O(5)	3743(2)	2409(1)	1167(1)	59(1)
O(6)	3027(3)	1295(2)	344(2)	86(1)
N(1)	3028(3)	4621(2)	1031(2)	64(1)
N(2)	2676(3)	1911(2)	734(2)	57(1)
N(11)	2081(3)	2566(1)	2554(1)	43(1)
N(12)	1123(2)	2738(1)	3094(1)	40(1)
N(21)	-267(3)	3662(2)	1553(1)	47(1)
N(22)	-969(2)	3570(2)	2203(1)	42(1)
C(13)	1550(3)	2185(2)	3737(2)	50(1)
C(14)	2748(4)	1625(2)	3600(2)	57(1)
C(15)	3038(3)	1885(2)	2860(2)	52(1)
C(23)	-2584(3)	3750(2)	1984(2)	57(1)
C(24)	-2929(4)	3923(3)	1185(2)	69(1)
C(25)	-1467(3)	3855(2)	935(2)	59(1)
C(31)	88(3)	3551(2)	3021(1)	39(1)
C(41)	-1038(3)	3466(2)	3618(2)	43(1)
C(42)	-2009(3)	2701(2)	3599(2)	54(1)
C(43)	-3051(4)	2617(2)	4123(2)	58(1)
C(44)	-3141(4)	3295(2)	4663(2)	60(1)
C(45)	-2188(4)	4045(2)	4685(2)	57(1)
C(46)	-1130(3)	4132(2)	4167(2)	48(1)
C(51)	1146(3)	4391(2)	3134(1)	39(1)
C(52)	461(3)	5213(2)	2876(2)	51(1)
C(53)	1386(4)	5991(2)	2997(2)	58(1)
C(54)	3007(4)	5953(2)	3353(2)	56(1)
C(55)	3699(4)	5139(2)	3611(2)	53(1)
C(56)	2776(3)	4360(2)	3513(2)	45(1)

Table I-2. Hydrogen coordinates (x 10^4) and isotropic displacement parameters ($Å^2$ x 10^3) for [(dpdpm)Ni(η2-NO3)2] (**2.1**).

	x	y	z	U_{eq}
H(13)	1104	2187	4193	60
H(14)	3260	1166	3931	68
H(15)	3803	1618	2611	62
H(23)	-3321	3754	2322	68
H(24)	-3944	4059	867	83
H(25)	-1344	3934	410	71
H(42)	-1955	2245	3232	64
H(43)	-3689	2104	4111	70
H(44)	-3850	3243	5013	72
H(45)	-2251	4500	5052	68
H(46)	-481	4643	4190	57
H(52)	-631	5243	2619	61
H(53)	904	6543	2836	69
H(54)	3634	6474	3420	67
H(55)	4799	5111	3853	64
H(56)	3250	3815	3702	54

Table I-3. Anisotropic parameters ($Å^2$ x 10^3) for [(dpdpm)Ni(η2-NO3)2] (**2.1**).

The anisotropic displacement factor exponent takes the form:

$$-2\pi^2 [h^2 a^{*2} U_{11} + ... + 2 h k a^* b^* U_{12}]$$

	U11	U22	U33	U23	U13	U12
Ni	40(1)	49(1)	45(1)	-2(1)	13(1)	4(1)
O(1)	61(1)	59(1)	63(1)	0(1)	21(1)	-4(1)
O(2)	68(1)	79(2)	56(1)	9(1)	20(1)	7(1)
O(3)	102(2)	74(2)	134(3)	44(2)	41(2)	-4(2)
O(4)	52(1)	74(1)	64(1)	-19(1)	13(1)	2(1)
O(5)	48(1)	63(1)	69(1)	-6(1)	17(1)	8(1)
O(6)	106(2)	78(2)	77(2)	-24(1)	25(1)	31(2)
N(1)	62(2)	59(2)	76(2)	16(1)	29(1)	10(1)
N(2)	64(2)	56(2)	52(1)	-4(1)	18(1)	12(1)
N(11)	43(1)	42(1)	46(1)	-3(1)	12(1)	4(1)
N(12)	42(1)	38(1)	42(1)	0(1)	12(1)	1(1)
N(21)	43(1)	59(1)	39(1)	-1(1)	10(1)	6(1)
N(22)	35(1)	53(1)	38(1)	-5(1)	9(1)	2(1)
C(13)	55(2)	48(2)	46(1)	4(1)	10(1)	-5(1)
C(14)	58(2)	47(2)	62(2)	10(1)	5(1)	7(1)
C(15)	49(2)	46(2)	61(2)	-2(1)	10(1)	8(1)
C(23)	35(1)	78(2)	58(2)	-4(2)	11(1)	6(1)
C(24)	39(2)	107(3)	58(2)	-1(2)	2(1)	17(2)
C(25)	47(2)	83(2)	46(2)	1(2)	5(1)	15(2)
C(31)	39(1)	42(1)	37(1)	-2(1)	10(1)	0(1)
C(41)	41(1)	48(1)	41(1)	-1(1)	15(1)	-1(1)
C(42)	54(2)	52(2)	58(2)	-11(1)	21(1)	-11(1)
C(43)	52(2)	64(2)	63(2)	0(2)	21(1)	-15(1)
C(44)	54(2)	73(2)	58(2)	2(2)	25(1)	-1(2)
C(45)	64(2)	60(2)	53(2)	-8(1)	27(1)	1(1)
C(46)	50(1)	47(1)	48(1)	-3(1)	16(1)	-2(1)
C(51)	41(1)	40(1)	39(1)	-1(1)	13(1)	-2(1)
C(52)	48(1)	47(2)	58(2)	9(1)	10(1)	4(1)
C(53)	66(2)	42(1)	66(2)	11(1)	18(2)	-1(1)
C(54)	66(2)	49(2)	57(2)	-3(1)	23(1)	-15(1)
C(55)	47(1)	59(2)	55(2)	-7(1)	12(1)	-11(1)
C(56)	44(1)	44(1)	47(1)	-3(1)	9(1)	1(1)

Table I-4. Bond lengths [Å] and angles [°] for [(dpdpm)Ni(η2-NO3)2] (**2.1**).

Ni-N(21)	1.994(2)	O(5)-NI-O(2)	89.65(9)
Ni-N(11)	2.027(2)	N(1)-O(1)-NI	.92.19(18)
Ni-O(1)	2.080(2)	N(1)-O(2)-NI	90.70(17)
Ni-O(4)	2.081(2)	N(2)-O(4)-NI	91.89(16)
Ni-O(5)	2.093(2)	N(2)-O(5)-NI	91.41(15)
Ni-O(2)	2.113(2)	O(3)-N(1)-O(1)	122.2(3)
O(1)-N(1)	1.269(3)	O(3)-N(1)-O(2)	122.3(3)
O(2)-N(1)	1.269(4)	O(1)-N(1)-O(2)	115.5(3)
O(3)-N(1)	1.218(3)	O(6)-N(2)-O(5)	122.5(3)
O(4)-N(2)	1.274(3)	O(6)-N(2)-O(4)	122.6(3)
O(5)-N(2)	1.271(3)	O(5)-N(2)-O(4)	114.9(2)
O(6)-N(2)	1.204(3)	C(15)-N(11)-N(12)	105.7(2)
N(11)-C(15)	1.328(3)	C(15)-N(11)-NI	128.85(19)
N(11)-N(12)	1.367(3)	N(12)-N(11)-NI	125.37(16)
N(12)-C(13)	1.356(3)	C(13)-N(12)-N(11)	109.7(2)
N(12)-C(31)	1.479(3)	C(13)-N(12)-C(31)	127.9(2)
N(21)-C(25)	1.325(3)	N(11)-N(12)-C(31)	121.03(19)
N(21)-N(22)	1.366(3)	C(25)-N(21)-N(22)	106.1(2)
N(22)-C(23)	1.355(3)	C(25)-N(21)-NI	126.34(19)
N(22)-C(31)	1.487(3)	N(22)-N(21)-NI	124.95(16)
C(13)-C(14)	1.363(4)	C(23)-N(22)-N(21)	109.6(2)
C(14)-C(15)	1.388(4)	C(23)-N(22)-C(31)	128.8(2)
C(23)-C(24)	1.356(5)	N(21)-N(22)-C(31)	119.16(19)
C(24)-C(25)	1.385(4)	N(12)-C(13)-C(14)	108.1(2)
C(31)-C(51)	1.521(3)	C(13)-C(14)-C(15)	105.2(2)
C(31)-C(41)	1.532(3)	N(11)-C(15)-C(14)	111.2(3)
C(41)-C(46)	1.375(4)	N(22)-C(23)-C(24)	107.7(3)
C(41)-C(42)	1.396(4)	C(23)-C(24)-C(25)	106.1(3)
C(42)-C(43)	1.380(4)	N(21)-C(25)-C(24)	110.4(3)
C(43)-C(44)	1.377(4)	N(12)-C(31)-N(22)	108.57(19)
C(44)-C(45)	1.368(4)	N(12)-C(31)-C(51)	110.00(19)
C(45)-C(46)	1.385(4)	N(22)-C(31)-C(51)	108.7(2)
C(51)-C(52)	1.382(4)	N(12)-C(31)-C(41)	108.2(2)
C(51)-C(56)	1.386(3)	N(22)-C(31)-C(41)	107.05(19)
C(52)-C(53)	1.385(4)	C(51)-C(31)-C(41)	114.2(2)
C(53)-C(54)	1.370(4)	C(46)-C(41)-C(42)	119.0(2)
C(54)-C(55)	1.373(4)	C(46)-C(41)-C(31)	121.5(2)
C(55)-C(56)	1.383(4)	C(42)-C(41)-C(31)	119.5(2)
N(21)-NI-N(11)	89.61(9)	C(43)-C(42)-C(41)	120.4(3)
N(21)-NI-O(1)	102.42(9)	C(44)-C(43)-C(42)	119.8(3)
N(11)-NI-O(1)	105.89(9)	C(45)-C(44)-C(43)	120.0(3)
N(21)-NI-O(4)	97.75(9)	C(44)-C(45)-C(46)	120.6(3)
N(11)-NI-O(4)	97.83(9)	C(41)-C(46)-C(45)	120.1(3)
O(1)-NI-O(4)	148.73(9)	C(52)-C(51)-C(56)	118.7(2)
N(21)-NI-O(5)	159.56(9)	C(52)-C(51)-C(31)	119.5(2)
N(11)-NI-O(5)	93.28(9)	C(56)-C(51)-C(31)	121.7(2)
O(1)-NI-O(5)	96.23(9)	C(51)-C(52)-C(53)	120.5(3)
O(4)-NI-O(5)	61.81(8)	C(54)-C(53)-C(52)	120.4(3)
N(21)-NI-O(2)	91.91(9)	C(53)-C(54)-C(55)	119.5(3)
N(11)-NI-O(2)	167.40(9)	C(54)-C(55)-C(56)	120.6(3)
O(1)-NI-O(2)	61.58(9)	C(55)-C(56)-C(51)	120.2(3)
O(4)-NI-O(2)	94.35(10)		

Symmetry transformations used to generate equivalent atoms:

Table I-5. Torsion angles [°] for [(dpdpm)Ni(η2-NO3)2](2.1).

N(21)-NI-O(1)-N(1)	-85.08(17)	C(25)-N(21)-N(22)-C(31)	-166.7(2)
N(11)-NI-O(1)-N(1)	-178.26(15)	NI-N(21)-N(22)-C(31)	30.6(3)
O(4)-NI-O(1)-N(1)	43.9(3)	N(11)-N(12)-C(13)-C(14)	-2.5(3)
O(5)-NI-O(1)-N(1)	86.52(17)	C(31)-N(12)-C(13)-C(14)	-168.8(2)
O(2)-NI-O(1)-N(1)	0.31(15)	N(12)-C(13)-C(14)-C(15)	1.5(3)
N(21)-NI-O(2)-N(1)	102.79(17)	N(12)-N(11)-C(15)-C(14)	-1.5(3)
N(11)-NI-O(2)-N(1)	6.0(5)	NI-N(11)-C(15)-C(14)	-179.17(19)
O(1)-NI-O(2)-N(1)	-0.31(15)	C(13)-C(14)-C(15)-N(11)	0.0(3)
O(4)-NI-O(2)-N(1)	-159.28(16)	N(21)-N(22)-C(23)-C(24)	2.3(4)
O(5)-NI-O(2)-N(1)	-97.59(17)	C(31)-N(22)-C(23)-C(24)	164.2(3)
N(21)-NI-O(4)-N(2)	178.82(17)	N(22)-C(23)-C(24)-C(25)	-0.9(4)
N(11)-NI-O(4)-N(2)	-90.50(17)	N(22)-N(21)-C(25)-C(24)	2.2(4)
O(1)-NI-O(4)-N(2)	48.9(3)	NI-N(21)-C(25)-C(24)	164.6(2)
O(5)-NI-O(4)-N(2)	-0.96(15)	C(23)-C(24)-C(25)-N(21)	-0.8(4)
O(2)-NI-O(4)-N(2)	86.29(17)	C(13)-N(12)-C(31)-N(22)	-140.5(2)
N(21)-NI-O(5)-N(2)	0.4(4)	N(11)-N(12)-C(31)-N(22)	54.5(3)
N(11)-NI-O(5)-N(2)	98.09(17)	C(13)-N(12)-C(31)-C(51)	100.7(3)
O(1)-NI-O(5)-N(2)	-155.52(17)	N(11)-N(12)-C(31)-C(51)	-64.3(3)
O(4)-NI-O(5)-N(2)	0.97(16)	C(13)-N(12)-C(31)-C(41)	-24.7(3)
O(2)-NI-O(5)-N(2)	-94.16(17)	N(11)-N(12)-C(31)-C(41)	170.4(2)
NI-O(1)-N(1)-O(3)	179.9(3)	C(23)-N(22)-C(31)-N(12)	134.9(3)
NI-O(1)-N(1)-O(2)	-0.5(2)	N(21)-N(22)-C(31)-N(12)	-64.8(3)
NI-O(2)-N(1)-O(3)	-179.9(3)	C(23)-N(22)-C(31)-C(51)	-105.5(3)
NI-O(2)-N(1)-O(1)	0.5(2)	N(21)-N(22)-C(31)-C(51)	54.9(3)
NI-O(5)-N(2)-O(6)	177.6(3)	C(23)-N(22)-C(31)-C(41)	18.3(4)
NI-O(5)-N(2)-O(4)	-1.5(2)	N(21)-N(22)-C(31)-C(41)	178.7(2)
NI-O(4)-N(2)-O(6)	-177.5(3)	N(12)-C(31)-C(41)-C(46)	126.8(3)
NI-O(4)-N(2)-O(5)	1.5(2)	N(22)-C(31)-C(41)-C(46)	-116.4(3)
N(21)-NI-N(11)-C(15)	159.9(2)	C(51)-C(31)-C(41)-C(46)	3.9(3)
O(1)-NI-N(11)-C(15)	-97.2(2)	N(12)-C(31)-C(41)-C(42)	-54.0(3)
O(4)-NI-N(11)-C(15)	62.2(2)	N(22)-C(31)-C(41)-C(42)	62.8(3)
O(5)-NI-N(11)-C(15)	0.2(2)	C(51)-C(31)-C(41)-C(42)	-176.9(2)
O(2)-NI-N(11)-C(15)	-103.0(4)	C(46)-C(41)-C(42)-C(43)	0.2(4)
N(21)-NI-N(11)-N(12)	-17.3(2)	C(31)-C(41)-C(42)-C(43)	-179.0(3)
O(1)-NI-N(11)-N(12)	85.5(2)	C(41)-C(42)-C(43)-C(44)	0.5(5)
O(4)-NI-N(11)-N(12)	-115.12(19)	C(42)-C(43)-C(44)-C(45)	-0.7(5)
O(5)-NI-N(11)-N(12)	-177.11(19)	C(43)-C(44)-C(45)-C(46)	0.2(5)
O(2)-NI-N(11)-N(12)	79.7(4)	C(42)-C(41)-C(46)-C(45)	-0.7(4)
C(15)-N(11)-N(12)-C(13)	2.4(3)	C(31)-C(41)-C(46)-C(45)	178.5(3)
I-N(11)-N(12)-C(13)	-179.77(17)	C(44)-C(45)-C(46)-C(41)	0.5(5)
C(15)-N(11)-N(12)-C(31)	169.8(2)	N(12)-C(31)-C(51)-C(52)	162.2(2)
NI-N(11)-N(12)-C(31)	-12.3(3)	N(22)-C(31)-C(51)-C(52)	43.5(3)
N(11)-NI-N(21)-C(25)	-151.1(3)	C(41)-C(31)-C(51)-C(52)	-76.0(3)
O(1)-NI-N(21)-C(25)	102.8(3)	N(12)-C(31)-C(51)-C(56)	-19.9(3)
O(4)-NI-N(21)-C(25)	-53.2(3)	N(22)-C(31)-C(51)-C(56)	-138.7(2)
O(5)-NI-N(21)-C(25)	-52.7(4)	C(41)-C(31)-C(51)-C(56)	101.9(3)
O(2)-NI-N(21)-C(25)	41.5(3)	C(56)-C(51)-C(52)-C(53)	-0.2(4)
N(11)-NI-N(21)-N(22)	8.2(2)	C(31)-C(51)-C(52)-C(53)	177.7(3)
O(1)-NI-N(21)-N(22)	-98.0(2)	C(51)-C(52)-C(53)-C(54)	2.0(5)
O(4)-NI-N(21)-N(22)	106.0(2)	C(52)-C(53)-C(54)-C(55)	-1.9(5)
O(2)-NI-N(21)-N(22)	-159.3(2)	C(53)-C(54)-C(55)-C(56)	0.1(4)
C(25)-N(21)-N(22)-C(23)	-2.8(3)	C(54)-C(55)-C(56)-C(51)	1.7(4)
NI-N(21)-N(22)-C(23)	-165.5(2)	C(52)-C(51)-C(56)-C(55)	-1.6(4)
		C(31)-C(51)-C(56)-C(55)	-179.4(2)

Symmetry transformations used to generate equivalent atoms

Table I-6. Atomic coordinates (x 10^4) and equivalent isotropic displacement parameters ($Å^2$ x 10^3) for [(dpdpm)Ni(η1-NO3)(CH3CN)][NO3] (**2.2**).

U_{eq} is defined as one third of the trace of the orthogonalized Uij tensor.

	Occ.	x	y	z	U_{eq}
Ni	1	6386(1)	10966(1)	3059(1)	27(1)
N(1)	1	5220(2)	12367(2)	1754(1)	36(1)
N(2)	1	7407(2)	12573(2)	4180(1)	40(1)
N(3)	1	4106(2)	11140(2)	3607(1)	36(1)
N(11)	1	6652(2)	8814(2)	3605(1)	30(1)
N(12)	1	7895(2)	7890(2)	3459(1)	28(1)
N(21)	1	8632(2)	10863(2)	2512(1)	27(1)
N(22)	1	9594(2)	9638(2)	2534(1)	27(1)
O(1)	1	5258(2)	10984(2)	1957(1)	39(1)
O(2)	1	5898(2)	12972(2)	2229(1)	36(1)
O(3)	1	4559(2)	13077(2)	1149(1)	55(1)
O(4)	1	7262(2)	11347(2)	4104(1)	43(1)
O(5)	0.50	7627(8)	13565(5)	3515(3)	69(2)
O(55)	0.50	6541(9)	13603(6)	3741(4)	84(2)
O(6)	1	7889(2)	12819(2)	4817(1)	58(1)
C(1)	1	2858(3)	11267(3)	3894(1)	37(1)
C(2)	1	1254(3)	11423(4)	4275(2)	60(1)
C(13)	1	7775(3)	6590(2)	4020(1)	38(1)
C(14)	1	6478(3)	6702(2)	4552(1)	44(1)
C(15)	1	5818(3)	8099(2)	4277(1)	37(1)
C(23)	1	11065(2)	10008(2)	2169(1)	34(1)
C(24)	1	11066(3)	11492(2)	1936(1)	38(1)
C(25)	1	9533(2)	11969(2)	2166(1)	32(1)
C(31)	1	8900(2)	8189(2)	2666(1)	29(1)
C(41)	1	10314(3)	7063(2)	2764(1)	33(1)
C(42)	1	11344(3)	7021(2)	3382(1)	40(1)
C(43)	1	12672(3)	6066(3)	3467(2)	47(1)
C(44)	1	12976(3)	5137(3)	2936(2)	51(1)
C(45)	1	11951(3)	5171(3)	2326(2)	52(1)
C(46)	1	10616(3)	6125(2)	2236(2)	42(1)
C(51)	1	7891(3)	8177(2)	1942(1)	34(1)
C(52)	1	8228(3)	9073(3)	1168(1)	43(1)
C(53)	1	7348(4)	9005(4)	503(2)	58(1)
C(54)	1	6176(4)	8038(5)	612(2)	77(1)
C(55)	1	5882(5)	7111(5)	1376(2)	88(1)
C(56)	1	6719(4)	7188(4)	2049(2)	63(1)
C(103)	0.50	1710(11)	7124(7)	-8(5)	79(2)
C(104)	0.50	1823(11)	5586(8)	-51(8)	118(4)
O(105)	0.50	463(9)	4886(6)	412(4)	108(2)
C(106)	0.50	-968(17)	5138(14)	-18(14)	271(14)
C(107)	0.50	-1901(13)	3832(13)	129(7)	99(3)

Table I-7. Hydrogen coordinates (x 10^4) and isotropic displacement parameters ($Å^2$ x 10^3) for [(dpdpm)Ni(η1-NO3)(CH3CN)][NO3] (**2.2**).

	Occ.	x	y	z	U_{eq}
H(2A)	1	1243	10998	4861	90
H(2B)	1	528	10937	4029	90
H(2C)	1	932	12438	4185	90
H(13)	1	8458	5771	4036	46
H(14)	1	6109	5989	5005	52
H(15)	1	4915	8484	4529	45
H(23)	1	11918	9364	2092	41
H(24)	1	11909	12060	1679	45
H(25)	1	9186	12943	2087	39
H(42)	1	11138	7639	3741	48
H(43)	1	13359	6049	3879	56
H(44)	1	13867	4494	2991	61
H(45)	1	12157	4545	1971	62
H(46)	1	9929	6136	1824	51
H(52)	1	9040	9723	1089	52
H(53)	1	7564	9623	-16	69
H(54)	1	5579	8005	171	93
H(55)	1	5113	6424	1444	106
H(56)	1	6489	6576	2568	75
H(10A)	0.50	2606	7612	-324	119
H(10B)	0.50	1710	7184	561	119
H(10C)	0.50	738	7579	-234	119
H(10D)	0.50	1847	5516	-625	141
H(10E)	0.50	2796	5115	182	141
H(10F)	0.50	-693	5469	-609	325
H(10G)	0.50	-1622	5907	161	325
H(10H)	0.50	-2870	4068	-151	148
H(10I)	0.50	-2157	3486	715	148
H(10J)	0.50	-1286	3088	-80	148

Table II-21. Bond lengths [Å] and angles [°] for [(dpdpm)NiBr(H_2O)$_2$(CH_3CN)][Br] (**3.3**).

Ni-O(2)	2.0640(15)	N(21)-NI-BR1	175.49(5)
Ni-N(11)	2.0766(17)	N(1)-NI-BR1	90.85(5)
Ni-N(21)	2.0857(17)	O(1)-NI-BR1	86.75(4)
Ni-N(1)	2.0957(17)	C(1)-N(1)-NI	163.98(17)
Ni-O(1)	2.0984(15)	C(15)-N(11)-N(12)	105.19(16)
Ni-Br(1)	2.5681(4)	C(15)-N(11)-NI	125.77(13)
N(1)-C(1)	1.136(3)	N(12)-N(11)-NI	126.52(12)
N(2)-C(2)	1.136(3)	C(13)-N(12)-N(11)	110.55(16)
N(11)-C(15)	1.334(2)	C(13)-N(12)-C(31)	126.57(16)
N(11)-N(12)	1.367(2)	N(11)-N(12)-C(31)	120.24(16)
N(12)-C(13)	1.355(3)	C(25)-N(21)-N(22)	105.60(16)
N(12)-C(31)	1.482(2)	C(25)-N(21)-NI	125.40(14)
N(21)-C(25)	1.333(3)	N(22)-N(21)-NI	128.28(12)
N(21)-N(22)	1.362(2)	C(23)-N(22)-N(21)	110.75(16)
N(22)-C(23)	1.359(3)	C(23)-N(22)-C(31)	127.05(17)
N(22)-C(31)	1.479(2)	N(21)-N(22)-C(31)	121.29(15)
C(1)-C(3)	1.464(3)	N(1)-C(1)-C(3)	178.6(2)
C(2)-C(4)	1.460(3)	N(2)-C(2)-C(4)	177.6(3)
C(13)-C(14)	1.366(3)	N(12)-C(13)-C(14)	107.82(18)
C(14)-C(15)	1.395(3)	C(13)-C(14)-C(15)	105.11(18)
C(23)-C(24)	1.372(3)	N(11)-C(15)-C(14)	111.28(18)
C(24)-C(25)	1.395(3)	N(22)-C(23)-C(24)	107.16(18)
C(31)-C(51)	1.532(3)	C(23)-C(24)-C(25)	105.53(18)
C(31)-C(41)	1.537(3)	N(21)-C(25)-C(24)	110.90(19)
C(41)-C(42)	1.386(3)	N(22)-C(31)-N(12)	109.45(15)
C(41)-C(46)	1.401(3)	N(22)-C(31)-C(51)	110.32(16)
C(42)-C(43)	1.398(3)	N(12)-C(31)-C(51)	109.12(15)
C(43)-C(44)	1.384(4)	N(22)-C(31)-C(41)	107.21(15)
C(44)-C(45)	1.390(3)	N(12)-C(31)-C(41)	108.29(15)
C(45)-C(46)	1.388(3)	C(51)-C(31)-C(41)	112.38(16)
C(51)-C(56)	1.393(3)	C(42)-C(41)-C(46)	119.74(19)
C(51)-C(52)	1.394(3)	C(42)-C(41)-C(31)	121.79(18)
C(52)-C(53)	1.390(3)	C(46)-C(41)-C(31)	118.47(18)
C(53)-C(54)	1.387(3)	C(41)-C(42)-C(43)	120.0(2)
C(54)-C(55)	1.390(3)	C(44)-C(43)-C(42)	120.1(2)
C(55)-C(56)	1.392(3)	C(43)-C(44)-C(45)	120.0(2)
O(2)-NI-N(11)	174.83(7)	C(46)-C(45)-C(44)	120.3(2)
O(2)-NI-N(21)	89.43(7)	C(45)-C(46)-C(41)	119.9(2)
N(11)-NI-N(21)	86.31(7)	C(56)-C(51)-C(52)	119.87(18)
O(2)-NI-N(1)	83.66(7)	C(56)-C(51)-C(31)	120.20(17)
N(11)-NI-N(1)	99.52(7)	C(52)-C(51)-C(31)	119.78(18)
N(21)-NI-N(1)	93.53(6)	C(53)-C(52)-C(51)	119.82(19)
O(2)-NI-O(1)	87.92(7)	C(54)-C(53)-C(52)	120.3(2)
N(11)-NI-O(1)	89.05(6)	C(53)-C(54)-C(55)	120.1(2)
N(21)-NI-O(1)	88.76(6)	C(54)-C(55)-C(56)	119.9(2)
N(1)-NI-O(1)	171.25(7)	C(55)-C(56)-C(51)	120.08(19)
O(2)-NI-BR1	89.98(5)	Symmetry transformations used to generate equivalent atoms:	
N(11)-NI-BR1	94.03(5)		

Table II-22. Torsion angles [°] for [(dpdpm)NiBr(H_2O)$_2$(CH_3CN)][Br] (**3.3**).

O(2)-NI-N(1)-C(1)	-3.7(6)
N(11)-NI-N(1)-C(1)	-179.5(6)
N(21)-NI-N(1)-C(1)	-92.7(6)
O(1)-NI-N(1)-C(1)	12.3(9)
BR1-NI-N(1)-C(1)	86.2(6)
O(2)-NI-N(11)-C(15)	121.8(7)
N(21)-NI-N(11)-C(15)	156.46(17)
N(1)-NI-N(11)-C(15)	-110.57(16)
O(1)-NI-N(11)-C(15)	67.65(16)
BR1-NI-N(11)-C(15)	-19.03(16)
O(2)-NI-N(11)-N(12)	-37.5(8)
N(21)-NI-N(11)-N(12)	-2.85(15)
N(1)-NI-N(11)-N(12)	90.12(15)
O(1)-NI-N(11)-N(12)	-91.67(15)
BR1-NI-N(11)-N(12)	-178.34(14)
C(15)-N(11)-N(12)-C(13)	2.0(2)
NI-N(11)-N(12)-C(13)	164.69(13)
C(15)-N(11)-N(12)-C(31)	164.73(16)
NI-N(11)-N(12)-C(31)	-32.5(2)
O(2)-NI-N(21)-C(25)	18.72(17)
N(11)-NI-N(21)-C(25)	-158.34(17)
N(1)-NI-N(21)-C(25)	102.33(17)
O(1)-NI-N(21)-C(25)	-69.22(17)
BR1-NI-N(21)-C(25)	-63.8(7)
O(2)-NI-N(21)-N(22)	-172.46(16)
N(11)-NI-N(21)-N(22)	10.48(15)
N(1)-NI-N(21)-N(22)	-88.84(16)
O(1)-NI-N(21)-N(22)	99.61(16)
BR1-NI-N(21)-N(22)	105.0(6)
C(25)-N(21)-N(22)-C(23)	-2.6(2)
NI-N(21)-N(22)-C(23)	-173.15(14)
C(25)-N(21)-N(22)-C(31)	-172.43(16)
NI-N(21)-N(22)-C(31)	17.0(2)
NI-N(1)-C(1)-C(3)	-3(10)
N(11)-N(12)-C(13)-C(14)	-1.7(2)
C(31)-N(12)-C(13)-C(14)	-163.13(18)
N(12)-C(13)-C(14)-C(15)	0.7(2)
N(12)-N(11)-C(15)-C(14)	-1.5(2)
NI-N(11)-C(15)-C(14)	-164.38(14)
C(13)-C(14)-C(15)-N(11)	0.5(2)
N(21)-N(22)-C(23)-C(24)	2.2(2)
C(31)-N(22)-C(23)-C(24)	171.27(18)
N(22)-C(23)-C(24)-C(25)	-0.8(2)
N(22)-N(21)-C(25)-C(24)	2.0(2)
NI-N(21)-C(25)-C(24)	172.94(14)
C(23)-C(24)-C(25)-N(21)	-0.8(2)
C(23)-N(22)-C(31)-N(12)	138.21(19)
N(21)-N(22)-C(31)-N(12)	-53.7(2)
C(23)-N(22)-C(31)-C(51)	-101.7(2)
N(21)-N(22)-C(31)-C(51)	66.4(2)
C(23)-N(22)-C(31)-C(41)	21.0(3)
N(21)-N(22)-C(31)-C(41)	-170.97(16)
C(13)-N(12)-C(31)-N(22)	-137.91(19)
N(11)-N(12)-C(31)-N(22)	62.3(2)
C(13)-N(12)-C(31)-C(51)	101.3(2)
N(11)-N(12)-C(31)-C(51)	-58.5(2)
C(13)-N(12)-C(31)-C(41)	-21.3(2)
N(11)-N(12)-C(31)-C(41)	178.86(16)
N(22)-C(31)-C(41)-C(42)	-120.5(2)
N(12)-C(31)-C(41)-C(42)	121.5(2)
C(51)-C(31)-C(41)-C(42)	0.9(3)
N(22)-C(31)-C(41)-C(46)	58.9(2)
N(12)-C(31)-C(41)-C(46)	-59.1(2)
C(51)-C(31)-C(41)-C(46)	-179.74(18)
C(46)-C(41)-C(42)-C(43)	-1.2(3)
C(31)-C(41)-C(42)-C(43)	178.20(19)
C(41)-C(42)-C(43)-C(44)	-0.6(3)
C(42)-C(43)-C(44)-C(45)	2.1(3)
C(43)-C(44)-C(45)-C(46)	-1.7(3)
C(44)-C(45)-C(46)-C(41)	-0.1(3)
C(42)-C(41)-C(46)-C(45)	1.6(3)
C(31)-C(41)-C(46)-C(45)	-177.85(19)
N(22)-C(31)-C(51)-C(56)	34.1(2)
N(12)-C(31)-C(51)-C(56)	154.41(18)
C(41)-C(31)-C(51)-C(56)	-85.5(2)
N(22)-C(31)-C(51)-C(52)	-150.26(18)
N(12)-C(31)-C(51)-C(52)	-30.0(2)
C(41)-C(31)-C(51)-C(52)	90.2(2)
C(56)-C(51)-C(52)-C(53)	-0.4(3)
C(31)-C(51)-C(52)-C(53)	-176.01(19)
C(51)-C(52)-C(53)-C(54)	-0.1(3)
C(52)-C(53)-C(54)-C(55)	0.6(3)
C(53)-C(54)-C(55)-C(56)	-0.6(4)
C(54)-C(55)-C(56)-C(51)	0.2(3)
C(52)-C(51)-C(56)-C(55)	0.3(3)
C(31)-C(51)-C(56)-C(55)	175.94(19)

Symmetry transformations used to generate equivalent atoms:

Table II-23. Bond lengths [Å] and angles [°] related to the hydrogen bonding for [(dpdpm)NiBr(H_2O)$_2$(CH_3CN)][Br] (**3.3**).

D-H	..A	d(D-H)	d(H..A)	d(D..A)	<DHA
O(1)-H(1A)	BR2	0.75(3)	2.63(3)	3.3540(16)	163(3)
O(1)-H(1B)	BR2#1	0.89(3)	2.34(3)	3.2268(16)	178(3)
O(2)-H(2A)	BR2	0.70(3)	2.49(3)	3.1785(16)	174(3)
O(2)-H(2B)	BR1#2	0.87(3)	2.40(3)	3.2619(16)	168(3)

Symmetry transformations used to generate equivalent atoms:

#1 -x+2,-y+1,-z+1 #2 -x+1,-y+2,-z+1

Table II-24. Atomic coordinates (x 10^4) and equivalent isotropic displacement parameters (Å^2 x 10^3) for [(dpdpm)$_2$NiBr$_2$] (**3.4**).

U_{eq} is defined as one third of the trace of the orthogonalized Uij tensor.

	Occ.	x	y	z	U_{eq}
Br(1)	1	-918(1)	8686(1)	4205(1)	29(1)
Br(2)	1	1042(1)	10249(1)	4795(1)	34(1)
Ni	1	608(1)	9471(1)	3649(1)	19(1)
N(21)	1	1797(1)	10182(1)	3236(1)	25(1)
N(22)	1	2822(1)	10116(1)	3395(1)	26(1)
N(11)	1	1741(1)	8656(1)	3947(1)	23(1)
N(12)	1	2776(1)	8832(1)	4005(1)	25(1)
N(31)	1	353(1)	8850(1)	2727(1)	21(1)
N(32)	1	-460(1)	8943(1)	2287(1)	22(1)
N(41)	1	-546(1)	10266(1)	3329(1)	22(1)
N(42)	1	-1255(1)	10110(1)	2825(1)	21(1)
C(23)	1	3322(2)	10808(2)	3230(1)	36(1)
C(24)	1	2608(2)	11335(2)	2981(1)	40(1)
C(25)	1	1669(2)	10923(2)	3005(1)	32(1)
C(13)	1	3240(2)	8282(2)	4421(1)	35(1)
C(14)	1	2506(2)	7766(2)	4651(1)	35(1)
C(15)	1	1584(2)	8024(1)	4354(1)	28(1)
C(33)	1	-469(2)	8329(1)	1822(1)	30(1)
C(34)	1	322(2)	7818(1)	1980(1)	33(1)
C(35)	1	810(2)	8167(1)	2552(1)	27(1)
C(43)	1	-2123(2)	10562(2)	2919(1)	30(1)
C(44)	1	-1988(2)	11003(2)	3507(1)	34(1)
C(45)	1	-1002(2)	10793(1)	3744(1)	28(1)
C(51)	1	3334(2)	9328(1)	3494(1)	25(1)

C(61)	1	-952(2)	9732(1)	2164(1)	21(1)
C(71)	1	3381(2)	8872(2)	2810(1)	26(1)
C(72)	1	3589(2)	8052(2)	2801(1)	35(1)
C(73)	1	3709(2)	7648(2)	2184(2)	43(1)
C(74)	1	3619(2)	8061(2)	1576(1)	46(1)
C(75)	1	3401(2)	8866(2)	1577(1)	43(1)
C(76)	1	3284(2)	9278(2)	2194(1)	33(1)
C(81)	1	4408(2)	9501(2)	3799(1)	31(1)
C(82)	1	4440(2)	9928(2)	4417(1)	40(1)
C(83)	1	5395(2)	10072(3)	4725(1)	51(1)
C(84)	1	6296(2)	9794(3)	4428(2)	58(1)
C(85)	1	6264(2)	9369(2)	3824(1)	47(1)
C(86)	1	5317(2)	9235(2)	3502(1)	36(1)
C(91)	1	-181(2)	10291(1)	1804(1)	24(1)
C(92)	1	-349(2)	11122(2)	1799(1)	33(1)
C(93)	1	345(2)	11637(2)	1489(1)	38(1)
C(94)	1	1224(2)	11336(2)	1174(1)	40(1)
C(95)	1	1394(2)	10512(2)	1158(1)	38(1)
C(96)	1	700(2)	9992(2)	1477(1)	29(1)
C(101)	1	-1964(2)	9565(1)	1772(1)	25(1)
C(102)	1	-2648(2)	8989(2)	2034(1)	33(1)
C(103)	1	-3564(2)	8811(2)	1694(1)	42(1)
C(104)	1	-3810(2)	9205(2)	1086(1)	47(1)
C(105)	1	-3136(2)	9769(2)	829(1)	44(1)
C(106)	1	-2212(2)	9960(2)	1167(1)	33(1)
C(1A)	0.54(3)	5189(15)	6375(8)	3996(6)	100(5)
Cl(1A)	0.54(3)	5806(4)	7298(4)	3923(4)	79(2)
Cl(2A)	0.54(3)	4947(13)	5941(4)	3204(5)	102(2)
C(1B)	0.46(3)	5280(20)	6215(12)	3881(8)	124(8)
Cl(1B)	0.46(3)	4717(4)	5920(4)	3117(3)	71(1)
Cl(2B)	0.46(3)	5859(10)	7152(8)	3828(6)	120(3)
C(3A)	0.524(18)	7354(8)	7131(7)	356(6)	56(2)
Cl(3A)	0.524(18)	6401(3)	7075(5)	-278(3)	90(2)
Cl(4A)	0.524(18)	8238(7)	7874(6)	195(5)	97(3)
C(3B)	0.476(18)	7370(11)	7138(11)	169(12)	125(9)
Cl(3B)	0.476(18)	6073(9)	7249(3)	40(8)	128(3)
Cl(4B)	0.476(18)	8166(6)	7981(4)	98(4)	62(1)

Table II-25. Hydrogen coordinates (x 10^4) and isotropic displacement parameters ($Å^2$ x 10^3) for [$(dpdpm)_2NiBr_2$] (**3.4**).

	Occ.	x	y	z	U_{eq}
H(23)	1	4037	10905	3278	44
H(24)	1	2725	11864	2827	47
H(25)	1	1027	11142	2873	38
H(13)	1	3951	8264	4529	41
H(14)	1	2599	7328	4949	42
H(15)	1	934	7782	4429	33
H(33)	1	-940	8269	1458	36
H(34)	1	503	7337	1756	39
H(35)	1	1385	7944	2779	32
H(43)	1	-2710	10571	2634	36
H(44)	1	-2458	11367	3706	40
H(45)	1	-700	10997	4146	34
H(72)	1	3650	7768	3215	42
H(73)	1	3851	7092	2182	52
H(74)	1	3707	7787	1160	56
H(75)	1	3330	9143	1161	51
H(76)	1	3139	9833	2192	39
H(82)	1	3824	10114	4620	48
H(83)	1	5426	10361	5138	62
H(84)	1	6939	9895	4639	70
H(85)	1	6881	9170	3629	56
H(86)	1	5295	8962	3081	44
H(92)	1	-945	11333	2011	39
H(93)	1	220	12195	1491	46
H(94)	1	1705	11690	972	48
H(95)	1	1980	10304	931	46
H(96)	1	826	9434	1471	35
H(102)	1	-2486	8721	2444	40
H(103)	1	-4020	8423	1873	50
H(104)	1	-4432	9085	855	56
H(105)	1	-3299	10032	417	53
H(106)	1	-1762	10351	986	39
H(1A1)	0.54(3)	4530	6447	4239	120
H(1A2)	0.54(3)	5623	6010	4266	120
H(1B1)	0.46(3)	4751	6225	4239	149
H(1B2)	0.46(3)	5809	5817	4012	149
H(3A1)	0.524(18)	7021	7233	798	67
H(3A2)	0.524(18)	7715	6612	386	67
H(3B1)	0.476(18)	7622	6734	-156	150
H(3B2)	0.476(18)	7468	6914	628	150

Table II-26. Anisotropic parameters ($Å^2$ x 10^3) for [$(dpdpm)_2NiBr_2$] (**3.4**).

The anisotropic displacement factor exponent takes the form:

$$-2\pi^2 [h^2 a^{*2} U_{11} + ... + 2 h k a^* b^* U_{12}]$$

	U11	U22	U33	U23	U13	U12
Br(1)	24(1)	28(1)	34(1)	4(1)	6(1)	-2(1)
Br(2)	40(1)	40(1)	21(1)	-6(1)	-2(1)	-6(1)
Ni	19(1)	22(1)	16(1)	1(1)	-1(1)	-1(1)
N(21)	22(1)	31(1)	22(1)	3(1)	-1(1)	-4(1)
N(22)	22(1)	33(1)	21(1)	-3(1)	0(1)	-6(1)
N(11)	19(1)	29(1)	21(1)	3(1)	-1(1)	-1(1)
N(12)	16(1)	41(1)	18(1)	2(1)	-2(1)	0(1)
N(31)	19(1)	26(1)	18(1)	0(1)	-3(1)	1(1)
N(32)	23(1)	24(1)	20(1)	-3(1)	-3(1)	1(1)
N(41)	25(1)	23(1)	18(1)	0(1)	-1(1)	2(1)
N(42)	22(1)	25(1)	17(1)	1(1)	1(1)	3(1)
C(23)	32(1)	40(1)	37(1)	-1(1)	1(1)	-13(1)
C(24)	43(1)	35(1)	41(1)	5(1)	1(1)	-12(1)
C(25)	36(1)	30(1)	28(1)	7(1)	-1(1)	-4(1)
C(13)	26(1)	53(1)	26(1)	8(1)	-5(1)	7(1)
C(14)	32(1)	43(1)	30(1)	12(1)	-4(1)	8(1)
C(15)	26(1)	31(1)	26(1)	5(1)	-3(1)	-1(1)
C(33)	36(1)	30(1)	24(1)	-8(1)	-7(1)	1(1)
C(34)	40(1)	27(1)	30(1)	-10(1)	-3(1)	5(1)
C(35)	25(1)	27(1)	28(1)	-2(1)	-3(1)	4(1)
C(43)	27(1)	32(1)	30(1)	-1(1)	2(1)	7(1)
C(44)	35(1)	33(1)	32(1)	-4(1)	7(1)	9(1)
C(45)	38(1)	23(1)	23(1)	-2(1)	2(1)	2(1)
C(51)	20(1)	35(1)	20(1)	1(1)	-1(1)	-3(1)
C(61)	22(1)	25(1)	16(1)	1(1)	-2(1)	4(1)
C(71)	18(1)	39(1)	22(1)	-1(1)	-1(1)	-3(1)
C(72)	34(1)	42(1)	28(1)	-2(1)	-4(1)	1(1)
C(73)	44(1)	43(1)	43(1)	-11(1)	-6(1)	1(1)
C(74)	48(1)	60(2)	32(1)	-20(1)	-1(1)	-4(1)
C(75)	50(2)	58(2)	20(1)	-2(1)	0(1)	-4(1)
C(76)	35(1)	42(1)	22(1)	1(1)	3(1)	-3(1)
C(81)	19(1)	49(1)	24(1)	0(1)	-2(1)	-6(1)
C(82)	27(1)	68(2)	26(1)	-9(1)	-3(1)	-9(1)
C(83)	35(1)	92(2)	27(1)	-10(1)	-5(1)	-17(2)
C(84)	28(1)	110(3)	38(1)	2(2)	-9(1)	-24(2)
C(85)	18(1)	85(2)	39(1)	2(1)	2(1)	-6(1)
C(86)	23(1)	58(2)	28(1)	-2(1)	1(1)	-5(1)
C(91)	25(1)	29(1)	17(1)	4(1)	-3(1)	-1(1)
C(92)	37(1)	32(1)	30(1)	6(1)	3(1)	4(1)
C(93)	47(1)	32(1)	36(1)	13(1)	3(1)	-3(1)
C(94)	42(1)	50(1)	29(1)	13(1)	4(1)	-13(1)
C(95)	34(1)	54(2)	26(1)	7(1)	5(1)	0(1)

C(96)	29(1)	36(1)	22(1)	1(1)	2(1)	2(1)
C(101)	19(1)	36(1)	20(1)	-4(1)	-3(1)	4(1)
C(102)	29(1)	42(1)	29(1)	-1(1)	-4(1)	-4(1)
C(103)	26(1)	60(2)	40(1)	-10(1)	0(1)	-7(1)
C(104)	25(1)	79(2)	37(1)	-15(1)	-8(1)	5(1)
C(105)	31(1)	78(2)	23(1)	-3(1)	-4(1)	15(1)
C(106)	26(1)	51(1)	21(1)	1(1)	1(1)	10(1)
C(1A)	175(12)	60(6)	65(6)	33(5)	55(8)	23(6)
Cl(1A)	68(2)	88(2)	80(2)	34(2)	-23(2)	13(2)
Cl(2A)	135(5)	75(2)	96(3)	7(2)	56(3)	15(3)
C(1B)	240(20)	72(8)	59(7)	14(6)	-53(12)	30(11)
Cl(1B)	57(2)	86(2)	71(2)	34(2)	-1(2)	-9(2)
Cl(2B)	105(5)	143(6)	111(4)	-5(4)	-34(3)	-23(4)
C(3A)	69(5)	58(4)	40(5)	26(3)	6(4)	13(4)
Cl(3A)	67(2)	106(3)	97(3)	17(2)	-10(2)	-7(2)
Cl(4A)	125(4)	120(5)	47(2)	-19(3)	-22(2)	-18(4)
C(3B)	162(15)	120(12)	92(13)	52(9)	64(10)	71(11)
Cl(3B)	120(4)	105(3)	158(7)	-24(3)	-38(5)	18(3)
Cl(4B)	96(2)	58(2)	32(2)	-9(1)	-4(2)	12(2)

Table II-27. Bond lengths [Å] and angles [°] for $[(dpdpm)_2NiBr_2]$ **(3.4)**.

Br(1)-Ni	2.5971(4)	C(94)-C(95)	1.387(5)
Br(2)-Ni	2.6476(4)	C(95)-C(96)	1.390(4)
Ni-N(11)	2.0740(19)	C(101)-C(106)	1.390(3)
Ni-N(41)	2.0835(18)	C(101)-C(102)	1.397(3)
Ni-N(21)	2.0949(19)	C(102)-C(103)	1.386(4)
Ni-N(31)	2.1031(17)	C(103)-C(104)	1.393(4)
N(21)-C(25)	1.320(3)	C(104)-C(105)	1.373(5)
N(21)-N(22)	1.361(3)	C(105)-C(106)	1.397(4)
N(22)-C(23)	1.355(3)	C(1a)-Cl(1a)	1.733(9)
N(22)-C(51)	1.477(3)	C(1a)-Cl(2a)	1.736(10)
N(11)-C(15)	1.332(3)	C(1b)-Cl(2b)	1.726(12)
N(11)-N(12)	1.370(2)	C(1b)-Cl(1b)	1.732(11)
N(12)-C(13)	1.360(3)	C(3a)-Cl(4a)	1.708(10)
N(12)-C(51)	1.482(3)	C(3a)-Cl(3a)	1.747(9)
N(31)-C(35)	1.321(3)	C(3b)-Cl(3b)	1.699(13)
N(31)-N(32)	1.365(2)	C(3b)-Cl(4b)	1.741(13)
N(32)-C(33)	1.365(3)	N(11)-NI-N(41)	178.34(7)
N(32)-C(61)	1.475(3)	N(11)-NI-N(21)	87.84(7)
N(41)-C(45)	1.330(3)	N(41)-NI-N(21)	92.76(7)
N(41)-N(42)	1.368(2)	N(11)-NI-N(31)	91.74(7)
N(42)-C(43)	1.359(3)	N(41)-NI-N(31)	86.69(7)
N(42)-C(61)	1.487(2)	N(21)-NI-N(31)	93.41(7)
C(23)-C(24)	1.359(4)	N(11)-NI-BR1	94.94(5)
C(24)-C(25)	1.391(4)	N(41)-NI-BR1	84.55(5)
C(13)-C(14)	1.353(4)	N(21)-NI-BR1	175.74(6)
C(14)-C(15)	1.389(3)	N(31)-NI-BR1	89.73(5)
C(33)-C(34)	1.360(4)	N(11)-NI-BR2	86.05(5)
C(34)-C(35)	1.408(3)	N(41)-NI-BR2	95.54(5)
C(43)-C(44)	1.374(3)	N(21)-NI-BR2	84.13(5)
C(44)-C(45)	1.395(4)	N(31)-NI-BR2	176.75(5)
C(51)-C(81)	1.534(3)	BR1-NI-BR2	92.827(13)
C(51)-C(71)	1.539(3)	C(25)-N(21)-N(22)	105.89(19)
C(61)-C(91)	1.531(3)	C(25)-N(21)-NI	124.47(17)
C(61)-C(101)	1.537(3)	N(22)-N(21)-NI	125.14(14)
C(71)-C(76)	1.386(3)	C(23)-N(22)-N(21)	109.7(2)
C(71)-C(72)	1.388(4)	C(23)-N(22)-C(51)	124.78(19)
C(72)-C(73)	1.389(4)	N(21)-N(22)-C(51)	122.25(18)
C(73)-C(74)	1.377(4)	C(15)-N(11)-N(12)	105.39(18)
C(74)-C(75)	1.366(5)	C(15)-N(11)-NI	125.19(15)
C(75)-C(76)	1.395(4)	N(12)-N(11)-NI	124.68(15)
C(81)-C(86)	1.380(4)	C(13)-N(12)-N(11)	109.52(19)
C(81)-C(82)	1.401(3)	C(13)-N(12)-C(51)	124.34(18)
C(82)-C(83)	1.390(4)	N(11)-N(12)-C(51)	122.27(17)
C(83)-C(84)	1.377(5)	C(35)-N(31)-N(32)	105.89(17)
C(84)-C(85)	1.378(5)	C(35)-N(31)-NI	125.04(14)
C(85)-C(86)	1.391(4)	N(32)-N(31)-NI	127.27(13)
C(91)-C(96)	1.394(3)	N(31)-N(32)-C(33)	110.05(18)
C(91)-C(92)	1.397(3)	N(31)-N(32)-C(61)	122.17(16)
C(92)-C(93)	1.379(4)	C(33)-N(32)-C(61)	123.48(17)
C(93)-C(94)	1.381(4)	C(45)-N(41)-N(42)	105.74(18)
		C(45)-N(41)-NI	123.18(15)

N(42)-N(41)-NI	124.84(13)	C(74)-C(75)-C(76)	120.2(3)
C(43)-N(42)-N(41)	110.16(17)	C(71)-C(76)-C(75)	120.2(3)
C(43)-N(42)-C(61)	124.50(17)	C(86)-C(81)-C(82)	120.1(2)
N(41)-N(42)-C(61)	122.13(16)	C(86)-C(81)-C(51)	122.7(2)
N(22)-C(23)-C(24)	108.1(2)	C(82)-C(81)-C(51)	117.2(2)
C(23)-C(24)-C(25)	104.9(2)	C(83)-C(82)-C(81)	119.2(3)
N(21)-C(25)-C(24)	111.2(2)	C(84)-C(83)-C(82)	120.3(3)
C(14)-C(13)-N(12)	108.5(2)	C(83)-C(84)-C(85)	120.6(2)
C(13)-C(14)-C(15)	105.2(2)	C(84)-C(85)-C(86)	119.8(3)
N(11)-C(15)-C(14)	111.3(2)	C(81)-C(86)-C(85)	120.1(2)
C(34)-C(33)-N(32)	107.90(19)	C(96)-C(91)-C(92)	118.4(2)
C(33)-C(34)-C(35)	104.9(2)	C(96)-C(91)-C(61)	121.6(2)
N(31)-C(35)-C(34)	111.16(19)	C(92)-C(91)-C(61)	120.0(2)
N(42)-C(43)-C(44)	107.7(2)	C(93)-C(92)-C(91)	121.0(2)
C(43)-C(44)-C(45)	105.1(2)	C(92)-C(93)-C(94)	120.2(2)
N(41)-C(45)-C(44)	111.2(2)	C(93)-C(94)-C(95)	119.8(2)
N(22)-C(51)-N(12)	111.41(17)	C(94)-C(95)-C(96)	120.1(3)
N(22)-C(51)-C(81)	106.66(18)	C(95)-C(96)-C(91)	120.5(2)
N(12)-C(51)-C(81)	106.11(16)	C(106)-C(101)-C(102)	119.4(2)
N(22)-C(51)-C(71)	109.87(17)	C(106)-C(101)-C(61)	122.4(2)
N(12)-C(51)-C(71)	109.41(18)	C(102)-C(101)-C(61)	118.28(19)
C(81)-C(51)-C(71)	113.33(18)	C(103)-C(102)-C(101)	120.3(2)
N(32)-C(61)-N(42)	110.26(15)	C(102)-C(103)-C(104)	120.3(3)
N(32)-C(61)-C(91)	109.49(17)	C(105)-C(104)-C(103)	119.3(2)
N(42)-C(61)-C(91)	108.31(16)	C(104)-C(105)-C(106)	121.3(3)
N(32)-C(61)-C(101)	106.57(16)	C(101)-C(106)-C(105)	119.5(3)
N(42)-C(61)-C(101)	106.73(16)	CL1A-C(1A)-CL2A	112.1(6)
C(91)-C(61)-C(101)	115.40(16)	CL2B-C(1B)-CL1B	112.6(9)
C(76)-C(71)-C(72)	118.9(2)	CL4A-C(3A)-CL3A	112.1(7)
C(76)-C(71)-C(51)	120.8(2)	CL3B-C(3B)-CL4B	118.70(11)
C(72)-C(71)-C(51)	120.1(2)		
C(71)-C(72)-C(73)	120.4(2)		
C(74)-C(73)-C(72)	120.0(3)		
C(75)-C(74)-C(73)	120.2(3)		

Symmetry transformations used to generate equivalent atoms:

Table II-28. Torsion angles [°] for [(dpdpm)$_2$NiBr$_2$] (**3.4**).

N(11)-NI-N(21)-C(25)	-170.70(19)	BR2-NI-N(41)-N(42)	-165.01(15)
N(41)-NI-N(21)-C(25)	10.85(19)	C(45)-N(41)-N(42)-C(43)	2.3(2)
N(31)-NI-N(21)-C(25)	97.69(19)	NI-N(41)-N(42)-C(43)	154.99(15)
BR1-NI-N(21)-C(25)	-39.9(8)	C(45)-N(41)-N(42)-C(61)	162.82(17)
BR2-NI-N(21)-C(25)	-84.45(18)	NI-N(41)-N(42)-C(61)	-44.4(2)
N(11)-NI-N(21)-N(22)	-17.92(18)	N(21)-N(22)-C(23)-C(24)	1.9(3)
N(41)-NI-N(21)-N(22)	163.62(18)	C(51)-N(22)-C(23)-C(24)	161.7(2)
N(31)-NI-N(21)-N(22)	-109.53(18)	N(22)-C(23)-C(24)-C(25)	-0.3(3)
BR1-NI-N(21)-N(22)	112.9(7)	N(22)-N(21)-C(25)-C(24)	2.6(3)
BR2-NI-N(21)-N(22)	68.33(17)	NI-N(21)-C(25)-C(24)	159.69(18)
C(25)-N(21)-N(22)-C(23)	-2.7(2)	C(23)-C(24)-C(25)-N(21)	-1.5(3)
NI-N(21)-N(22)-C(23)	-159.64(16)	N(11)-N(12)-C(13)-C(14)	-2.0(3)
C(25)-N(21)-N(22)-C(51)	-163.20(19)	C(51)-N(12)-C(13)-C(14)	-160.2(2)
NI-N(21)-N(22)-C(51)	39.9(3)	N(12)-C(13)-C(14)-C(15)	0.5(3)
N(41)-NI-N(11)-C(15)	-78(3)	N(12)-N(11)-C(15)-C(14)	-2.5(3)
N(21)-NI-N(11)-C(15)	170.75(19)	NI-N(11)-C(15)-C(14)	-158.84(17)
N(31)-NI-N(11)-C(15)	-95.90(19)	C(13)-C(14)-C(15)-N(11)	1.3(3)
BR1-NI-N(11)-C(15)	-6.02(18)	N(31)-N(32)-C(33)-C(34)	2.2(3)
BR2-NI-N(11)-C(15)	86.48(18)	C(61)-N(32)-C(33)-C(34)	159.3(2)
N(41)-NI-N(11)-N(12)	130(2)	N(32)-C(33)-C(34)-C(35)	-1.0(3)
N(21)-NI-N(11)-N(12)	18.79(16)	N(32)-N(31)-C(35)-C(34)	1.9(2)
N(31)-NI-N(11)-N(12)	112.15(16)	NI-N(31)-C(35)-C(34)	167.51(16)
BR1-NI-N(11)-N(12)	-157.98(15)	C(33)-C(34)-C(35)-N(31)	-0.6(3)
BR2-NI-N(11)-N(12)	-65.47(16)	N(41)-N(42)-C(43)-C(44)	-1.8(3)
C(15)-N(11)-N(12)-C(13)	2.7(3)	C(61)-N(42)-C(43)-C(44)	-161.77(19)
NI-N(11)-N(12)-C(13)	159.25(16)	N(42)-C(43)-C(44)-C(45)	0.6(3)
C(15)-N(11)-N(12)-C(51)	161.4(2)	N(42)-N(41)-C(45)-C(44)	-1.9(2)
NI-N(11)-N(12)-C(51)	-42.1(3)	NI-N(41)-C(45)-C(44)	-155.21(16)
N(11)-NI-N(31)-C(35)	3.74(18)	C(43)-C(44)-C(45)-N(41)	0.9(3)
N(41)-NI-N(31)-C(35)	-175.76(18)	C(23)-N(22)-C(51)-N(12)	148.8(2)
N(21)-NI-N(31)-C(35)	91.67(18)	N(21)-N(22)-C(51)-N(12)	-53.8(2)
BR1-NI-N(31)-C(35)	-91.20(17)	C(23)-N(22)-C(51)-C(81)	33.4(3)
BR2-NI-N(31)-C(35)	50.8(1)	N(21)-N(22)-C(51)-C(81)	-169.13(18)
N(11)-NI-N(31)-N(32)	166.22(16)	C(23)-N(22)-C(51)-C(71)	-89.8(2)
N(41)-NI-N(31)-N(32)	-13.27(16)	N(21)-N(22)-C(51)-C(71)	67.7(2)
N(21)-NI-N(31)-N(32)	-105.84(16)	C(13)-N(12)-C(51)-N(22)	-149.4(2)
BR1-NI-N(31)-N(32)	71.29(16)	N(11)-N(12)-C(51)-N(22)	55.1(3)
BR2-NI-N(31)-N(32)	-146.7(8)	C(13)-N(12)-C(51)-C(81)	-33.7(3)
C(35)-N(31)-N(32)-C(33)	-2.5(2)	N(11)-N(12)-C(51)-C(81)	170.8(2)
NI-N(31)-N(32)-C(33)	-167.71(15)	C(13)-N(12)-C(51)-C(71)	88.9(3)
C(35)-N(31)-N(32)-C(61)	-159.97(19)	N(11)-N(12)-C(51)-C(71)	-66.6(3)
NI-N(31)-N(32)-C(61)	34.9(2)	N(31)-N(32)-C(61)-N(42)	-52.4(2)
N(11)-NI-N(41)-C(45)	148(2)	C(33)-N(32)-C(61)-N(42)	153.3(2)
N(21)-NI-N(41)-C(45)	-101.16(18)	N(31)-N(32)-C(61)-C(91)	66.7(2)
N(31)-NI-N(41)-C(45)	165.57(19)	C(33)-N(32)-C(61)-C(91)	-87.7(2)
BR1-NI-N(41)-C(45)	75.53(18)	N(31)-N(32)-C(61)-C(101)	-167.84(16)
BR2-NI-N(41)-C(45)	-16.79(18)	C(33)-N(32)-C(61)-C(101)	37.8(3)
N(11)-NI-N(41)-N(42)	-1(3)	C(43)-N(42)-C(61)-N(32)	-144.0(2)
N(21)-NI-N(41)-N(42)	110.62(16)	N(41)-N(42)-C(61)-N(32)	58.2(2)
N(31)-NI-N(41)-N(42)	17.36(15)	C(43)-N(42)-C(61)-C(91)	96.2(2)
BR1-NI-N(41)-N(42)	-72.69(15)	N(41)-N(42)-C(61)-C(91)	-61.6(2)

C(43)-N(42)-C(61)-C(101)	-28.7(3)
N(41)-N(42)-C(61)-C(101)	173.59(17)
N(22)-C(51)-C(71)-C(76)	20.0(3)
N(12)-C(51)-C(71)-C(76)	142.6(2)
C(81)-C(51)-C(71)-C(76)	-99.2(3)
N(22)-C(51)-C(71)-C(72)	-164.2(2)
N(12)-C(51)-C(71)-C(72)	-41.6(3)
C(81)-C(51)-C(71)-C(72)	76.6(3)
C(76)-C(71)-C(72)-C(73)	0.6(4)
C(51)-C(71)-C(72)-C(73)	-175.2(2)
C(71)-C(72)-C(73)-C(74)	-0.1(4)
C(72)-C(73)-C(74)-C(75)	-0.7(5)
C(73)-C(74)-C(75)-C(76)	0.9(5)
C(72)-C(71)-C(76)-C(75)	-0.4(4)
C(51)-C(71)-C(76)-C(75)	175.4(2)
C(74)-C(75)-C(76)-C(71)	-0.4(4)
N(22)-C(51)-C(81)-C(86)	-124.1(3)
N(12)-C(51)-C(81)-C(86)	117.0(3)
C(71)-C(51)-C(81)-C(86)	-3.1(3)
N(22)-C(51)-C(81)-C(82)	57.9(3)
N(12)-C(51)-C(81)-C(82)	-61.0(3)
C(71)-C(51)-C(81)-C(82)	178.9(2)
C(86)-C(81)-C(82)-C(83)	-0.4(5)
C(51)-C(81)-C(82)-C(83)	177.7(3)
C(81)-C(82)-C(83)-C(84)	-0.4(6)
C(82)-C(83)-C(84)-C(85)	-0.1(6)
C(83)-C(84)-C(85)-C(86)	1.5(6)
C(82)-C(81)-C(86)-C(85)	1.8(4)
C(51)-C(81)-C(86)-C(85)	-176.2(3)
C(84)-C(85)-C(86)-C(81)	-2.3(5)
N(32)-C(61)-C(91)-C(96)	17.3(3)
N(42)-C(61)-C(91)-C(96)	137.61(19)
C(101)-C(61)-C(91)-C(96)	-102.9(2)
N(32)-C(61)-C(91)-C(92)	-162.5(2)
N(42)-C(61)-C(91)-C(92)	-42.2(3)
C(101)-C(61)-C(91)-C(92)	77.3(3)
C(96)-C(91)-C(92)-C(93)	-1.0(4)
C(61)-C(91)-C(92)-C(93)	178.8(2)
C(91)-C(92)-C(93)-C(94)	0.1(4)
C(92)-C(93)-C(94)-C(95)	1.5(4)
C(93)-C(94)-C(95)-C(96)	-2.1(4)
C(94)-C(95)-C(96)-C(91)	1.2(4)
C(92)-C(91)-C(96)-C(95)	0.4(3)
C(61)-C(91)-C(96)-C(95)	-179.4(2)
N(32)-C(61)-C(101)-C(106)	-128.3(2)
N(42)-C(61)-C(101)-C(106)	113.8(2)
C(91)-C(61)-C(101)-C(106)	-6.6(3)
N(32)-C(61)-C(101)-C(102)	51.0(2)
N(42)-C(61)-C(101)-C(102)	-66.9(2)
C(91)-C(61)-C(101)-C(102)	172.7(2)
C(106)-C(101)-C(102)-C(103)	0.1(4)
C(61)-C(101)-C(102)-C(10)	-179.2(2)
C(101)-C(102)-C(103)-C(104)	0.0(4)
C(102)-C(103)-C(104)-C(105)	0.1(4)
C(103)-C(104)-C(105)-C(106)	-0.5(4)
C(102)-C(101)-C(106)-C(105)	-0.5(3)
C(61)-C(101)-C(106)-C(105)	178.8(2)
C(104)-C(105)-C(106)-C(101)	0.7(4)

Symmetry transformations used to generate equivalent atoms:

Table II-29. Atomic coordinates (x 10^4) and equivalent isotropic displacement parameters ($Å^2$ x 10^3) for [$(dpdpm)_2NiBr(H_2O)$][Br] **(3.5)**.

U_{eq} is defined as one third of the trace of the orthogonalized Uij tensor.

	x	y	z	U_{eq}
Br(1)	-1832(1)	6257(1)	1872(1)	20(1)
Br(2)	2004(1)	4526(1)	3848(1)	19(1)
Ni	-515(1)	6606(1)	3347(1)	13(1)
N(21)	593(2)	6656(2)	4529(2)	14(1)
N(22)	1657(2)	6855(2)	4777(2)	15(1)
N(11)	857(2)	6676(2)	2926(2)	13(1)
N(12)	1908(2)	6693(2)	3415(2)	13(1)
N(31)	-922(2)	7826(2)	3161(2)	15(1)
N(32)	-1719(2)	8248(2)	3362(2)	13(1)
N(41)	-1814(2)	6492(2)	3810(2)	14(1)
N(42)	-2548(2)	7090(2)	3823(2)	13(1)
C(23)	2079(3)	6777(2)	5617(2)	18(1)
C(24)	1290(3)	6490(2)	5915(2)	19(1)
C(25)	382(3)	6418(2)	5214(2)	16(1)
C(13)	2560(3)	6487(2)	2956(2)	18(1)
C(14)	1932(3)	6304(2)	2168(2)	18(1)
C(15)	880(3)	6420(2)	2182(2)	18(1)
C(33)	-1821(3)	9020(2)	3028(2)	17(1)
C(34)	-1127(3)	9081(2)	2571(2)	18(1)
C(35)	-590(3)	8329(2)	2667(2)	17(1)
C(43)	-3458(3)	6754(2)	3920(2)	15(1)
C(44)	-3337(3)	5921(2)	3941(2)	17(1)
C(45)	-2315(3)	5790(2)	3863(2)	18(1)
C(51)	2230(3)	7171(2)	4200(2)	13(1)
C(61)	-2199(3)	7958(2)	4006(2)	13(1)
C(71)	1973(2)	8074(2)	3983(2)	14(1)
C(72)	1702(3)	8581(2)	4556(2)	17(1)
C(73)	1509(3)	9410(2)	4373(2)	20(1)
C(74)	1600(3)	9733(2)	3632(2)	21(1)
C(75)	1918(3)	9235(2)	3078(2)	19(1)
C(76)	2097(3)	8408(2)	3257(2)	18(1)
C(81)	3434(3)	7035(2)	4644(2)	15(1)
C(82)	3806(3)	6236(2)	4873(2)	18(1)
C(83)	4867(3)	6114(2)	5347(2)	20(1)
C(84)	5575(3)	6771(2)	5593(2)	19(1)
C(85)	5210(3)	7558(2)	5343(2)	19(1)
C(86)	4141(3)	7689(2)	4869(2)	17(1)
C(91)	-1395(3)	8019(2)	4883(2)	13(1)
C(92)	-1560(3)	7562(2)	5532(2)	17(1)
C(93)	-909(3)	7686(2)	6345(2)	21(1)
C(94)	-74(3)	8254(2)	6518(2)	21(1)
C(95)	100(3)	8695(2)	5867(2)	20(1)
C(96)	-553(3)	8586(2)	5055(2)	17(1)
C(101)	-3201(3)	8482(2)	3916(2)	13(1)
C(102)	-3244(3)	9024(2)	4544(2)	17(1)
C(103)	-4137(3)	9520(2)	4446(2)	21(1)

C(104)	-5008(3)	9463(2)	3732(2)	21(1)
C(105)	-4970(3)	8926(2)	3098(2)	22(1)
C(106)	-4063(3)	8448(2)	3185(2)	18(1)
O(1)	-327(2)	5326(1)	3413(2)	18(1)

Table II-30. Hydrogen coordinates (x 10^4) and isotropic displacement parameters ($Å^2$ x 10^3) for $[(dpdpm)_2NiBr(H_2O)][Br]$ **(3.5)**.

	x	y	z	U_{eq}
H(23)	2797	6901	5938	22
H(24)	1343	6364	6478	23
H(25)	-299	6224	5229	20
H(13)	3324	6473	3150	21
H(14)	2163	6133	1710	21
H(15)	259	6328	1718	21
H(33)	-2291	9436	3104	20
H(34)	-1026	9538	2253	22
H(35)	-55	8194	2411	20
H(43)	-4068	7045	3967	18
H(44)	-3839	5521	3995	20
H(45)	-2011	5264	3849	21
H(72)	1650	8364	5067	21
H(73)	1315	9756	4758	24
H(74)	1445	10295	3504	25
H(75)	2013	9458	2583	23
H(76)	2307	8065	2878	21
H(82)	3333	5783	4704	22
H(83)	5116	5574	5507	24
H(84)	6297	6682	5926	22
H(85)	5690	8008	5495	23
H(86)	3897	8228	4700	20
H(92)	-2117	7164	5419	21
H(93)	-1034	7381	6788	26
H(94)	371	8338	7075	25
H(95)	675	9078	5979	23
H(96)	-429	8895	4615	20
H(102)	-2656	9055	5042	21
H(103)	-4150	9900	4871	25
H(104)	-5630	9789	3674	26
H(105)	-5565	8887	2606	26
H(106)	-4030	8095	2744	21
H(1A)	350(30)	5170(20)	3540(20)	27
H(1B)	-570(30)	5200(30)	2960(30)	27

Table II-31. Anisotropic parameters ($Å^2$ x 10^3) for $[(dpdpm)_2NiBr(H_2O)][Br]$ **(3.5)**.

The anisotropic displacement factor exponent takes the form:

$$-2\pi^2 [h^2 a^{*2} U_{11} + \ldots + 2 h k a^* b^* U_{12}]$$

	U11	U22	U33	U23	U13	U12
Br(1)	17(1)	23(1)	18(1)	-2(1)	2(1)	1(1)
Br(2)	18(1)	14(1)	23(1)	1(1)	2(1)	1(1)
Ni	13(1)	11(1)	16(1)	0(1)	5(1)	1(1)
N(21)	12(1)	14(1)	16(1)	0(1)	5(1)	0(1)
N(22)	16(1)	10(1)	18(2)	0(1)	4(1)	0(1)
N(11)	12(1)	13(1)	15(1)	0(1)	3(1)	-2(1)
N(12)	15(1)	10(1)	15(1)	0(1)	5(1)	-1(1)
N(31)	14(1)	14(1)	17(2)	-1(1)	6(1)	2(1)
N(32)	13(1)	12(1)	15(1)	0(1)	5(1)	1(1)
N(41)	14(1)	12(1)	17(2)	0(1)	5(1)	1(1)
N(42)	12(1)	10(1)	17(1)	0(1)	4(1)	1(1)
C(23)	17(2)	18(2)	16(2)	-2(1)	0(1)	2(1)
C(24)	23(2)	19(2)	17(2)	4(1)	7(2)	5(1)
C(25)	17(2)	15(2)	18(2)	0(1)	6(1)	2(1)
C(13)	15(2)	15(2)	25(2)	1(1)	10(2)	2(1)
C(14)	22(2)	18(2)	16(2)	-1(1)	10(1)	2(1)
C(15)	21(2)	18(2)	16(2)	-1(1)	8(1)	0(1)
C(33)	17(2)	13(2)	18(2)	2(1)	2(1)	2(1)
C(34)	20(2)	16(2)	18(2)	6(1)	4(1)	1(1)
C(35)	15(2)	19(2)	17(2)	4(1)	6(1)	1(1)
C(43)	13(2)	19(2)	15(2)	-1(1)	7(1)	-2(1)
C(44)	19(2)	17(2)	17(2)	-1(1)	7(1)	-5(1)
C(45)	24(2)	12(2)	18(2)	1(1)	8(2)	-3(1)
C(51)	14(2)	13(2)	13(2)	-2(1)	5(1)	-2(1)
C(61)	15(2)	8(2)	15(2)	-2(1)	4(1)	1(1)
C(71)	9(2)	12(2)	21(2)	0(1)	2(1)	-2(1)
C(72)	17(2)	16(2)	20(2)	-1(1)	7(1)	-1(1)
C(73)	20(2)	14(2)	30(2)	-6(2)	12(2)	-2(1)
C(74)	19(2)	12(2)	32(2)	1(2)	8(2)	-1(1)
C(75)	21(2)	16(2)	20(2)	3(1)	7(2)	-2(1)
C(76)	16(2)	16(2)	20(2)	-4(1)	6(1)	-2(1)
C(81)	14(2)	19(2)	14(2)	-1(1)	5(1)	2(1)
C(82)	17(2)	16(2)	21(2)	-4(2)	4(1)	-2(1)
C(83)	21(2)	17(2)	23(2)	2(2)	6(2)	5(1)
C(84)	11(2)	27(2)	18(2)	-1(2)	4(1)	2(1)
C(85)	18(2)	21(2)	20(2)	-7(2)	8(2)	-6(1)
C(86)	17(2)	16(2)	19(2)	-2(1)	7(1)	0(1)
C(91)	13(2)	11(2)	16(2)	-2(1)	6(1)	4(1)
C(92)	18(2)	14(2)	19(2)	1(1)	4(1)	1(1)
C(93)	28(2)	18(2)	17(2)	3(2)	6(2)	3(2)
C(94)	21(2)	19(2)	20(2)	0(2)	1(2)	6(1)
C(95)	16(2)	17(2)	24(2)	-5(2)	3(1)	0(1)

C(96)	18(2)	15(2)	18(2)	0(1)	7(1)	3(1)
C(101)	14(2)	9(1)	18(2)	1(1)	7(1)	0(1)
C(102)	18(2)	15(2)	20(2)	0(1)	8(1)	-2(1)
C(103)	19(2)	16(2)	31(2)	-3(2)	13(2)	0(1)
C(104)	16(2)	16(2)	33(2)	6(2)	10(2)	2(1)
C(105)	16(2)	23(2)	24(2)	7(2)	3(2)	-2(1)
C(106)	18(2)	17(2)	18(2)	2(1)	5(1)	0(1)
O(1)	18(1)	12(1)	24(1)	-1(1)	6(1)	1(1)

Table II-32. Bond lengths [Å] and angles [°] for $[(dpdpm)_2NiBr(H_2O)][Br]$ (3.5).

Br(1)-Ni	2.6146(7)	C(94)-C(95)	1.385(5)
Ni-N(31)	2.061(3)	C(95)-C(96)	1.383(5)
Ni-N(21)	2.074(3)	C(101)-C(102)	1.392(4)
Ni-N(41)	2.076(3)	C(101)-C(106)	1.392(4)
Ni-O(1)	2.106(2)	C(102)-C(103)	1.387(5)
Ni-N(11)	2.116(3)	C(103)-C(104)	1.384(5)
N(21)-C(25)	1.321(4)	C(104)-C(105)	1.392(5)
N(21)-N(22)	1.362(4)	C(105)-C(106)	1.388(5)
N(22)-C(23)	1.357(4)		
N(22)-C(51)	1.485(4)	N(31)-NI-N(21)	100.39(11)
N(11)-C(15)	1.328(4)	N(31)-NI-N(41)	86.65(11)
N(11)-N(12)	1.369(3)	N(21)-NI-N(41)	93.16(11)
N(12)-C(13)	1.352(4)	N(31)-NI-O(1)	171.52(11)
N(12)-C(51)	1.481(4)	N(21)-NI-O(1)	87.23(10)
N(31)-C(35)	1.330(4)	N(41)-NI-O(1)	89.22(10)
N(31)-N(32)	1.372(4)	N(31)-NI-N(11)	95.84(11)
N(32)-C(33)	1.370(4)	N(21)-NI-N(11)	84.49(11)
N(32)-C(61)	1.484(4)	N(41)-NI-N(11)	176.84(11)
N(41)-C(45)	1.336(4)	O(1)-NI-N(11)	88.56(10)
N(41)-N(42)	1.373(3)	N(31)-NI-BR1	90.10(8)
N(42)-C(43)	1.361(4)	N(21)-NI-BR1	169.51(8)
N(42)-C(61)	1.492(4)	N(41)-NI-BR1	87.67(8)
C(23)-C(24)	1.358(5)	O(1)-NI-BR1	82.33(7)
C(24)-C(25)	1.400(5)	N(11)-NI-BR1	94.26(8)
C(13)-C(14)	1.362(5)	C(25)-N(21)-N(22)	105.4(3)
C(14)-C(15)	1.393(5)	C(25)-N(21)-NI	123.7(2)
C(33)-C(34)	1.357(5)	N(22)-N(21)-NI	130.7(2)
C(34)-C(35)	1.400(4)	C(23)-N(22)-N(21)	110.5(3)
C(43)-C(44)	1.369(5)	C(23)-N(22)-C(51)	125.9(3)
C(44)-C(45)	1.394(5)	N(21)-N(22)-C(51)	123.5(3)
C(51)-C(71)	1.533(4)	C(15)-N(11)-N(12)	105.5(3)
C(51)-C(81)	1.536(4)	C(15)-N(11)-NI	124.1(2)
C(61)-C(91)	1.531(4)	N(12)-N(11)-NI	126.5(2)
C(61)-C(101)	1.531(4)	C(13)-N(12)-N(11)	109.9(3)
C(71)-C(76)	1.388(5)	C(13)-N(12)-C(51)	125.6(3)
C(71)-C(72)	1.395(5)	N(11)-N(12)-C(51)	120.5(3)
C(72)-C(73)	1.395(5)	C(35)-N(31)-N(32)	104.9(3)
C(73)-C(74)	1.391(5)	C(35)-N(31)-NI	125.1(2)
C(74)-C(75)	1.392(5)	N(32)-N(31)-NI	128.9(2)
C(75)-C(76)	1.388(5)	C(33)-N(32)-N(31)	110.4(3)
C(81)-C(86)	1.388(5)	C(33)-N(32)-C(61)	125.6(3)
C(81)-C(82)	1.405(4)	N(31)-N(32)-C(61)	122.5(3)
C(82)-C(83)	1.386(5)	C(45)-N(41)-N(42)	104.6(3)
C(83)-C(84)	1.394(5)	C(45)-N(41)-NI	125.0(2)
C(84)-C(85)	1.391(5)	N(42)-N(41)-NI	126.5(2)
C(85)-C(86)	1.397(4)	C(43)-N(42)-N(41)	110.6(3)
C(91)-C(92)	1.392(5)	C(43)-N(42)-C(61)	125.5(3)
C(91)-C(96)	1.398(4)	N(41)-N(42)-C(61)	120.6(2)
C(92)-C(93)	1.388(5)	N(22)-C(23)-C(24)	107.6(3)
C(93)-C(94)	1.393(5)	C(23)-C(24)-C(25)	105.1(3)
		N(21)-C(25)-C(24)	111.3(3)

N(12)-C(13)-C(14)	108.2(3)	C(75)-C(76)-C(71)	121.1(3)
C(13)-C(14)-C(15)	105.0(3)	C(86)-C(81)-C(82)	119.8(3)
N(11)-C(15)-C(14)	111.2(3)	C(86)-C(81)-C(51)	121.1(3)
C(34)-C(33)-N(32)	107.5(3)	C(82)-C(81)-C(51)	119.0(3)
C(33)-C(34)-C(35)	105.4(3)	C(83)-C(82)-C(81)	119.5(3)
N(31)-C(35)-C(34)	111.6(3)	C(82)-C(83)-C(84)	121.0(3)
N(42)-C(43)-C(44)	107.8(3)	C(85)-C(84)-C(83)	119.2(3)
C(43)-C(44)-C(45)	104.9(3)	C(84)-C(85)-C(86)	120.4(3)
N(41)-C(45)-C(44)	112.0(3)	C(81)-C(86)-C(85)	120.2(3)
N(12)-C(51)-N(22)	109.6(3)	C(92)-C(91)-C(96)	119.4(3)
N(12)-C(51)-C(71)	108.3(3)	C(92)-C(91)-C(61)	119.8(3)
N(22)-C(51)-C(71)	111.9(3)	C(96)-C(91)-C(61)	120.6(3)
N(12)-C(51)-C(81)	109.1(3)	C(93)-C(92)-C(91)	120.0(3)
N(22)-C(51)-C(81)	106.0(3)	C(92)-C(93)-C(94)	120.6(3)
C(71)-C(51)-C(81)	111.9(3)	C(95)-C(94)-C(93)	119.2(3)
N(32)-C(61)-N(42)	108.8(2)	C(96)-C(95)-C(94)	120.8(3)
N(32)-C(61)-C(91)	111.4(3)	C(95)-C(96)-C(91)	120.1(3)
N(42)-C(61)-C(91)	109.8(3)	C(102)-C(101)-C(106)	119.2(3)
N(32)-C(61)-C(101)	106.6(3)	C(102)-C(101)-C(61)	120.7(3)
N(42)-C(61)-C(101)	108.2(2)	C(106)-C(101)-C(61)	120.1(3)
C(91)-C(61)-C(101)	111.9(3)	C(103)-C(102)-C(101)	120.5(3)
C(76)-C(71)-C(72)	119.6(3)	C(104)-C(103)-C(102)	120.1(3)
C(76)-C(71)-C(51)	120.8(3)	C(103)-C(104)-C(105)	119.8(3)
C(72)-C(71)-C(51)	119.3(3)	C(106)-C(105)-C(104)	120.1(3)
C(73)-C(72)-C(71)	119.4(3)	C(105)-C(106)-C(101)	120.3(3)
C(74)-C(73)-C(72)	120.5(3)		
C(73)-C(74)-C(75)	120.0(3)		
C(76)-C(75)-C(74)	119.2(3)		

Symmetry transformations used to generate equivalent atoms:

Table II-33. Torsion angles [°] for [(dpdpm)$_2$NiBr(H$_2$O)][Br] (**3.5**).

N(31)-NI-N(21)-C(25)	104.4(3)	BR1-NI-N(41)-N(42)	-85.2(2)
N(41)-NI-N(21)-C(25)	17.3(3)	C(45)-N(41)-N(42)-C(43)	2.7(4)
O(1)-NI-N(21)-C(25)	-71.8(3)	NI-N(41)-N(42)-C(43)	161.1(2)
N(11)-NI-N(21)-C(25)	-160.6(3)	C(45)-N(41)-N(42)-C(61)	163.3(3)
BR1-NI-N(21)-C(25)	-77.0(5)	NI-N(41)-N(42)-C(61)	-38.4(4)
N(31)-NI-N(21)-N(22)	-81.4(3)	N(21)-N(22)-C(23)-C(24)	2.5(4)
N(41)-NI-N(21)-N(22)	-168.6(3)	C(51)-N(22)-C(23)-C(24)	178.3(3)
O(1)-NI-N(21)-N(22)	102.3(3)	N(22)-C(23)-C(24)-C(25)	-1.1(4)
N(11)-NI-N(21)-N(22)	13.5(3)	N(22)-N(21)-C(25)-C(24)	2.2(4)
BR1-NI-N(21)-N(22)	97.1(5)	NI-N(21)-C(25)-C(24)	177.6(2)
C(25)-N(21)-N(22)-C(23)	-2.9(4)	C(23)-C(24)-C(25)-N(21)	-0.7(4)
NI-N(21)-N(22)-C(23)	-177.9(2)	N(11)-N(12)-C(13)-C(14)	-2.3(4)
C(25)-N(21)-N(22)-C(51)	-178.8(3)	C(51)-N(12)-C(13)-C(14)	-159.8(3)
NI-N(21)-N(22)-C(51)	6.3(4)	N(12)-C(13)-C(14)-C(15)	0.7(4)
N(31)-NI-N(11)-C(15)	-102.8(3)	N(12)-N(11)-C(15)-C(14)	-2.6(4)
N(21)-NI-N(11)-C(15)	157.3(3)	NI-N(11)-C(15)-C(14)	-161.5(2)
N(41)-NI-N(11)-C(15)	115.30(19)	C(13)-C(14)-C(15)-N(11)	1.2(4)
O(1)-NI-N(11)-C(15)	69.9(3)	N(31)-N(32)-C(33)-C(34)	3.3(4)
BR1-NI-N(11)-C(15)	-12.3(3)	C(61)-N(32)-C(33)-C(34)	170.0(3)
N(31)-NI-N(11)-N(12)	102.8(2)	N(32)-C(33)-C(34)-C(35)	-1.7(4)
N(21)-NI-N(11)-N(12)	2.8(2)	N(32)-N(31)-C(35)-C(34)	2.4(4)
N(41)-NI-N(11)-N(12)	-39(2)	NI-N(31)-C(35)-C(34)	171.0(2)
O(1)-NI-N(11)-N(12)	-84.5(2)	C(33)-C(34)-C(35)-N(31)	-0.4(4)
BR1-NI-N(11)-N(12)	-166.7(2)	N(41)-N(42)-C(43)-C(44)	-2.3(4)
C(15)-N(11)-N(12)-C(13)	3.0(3)	C(61)-N(42)-C(43)-C(44)	-161.7(3)
NI-N(11)-N(12)-C(13)	161.2(2)	N(42)-C(43)-C(44)-C(45)	0.9(4)
C(15)-N(11)-N(12)-C(51)	161.8(3)	N(42)-N(41)-C(45)-C(44)	-2.2(4)
NI-N(11)-N(12)-C(51)	-40.0(4)	NI-N(41)-C(45)-C(44)	-161.0(2)
N(21)-NI-N(31)-C(35)	104.8(3)	C(43)-C(44)-C(45)-N(41)	0.9(4)
N(41)-NI-N(31)-C(35)	-162.6(3)	C(13)-N(12)-C(51)-N(22)	-143.9(3)
O(1)-NI-N(31)-C(35)	-101.5(8)	N(11)-N(12)-C(51)-N(22)	60.8(4)
N(11)-NI-N(31)-C(35)	19.4(3)	C(13)-N(12)-C(51)-C(71)	93.8(4)
BR1-NI-N(31)-C(35)	-74.9(3)	N(11)-N(12)-C(51)-C(71)	-61.5(4)
N(21)-NI-N(31)-N(32)	-89.3(3)	C(13)-N(12)-C(51)-C(81)	-28.3(4)
N(41)-NI-N(31)-N(32)	3.3(3)	N(11)-N(12)-C(51)-C(81)	176.4(3)
O(1)-NI-N(31)-N(32)	64.3(8)	C(23)-N(22)-C(51)-N(12)	141.4(3)
N(11)-NI-N(31)-N(32)	-174.8(3)	N(21)-N(22)-C(51)-N(12)	-43.3(4)
BR1-NI-N(31)-N(32)	90.9(3)	C(23)-N(22)-C(51)-C(71)	-98.5(4)
C(35)-N(31)-N(32)-C(33)	-3.5(4)	N(21)-N(22)-C(51)-C(71)	76.8(4)
NI-N(31)-N(32)-C(33)	-171.5(2)	C(23)-N(22)-C(51)-C(81)	23.8(4)
C(35)-N(31)-N(32)-C(61)	-170.6(3)	N(21)-N(22)-C(51)-C(81)	-161.0(3)
NI-N(31)-N(32)-C(61)	21.3(4)	C(33)-N(32)-C(61)-N(42)	143.2(3)
N(31)-NI-N(41)-C(45)	159.2(3)	N(31)-N(32)-C(61)-N(42)	-51.6(4)
N(21)-NI-N(41)-C(45)	-100.6(3)	C(33)-N(32)-C(61)-C(91)	-95.6(4)
O(1)-NI-N(41)-C(45)	-13.4(3)	N(31)-N(32)-C(61)-C(91)	69.5(4)
N(11)-NI-N(41)-C(45)	-59(2)	C(33)-N(32)-C(61)-C(101)	26.7(4)
BR1-NI-N(41)-C(45)	68.9(3)	N(31)-N(32)-C(61)-C(101)	-168.1(3)
N(31)-NI-N(41)-N(42)	5.0(3)	C(43)-N(42)-C(61)-N(32)	-141.8(3)
N(21)-NI-N(41)-N(42)	105.2(3)	N(41)-N(42)-C(61)-N(32)	60.7(4)
O(1)-NI-N(41)-N(42)	-167.6(3)	C(43)-N(42)-C(61)-C(91)	96.1(4)
N(11)-NI-N(41)-N(42)	147.10(19)	N(41)-N(42)-C(61)-C(91)	-61.4(4)

C(43)-N(42)-C(61)-C(101)	-26.4(4)
N(41)-N(42)-C(61)-C(101)	176.1(3)
N(12)-C(51)-C(71)-C(76)	-36.2(4)
N(22)-C(51)-C(71)-C(76)	-157.1(3)
C(81)-C(51)-C(71)-C(76)	84.1(4)
N(12)-C(51)-C(71)-C(72)	149.4(3)
N(22)-C(51)-C(71)-C(72)	28.5(4)
C(81)-C(51)-C(71)-C(72)	-90.3(4)
C(76)-C(71)-C(72)-C(73)	3.0(5)
C(51)-C(71)-C(72)-C(73)	177.5(3)
C(71)-C(72)-C(73)-C(74)	-0.9(5)
C(72)-C(73)-C(74)-C(75)	-2.0(5)
C(73)-C(74)-C(75)-C(76)	2.8(5)
C(74)-C(75)-C(76)-C(71)	-0.6(5)
C(72)-C(71)-C(76)-C(75)	-2.3(5)
C(51)-C(71)-C(76)-C(75)	-176.7(3)
N(12)-C(51)-C(81)-C(86)	125.2(3)
N(22)-C(51)-C(81)-C(86)	-116.9(3)
C(71)-C(51)-C(81)-C(86)	5.4(4)
N(12)-C(51)-C(81)-C(82)	-59.1(4)
N(22)-C(51)-C(81)-C(82)	58.8(4)
C(71)-C(51)-C(81)-C(82)	-178.9(3)
C(86)-C(81)-C(82)-C(83)	2.3(5)
C(51)-C(81)-C(82)-C(83)	-173.5(3)
C(81)-C(82)-C(83)-C(84)	-0.7(5)
C(82)-C(83)-C(84)-C(85)	-1.2(5)
C(83)-C(84)-C(85)-C(86)	1.5(5)
C(82)-C(81)-C(86)-C(85)	-1.9(5)
C(51)-C(81)-C(86)-C(85)	173.8(3)
C(84)-C(85)-C(86)-C(81)	0.0(5)
N(32)-C(61)-C(91)-C(92)	-160.6(3)
N(42)-C(61)-C(91)-C(92)	-40.0(4)
C(101)-C(61)-C(91)-C(92)	80.2(4)
N(32)-C(61)-C(91)-C(96)	25.4(4)
N(42)-C(61)-C(91)-C(96)	146.0(3)
C(101)-C(61)-C(91)-C(96)	-93.8(4)
C(96)-C(91)-C(92)-C(93)	1.7(5)
C(61)-C(91)-C(92)-C(93)	-172.4(3)
C(91)-C(92)-C(93)-C(94)	-1.4(5)
C(92)-C(93)-C(94)-C(95)	0.0(5)
C(93)-C(94)-C(95)-C(96)	0.9(5)
C(94)-C(95)-C(96)-C(91)	-0.5(5)
C(92)-C(91)-C(96)-C(95)	-0.8(5)
C(61)-C(91)-C(96)-C(95)	173.3(3)
N(32)-C(61)-C(101)-C(102	-113.4(3)
N(42)-C(61)-C(101)-C(102)	129.8(3)
C(91)-C(61)-C(101)-C(102)	8.6(4)
N(32)-C(61)-C(101)-C(106)	63.7(4)
N(42)-C(61)-C(101)-C(106)	-53.2(4)
C(91)-C(61)-C(101)-C(106	-174.4(3)
C(106)-C(101)-C(102)-C(103)	0.6(5)
C(61)-C(101)-C(102)-C(103	177.6(3)
C(101)-C(102)-C(103)-C(104)	1.8(5)
C(102)-C(103)-C(104)-C(105	-2.2(5)
C(103)-C(104)-C(105)-C(106)	0.3(5)
C(104)-C(105)-C(106)-C(101)	2.1(5)
C(102)-C(101)-C(106)-C(105	-2.5(5)
C(61)-C(101)-C(106)-C(10	-179.6(3)

Symmetry transformations used to generate equivalent atoms:

Table II-34. Bond lengths [Å] and angles [°] related to the hydrogen bonding for $[(dpdpm)_2NiBr(H_2O)][Br]$ (**3.5**).

D-H	..A	d(D-H)	d(H..A)	d(D..A)	<DHA
O(1)-H(1A)	BR2	0.88(4)	2.31(4)	3.183(2)	170(4)
O(1)-H(1B)	BR1	0.76(4)	2.68(4)	3.130(3)	120(4)

Symmetry transformations used to generate equivalent atoms:

Chapter 3

$[(L_2L'NiBr_2)(AgBr)]_2$: A Tetrametallic Ensemble Arising From Halophilicity of Silver

Supplementary material

Table III-1 Atomic coordinates and equivalent isotropic displacement parameters ($Å^2 \times 10^3$) for [{(dpdpm)(CH_3CN)$NiBr_2$}($AgBr$)]$_2$ (**4.1**).

Table III-2 Hydrogen coordinates ($\times 10^4$) and isotropic displacement parameters ($Å^2 \times 10^3$) for [{(dpdpm)(CH_3CN)$NiBr_2$}($AgBr$)]$_2$ (**4.1**).

Table III-3 Anisotropic displacement parameters ($Å^2 \times 10^3$) for [{(dpdpm)(CH_3CN)$NiBr_2$}($AgBr$)]$_2$ (**4.1**).

Table III-4 Bond length [A] and angles [°] for [{(dpdpm)(CH_3CN)$NiBr_2$}($AgBr$)]$_2$ (**4.1**).

Table III-5 Torsion angles [°] for [{(dpdpm)(CH_3CN)$NiBr_2$}($AgBr$)]$_2$ (**4.1**).

Table III-6 Atomic coordinates and equivalent isotropic displacement parameters ($Å^2 \times 10^3$) for [(dpdpm)$NiBr(CH_3CN)_3$][PF_6] (**4.2**).

Table III-7 Hydrogen coordinates ($\times 10^4$) and isotropic displacement parameters ($Å^2 \times 10^3$) for [(dpdpm)$NiBr(CH_3CN)_3$][PF_6] (**4.2**).

Table III-8 Anisptropic displacement parameters ($Å^2 \times 10^3$) for [(dpdpm)$NiBr(CH_3CN)_3$][PF_6] (**4.2**).

Table III-9 Bond length [Å] and angles [deg] for [(dpdpm)$NiBr(CH_3CN)_3$][PF_6] (**4.2**).

Table III-10 Torsion angles [°] for [(dpdpm)$NiBr(CH_3CN)_3$][PF_6] (**4.2**).

Table III-1. Atomic coordinates (x 10^4) and equivalent isotropic displacement parameters ($Å^2$ x 10^3) for $[(dpdpm)NiBr_3Ag(CH_3CN)]_2$ **(4.1)**.

U_{eq} is defined as one third of the trace of the orthogonalized Uij tensor.

	x	y	z	U_{eq}
Br(1)	3111(1)	1798(1)	-83(1)	36(1)
Br(2)	4089(1)	3219(1)	1621(1)	32(1)
Br(3)	6629(1)	3790(1)	52(1)	36(1)
Ag	4510(1)	3893(1)	379(1)	39(1)
Ni	2701(1)	1536(1)	1072(1)	26(1)
N(1)	3812(3)	-24(4)	1297(2)	36(1)
N(11)	1466(3)	81(3)	861(2)	26(1)
N(12)	405(3)	126(3)	1070(2)	23(1)
N(21)	1359(3)	2853(3)	1052(2)	25(1)
N(22)	318(3)	2502(3)	1244(2)	23(1)
C(1)	4291(3)	-1005(5)	1392(2)	34(1)
C(2)	4913(4)	-2282(5)	1502(3)	45(1)
C(13)	-227(4)	-957(4)	828(2)	30(1)
C(14)	449(4)	-1713(4)	458(2)	34(1)
C(15)	1492(4)	-1030(4)	496(2)	30(1)
C(23)	-426(3)	3545(4)	1146(2)	28(1)
C(24)	133(4)	4591(4)	872(2)	32(1)
C(25)	1244(3)	4121(4)	818(2)	28(1)
C(31)	203(3)	1168(4)	1559(2)	23(1)
C(41)	-1015(3)	1041(4)	1755(2)	24(1)
C(46)	-1965(3)	1098(4)	1275(2)	29(1)
C(45)	-3070(3)	1017(4)	1454(2)	33(1)
C(44)	-3246(3)	865(4)	2104(2)	34(1)
C(43)	-2310(4)	788(5)	2590(2)	32(1)
C(42)	-1203(3)	889(4)	2420(2)	27(1)
C(51)	1133(3)	1037(4)	2148(2)	24(1)
C(52)	1640(3)	-206(4)	2320(2)	29(1)
C(53)	2427(4)	-313(5)	2881(2)	36(1)
C(54)	2672(4)	780(5)	3282(2)	37(1)
C(55)	2168(4)	2017(5)	3122(2)	36(1)
C(56)	1396(3)	2157(4)	2547(2)	29(1)

Table III-2. Hydrogen coordinates (x 10^4) and isotropic displacement parameters ($Å^2$ x 10^3) for $[(dpdpm)NiBr_3Ag(CH_3CN)]_2$ (**4.1**).

	x	y	z	U_{eq}
H(2A)	4372	-3041	1436	68
H(2B)	5298	-2305	1954	68
H(2C)	5486	-2358	1190	68
H(13)	-995	-1155	901	36
H(14)	246	-2530	226	41
H(15)	2136	-1319	288	35
H(23)	-1197	3555	1248	33
H(24)	-173	5456	744	38
H(25)	1830	4625	643	34
H(46)	-1853	1194	823	35
H(45)	-3709	1066	1125	40
H(44)	-4005	813	2223	41
H(43)	-2433	666	3038	39
H(42)	-568	855	2753	32
H(52)	1449	-983	2055	35
H(53)	2797	-1155	2986	43
H(54)	3190	688	3673	44
H(55)	2344	2777	3401	43
H(56)	1057	3012	2433	35

Table III-3. Anisotropic parameters ($Å^2$ x 10^3) for $[(dpdpm)NiBr_3Ag(CH_3CN)]_2$ **(4.1)**.

The anisotropic displacement factor exponent takes the form:

$$-2\pi^2 [h^2 a^{*2} U_{11} + ... + 2 h k a^* b^* U_{12}]$$

	U11	U22	U33	U23	U13	U12
Br(1)	32(1)	45(1)	31(1)	-5(1)	8(1)	-14(1)
Br(2)	23(1)	39(1)	33(1)	-4(1)	1(1)	-3(1)
Br(3)	24(1)	36(1)	48(1)	4(1)	7(1)	3(1)
Ag	29(1)	40(1)	49(1)	3(1)	9(1)	-5(1)
Ni	18(1)	29(1)	30(1)	-1(1)	3(1)	0(1)
N(1)	22(2)	39(2)	46(2)	2(2)	2(1)	4(2)
N(11)	19(1)	29(2)	30(2)	-2(1)	4(1)	1(1)
N(12)	20(1)	22(2)	27(2)	-2(1)	3(1)	-1(1)
N(21)	15(1)	28(2)	31(2)	3(1)	4(1)	-2(1)
N(22)	18(1)	25(2)	27(2)	1(1)	4(1)	0(1)
C(1)	20(2)	41(3)	41(3)	-2(2)	0(2)	-1(2)
C(2)	38(2)	45(3)	50(3)	-3(2)	-2(2)	16(2)
C(13)	27(2)	27(2)	35(2)	-1(2)	2(2)	-8(2)
C(14)	41(2)	22(2)	39(3)	-3(2)	6(2)	-5(2)
C(15)	28(2)	33(2)	27(2)	-3(2)	4(2)	1(2)
C(23)	25(2)	29(2)	30(2)	2(2)	4(2)	4(2)
C(24)	32(2)	24(2)	39(2)	4(2)	3(2)	5(2)
C(25)	29(2)	27(2)	29(2)	4(2)	4(2)	-5(2)
C(31)	19(2)	23(2)	26(2)	-2(1)	3(1)	1(1)
C(41)	18(2)	21(2)	33(2)	1(1)	5(1)	-4(1)
C(46)	24(2)	34(2)	28(2)	1(2)	3(2)	1(2)
C(45)	20(2)	36(2)	42(3)	0(2)	-1(2)	-1(2)
C(44)	20(2)	34(2)	50(3)	2(2)	8(2)	0(2)
C(43)	26(2)	38(2)	35(2)	5(2)	12(2)	-1(2)
C(42)	24(2)	26(2)	32(2)	2(2)	4(2)	0(2)
C(51)	18(2)	28(2)	25(2)	3(1)	2(1)	-1(1)
C(52)	28(2)	26(2)	34(2)	3(2)	5(2)	0(2)
C(53)	26(2)	39(2)	42(3)	14(2)	1(2)	3(2)
C(54)	26(2)	49(3)	33(2)	6(2)	-5(2)	-7(2)
C(55)	29(2)	45(3)	32(2)	-6(2)	-3(2)	-9(2)
C(56)	24(2)	31(2)	31(2)	-1(2)	2(2)	-2(2)

Table III-4. Bond lengths [Å] and angles [°] for $[(dpdpm)NiBr_3Ag(CH_3CN)]_2$ **(4.1)**.

		Ag-Br(3)#1	2.7397(6)
Br(1)-Ni	2.4713(8)	Ag-Ag#1	2.9794(7)
Br(1)-Ag	2.7371(5)	Ni-N(1)	2.033(4)
Br(2)-Ni	2.4975(8)	Ni-N(21)	2.036(3) Ni-
Br(2)-Ag	2.7188(6)	N(11)	2.050(3)
Br(3)-Ag	2.6465(5)	N(1)-C(1)	1.124(6)
Br(3)-Ag#1	2.7397(6)	N(11)-C(15)	1.326(5)

N(11)-N(12)	1.360(4)	N(21)-NI-BR2	92.77(9)
N(12)-C(13)	1.360(5)	N(11)-NI-BR2	165.49(10)
N(12)-C(31)	1.471(5)	BR1-NI-BR2	99.84(3)
N(21)-C(25)	1.338(5)	C(1)-N(1)-NI	169.8(4)
N(21)-N(22)	1.368(4)	C(15)-N(11)-N(12)	106.5(3)
N(22)-C(23)	1.349(5)	C(15)-N(11)-NI	129.4(3)
N(22)-C(31)	1.476(5)	N(12)-N(11)-NI	124.0(2)
C(1)-C(2)	1.460(6)	N(11)-N(12)-C(13)	109.9(3)
C(13)-C(14)	1.374(6)	N(11)-N(12)-C(31)	117.4(3)
C(14)-C(15)	1.391(6)	C(13)-N(12)-C(31)	132.2(3)
C(23)-C(24)	1.375(6)	C(25)-N(21)-N(22)	106.4(3)
C(24)-C(25)	1.398(6)	C(25)-N(21)-NI	130.4(3)
C(31)-C(41)	1.530(5)	N(22)-N(21)-NI	123.0(2)
C(31)-C(51)	1.533(5)	C(23)-N(22)-N(21)	110.3(3)
C(41)-C(46)	1.398(5)	C(23)-N(22)-C(31)	130.8(3)
C(41)-C(42)	1.406(6)	N(21)-N(22)-C(31)	118.7(3)
C(46)-C(45)	1.388(6)	N(1)-C(1)-C(2)	178.9(5)
C(45)-C(44)	1.373(7)	N(12)-C(13)-C(14)	107.5(4)
C(44)-C(43)	1.394(6)	C(13)-C(14)-C(15)	105.4(4)
C(43)-C(42)	1.385(5)	N(11)-C(15)-C(14)	110.7(4)
C(51)-C(56)	1.386(6)	N(22)-C(23)-C(24)	107.5(3)
C(51)-C(52)	1.390(5)	C(23)-C(24)-C(25)	106.0(4)
C(52)-C(53)	1.390(6)	N(21)-C(25)-C(24)	109.8(4)
C(53)-C(54)	1.364(7)	N(12)-C(31)-N(22)	107.2(3)
C(54)-C(55)	1.378(7)	N(12)-C(31)-C(41)	110.3(3)
C(55)-C(56)	1.404(6)	N(22)-C(31)-C(41)	108.8(3)
NI-BR1-AG	85.67(2)	N(12)-C(31)-C(51)	108.5(3)
NI-BR2-AG	85.55(2)	N(22)-C(31)-C(51)	108.9(3)
AG-BR3-AG#1	67.142(15)	C(41)-C(31)-C(51)	112.9(3)
BR3-AG-BR2	120.049(1)	C(46)-C(41)-C(42)	118.7(4)
BR3-AG-BR1	115.312(1)	C(46)-C(41)-C(31)	120.4(4)
BR2-AG-BR1	88.345(16)	C(42)-C(41)-C(31)	120.9(3)
BR3-AG-BR3#1	112.858(1)	C(45)-C(46)-C(41)	120.4(4)
BR2-AG-BR3#1	111.657(1)	C(44)-C(45)-C(46)	120.6(4)
BR1-AG-BR3#1	105.507(1)	C(45)-C(44)-C(43)	120.0(4)
BR3-AG-AG#1	57.923(14)	C(42)-C(43)-C(44)	120.2(4)
BR2-AG-AG#1	141.64(2)	C(43)-C(42)-C(41)	120.2(4)
BR1-AG-AG#1	128.73(2)	C(56)-C(51)-C(52)	119.6(4)
BR3#1-AG-AG#1	54.935(15)	C(56)-C(51)-C(31)	119.0(3)
N(1)-NI-N(21)	163.79(14)	C(52)-C(51)-C(31)	121.2(3)
N(1)-NI-N(11)	86.37(14)	C(53)-C(52)-C(51)	120.0(4)
N(21)-NI-N(11)	85.21(13)	C(54)-C(53)-C(52)	120.6(4)
N(1)-NI-BR1	96.03(11)	C(53)-C(54)-C(55)	120.1(4)
N(21)-NI-BR1	98.44(10)	C(54)-C(55)-C(56)	120.2(4)
N(11)-NI-BR1	94.67(10)	C(51)-C(56)-C(55)	119.5(4)
N(1)-NI-BR2	91.93(11)		

Symmetry transformations used to generate equivalent atoms:

#1 -x+1,-y+1,-z

Table III-5. Torsion angles [°] for [(dpdpm)Ni Br_3 Ag $(CH_3CN)]_2$ (**4.1**).

AG#1-BR3-AG-BR2	-134.95(3)
AG#1-BR3-AG-BR1	121.35(2)
AG#1-BR3-AG-BR3#1	0
NI-BR2-AG-BR3	-124.02(2)
NI-BR2-AG-BR1	-5.50(2)
NI-BR2-AG-BR3#1	100.54(2)
NI-BR2-AG-AG#1	160.91(3)
NI-BR1-AG-BR3	128.28(2)
NI-BR1-AG-BR2	5.56(2)
NI-BR1-AG-BR3#1	-106.47(2)
NI-BR1-AG-AG#1	-163.67(3)
AG-BR1-NI-N(1)	-99.16(11)
AG-BR1-NI-N(21)	88.18(9)
AG-BR1-NI-N(11)	174.01(9)
AG-BR1-NI-BR2	-6.14(2)
AG-BR2-NI-N(1)	102.64(11)
AG-BR2-NI-N(21)	-92.88(9)
AG-BR2-NI-N(11)	-174.4(4)
AG-BR2-NI-BR1	6.18(2)
N(21)-NI-N(1)-C(1)	62(2)
N(11)-NI-N(1)-C(1)	3(2)
BR1-NI-N(1)-C(1)	-91(2)
BR2-NI-N(1)-C(1)	169(2)
N(1)-NI-N(11)-C(15)	-48.3(4)
N(21)-NI-N(11)-C(15)	145.6(4)
BR1-NI-N(11)-C(15)	47.5(4)
BR2-NI-N(11)-C(15)	-131.9(4)
N(1)-NI-N(11)-N(12)	134.0(3)
N(21)-NI-N(11)-N(12)	-32.1(3)
BR1-NI-N(11)-N(12)	-130.2(3)
BR2-NI-N(11)-N(12)	50.4(6)
C(15)-N(11)-N(12)-C(13)	-0.4(4)
NI-N(11)-N(12)-C(13)	177.7(3)
C(15)-N(11)-N(12)-C(31)	172.0(3)
NI-N(11)-N(12)-C(31)	-9.9(4)
N(1)-NI-N(21)-C(25)	159.6(5)
N(11)-NI-N(21)-C(25)	-141.4(4)
BR1-NI-N(21)-C(25)	-47.4(4)
BR2-NI-N(21)-C(25)	53.0(4)
N(1)-NI-N(21)-N(22)	-26.2(7)
N(11)-NI-N(21)-N(22)	32.7(3)
BR1-NI-N(21)-N(22)	126.7(3)
BR2-NI-N(21)-N(22)	-132.9(3)
C(25)-N(21)-N(22)-C(23)	-1.4(4)
NI-N(21)-N(22)-C(23)	-176.8(3)
C(25)-N(21)-N(22)-C(31)	-176.7(3)
NI-N(21)-N(22)-C(31)	8.0(4)
NI-N(1)-C(1)-C(2)	74(26)
N(11)-N(12)-C(13)-C(14)	0.2(5)
C(31)-N(12)-C(13)-C(14)	-170.6(4)
N(12)-C(13)-C(14)-C(15)	0.1(5)
N(12)-N(11)-C(15)-C(14)	0.5(5)
NI-N(11)-C(15)-C(14)	-177.5(3)
C(13)-C(14)-C(15)-N(11)	-0.3(5)
N(21)-N(22)-C(23)-C(24)	1.2(5)
C(31)-N(22)-C(23)-C(24)	175.7(4)
N(22)-C(23)-C(24)-C(25)	-0.6(5)
N(22)-N(21)-C(25)-C(24)	1.0(5)
NI-N(21)-C(25)-C(24)	175.9(3)
C(23)-C(24)-C(25)-N(21)	-0.3(5)
N(11)-N(12)-C(31)-N(22)	63.7(4)
C(13)-N(12)-C(31)-N(22)	-126.0(4)
N(11)-N(12)-C(31)-C(41)	-178.0(3)
C(13)-N(12)-C(31)-C(41)	-7.7(6)
N(11)-N(12)-C(31)-C(51)	-53.8(4)
C(13)-N(12)-C(31)-C(51)	116.6(4)
C(23)-N(22)-C(31)-N(12)	122.7(4)
N(21)-N(22)-C(31)-N(12)	-63.2(4)
C(23)-N(22)-C(31)-C(41)	3.4(5)
N(21)-N(22)-C(31)-C(41)	177.5(3)
C(23)-N(22)-C(31)-C(51)	-120.1(4)
N(21)-N(22)-C(31)-C(51)	54.0(4)
N(12)-C(31)-C(41)-C(46)	-56.5(5)
N(22)-C(31)-C(41)-C(46)	60.8(4)
C(51)-C(31)-C(41)-C(46)	-178.2(3)
N(12)-C(31)-C(41)-C(42)	124.6(4)
N(22)-C(31)-C(41)-C(42)	-118.1(4)
C(51)-C(31)-C(41)-C(42)	3.0(5)
C(42)-C(41)-C(46)-C(45)	0.5(6)
C(31)-C(41)-C(46)-C(45)	-178.4(4)
C(41)-C(46)-C(45)-C(44)	-0.6(6)
C(46)-C(45)-C(44)-C(43)	-0.2(7)
C(45)-C(44)-C(43)-C(42)	1.2(7)
C(44)-C(43)-C(42)-C(41)	-1.3(6)
C(46)-C(41)-C(42)-C(43)	0.5(6)
C(31)-C(41)-C(42)-C(43)	179.4(4)
N(12)-C(31)-C(51)-C(56)	156.3(3)
N(22)-C(31)-C(51)-C(56)	39.9(5)
C(41)-C(31)-C(51)-C(56)	-81.1(4)
N(12)-C(31)-C(51)-C(52)	-29.5(5)
N(22)-C(31)-C(51)-C(52)	-145.8(4)
C(41)-C(31)-C(51)-C(52)	93.2(4)
C(56)-C(51)-C(52)-C(53)	-1.6(6)
C(31)-C(51)-C(52)-C(53)	-175.8(4)
C(51)-C(52)-C(53)-C(54)	2.8(6)
C(52)-C(53)-C(54)-C(55)	-2.2(7)
C(53)-C(54)-C(55)-C(56)	0.4(7)
C(52)-C(51)-C(56)-C(55)	-0.3(6)
C(31)-C(51)-C(56)-C(55)	174.1(4)
C(54)-C(55)-C(56)-C(51)	0.9(6)

Table III-6. Atomic coordinates (x 10^4) and equivalent isotropic displacement parameters ($Å^2$ x 10^3) for for [(dpdpm)NiBr(CH_3CN)$_3$][PF6] (**4.2**).

U_{eq} is defined as one third of the trace of the orthogonalized Uij tensor.

	Occ.	x	y	z	U_{eq}
Br	1	4569(1)	2377(1)	392(1)	18(1)
Ni	1	6739(1)	2575(1)	-172(1)	12(1)
P	1	3222(1)	2407(1)	5309(1)	19(1)
F(1)	1	3199(2)	988(2)	5334(2)	31(1)
F(2)	1	2252(2)	2333(3)	4278(2)	45(1)
F(3)	1	3282(3)	3838(2)	5306(2)	48(1)
F(4)	1	4200(2)	2489(2)	6359(2)	32(1)
F(5)	1	2157(2)	2363(3)	6146(2)	37(1)
F(6)	1	4289(2)	2457(2)	4487(2)	26(1)
N(1)	1	6346(3)	1224(3)	-1340(2)	19(1)
N(2)	1	6352(2)	3764(3)	-1438(2)	18(1)
N(3)	1	8548(3)	2617(3)	-701(2)	17(1)
N(11)	1	7195(2)	1429(2)	1070(2)	14(1)
N(12)	1	7489(2)	1720(2)	2156(2)	14(1)
N(21)	1	7087(2)	3949(2)	957(2)	13(1)
N(22)	1	7423(2)	3850(2)	2058(2)	12(1)
C(1)	1	6123(3)	560(3)	-2043(3)	21(1)
C(2)	1	5850(4)	-305(4)	-2939(3)	33(1)
C(3)	1	6136(3)	4435(3)	-2109(3)	17(1)
C(4)	1	5885(3)	5320(4)	-2952(3)	25(1)
C(5)	1	9438(3)	2409(3)	-1040(3)	20(1)
C(6)	1	10573(4)	2140(4)	-1480(4)	34(1)
C(13)	1	7429(3)	717(3)	2786(3)	18(1)
C(14)	1	7043(3)	-228(3)	2096(3)	21(1)
C(15)	1	6898(3)	264(3)	1040(3)	18(1)
C(23)	1	7299(3)	4887(3)	2599(3)	17(1)
C(24)	1	6815(3)	5656(3)	1842(3)	17(1)
C(25)	1	6695(3)	5032(3)	839(3)	15(1)
C(31)	1	8143(3)	2885(3)	2480(2)	14(1)
C(41)	1	8235(3)	2981(3)	3750(3)	17(1)
C(42)	1	7172(3)	2844(3)	4307(3)	21(1)
C(43)	1	7228(4)	2985(4)	5451(3)	25(1)
C(44)	1	8332(4)	3264(4)	6045(3)	28(1)
C(45)	1	9388(3)	3406(4)	5497(3)	27(1)
C(46)	1	9352(3)	3256(3)	4347(3)	21(1)
C(51)	1	9375(3)	2989(3)	1980(3)	15(1)
C(56)	1	9861(3)	4086(3)	1612(3)	20(1)
C(55)	1	11000(3)	4179(3)	1206(3)	24(1)
C(54)	1	11654(3)	3190(4)	1172(3)	26(1)
C(53)	1	11173(3)	2102(4)	1539(3)	23(1)
C(52)	1	10030(3)	1998(3)	1942(3)	20(1)
C(9)	0.50	86(18)	10086(17)	5104(17)	44(2)
C(10)	0.50	581(9)	9788(9)	4081(10)	44(2)
N(4)	0.50	988(9)	9571(8)	3281(9)	50(2)

Table III-7. Hydrogen coordinates (x 10^4) and isotropic displacement parameters ($Å^2$ x 10^3) for [(dpdpm)NiBr(CH_3CN)$_3$][PF6] (**4.2**).

	Occ.	x	y	z	U_{eq}
H(2A)	1	6601	-468	-3267	49
H(2B)	1	5293	12	-3508	49
H(2C)	1	5472	-1043	-2648	49
H(4A)	1	5580	6011	-2604	37
H(4B)	1	5274	4974	-3514	37
H(4C)	1	6631	5570	-3303	37
H(6A)	1	10472	2112	-2292	50
H(6B)	1	10798	1369	-1202	50
H(6C)	1	11212	2760	-1241	50
H(13)	1	7620	681	3563	22
H(14)	1	6903	-1039	2292	26
H(15)	1	6624	-178	386	21
H(23)	1	7509	5051	3364	20
H(24)	1	6608	6441	1974	20
H(25)	1	6375	5336	158	18
H(42)	1	6413	2656	3903	25
H(43)	1	6506	2890	5829	30
H(44)	1	8366	3359	6828	34
H(45)	1	10141	3606	5907	32
H(46)	1	10077	3339	3974	26
H(52)	1	9414	4765	1641	23
H(55)	1	11332	4923	951	29
H(54)	1	12436	3257	896	31
H(53)	1	11626	1426	1514	28
H(52)	1	9698	1251	2191	24
H(9A)	0.50	-600	10566	4945	66
H(9B)	0.50	711	10540	5585	66
H(9C)	0.50	-190	9355	5477	66

Table III-8. Anisotropic parameters ($Å^2$ x 10^3) for [(dpdpm)NiBr(CH_3CN)$_3$][PF6] (**4.2**).

The anisotropic displacement factor exponent takes the form:

$$-2\pi^2 [h^2 a^{*2} U_{11} + \ldots + 2 h k a^* b^* U_{12}]$$

	U11	U22	U33	U23	U13	U12
Br	14(1)	17(1)	22(1)	0(1)	5(1)	2(1)
Ni	14(1)	14(1)	9(1)	0(1)	3(1)	2(1)
P	24(1)	22(1)	11(1)	2(1)	8(1)	5(1)
F(1)	50(1)	23(1)	21(1)	2(1)	12(1)	-2(1)
F(2)	32(1)	84(2)	20(1)	11(1)	-1(1)	14(1)
F(3)	100(2)	24(1)	27(1)	4(1)	32(1)	18(1)
F(4)	30(1)	48(2)	17(1)	-4(1)	3(1)	-5(1)
F(5)	31(1)	59(2)	25(1)	10(1)	16(1)	15(1)
F(6)	33(1)	27(1)	19(1)	-3(1)	15(1)	-3(1)
N(1)	20(1)	21(2)	17(1)	-3(1)	3(1)	3(1)
N(2)	16(1)	22(2)	14(1)	0(1)	3(1)	1(1)
N(3)	19(1)	22(2)	11(1)	2(1)	4(1)	2(1)
N(11)	16(1)	15(1)	11(1)	-2(1)	2(1)	3(1)
N(12)	14(1)	16(1)	12(1)	1(1)	3(1)	3(1)
N(21)	14(1)	16(1)	10(1)	1(1)	3(1)	2(1)
N(22)	12(1)	16(1)	9(1)	-1(1)	2(1)	2(1)
C(1)	22(2)	24(2)	17(2)	-2(1)	6(1)	3(1)
C(2)	38(2)	36(2)	25(2)	-15(2)	4(2)	0(2)
C(3)	17(2)	20(2)	14(2)	-2(1)	4(1)	2(1)
C(4)	29(2)	28(2)	17(2)	11(1)	2(1)	2(2)
C(5)	20(2)	25(2)	17(2)	1(1)	4(1)	2(1)
C(6)	24(2)	45(3)	35(2)	-7(2)	13(2)	10(2)
C(13)	20(2)	20(2)	16(2)	6(1)	3(1)	2(1)
C(14)	26(2)	18(2)	22(2)	5(1)	4(1)	3(1)
C(15)	20(2)	17(2)	17(2)	1(1)	3(1)	3(1)
C(23)	14(1)	22(2)	14(2)	-5(1)	4(1)	1(1)
C(24)	15(2)	15(2)	21(2)	-4(1)	5(1)	2(1)
C(25)	16(1)	15(2)	15(2)	0(1)	4(1)	1(1)
C(31)	15(1)	17(2)	11(1)	1(1)	3(1)	3(1)
C(41)	20(2)	19(2)	13(2)	1(1)	2(1)	3(1)
C(42)	21(2)	27(2)	15(2)	0(1)	3(1)	4(1)
C(43)	29(2)	33(2)	16(2)	0(1)	8(1)	7(2)
C(44)	34(2)	39(2)	13(2)	-1(1)	4(1)	9(2)
C(45)	25(2)	37(2)	17(2)	-2(1)	-5(1)	5(2)
C(46)	21(2)	26(2)	17(2)	0(1)	0(1)	5(1)
C(51)	15(2)	19(2)	11(1)	0(1)	1(1)	3(1)
C(56)	17(2)	22(2)	21(2)	1(1)	5(1)	2(1)
C(55)	19(2)	27(2)	27(2)	-2(1)	8(1)	-2(1)
C(54)	15(2)	37(2)	28(2)	2(2)	9(1)	4(2)
C(53)	17(2)	30(2)	25(2)	2(1)	6(1)	12(1)
C(52)	17(2)	23(2)	23(2)	5(1)	5(1)	6(1)
C(9)	35(4)	32(4)	60(6)	6(4)	-20(3)	-8(3)
C(10)	35(4)	32(4)	60(6)	6(4)	-20(3)	-8(3)
N(4)	51(5)	33(4)	63(6)	8(4)	-10(5)	-1(4)

Table III-9. Bond lengths [Å] and angles [°] for [(dpdpm)NiBr(CH_3CN)$_3$][PF6] (4.2).

Br-Ni	2.5458(6)	N(21)-NI-N(3)	96.04(11)
Ni-N(11)	2.050(3)	N(1)-NI-N(3)	84.89(11)
Ni-N(21)	2.055(3)	N(2)-NI-N(3)	87.90(11)
Ni-N(1)	2.070(3)	N(11)-NI-BR	89.04(8)
Ni-N(2)	2.085(3)	N(21)-NI-BR	87.87(7)
Ni-N(3)	2.151(3)	N(1)-NI-BR	91.24(8)
P-F(2)	1.583(2)	N(2)-NI-BR	93.24(8)
P-F(6)	1.600(2)	N(3)-NI-BR	175.92(8)
P-F(1)	1.601(2)	F(2)-P-F(6)	90.03(13)
P-F(4)	1.607(2)	F(2)-P-F(1)	90.71(15)
P-F(3)	1.610(3)	F(6)-P-F(1)	90.05(12)
P-F(5)	1.610(2)	F(2)-P-F(4)	179.58(16)
N(1)-C(1)	1.130(5)	F(6)-P-F(4)	90.29(12)
N(2)-C(3)	1.138(5)	F(1)-P-F(4)	89.57(13)
N(3)-C(5)	1.139(5)	F(2)-P-F(3)	90.93(17)
N(11)-C(15)	1.328(4)	F(6)-P-F(3)	89.44(13)
N(11)-N(12)	1.362(4)	F(1)-P-F(3)	178.28(17)
N(12)-C(13)	1.367(4)	F(4)-P-F(3)	88.79(16)
N(12)-C(31)	1.483(4)	F(2)-P-F(5)	90.54(14)
N(21)-C(25)	1.335(4)	F(6)-P-F(5)	179.40(14)
N(21)-N(22)	1.363(4)	F(1)-P-F(5)	90.13(14)
N(22)-C(23)	1.360(4)	F(4)-P-F(5)	89.14(13)
N(22)-C(31)	1.476(4)	F(3)-P-F(5)	90.37(15)
C(1)-C(2)	1.453(5)	C(1)-N(1)-NI	174.2(3)
C(3)-C(4)	1.459(5)	C(3)-N(2)-NI	178.2(3)
C(5)-C(6)	1.458(5)	C(5)-N(3)-NI	166.3(3)
C(13)-C(14)	1.370(5)	C(15)-N(11)-N(12)	106.1(3)
C(14)-C(15)	1.398(5)	C(15)-N(11)-NI	124.6(2)
C(23)-C(24)	1.376(5)	N(12)-N(11)-NI	126.4(2)
C(24)-C(25)	1.391(4)	N(11)-N(12)-C(13)	109.9(3)
C(31)-C(51)	1.533(4)	N(11)-N(12)-C(31)	120.9(3)
C(31)-C(41)	1.535(4)	C(13)-N(12)-C(31)	126.5(3)
C(41)-C(46)	1.399(5)	C(25)-N(21)-N(22)	105.7(3)
C(41)-C(42)	1.400(5)	C(25)-N(21)-NI	125.4(2)
C(42)-C(43)	1.388(5)	N(22)-N(21)-NI	126.3(2)
C(43)-C(44)	1.386(6)	C(23)-N(22)-N(21)	110.2(3)
C(44)-C(45)	1.387(6)	C(23)-N(22)-C(31)	125.8(3)
C(45)-C(46)	1.397(5)	N(21)-N(22)-C(31)	121.6(3)
C(51)-C(52)	1.387(5)	N(1)-C(1)-C(2)	179.1(4)
C(51)-C(56)	1.396(5)	N(2)-C(3)-C(4)	178.3(4)
C(56)-C(55)	1.387(5)	N(3)-C(5)-C(6)	179.6(4)
C(55)-C(54)	1.384(6)	N(12)-C(13)-C(14)	107.8(3)
C(54)-C(53)	1.385(6)	C(13)-C(14)-C(15)	104.9(3)
C(53)-C(52)	1.391(5)	N(11)-C(15)-C(14)	111.2(3)
C(9)-C(10)	1.44(3)	N(22)-C(23)-C(24)	107.8(3)
C(10)-N(4)	1.132(15)	C(23)-C(24)-C(25)	104.9(3)
N(11)-NI-N(21)	88.35(11)	N(21)-C(25)-C(24)	111.3(3)
N(11)-NI-N(1)	93.40(11)	N(22)-C(31)-N(12)	109.4(2)
N(21)-NI-N(1)	178.02(11)	N(22)-C(31)-C(51)	109.5(3)
N(11)-NI-N(2)	177.59(11)	N(12)-C(31)-C(51)	109.3(3)
N(21)-NI-N(2)	90.96(11)	N(22)-C(31)-C(41)	107.0(3)
N(1)-NI-N(2)	87.32(12)	N(12)-C(31)-C(41)	108.0(2)
N(11)-NI-N(3)	89.88(11)	C(51)-C(31)-C(41)	113.6(3)
		C(46)-C(41)-C(42)	120.0(3)
		C(46)-C(41)-C(31)	121.0(3)

C(42)-C(41)-C(31)	118.9(3)	C(55)-C(56)-C(51)	119.7(3)
C(43)-C(42)-C(41)	119.9(3)	C(54)-C(55)-C(56)	120.1(4)
C(44)-C(43)-C(42)	120.3(3)	C(55)-C(54)-C(53)	120.2(3)
C(43)-C(44)-C(45)	120.1(3)	C(54)-C(53)-C(52)	120.1(3)
C(44)-C(45)-C(46)	120.5(3)	C(51)-C(52)-C(53)	119.7(3)
C(45)-C(46)-C(41)	119.2(3)	N(4)-C(10)-C(9)	178.60(12)
C(52)-C(51)-C(56)	120.1(3)		
C(52)-C(51)-C(31)	119.5(3)		
C(56)-C(51)-C(31)	120.3(3)		

Symmetry transformations used to generate equivalent atoms:

Table III-10. Torsion angles [°] for [(dpdpm)NiBr(CH_3CN)$_3$][PF6] (**4.2**).

N(11)-NI-N(1)-C(1)	-171(3)	N(22)-N(21)-C(25)-C(24)	2.3(4)
N(21)-NI-N(1)-C(1)	36(5)	NI-N(21)-C(25)-C(24)	164.9(2)
N(2)-NI-N(1)-C(1)	6(3)	C(23)-C(24)-C(25)-N(21)	-0.5(4)
N(3)-NI-N(1)-C(1)	-82(3)	C(23)-N(22)-C(31)-N(12)	141.6(3)
BR-NI-N(1)-C(1)	100(3)	N(21)-N(22)-C(31)-N(12)	-57.6(3)
N(11)-NI-N(2)-C(3)	-94(9)	C(23)-N(22)-C(31)-C(51)	-98.7(3)
N(21)-NI-N(2)-C(3)	-20(9)	N(21)-N(22)-C(31)-C(51)	62.2(3)
N(1)-NI-N(2)-C(3)	159(9)	C(23)-N(22)-C(31)-C(41)	24.8(4)
N(3)-NI-N(2)-C(3)	-116(9)	N(21)-N(22)-C(31)-C(41)	-174.3(3)
BR-NI-N(2)-C(3)	68(9)	N(11)-N(12)-C(31)-N(22)	58.9(3)
N(11)-NI-N(3)-C(5)	68.10(11)	C(13)-N(12)-C(31)-N(22)	-141.9(3)
N(21)-NI-N(3)-C(5)	156.50(11)	N(11)-N(12)-C(31)-C(51)	-61.0(3)
N(1)-NI-N(3)-C(5)	-25.30(11)	C(13)-N(12)-C(31)-C(51)	98.2(3)
N(2)-NI-N(3)-C(5)	-112.80(11)	N(11)-N(12)-C(31)-C(41)	175.0(3)
BR-NI-N(3)-C(5)	-7(2)	C(13)-N(12)-C(31)-C(41)	-25.8(4)
N(21)-NI-N(11)-C(15)	161.8(3)	N(22)-C(31)-C(41)-C(46)	-115.1(3)
N(1)-NI-N(11)-C(15)	-17.3(3)	N(12)-C(31)-C(41)-C(46)	127.3(3)
N(2)-NI-N(11)-C(15)	-125(3)	C(51)-C(31)-C(41)-C(46)	5.9(4)
N(3)-NI-N(11)-C(15)	-102.2(3)	N(22)-C(31)-C(41)-C(42)	61.9(4)
BR-NI-N(11)-C(15)	73.9(3)	N(12)-C(31)-C(41)-C(42)	-55.8(4)
N(21)-NI-N(11)-N(12)	3.8(2)	C(51)-C(31)-C(41)-C(42)	-177.1(3)
N(1)-NI-N(11)-N(12)	-175.2(2)	C(46)-C(41)-C(42)-C(43)	0.2(5)
N(2)-NI-N(11)-N(12)	77(3)	C(31)-C(41)-C(42)-C(43)	-176.8(3)
N(3)-NI-N(11)-N(12)	99.9(3)	C(41)-C(42)-C(43)-C(44)	0.2(6)
BR-NI-N(11)-N(12)	-84.0(2)	C(42)-C(43)-C(44)-C(45)	0.1(6)
C(15)-N(11)-N(12)-C(13)	2.9(3)	C(43)-C(44)-C(45)-C(46)	-0.7(6)
NI-N(11)-N(12)-C(13)	164.2(2)	C(44)-C(45)-C(46)-C(41)	1.1(6)
C(15)-N(11)-N(12)-C(31)	165.3(3)	C(42)-C(41)-C(46)-C(45)	-0.8(5)
NI-N(11)-N(12)-C(31)	-33.5(4)	C(31)-C(41)-C(46)-C(45)	176.1(3)
N(11)-NI-N(21)-C(25)	-161.4(3)	N(22)-C(31)-C(51)-C(52)	-158.3(3)
N(1)-NI-N(21)-C(25)	-9(3)	N(12)-C(31)-C(51)-C(52)	-38.5(4)
N(2)-NI-N(21)-C(25)	20.9(3)	C(41)-C(31)-C(51)-C(52)	82.1(4)
N(3)-NI-N(21)-C(25)	108.9(3)	N(22)-C(31)-C(51)-C(56)	24.7(4)
BR-NI-N(21)-C(25)	-72.3(3)	N(12)-C(31)-C(51)-C(56)	144.5(3)
N(11)-NI-N(21)-N(22)	-2.4(2)	C(41)-C(31)-C(51)-C(56)	-94.8(4)
N(1)-NI-N(21)-N(22)	150(3)	C(52)-C(51)-C(56)-C(55)	0.2(5)
N(2)-NI-N(21)-N(22)	179.9(2)	C(31)-C(51)-C(56)-C(55)	177.2(3)
N(3)-NI-N(21)-N(22)	-92.1(2)	C(51)-C(56)-C(55)-C(54)	-0.4(5)
BR-NI-N(21)-N(22)	86.7(2)	C(56)-C(55)-C(54)-C(53)	0.3(6)
C(25)-N(21)-N(22)-C(23)	-3.3(3)	C(55)-C(54)-C(53)-C(52)	0.1(6)
NI-N(21)-N(22)-C(23)	-165.6(2)	C(56)-C(51)-C(52)-C(53)	0.1(5)
C(25)-N(21)-N(22)-C(31)	-166.8(3)	C(31)-C(51)-C(52)-C(53)	-176.9(3)
NI-N(21)-N(22)-C(31)	30.8(4)	C(54)-C(53)-C(52)-C(51)	-0.3(5)
NI-N(1)-C(1)-C(2)	142(28)		
NI-N(2)-C(3)-C(4)	52(19)		
NI-N(3)-C(5)-C(6)	60(73)		
N(11)-N(12)-C(13)-C(14)	-2.4(4)		
C(31)-N(12)-C(13)-C(14)	-163.5(3)		
N(12)-C(13)-C(14)-C(15)	0.8(4)		
N(12)-N(11)-C(15)-C(14)	-2.4(4)		
NI-N(11)-C(15)-C(14)	-164.1(2)		
C(13)-C(14)-C(15)-N(11)	1.0(4)		
N(21)-N(22)-C(23)-C(24)	3.0(3)		
C(31)-N(22)-C(23)-C(24)	165.7(3)		
N(22)-C(23)-C(24)-C(25)	-1.5(3)		

Chapter 4

Divers results of several studies

Supplementary material

Table IV-1 Crystal data and structure refinement for $[(dpdpm)Ni(\mu\text{-}Cl)Cl]_2$ (**5.6**)

Table IV-2 Atomic coordinates (x 10^4) and equivalent isotropic displacement parameters ($Å^2 \times 10^3$) for $[(dpdpm)Ni(\mu\text{-}Cl)Cl]_2$ (**5.6**)

Table IV-3 Hydrogen coordinates ($\times 10^4$) and isotropic displacement parameters ($Å^2 \times 10^3$) for $[(dpdpm)Ni(\mu\text{-}Cl)Cl]_2$ (**5.6**)

Table IV-4 Anisotropic displacement parameters ($Å^2 \times 10^3$) for $[(dpdpm)Ni(\mu\text{-}Cl)Cl]_2$ (**5.6**)

Table IV-5 Bond length [Å] and angles [°] for $[(dpdpm)Ni(\mu\text{-}Cl)Cl]_2$ (**5.6**)

Table IV-6 Torsion angles [°] for $[(dpdpm)Ni(\mu\text{-}Cl)Cl]_2$ (**5.6**)

Table IV-7 Crystal data and structure refinement for $[(dpdpm)NiCl(H_2O)_2]Cl$ (**5.7**).

Table IV-8 Atomic coordinates (x 10^4) and equivalent isotropic displacement parameters ($Å^2 \times 10^3$) for $[(dpdpm)NiCl(H_2O)_2]Cl$ (**5.7**).

Table IV-9 Hydrogen coordinates ($\times 10^4$) and isotropic displacement parameters ($Å^2 \times 10^3$) for $[(dpdpm)NiCl(H_2O)_2]Cl$ (**5.7**).

Table IV-10 Anisotropic parameters ($Å^2$ x 10^3) for $[(dpdpm)NiCl(H_2O)_2]Cl$ (**5.7**).

Table IV-11 Bond length [Å] and angles [°] for $[(dpdpm)NiCl(H_2O)_2]Cl$ (**5.7**).

Table IV-12 Torsion angles [°] for $[(dpdpm)NiCl(H_2O)_2]Cl$ (**5.7**).

Table IV-13 Bond lengths [Å] and angles [°] related to the hydrogen bonding for $[(dpdpm)NiCl(H_2O)_2]Cl$ (**5.7**).

Table IV-14 Crystal data and structure refinement for $[(dpdpm)_3Ni][I_3]_2$ (**5.8**)

Table IV-15. Atomic coordinates ($\times 10^4$) and equivalent isotropic displacement parameters ($Å^2$ x 10^3) for $[(dpdpm)_3Ni][I_3]_2$ (**5.8**)

Table IV-16. Hydrogen coordinates (× 10^4) and isotropic displacement parameters (Å^2 x 10^3) for $[(dpdpm)_3Ni][I_3]_2$ (**5.8**).

Table IV-17 Anisotropic parameters (Å^2 x 10^3) for $[(dpdpm)_3Ni][I_3]_2$ (**5.8**)

Table IV-18 Bond lengths [Å] and angles [deg.] for $[(dpdpm)_3Ni][I_3]_2$ (**5.8**)

Table IV-19 Torsion angles [°]for $[(dpdpm)_3Ni][I_3]_2$ (**5.8**)

Table IV-20 Crystal data and structure refinement for and $[(Pz)_6Ni][I]_2$ (**5.9**).

Table IV-21 Atomic coordinates (x 10^4) and equivalent isotropic displacement parameters (Å^2 x 10^3) for and $[(Pz)_6Ni][I]_2$ (**5.9**).

Table IV-22. Hydrogen coordinates (x 10^4) and isotropic displacement parameters (Å^2 x 10^3) for and $[(Pz)_6Ni][I]_2$ (**5.9**).

Table IV-23 Anisotropic parameters (Å^2 x 10^3) for $[(Pz)_6Ni][I]_2$ (**5.9**).

Table IV-24 Bond lengths [Å] and angles [°] for $[(Pz)_6Ni][I]_2$ (**5.9**).

Table IV-25 Torsion angles [°] for $[(Pz)_6Ni][I]_2$ (**5.9**).

Table IV-26 Crystal data and structure refinement for $[(Pz^{Me2})_2NiCl_2(H_2O)_2]$ (**5.10b**).

Table IV-27 Atomic coordinates (x 10^4) and equivalent isotropic displacement parameters (Å^2 x 10^3) for $[(Pz^{Me2})_2NiCl_2(H_2O)_2]$ (**5.10b**).

Table IV-28. Hydrogen coordinates (x 10^4) and isotropic displacement parameters (Å^2 x 10^3) for $[(Pz^{Me2})_2NiCl_2(H_2O)_2]$ (**5.10b**).

Table IV-29 Anisotropic parameters (Å^2 x 10^3) for $[(Pz^{Me2})_2NiCl_2(H_2O)_2]$ (**5.10b**).

Table IV-30 Bond lengths [Å] and angles [°] for $[(Pz^{Me2})_2NiCl_2(H_2O)_2]$ (**5.10b**).

Table IV-31 Torsion angles [°] for $[(Pz^{Me2})_2NiCl_2(H_2O)_2]$ (**5.10b**).

Table IV-32. Bond lengths [Å] and angles [°] related to the hydrogen bonding for $[(Pz^{Me2})_2NiCl_2(H_2O)_2]$ (**5.10b**).

Table IV-33 Crystal data and structure refinement for $[(Pz^{Me2})_2NiBr_2]$ (**5.11**).

Table IV-34 Atomic coordinates (x 10^4) and equivalent isotropic displacement parameters (Å^2 x 10^3) for $[(Pz^{Me2})_2NiBr_2]$ (**5.11**).

Table IV-35. Hydrogen coordinates (x 10^4) and isotropic displacement parameters (Å^2 x 10^3) for $[(Pz^{Me2})_2NiBr_2]$ (**5.11**).

Table IV-36 Anisotropic parameters (Å^2 x 10^3) for $[(Pz^{Me2})_2NiBr_2]$ (**5.11**).

Table IV-37 Bond lengths [Å] and angles [°] for $[(Pz^{Me2})_2NiBr_2]$ (**5.11**).

Table IV-38 Torsion angles [°] for $[(Pz^{Me2})_2NiBr_2]$ (**5.11**).

Table IV-39 Crystal data and structure refinement for $[(Pz^{Me2})_2PdCl_2]$ (**5.12**).

Table IV-40 Atomic coordinates (x 10^4) and equivalent isotropic displacement parameters ($Å^2$ x 10^3) for $[(Pz^{Me2})_2PdCl_2]$ (**5.12**).

Table IV-41 Hydrogen coordinates (x 10^4) and isotropic displacement parameters ($Å^2$ x 10^3) for $[(Pz^{Me2})_2PdCl_2]$ (**5.12**).

Table IV-42 Anisotropic parameters ($Å^2$ x 10^3) for $[(Pz^{Me2})_2PdCl_2]$ (**5.12**).

Table IV-43 Bond lengths [Å] and angles [°] for $[(Pz^{Me2})_2PdCl_2]$ (**5.12**).

Table IV-44. Torsion angles [°] for $[(Pz^{Me2})_2PdCl_2]$ (**5.12**).

Table IV-45. Bond lengths [Å] and angles [°] related to the hydrogen bonding for $[(Pz^{Me2})_2PdCl_2]$ (**5.12**).

Table IV-46 Crystal data and structure refinement for (dpdpm)$CuBr_2$ (**5.13**).

Table IV-47 Atomic coordinates (x 10^4) and equivalent isotropic displacement parameters ($Å^2$ x 10^3) for (dpdpm)$CuBr_2$ (**5.13**).

Table IV-48. Hydrogen coordinates (x 10^4) and isotropic displacement parameters ($Å^2$ x 10^3) for (dpdpm)$CuBr_2$ (**5.13**).

Table IV-49 Anisotropic parameters ($Å^2$ x 10^3) for (dpdpm)$CuBr_2$ (**5.13**).

Table IV-50 Bond lengths [Å] and angles [°] for (dpdpm)$CuBr_2$ (**5.13**).

Table IV-51 Torsion angles [°] for (dpdpm)$CuBr_2$ (**5.13**).

Table IV-52 Crystal data and structure refinement for $[(dpdpm)_2Ni(CH_3CN)_2][(FeBr_3)_2O]$ (**5.14**).

Table IV-53 Atomic coordinates (x 10^4) and equivalent isotropic displacement parameters ($Å^2$ x 10^3) for $[(dpdpm)_2Ni(CH_3CN)_2][(FeBr_3)_2O]$ (**5.14**).

Table IV-54. Hydrogen coordinates (x 10^4) and isotropic displacement parameters ($Å^2$ x 10^3) for $[(dpdpm)_2Ni(CH_3CN)_2][(FeBr_3)_2O]$ (**5.14**).

Table IV-55 Anisotropic parameters ($Å^2$ x 10^3) for $[(dpdpm)_2Ni(CH_3CN)_2][(FeBr_3)_2O]$ (**5.14**).

Table IV-56 Bond lengths [Å] and angles [°] for $[(dpdpm)_2Ni(CH_3CN)_2][(FeBr_3)_2O]$ (**5.14**).

Table IV-1. Crystal data and structure refinement for $[(dpdpm)Ni(\mu\text{-}Cl)Cl]_2$ (**5.6**).

Identification code	natha6
Empirical formula	C38 H32 Cl4 N8 Ni2
Formula weight	859.94
Temperature	100(2)K
Wavelength	1.54178 Å
Crystal system	Triclinic
Space group	P-1
Unit cell dimensions	a = 8.87110(10) Å α = 84.3600(10)° b = 9.0951(2) Å β = 80.8950(10)° c = 11.4915(2) Å γ = 84.4220(10)°
Volume	907.91(3)Å^3
Z	1
Density (calculated)	1.573 g/cm^3
Absorption coefficient	4.329 mm^{-1}
F(000)	440
Crystal size	0.18 x 0.11 x 0.06 mm
Theta range for data collection	3.91 to 72.91°
Index ranges	$-10 \le h \le 10$, $-11 \le k \le 11$, $-13 \le \ell \le 14$
Reflections collected	22124
Independent reflections	3453 [R_{int} = 0.024]
Absorption correction	Semi-empirical from equivalents
Max. and min. transmission	0.7100 and 0.5200
Refinement method	Full-matrix least-squares on F^2
Data / restraints / parameters	3453 / 0 / 235
Goodness-of-fit on F^2	1.072
Final R indices [I>2sigma(I)]	R_1 = 0.0312, wR_2 = 0.0865
R indices (all data)	R_1 = 0.0359, wR_2 = 0.0884
Largest diff. peak and hole	0.387 and -0.305 e/Å^3

Table IV-2. Atomic coordinates (x 10^4) and equivalent isotropic displacement parameters ($Å^2$ x 10^3) for $[(dpdpm)Ni(\mu\text{-}Cl)Cl]_2$ (**5.6**).

U_{eq} is defined as one third of the trace of the orthogonalized Uij tensor.

	x	y	z	U_{eq}
Ni	3982(1)	4834(1)	6424(1)	13(1)
Cl(1)	5043(1)	2707(1)	7339(1)	16(1)
Cl(2)	3869(1)	3982(1)	4531(1)	17(1)
N(11)	3817(2)	5982(2)	7899(1)	14(1)
N(12)	2517(2)	6683(2)	8457(1)	13(1)
N(21)	1670(2)	4670(2)	6897(1)	14(1)
N(22)	693(2)	5692(2)	7490(1)	13(1)
C(13)	2794(2)	7228(2)	9460(2)	17(1)
C(14)	4298(2)	6824(2)	9569(2)	19(1)
C(15)	4879(2)	6050(2)	8578(2)	18(1)
C(23)	-779(2)	5369(2)	7529(2)	19(1)
C(24)	-756(2)	4083(2)	7003(2)	22(1)
C(25)	796(2)	3686(2)	6619(2)	17(1)
C(31)	1218(2)	7084(2)	7793(2)	14(1)
C(41)	-128(2)	7839(2)	8587(2)	14(1)
C(42)	-928(2)	9115(2)	8152(2)	17(1)
C(43)	-2244(2)	9724(2)	8825(2)	20(1)
C(44)	-2749(2)	9075(2)	9943(2)	20(1)
C(45)	-1941(2)	7802(2)	10390(2)	20(1)
C(46)	-654(2)	7184(2)	9706(2)	18(1)
C(51)	1785(2)	8053(2)	6676(2)	14(1)
C(52)	2687(2)	9201(2)	6769(2)	17(1)
C(53)	3145(2)	10154(2)	5790(2)	19(1)
C(54)	2712(2)	9970(2)	4709(2)	20(1)
C(55)	1828(3)	8829(2)	4612(2)	21(1)
C(56)	1358(2)	7868(2)	5593(2)	17(1)

Table IV-3. Hydrogen coordinates (x 10^4) and isotropic displacement parameters ($Å^2$ x 10^3) for $[(dpdpm)Ni(\mu\text{-}Cl)Cl]_2$ (**5.6**).

	x	y	z	U_{eq}
H(13)	2077	7785	9986	21
H(14)	4830	7026	10183	23
H(15)	5905	5627	8413	22
H(23)	-1668	5939	7864	23
H(24)	-1608	3568	6917	27
H(25)	1173	2831	6215	21
H(42)	-574	9573	7392	20
H(43)	-2796	10584	8518	24
H(44)	-3641	9494	10405	24

H(45)	-2275	7362	11161	24
H(46)	-124	6304	10003	21
H(52)	2987	9328	7508	21
H(53)	3755	10935	5858	23
H(54)	3022	10625	4036	24
H(55)	1539	8701	3870	26
H(56)	747	7090	5520	20

Table IV-4. Anisotropic parameters ($Å^2 \times 10^3$) for $[(dpdpm)Ni(\mu\text{-}Cl)Cl]_2$ **(5.6)**.

The anisotropic displacement factor exponent takes the form:

$$-2\pi^2 [h^2 a^{*2} U_{11} + \ldots + 2 h k a^* b^* U_{12}]$$

	U11	U22	U33	U23	U13	U12
Ni	12(1)	13(1)	12(1)	-2(1)	0(1)	-1(1)
Cl(1)	17(1)	15(1)	15(1)	-2(1)	-1(1)	3(1)
Cl(2)	17(1)	20(1)	13(1)	-3(1)	1(1)	-7(1)
N(11)	13(1)	15(1)	15(1)	-5(1)	-1(1)	1(1)
N(12)	12(1)	13(1)	13(1)	-3(1)	-1(1)	1(1)
N(21)	12(1)	13(1)	15(1)	-4(1)	-1(1)	2(1)
N(22)	13(1)	11(1)	14(1)	-4(1)	0(1)	0(1)
C(13)	22(1)	16(1)	15(1)	-5(1)	-2(1)	0(1)
C(14)	22(1)	20(1)	19(1)	-5(1)	-8(1)	-3(1)
C(15)	16(1)	20(1)	20(1)	-3(1)	-4(1)	-1(1)
C(23)	12(1)	19(1)	27(1)	-7(1)	0(1)	-1(1)
C(24)	15(1)	21(1)	31(1)	-9(1)	-1(1)	-4(1)
C(25)	17(1)	14(1)	22(1)	-6(1)	-1(1)	-1(1)
C(31)	14(1)	12(1)	15(1)	-3(1)	-2(1)	0(1)
C(41)	14(1)	14(1)	16(1)	-7(1)	-1(1)	0(1)
C(42)	19(1)	15(1)	16(1)	-2(1)	-3(1)	1(1)
C(43)	21(1)	15(1)	23(1)	-5(1)	-5(1)	5(1)
C(44)	17(1)	19(1)	25(1)	-9(1)	2(1)	1(1)
C(45)	20(1)	20(1)	19(1)	-1(1)	3(1)	-2(1)
C(46)	20(1)	13(1)	19(1)	-1(1)	-1(1)	0(1)
C(51)	13(1)	13(1)	14(1)	-2(1)	0(1)	2(1)
C(52)	18(1)	17(1)	18(1)	-3(1)	-4(1)	-1(1)
C(53)	17(1)	15(1)	25(1)	-2(1)	1(1)	-3(1)
C(54)	24(1)	16(1)	16(1)	1(1)	4(1)	2(1)
C(55)	31(1)	18(1)	14(1)	-3(1)	-4(1)	1(1)
C(56)	21(1)	13(1)	17(1)	-4(1)	-4(1)	-1(1)

Table IV-5. Bond lengths [Å] and angles [°] for [(dpdpm)Ni(μ-Cl)Cl]$_2$ (**5.6**).

Ni-N(21)	2.0530(16)	NI#1-CL2-NI	94.299(18)
Ni-N(11)	2.0560(16)	C(15)-N(11)-N(12)	105.79(16)
Ni-Cl(1)	2.2999(5)	C(15)-N(11)-NI	127.80(14)
Ni-Cl(2)#1	2.3456(5)	N(12)-N(11)-NI	125.97(12)
Ni-Cl(2)	2.3989(5)	N(11)-N(12)-C(13)	110.47(15)
Cl(2)-Ni#1	2.3456(5)	N(11)-N(12)-C(31)	118.45(15)
N(11)-C(15)	1.324(3)	C(13)-N(12)-C(31)	128.83(16)
N(11)-N(12)	1.360(2)	C(25)-N(21)-N(22)	105.98(15)
N(12)-C(13)	1.363(2)	C(25)-N(21)-NI	129.35(14)
N(12)-C(31)	1.479(2)	N(22)-N(21)-NI	124.39(12)
N(21)-C(25)	1.332(2)	C(23)-N(22)-N(21)	110.04(16)
N(21)-N(22)	1.364(2)	C(23)-N(22)-C(31)	126.97(16)
N(22)-C(23)	1.358(2)	N(21)-N(22)-C(31)	121.82(15)
N(22)-C(31)	1.481(2)	N(12)-C(13)-C(14)	107.39(18)
C(13)-C(14)	1.370(3)	C(13)-C(14)-C(15)	105.00(18)
C(14)-C(15)	1.400(3)	N(11)-C(15)-C(14)	111.31(18)
C(23)-C(24)	1.366(3)	N(22)-C(23)-C(24)	108.03(18)
C(24)-C(25)	1.401(3)	C(23)-C(24)-C(25)	105.13(18)
C(31)-C(51)	1.529(3)	N(21)-C(25)-C(24)	110.76(18)
C(31)-C(41)	1.532(3)	N(12)-C(31)-N(22)	107.77(15)
C(41)-C(42)	1.392(3)	N(12)-C(31)-C(51)	108.06(15)
C(41)-C(46)	1.393(3)	N(22)-C(31)-C(51)	110.89(15)
C(42)-C(43)	1.394(3)	N(12)-C(31)-C(41)	109.89(15)
C(43)-C(44)	1.385(3)	N(22)-C(31)-C(41)	106.76(15)
C(44)-C(45)	1.399(3)	C(51)-C(31)-C(41)	113.34(16)
C(45)-C(46)	1.383(3)	C(42)-C(41)-C(46)	119.18(18)
C(51)-C(56)	1.387(3)	C(42)-C(41)-C(31)	120.06(18)
C(51)-C(52)	1.398(3)	C(46)-C(41)-C(31)	120.48(18)
C(52)-C(53)	1.383(3)	C(41)-C(42)-C(43)	120.39(19)
C(53)-C(54)	1.387(3)	C(44)-C(43)-C(42)	119.99(19)
C(54)-C(55)	1.383(3)	C(43)-C(44)-C(45)	119.87(19)
C(55)-C(56)	1.391(3)	C(46)-C(45)-C(44)	119.82(19)
N(21)-NI-N(11)	85.53(6)	C(45)-C(46)-C(41)	120.72(19)
N(21)-NI-CL1	103.19(5)	C(56)-C(51)-C(52)	119.56(18)
N(11)-NI-CL1	92.90(5)	C(56)-C(51)-C(31)	121.56(17)
N(21)-NI-CL2#1	153.64(5)	C(52)-C(51)-C(31)	118.78(17)
N(11)-NI-CL2#1	92.75(5)	C(53)-C(52)-C(51)	120.31(19)
CL1-NI-CL2#1	103.17(2)	C(52)-C(53)-C(54)	120.00(19)
N(21)-NI-CL2	90.21(5)	C(55)-C(54)-C(53)	119.84(19)
N(11)-NI-CL2	167.19(5)	C(54)-C(55)-C(56)	120.61(19)
CL1-NI-CL2	99.84(2)	C(51)-C(56)-C(55)	119.68(19)
CL2#1-NI-CL2	85.701(19)		

Symmetry transformations used to generate equivalent atoms:

#1 -x+1,-y+1,-z+1

Table IV-6. Torsion angles [°] for [(dpdpm)Ni(μ-Cl)Cl]$_2$ (**5.6**).

N(21)-NI-CL2-NI#1	153.93(5)
N(11)-NI-CL2-NI#1	83.5(2)
CL1-NI-CL2-NI#1	-102.64(2)
CL2#1-NI-CL2-NI#1	0
N(21)-NI-N(11)-C(15)	149.93(18)
CL1-NI-N(11)-C(15)	46.91(17)
CL2#1-NI-N(11)-C(15)	-56.43(17)
CL2-NI-N(11)-C(15)	-139.14(19)
N(21)-NI-N(11)-N(12)	-21.34(15)
CL1-NI-N(11)-N(12)	-124.36(15)
CL2#1-NI-N(11)-N(12)	132.30(15)
CL2-NI-N(11)-N(12)	49.6(3)
C(15)-N(11)-N(12)-C(13)	2.2(2)
NI-N(11)-N(12)-C(13)	174.99(13)
C(15)-N(11)-N(12)-C(31)	166.59(17)
NI-N(11)-N(12)-C(31)	-20.6(2)
N(11)-NI-N(21)-C(25)	-157.26(18)
CL1-NI-N(21)-C(25)	-65.32(18)
CL2#1-NI-N(21)-C(25)	115.55(17)
CL2-NI-N(21)-C(25)	34.83(17)
N(11)-NI-N(21)-N(22)	29.69(15)
CL1-NI-N(21)-N(22)	121.62(14)
CL2#1-NI-N(21)-N(22)	-57.5(2)
CL2-NI-N(21)-N(22)	-138.22(14)
C(25)-N(21)-N(22)-C(23)	-2.6(2)
NI-N(21)-N(22)-C(23)	171.83(13)
C(25)-N(21)-N(22)-C(31)	-170.98(17)
NI-N(21)-N(22)-C(31)	3.4(2)
N(11)-N(12)-C(13)-C(14)	-2.0(2)
C(31)-N(12)-C(13)-C(14)	-164.41(18)
N(12)-C(13)-C(14)-C(15)	1.1(2)
N(12)-N(11)-C(15)-C(14)	-1.5(2)
NI-N(11)-C(15)-C(14)	-174.12(14)
C(13)-C(14)-C(15)-N(11)	0.2(2)
N(21)-N(22)-C(23)-C(24)	2.8(2)
C(31)-N(22)-C(23)-C(24)	170.41(18)
N(22)-C(23)-C(24)-C(25)	-1.8(2)
N(22)-N(21)-C(25)-C(24)	1.4(2)
NI-N(21)-C(25)-C(24)	-172.59(14)
C(23)-C(24)-C(25)-N(21)	0.2(3)
N(11)-N(12)-C(31)-N(22)	63.3(2)
C(13)-N(12)-C(31)-N(22)	-135.53(19)
N(11)-N(12)-C(31)-C(51)	-56.6(2)
C(13)-N(12)-C(31)-C(51)	104.6(2)
N(11)-N(12)-C(31)-C(41)	179.27(16)
C(13)-N(12)-C(31)-C(41)	-19.5(3)
C(23)-N(22)-C(31)-N(12)	139.04(19)
N(21)-N(22)-C(31)-N(12)	-54.6(2)
C(23)-N(22)-C(31)-C(51)	-102.9(2)
N(21)-N(22)-C(31)-C(51)	63.4(2)
C(23)-N(22)-C(31)-C(41)	21.0(3)
N(21)-N(22)-C(31)-C(41)	-172.66(16)
N(12)-C(31)-C(41)-C(42)	135.20(18)
N(22)-C(31)-C(41)-C(42)	-108.19(19)
C(51)-C(31)-C(41)-C(42)	14.2(3)
N(12)-C(31)-C(41)-C(46)	-50.9(2)
N(22)-C(31)-C(41)-C(46)	65.7(2)
C(51)-C(31)-C(41)-C(46)	-171.91(18)
C(46)-C(41)-C(42)-C(43)	-0.4(3)
C(31)-C(41)-C(42)-C(43)	173.58(18)
C(41)-C(42)-C(43)-C(44)	1.2(3)
C(42)-C(43)-C(44)-C(45)	-0.5(3)
C(43)-C(44)-C(45)-C(46)	-0.9(3)
C(44)-C(45)-C(46)-C(41)	1.7(3)
C(42)-C(41)-C(46)-C(45)	-1.1(3)
C(31)-C(41)-C(46)-C(45)	-175.02(18)
N(12)-C(31)-C(51)-C(56)	138.22(18)
N(22)-C(31)-C(51)-C(56)	20.3(2)
C(41)-C(31)-C(51)-C(56)	-99.7(2)
N(12)-C(31)-C(51)-C(52)	-45.3(2)
N(22)-C(31)-C(51)-C(52)	-163.25(17)
C(41)-C(31)-C(51)-C(52)	76.7(2)
C(56)-C(51)-C(52)-C(53)	0.3(3)
C(31)-C(51)-C(52)-C(53)	-176.16(18)
C(51)-C(52)-C(53)-C(54)	-0.2(3)
C(52)-C(53)-C(54)-C(55)	-0.2(3)
C(53)-C(54)-C(55)-C(56)	0.4(3)
C(52)-C(51)-C(56)-C(55)	-0.1(3)
C(31)-C(51)-C(56)-C(55)	176.28(19)
C(54)-C(55)-C(56)-C(51)	-0.3(3)

Symmetry transformations used to generate equivalent atoms:

#1 -x+1,-y+1,-z+1

Table IV-7. Crystal data and structure refinement for [(dpdpm)NiCl(H_2O)$_2$]Cl (5.7).

Identification code	nath13
Empirical formula	C19 H22 Cl2 N4 Ni O3
Formula weight	484.02
Temperature	100(2)K
Wavelength	1.54178 Å
Crystal system	Triclinic
Space group	P-1
Unit cell dimensions	a = 9.9327(2) Å α = 80.5560(10)° b = 10.8080(2) Å β = 63.7130(10)° c = 11.1787(2) Å γ = 74.5640(10)°
Volume	1035.67(3)Å^3
Z	2
Density (calculated)	1.552 g/cm^3
Absorption coefficient	3.972 mm^{-1}
F(000)	500
Crystal size	0.32 x 0.23 x 0.07 mm
Theta range for data collection	4.25 to 72.87°
Index ranges	$-11 \leq h \leq 9$, $-13 \leq k \leq 13$, $-13 \leq \ell \leq 13$
Reflections collected	12516
Independent reflections	3950 [R_{int} = 0.036]
Absorption correction	Semi-empirical from equivalents
Max. and min. transmission	0.8100 and 0.5300
Refinement method	Full-matrix least-squares on F^2
Data / restraints / parameters	3950 / 3 / 286
Goodness-of-fit on F^2	1.100
Final R indices [I>2sigma(I)]	R_1 = 0.0521, wR_2 = 0.1528
R indices (all data)	R_1 = 0.0554, wR_2 = 0.1622
Largest diff. peak and hole	0.684 and -0.910 e/Å^3

Table IV-8. Atomic coordinates (x 10^4) and equivalent isotropic displacement parameters ($Å^2$ x 10^3) for [(dpdpm)NiCl(H_2O)$_2$]Cl **(5.7)**.

U_{eq} is defined as one third of the trace of the orthogonalized Uij tensor.

	x	y	z	U_{eq}
Ni	1158(1)	1258(1)	2886(1)	11(1)
Cl(1)	1532(1)	-976(1)	2980(1)	15(1)
Cl(2)	-6372(1)	2025(1)	5408(1)	19(1)
N(11)	892(3)	1614(2)	1154(2)	12(1)
N(12)	1773(3)	2295(2)	93(2)	11(1)
N(21)	3388(3)	1338(2)	1798(2)	12(1)
N(22)	3900(3)	2065(2)	642(2)	11(1)
O(1)	-1151(2)	1639(2)	4012(2)	15(1)
O(2)	1340(3)	1534(2)	4539(2)	22(1)
O(3)	-3034(3)	727(2)	3493(2)	20(1)
C(13)	1363(3)	2398(3)	-938(3)	13(1)
C(14)	198(3)	1758(3)	-532(3)	16(1)
C(15)	-53(3)	1280(3)	775(3)	14(1)
C(23)	5456(3)	1871(3)	78(3)	15(1)
C(24)	5970(3)	966(3)	885(3)	17(1)
C(25)	4657(3)	664(3)	1946(3)	15(1)
C(31)	2722(3)	3019(2)	300(3)	12(1)
C(41)	3505(3)	3796(2)	-993(3)	12(1)
C(42)	3164(3)	5138(3)	-1027(3)	14(1)
C(43)	3848(4)	5836(3)	-2208(3)	19(1)
C(44)	4893(3)	5203(3)	-3366(3)	18(1)
C(45)	5232(3)	3869(3)	-3342(3)	17(1)
C(46)	4521(3)	3167(3)	-2163(3)	15(1)
C(51)	1701(3)	3869(2)	1488(3)	11(1)
C(52)	119(3)	4245(3)	1908(3)	14(1)
C(53)	-765(3)	5079(3)	2943(3)	17(1)
C(54)	-63(4)	5574(3)	3525(3)	20(1)
C(55)	1529(4)	5210(3)	3098(3)	22(1)
C(56)	2403(3)	4349(3)	2099(3)	17(1)

Table IV-9. *Hydrogen coordinates* (x 10^4) *and isotropic displacement parameters* ($Å^2$ x 10^3) *for* [(dpdpm)NiCl(H_2O)$_2$]Cl (**5.7**).

	x	y	z	U_{eq}
H(13)	1802	2834	-1783	16
H(14)	-328	1659	-1031	20
H(15)	-795	786	1316	17
H(23)	6072	2282	-723	18
H(24)	7009	617	748	20
H(25)	4660	67	2671	18
H(42)	2461	5574	-239	17
H(43)	3603	6748	-2227	23
H(44)	5372	5683	-4170	22
H(45)	5948	3435	-4128	20
H(46)	4729	2256	-2156	18
H(52)	-364	3932	1489	17
H(53)	-1852	5308	3249	20
H(54)	-663	6160	4214	24
H(55)	2015	5554	3493	27
H(56)	3483	4084	1828	20
H(1A)	-1740(40)	1290(40)	3850(30)	21(9)
H(1B)	-1440(50)	1520(40)	4820(40)	31(11)
H(2A)	680(30)	1470(40)	5180(50)	38(13)
H(2B)	2080(40)	1700(50)	4640(60)	58(16)
H(3A)	-3910(50)	1150(30)	3910(40)	25(10)
H(3B)	-3000(50)	-10(40)	3680(50)	34(12)

Table IV-10. Anisotropic parameters ($Å^2$ x 10^3) for [(dpdpm)NiCl(H_2O)$_2$]Cl (**5.7**).

The anisotropic displacement factor exponent takes the form:

$$-2\pi^2 [h^2 a^{*2} U_{11} + \ldots + 2 h k a^* b^* U_{12}]$$

	U11	U22	U33	U23	U13	U12
Ni	14(1)	12(1)	7(1)	-1(1)	-3(1)	-5(1)
Cl(1)	20(1)	12(1)	10(1)	-1(1)	-1(1)	-5(1)
Cl(2)	20(1)	18(1)	21(1)	-5(1)	-7(1)	-7(1)
N(11)	13(1)	12(1)	11(1)	-1(1)	-3(1)	-6(1)
N(12)	17(1)	11(1)	8(1)	0(1)	-5(1)	-6(1)
N(21)	16(1)	13(1)	8(1)	0(1)	-4(1)	-5(1)
N(22)	14(1)	11(1)	9(1)	0(1)	-4(1)	-5(1)
O(1)	16(1)	19(1)	10(1)	-2(1)	-3(1)	-7(1)
O(2)	20(1)	40(1)	9(1)	-2(1)	-4(1)	-17(1)
O(3)	20(1)	23(1)	18(1)	2(1)	-5(1)	-10(1)
C(13)	15(1)	14(1)	11(1)	-1(1)	-6(1)	-4(1)
C(14)	22(2)	15(1)	14(1)	-2(1)	-8(1)	-7(1)
C(15)	16(1)	15(1)	14(1)	-2(1)	-5(1)	-6(1)
C(23)	17(1)	15(1)	11(1)	-3(1)	-2(1)	-5(1)
C(24)	15(1)	20(1)	17(1)	-3(1)	-7(1)	-3(1)
C(25)	21(2)	13(1)	12(1)	-1(1)	-7(1)	-4(1)
C(31)	14(1)	11(1)	11(1)	-2(1)	-5(1)	-4(1)
C(41)	12(1)	15(1)	12(1)	1(1)	-6(1)	-6(1)
C(42)	15(1)	16(1)	16(1)	-1(1)	-8(1)	-6(1)
C(43)	29(2)	13(1)	21(1)	4(1)	-14(1)	-10(1)
C(44)	20(2)	24(1)	13(1)	6(1)	-8(1)	-13(1)
C(45)	18(1)	22(1)	10(1)	-1(1)	-3(1)	-9(1)
C(46)	21(2)	15(1)	10(1)	0(1)	-6(1)	-8(1)
C(51)	13(1)	11(1)	10(1)	0(1)	-4(1)	-4(1)
C(52)	19(1)	12(1)	12(1)	0(1)	-6(1)	-6(1)
C(53)	15(1)	14(1)	16(1)	-1(1)	-3(1)	-1(1)
C(54)	26(2)	17(1)	14(1)	-6(1)	-5(1)	1(1)
C(55)	26(2)	25(2)	20(2)	-10(1)	-11(1)	-5(1)
C(56)	14(1)	20(1)	18(1)	-6(1)	-6(1)	-3(1)

Table IV-11. Bond lengths [Å] and angles [°] for [(dpdpm)NiCl(H_2O)$_2$]Cl **(5.7)**.

Ni-O(2)	2.011(2)	C(15)-N(11)-N(12)	106.1(2)
Ni-N(21)	2.019(2)	C(15)-N(11)-NI	131.80(18)
Ni-N(11)	2.030(2)	N(12)-N(11)-NI	122.05(17)
Ni-O(1)	2.030(2)	N(11)-N(12)-C(13)	110.4(2)
Ni-Cl(1)	2.3352(7)	N(11)-N(12)-C(31)	118.5(2)
N(11)-C(15)	1.332(3)	C(13)-N(12)-C(31)	129.6(2)
N(11)-N(12)	1.361(3)	C(25)-N(21)-N(22)	105.6(2)
N(12)-C(13)	1.363(3)	C(25)-N(21)-NI	130.45(19)
N(12)-C(31)	1.483(3)	N(22)-N(21)-NI	123.79(17)
N(21)-C(25)	1.343(4)	C(23)-N(22)-N(21)	111.2(2)
N(21)-N(22)	1.358(3)	C(23)-N(22)-C(31)	131.1(2)
N(22)-C(23)	1.356(4)	N(21)-N(22)-C(31)	117.2(2)
N(22)-C(31)	1.484(3)	N(12)-C(13)-C(14)	107.4(2)
C(13)-C(14)	1.372(4)	C(13)-C(14)-C(15)	105.4(2)
C(14)-C(15)	1.400(4)	N(11)-C(15)-C(14)	110.6(2)
C(23)-C(24)	1.372(4)	N(22)-C(23)-C(24)	106.9(2)
C(24)-C(25)	1.394(4)	C(23)-C(24)-C(25)	106.0(3)
C(31)-C(51)	1.532(3)	N(21)-C(25)-C(24)	110.3(2)
C(31)-C(41)	1.535(4)	N(12)-C(31)-N(22)	107.5(2)
C(41)-C(42)	1.397(4)	N(12)-C(31)-C(51)	109.2(2)
C(41)-C(46)	1.397(4)	N(22)-C(31)-C(51)	108.3(2)
C(42)-C(43)	1.387(4)	N(12)-C(31)-C(41)	109.3(2)
C(43)-C(44)	1.395(4)	N(22)-C(31)-C(41)	110.0(2)
C(44)-C(45)	1.389(4)	C(51)-C(31)-C(41)	112.5(2)
C(45)-C(46)	1.394(4)	C(42)-C(41)-C(46)	119.3(2)
C(51)-C(52)	1.387(4)	C(42)-C(41)-C(31)	120.6(2)
C(51)-C(56)	1.397(4)	C(46)-C(41)-C(31)	120.1(2)
C(52)-C(53)	1.394(4)	C(43)-C(42)-C(41)	120.2(3)
C(53)-C(54)	1.383(4)	C(42)-C(43)-C(44)	120.3(3)
C(54)-C(55)	1.394(5)	C(45)-C(44)-C(43)	119.8(3)
C(55)-C(56)	1.386(4)	C(44)-C(45)-C(46)	120.0(3)
O(2)-NI-N(21)	89.43(9)	C(45)-C(46)-C(41)	120.3(3)
O(2)-NI-N(11)	161.17(10)	C(52)-C(51)-C(56)	119.3(2)
N(21)-NI-N(11)	87.72(9)	C(52)-C(51)-C(31)	121.8(2)
O(2)-NI-O(1)	86.05(9)	C(56)-C(51)-C(31)	118.7(2)
N(21)-NI-O(1)	166.13(9)	C(51)-C(52)-C(53)	120.4(3)
N(11)-NI-O(1)	92.34(9)	C(54)-C(53)-C(52)	120.1(3)
O(2)-NI-CL1	101.78(7)	C(53)-C(54)-C(55)	119.8(3)
N(21)-NI-CL1	96.59(7)	C(56)-C(55)-C(54)	120.1(3)
N(11)-NI-CL1	97.03(6)	C(55)-C(56)-C(51)	120.3(3)
O(1)-NI-CL1	97.17(6)		

Symmetry transformations used to generate equivalent atoms:

Table IV-12. Torsion angles [°] for [(dpdpm)NiCl(H_2O)$_2$]Cl (**5.7**).

O(2)-NI-N(11)-C(15)	-128.0(3)	C(13)-N(12)-C(31)-C(51)	112.4(3)
N(21)-NI-N(11)-C(15)	150.5(2)	N(11)-N(12)-C(31)-C(41)	-175.3(2)
O(1)-NI-N(11)-C(15)	-43.3(2)	C(13)-N(12)-C(31)-C(41)	-11.0(4)
CL1-NI-N(11)-C(15)	54.2(2)	C(23)-N(22)-C(31)-N(12)	124.8(3)
O(2)-NI-N(11)-N(12)	52.9(4)	N(21)-N(22)-C(31)-N(12)	-63.9(3)
N(21)-NI-N(11)-N(12)	-28.60(19)	C(23)-N(22)-C(31)-C(51)	-117.4(3)
O(1)-NI-N(11)-N(12)	137.52(19)	N(21)-N(22)-C(31)-C(51)	53.8(3)
CL1-NI-N(11)-N(12)	-124.96(18)	C(23)-N(22)-C(31)-C(41)	5.9(4)
C(15)-N(11)-N(12)-C(13)	0.8(3)	N(21)-N(22)-C(31)-C(41)	177.1(2)
NI-N(11)-N(12)-C(13)	-179.88(17)	N(12)-C(31)-C(41)-C(42)	116.5(3)
C(15)-N(11)-N(12)-C(31)	167.9(2)	N(22)-C(31)-C(41)-C(42)	-125.8(3)
NI-N(11)-N(12)-C(31)	-12.8(3)	C(51)-C(31)-C(41)-C(42)	-5.0(3)
O(2)-NI-N(21)-C(25)	54.3(2)	N(12)-C(31)-C(41)-C(46)	-60.9(3)
N(11)-NI-N(21)-C(25)	-144.3(2)	N(22)-C(31)-C(41)-C(46)	56.9(3)
O(1)-NI-N(21)-C(25)	125.2(4)	C(51)-C(31)-C(41)-C(46)	177.7(2)
CL1-NI-N(21)-C(25)	-47.5(2)	C(46)-C(41)-C(42)-C(43)	-1.0(4)
O(2)-NI-N(21)-N(22)	-131.7(2)	C(31)-C(41)-C(42)-C(43)	-178.4(3)
N(11)-NI-N(21)-N(22)	29.7(2)	C(41)-C(42)-C(43)-C(44)	-0.6(4)
O(1)-NI-N(21)-N(22)	-60.9(4)	C(42)-C(43)-C(44)-C(45)	1.0(4)
CL1-NI-N(21)-N(22)	126.47(19)	C(43)-C(44)-C(45)-C(46)	0.4(4)
C(25)-N(21)-N(22)-C(23)	-0.7(3)	C(44)-C(45)-C(46)-C(41)	-2.1(4)
NI-N(21)-N(22)-C(23)	-175.95(17)	C(42)-C(41)-C(46)-C(45)	2.4(4)
C(25)-N(21)-N(22)-C(31)	-173.7(2)	C(31)-C(41)-C(46)-C(45)	179.8(3)
NI-N(21)-N(22)-C(31)	11.1(3)	N(12)-C(31)-C(51)-C(52)	-22.5(3)
N(11)-N(12)-C(13)-C(14)	-0.5(3)	N(22)-C(31)-C(51)-C(52)	-139.2(2)
C(31)-N(12)-C(13)-C(14)	-165.8(2)	C(41)-C(31)-C(51)-C(52)	99.0(3)
N(12)-C(13)-C(14)-C(15)	0.1(3)	N(12)-C(31)-C(51)-C(56)	162.1(2)
N(12)-N(11)-C(15)-C(14)	-0.7(3)	N(22)-C(31)-C(51)-C(56)	45.4(3)
NI-N(11)-C(15)-C(14)	-179.98(19)	C(41)-C(31)-C(51)-C(56)	-76.4(3)
C(13)-C(14)-C(15)-N(11)	0.4(3)	C(56)-C(51)-C(52)-C(53)	-0.9(4)
N(21)-N(22)-C(23)-C(24)	1.2(3)	C(31)-C(51)-C(52)-C(53)	-176.3(2)
C(31)-N(22)-C(23)-C(24)	172.8(2)	C(51)-C(52)-C(53)-C(54)	2.3(4)
N(22)-C(23)-C(24)-C(25)	-1.1(3)	C(52)-C(53)-C(54)-C(55)	-1.7(4)
N(22)-N(21)-C(25)-C(24)	0.0(3)	C(53)-C(54)-C(55)-C(56)	-0.4(5)
NI-N(21)-C(25)-C(24)	174.77(19)	C(54)-C(55)-C(56)-C(51)	1.8(5)
C(23)-C(24)-C(25)-N(21)	0.7(3)	C(52)-C(51)-C(56)-C(55)	-1.2(4)
N(11)-N(12)-C(31)-N(22)	65.3(3)	C(31)-C(51)-C(56)-C(55)	174.4(3)
C(13)-N(12)-C(31)-N(22)	-130.4(3)		
N(11)-N(12)-C(31)-C(51)	-51.9(3)		

Symmetry transformations used to generate equivalent atoms:

Table IV-13. Bond lengths [Å] and angles [°] related to the hydrogen bonding for [(dpdpm)NiCl(H_2O)$_2$]Cl (**5.7**).

D-H	..A	d(D-H)	d(H..A)	d(D..A)	<DHA
O(1)-H(1A)	O(3)	0.87(4)	1.77(4)	2.634(3)	175(4)
O(1)-H(1B)	CL1#1	0.82(4)	2.39(4)	3.192(2)	164(4)
O(2)-H(2A)	CL1#1	0.74(4)	2.36(4)	3.090(2)	168(5)
O(2)-H(2B)	CL2#2	0.86(4)	2.18(5)	3.025(2)	166(5)
O(3)-H(3A)	CL2	0.83(4)	2.31(4)	3.125(2)	168(4)
O(3)-H(3B)	CL2#3	0.79(4)	2.36(5)	3.129(2)	165(4)

Symmetry transformations used to generate equivalent atoms:

#1 -x,-y,-z+1 #2 x+1,y,z #3 -x-1,-y,-z+1

Table IV-14. Crystal data and structure refinement for 'C245 H232 Cl10 I24 N48 Ni4 O3' (**5.8**)

Identification code	nath15
Empirical formula	4(C57H48N12Ni), 8(I3), 3(C4H10O), 5(CH2Cl2)
Formula weight	7531.73
Temperature	100(2)K
Wavelength	1.54178 $A
Crystal system	Monoclinic
Space group	P21/n
Unit cell dimensions	a = 12.5268(4) $A alpha = 90 deg. b = 26.8473(7) $A beta = 103.382(2) deg. c = 20.4728(7) $A gamma = 90 deg.
Volume	6698.3(4)$A^3
Z	1
Density (calculated)	1.867 Mg/m^3
Absorption coefficient	23.433 mm^*1
F(000)	3616
Crystal size	0.24 x 0.18 x 0.06 mm
Theta range for data collection	2.76 to 72.92 deg.
Index ranges	-15<=h<=15, -32<=k<=32, -23<=l<=25
Reflections collected	81682
Independent reflections	13304 [R(int) = 0.076]
Absorption correction	Semi-empirical from equivalents
Max. and min. transmission	0.4300 and 0.1100
Refinement method	Full-matrix least-squares on F^2
Data / restraints / parameters	13304 / 16 / 784
Goodness-of-fit on F^2	0.995
Final R indices [I>2sigma(I)]	R1 = 0.0520, wR2 = 0.1287
R indices (all data)	R1 = 0.0740, wR2 = 0.1358
Largest diff. peak and hole	2.029 and -1.069 e.$A^*3

Table IV-15. Atomic coordinates (x 10^4) and equivalent isotropic displacement parameters ($A^2 x 10^3) for 'C245 H232 Cl10 I24 N48 Ni4 O3' (5.8)

U(eq) is defined as one third of the trace of the orthogonalized Uij tensor.

	Occ.	x	y	z	U(eq)
I(1)	1	6181(1)	332(1)	7218(1)	25(1)
I(2)	1	3071(1)	2566(1)	8375(1)	26(1)
I(3)	1	4292(1)	3428(1)	8988(1)	30(1)
I(4)	1	3890(1)	584(1)	6748(1)	31(1)
I(5)	1	8551(1)	119(1)	7717(1)	29(1)
I(6)	1	1682(1)	1739(1)	7718(1)	34(1)
Ni(1)	1	7993(1)	2978(1)	6637(1)	13(1)
N(111)	1	7888(5)	2232(2)	6864(3)	12(1)
N(112)	1	7446(5)	1852(2)	6441(3)	15(1)
N(121)	1	6917(5)	2813(2)	5697(3)	14(1)
N(122)	1	6754(5)	2342(2)	5435(3)	14(1)
N(211)	1	9307(5)	2797(2)	6167(3)	15(1)
N(212)	1	9578(5)	3073(2)	5668(3)	14(1)
N(221)	1	8154(5)	3718(2)	6302(3)	15(1)
N(222)	1	8633(5)	3846(2)	5792(3)	15(1)
N(311)	1	9027(5)	3141(2)	7577(3)	13(1)
N(312)	1	8727(5)	3407(2)	8075(3)	14(1)
N(321)	1	6698(5)	3201(2)	7055(3)	14(1)
N(322)	1	6787(5)	3462(2)	7642(3)	15(1)
C(113)	1	7805(6)	1404(2)	6708(4)	18(2)
C(114)	1	8523(7)	1493(3)	7312(4)	23(2)
C(115)	1	8556(6)	2010(2)	7389(4)	17(2)
C(123)	1	6410(6)	2361(3)	4755(4)	20(2)
C(124)	1	6382(6)	2854(3)	4560(4)	20(2)
C(125)	1	6712(5)	3123(3)	5170(4)	17(2)
C(131)	1	6502(6)	1932(2)	5863(4)	15(1)
C(141)	1	6368(6)	1449(2)	5446(3)	15(1)
C(142)	1	5453(6)	1143(2)	5397(4)	17(2)
C(143)	1	5362(6)	702(2)	5042(4)	18(2)
C(144)	1	6168(6)	560(3)	4724(4)	20(2)
C(145)	1	7083(7)	860(3)	4771(4)	23(2)
C(146)	1	7181(6)	1304(3)	5130(4)	20(2)
C(151)	1	5477(6)	2068(2)	6105(4)	17(2)
C(152)	1	5363(6)	1933(2)	6732(4)	20(2)
C(153)	1	4370(6)	2029(3)	6920(4)	23(2)
C(154)	1	3514(6)	2260(3)	6484(4)	23(2)
C(155)	1	3624(6)	2391(3)	5844(4)	24(2)
C(156)	1	4601(6)	2290(3)	5658(4)	20(2)
C(213)	1	10129(6)	2786(3)	5311(4)	23(2)
C(214)	1	10188(6)	2313(3)	5576(4)	21(2)
C(215)	1	9665(6)	2341(3)	6101(4)	17(2)
C(223)	1	8239(6)	4296(3)	5531(4)	19(2)
C(224)	1	7484(7)	4454(3)	5867(4)	24(2)
C(225)	1	7466(6)	4088(2)	6343(4)	18(2)
C(231)	1	9675(5)	3625(2)	5721(4)	13(1)
C(241)	1	9901(6)	3820(2)	5063(4)	16(2)
C(242)	1	10787(6)	4129(3)	5061(4)	20(2)
C(243)	1	10935(7)	4322(3)	4450(4)	28(2)
C(244)	1	10225(7)	4216(3)	3864(4)	27(2)
C(245)	1	9337(7)	3901(3)	3858(4)	24(2)
C(246)	1	9158(7)	3708(3)	4452(4)	24(2)

C(251)	1	10590(6)	3757(3)	6325(4)	18(2)
C(252)	1	11507(6)	3460(3)	6520(4)	22(2)
C(253)	1	12342(7)	3585(3)	7064(4)	28(2)
C(254)	1	12284(7)	4025(3)	7410(4)	34(2)
C(255)	1	11375(7)	4328(3)	7229(4)	33(2)
C(256)	1	10521(7)	4197(3)	6683(4)	24(2)
C(313)	1	9640(6)	3589(2)	8510(4)	17(2)
C(314)	1	10539(6)	3438(2)	8279(4)	17(2)
C(315)	1	10103(6)	3161(2)	7700(4)	18(2)
C(323)	1	5834(6)	3709(2)	7633(4)	19(2)
C(324)	1	5140(6)	3622(3)	7025(4)	21(2)
C(325)	1	5699(6)	3308(2)	6677(4)	18(2)
C(331)	1	7646(6)	3338(2)	8248(4)	14(1)
C(341)	1	7565(6)	3705(3)	8800(4)	15(1)
C(342)	1	7407(6)	3540(3)	9418(4)	20(2)
C(343)	1	7281(6)	3883(3)	9897(4)	26(2)
C(344)	1	7320(6)	4393(3)	9768(4)	26(2)
C(345)	1	7494(6)	4556(3)	9162(4)	28(2)
C(346)	1	7625(6)	4215(3)	8680(4)	19(2)
C(351)	1	7527(6)	2792(2)	8451(4)	16(2)
C(352)	1	8432(6)	2544(3)	8824(4)	18(2)
C(353)	1	8310(7)	2064(3)	9059(4)	25(2)
C(354)	1	7296(7)	1841(3)	8941(4)	23(2)
C(355)	1	6394(7)	2093(3)	8579(4)	27(2)
C(356)	1	6505(6)	2577(3)	8334(4)	17(2)
Cl(1)	1	698(2)	-118(1)	6302(2)	68(1)
Cl(2)	1	52(2)	889(1)	5844(2)	60(1)
C(1)	1	600(8)	509(4)	6539(5)	46(3)
Cl(3)	0.25	10516(10)	1029(4)	-1022(5)	64(3)
Cl(4)	0.25	9372(14)	955(5)	109(7)	84(5)
C(2)	0.25	9620(40)	676(15)	-650(20)	47(12)
C(11)	0.75	7673(12)	-169(4)	1183(5)	57(4)
C(12)	0.75	8387(8)	261(3)	1109(4)	37(3)
O(13)	0.75	8503(7)	302(3)	449(4)	56(3)
C(14)	0.75	9157(12)	713(4)	348(6)	63(5)
C(15)	0.75	9321(14)	687(5)	-362(7)	76(7)

Table IV-16. Hydrogen coordinates (x 10^4) and isotropic displacement parameters ($A^2 x 10^3) for 'C245 H232 Cl10 I24 N48 Ni4 O3' (**5.8**).

	Occ.	x	y	z	U(eq)
H(113)	1	7598	1087	6514	22
H(114)	1	8916	1253	7616	27
H(115)	1	8993	2181	7763	21
H(123)	1	6221	2083	4464	24
H(124)	1	6186	2984	4117	24
H(125)	1	6779	3475	5200	20
H(142)	1	4886	1240	5608	21
H(143)	1	4740	494	5019	21
H(144)	1	6098	259	4474	24
H(145)	1	7646	762	4557	28
H(146)	1	7809	1508	5158	24
H(152)	1	5952	1775	7038	24
H(153)	1	4292	1934	7353	28
H(154)	1	2853	2329	6619	27
H(155)	1	3035	2548	5537	28
H(156)	1	4671	2374	5219	24
H(213)	1	10421	2892	4946	27
H(214)	1	10518	2028	5429	25
H(215)	1	9574	2068	6378	20
H(223)	1	8456	4468	5177	23
H(224)	1	7060	4751	5792	29
H(225)	1	7017	4100	6659	21
H(242)	1	11291	4210	5470	25
H(243)	1	11547	4531	4450	33
H(244)	1	10329	4355	3456	32
H(245)	1	8851	3817	3444	29
H(246)	1	8538	3503	4447	29
H(252)	1	11566	3164	6275	27
H(253)	1	12956	3370	7200	34
H(254)	1	12872	4118	7773	41
H(255)	1	11327	4625	7474	40
H(256)	1	9896	4406	6555	29
H(313)	1	9653	3783	8899	20
H(314)	1	11290	3508	8471	20
H(315)	1	10531	3007	7430	21
H(323)	1	5680	3905	7986	22
H(324)	1	4420	3751	6869	25
H(325)	1	5413	3186	6235	21
H(342)	1	7387	3194	9509	24
H(343)	1	7167	3772	10316	31
H(344)	1	7228	4627	10098	32
H(345)	1	7523	4903	9075	34
H(346)	1	7756	4329	8265	23
H(352)	1	9133	2699	8920	22
H(353)	1	8936	1890	9305	31
H(354)	1	7219	1516	9107	28
H(355)	1	5691	1940	8493	32
H(356)	1	5880	2753	8091	20
H(1A)	1	127	530	6865	55
H(1B)	1	1338	633	6764	55
H(2A)	0.25	9945	341	-537	56
H(2B)	0.25	8916	634	-977	56
H(11A)	0.75	7606	-191	1650	86
H(11B)	0.75	7999	-477	1061	86
H(11C)	0.75	6944	-123	887	86

H(12A)	0.75	8062	572	1238	44
H(12B)	0.75	9118	217	1415	44
H(14A)	0.75	9876	701	675	75
H(14B)	0.75	8788	1028	414	75
H(15A)	0.75	9760	972	-444	114
H(15B)	0.75	8606	694	-682	114
H(15C)	0.75	9704	377	-420	114

Table IV-17. Anisotropic parameters ($A^2 x 10^3) for 'C245 H232 Cl10 I24 N48 Ni4 O3' **(5.8)**

The anisotropic displacement factor exponent takes the form:

$$-2\pi^2 [h^2 a^{*2} U11 + ... + 2 h k a^* b^* U12]$$

	U11	U22	U33	U23	U13	U12
I(1)	37(1)	15(1)	29(1)	-1(1)	19(1)	-2(1)
I(2)	22(1)	33(1)	26(1)	8(1)	14(1)	10(1)
I(3)	28(1)	35(1)	31(1)	7(1)	16(1)	4(1)
I(4)	34(1)	25(1)	38(1)	3(1)	15(1)	-2(1)
I(5)	36(1)	14(1)	38(1)	3(1)	11(1)	-4(1)
I(6)	26(1)	46(1)	32(1)	-3(1)	8(1)	5(1)
Ni(1)	14(1)	8(1)	17(1)	1(1)	6(1)	0(1)
N(111)	13(3)	10(2)	15(3)	3(2)	5(2)	-2(2)
N(112)	16(3)	9(2)	21(3)	0(2)	8(3)	0(2)
N(121)	14(3)	13(3)	17(3)	0(2)	6(2)	-4(2)
N(122)	11(3)	14(3)	18(3)	-2(2)	7(2)	-2(2)
N(211)	16(3)	12(3)	17(3)	0(2)	6(2)	-3(2)
N(212)	15(3)	7(2)	21(3)	1(2)	8(2)	2(2)
N(221)	18(3)	10(2)	18(3)	0(2)	9(2)	-1(2)
N(222)	15(3)	9(2)	22(3)	3(2)	8(3)	-1(2)
N(311)	13(3)	13(3)	16(3)	-4(2)	6(2)	-2(2)
N(312)	15(3)	9(2)	19(3)	0(2)	7(2)	2(2)
N(321)	16(3)	10(2)	20(3)	0(2)	8(2)	-1(2)
N(322)	19(3)	10(2)	17(3)	-1(2)	10(2)	-2(2)
C(113)	20(4)	9(3)	26(4)	0(3)	10(3)	-2(3)
C(114)	34(5)	10(3)	27(4)	6(3)	13(4)	0(3)
C(115)	20(4)	12(3)	20(4)	3(3)	7(3)	-1(3)
C(123)	13(4)	25(4)	22(4)	-4(3)	4(3)	-5(3)
C(124)	13(4)	27(4)	20(4)	1(3)	5(3)	0(3)
C(125)	11(4)	18(3)	22(4)	8(3)	6(3)	0(3)
C(131)	12(4)	16(3)	18(4)	0(3)	5(3)	-3(3)
C(141)	16(4)	14(3)	13(4)	-2(3)	3(3)	0(3)
C(142)	19(4)	13(3)	21(4)	5(3)	8(3)	-2(3)
C(143)	20(4)	13(3)	19(4)	5(3)	2(3)	-3(3)
C(144)	26(4)	13(3)	23(4)	0(3)	7(3)	3(3)
C(145)	30(5)	14(3)	28(5)	-2(3)	12(4)	6(3)
C(146)	19(4)	17(3)	29(4)	-5(3)	14(3)	-5(3)
C(151)	18(4)	11(3)	26(4)	-6(3)	14(3)	-2(3)
C(152)	18(4)	14(3)	28(4)	4(3)	7(3)	3(3)
C(153)	24(4)	21(4)	25(4)	-3(3)	9(3)	-3(3)
C(154)	16(4)	24(4)	32(5)	1(3)	15(3)	1(3)
C(155)	17(4)	20(3)	33(5)	2(3)	5(3)	4(3)
C(156)	25(4)	18(3)	18(4)	1(3)	9(3)	-5(3)
C(213)	31(5)	18(3)	25(4)	-3(3)	17(3)	-2(3)
C(214)	21(4)	13(3)	30(4)	-5(3)	8(3)	5(3)
C(215)	13(4)	16(3)	22(4)	-2(3)	5(3)	1(3)
C(223)	22(4)	16(3)	19(4)	5(3)	4(3)	-1(3)

C(224)	34(5)	10(3)	33(5)	4(3)	17(4)	7(3)
C(225)	23(4)	8(3)	25(4)	-2(3)	13(3)	4(3)
C(231)	11(4)	8(3)	25(4)	-1(3)	11(3)	-3(2)
C(241)	16(4)	11(3)	26(4)	2(3)	13(3)	2(3)
C(242)	24(4)	15(3)	25(4)	2(3)	11(3)	-3(3)
C(243)	29(5)	20(4)	38(5)	2(4)	18(4)	-3(3)
C(244)	28(5)	24(4)	33(5)	8(4)	18(4)	1(3)
C(245)	30(5)	25(4)	20(4)	0(3)	11(3)	-1(3)
C(246)	27(4)	17(3)	34(5)	2(3)	17(4)	-2(3)
C(251)	20(4)	15(3)	21(4)	2(3)	9(3)	-4(3)
C(252)	15(4)	24(4)	31(4)	8(3)	10(3)	-4(3)
C(253)	26(5)	32(4)	29(5)	14(4)	13(4)	-6(3)
C(254)	23(5)	48(5)	27(5)	6(4)	-2(4)	-18(4)
C(255)	41(6)	28(4)	28(5)	-5(4)	3(4)	-15(4)
C(256)	29(5)	16(3)	27(4)	-3(3)	6(3)	-5(3)
C(313)	23(4)	15(3)	14(4)	-2(3)	9(3)	0(3)
C(314)	8(3)	17(3)	25(4)	0(3)	1(3)	1(3)
C(315)	19(4)	15(3)	20(4)	2(3)	8(3)	7(3)
C(323)	26(4)	11(3)	24(4)	5(3)	17(3)	-1(3)
C(324)	10(4)	19(3)	37(5)	6(3)	11(3)	6(3)
C(325)	21(4)	11(3)	21(4)	1(3)	6(3)	-3(3)
C(331)	14(4)	8(3)	19(4)	2(3)	5(3)	-3(2)
C(341)	12(4)	16(3)	19(4)	-3(3)	5(3)	1(3)
C(342)	15(4)	22(3)	23(4)	3(3)	5(3)	0(3)
C(343)	25(4)	33(4)	24(4)	-2(4)	16(3)	-6(3)
C(344)	21(4)	25(4)	33(5)	-16(4)	5(3)	-5(3)
C(345)	23(5)	21(4)	44(5)	-6(4)	12(4)	-2(3)
C(346)	19(4)	15(3)	24(4)	2(3)	7(3)	3(3)
C(351)	26(4)	10(3)	15(4)	-1(3)	10(3)	-1(3)
C(352)	22(4)	18(3)	15(4)	-1(3)	7(3)	-1(3)
C(353)	36(5)	20(4)	21(4)	6(3)	9(4)	6(3)
C(354)	35(5)	16(3)	21(4)	1(3)	11(3)	-2(3)
C(355)	30(5)	20(4)	30(5)	8(3)	8(4)	-8(3)
C(356)	14(4)	15(3)	23(4)	4(3)	5(3)	-2(3)
Cl(1)	56(2)	39(1)	107(3)	10(2)	15(2)	11(1)
Cl(2)	60(2)	53(2)	72(2)	20(1)	29(2)	17(1)
C(1)	36(6)	49(6)	58(7)	3(5)	24(5)	6(5)
Cl(3)	84(9)	60(7)	43(6)	-13(5)	3(6)	-39(6)
Cl(4)	104(12)	57(8)	75(10)	15(8)	-12(8)	2(8)
C(2)	50(15)	38(14)	53(15)	13(9)	17(9)	-7(9)
C(11)	84(12)	51(8)	27(7)	-25(7)	-6(7)	-7(8)
C(12)	37(7)	32(6)	36(7)	-8(5)	-2(5)	30(5)
O(13)	34(5)	37(5)	85(8)	-22(5)	-13(5)	17(4)
C(14)	47(10)	28(7)	101(16)	-30(9)	-8(9)	4(7)
C(15)	64(13)	18(7)	130(20)	8(10)	-20(13)	-7(7)

Table IV-18. Bond lengths [$A] and angles [deg.]
for 'C245 H232 Cl10 I24 N48 Ni4 O3' (**5.8**)

I(1)-I(4)	2.8887(8)
I(1)-I(5)	2.9629(8)
I(2)-I(3)	2.8953(8)
I(2)-I(6)	2.9470(8)
Ni(1)-N(111)	2.068(5)
Ni(1)-N(321)	2.089(6)
Ni(1)-N(311)	2.103(6)
Ni(1)-N(121)	2.125(6)
Ni(1)-N(221)	2.126(6)
Ni(1)-N(211)	2.145(6)
N(111)-C(115)	1.339(9)
N(111)-N(112)	1.368(7)
N(112)-C(113)	1.356(8)
N(112)-C(131)	1.481(9)
N(121)-C(125)	1.338(8)
N(121)-N(122)	1.372(7)
N(122)-C(123)	1.360(9)
N(122)-C(131)	1.485(8)
N(211)-C(215)	1.322(8)
N(211)-N(212)	1.368(8)
N(212)-C(213)	1.356(9)
N(212)-C(231)	1.487(7)
N(221)-C(225)	1.329(8)
N(221)-N(222)	1.363(7)
N(222)-C(223)	1.365(8)
N(222)-C(231)	1.473(8)
N(311)-C(315)	1.314(9)
N(311)-N(312)	1.366(7)
N(312)-C(313)	1.366(9)
N(312)-C(331)	1.488(9)
N(321)-C(325)	1.341(9)
N(321)-N(322)	1.373(8)
N(322)-C(323)	1.362(9)
N(322)-C(331)	1.480(9)
C(113)-C(114)	1.371(11)
C(114)-C(115)	1.396(9)
C(123)-C(124)	1.381(10)
C(124)-C(125)	1.417(10)
C(131)-C(151)	1.524(9)
C(131)-C(141)	1.540(9)
C(141)-C(146)	1.384(9)
C(141)-C(142)	1.394(9)
C(142)-C(143)	1.380(9)
C(143)-C(144)	1.376(10)
C(144)-C(145)	1.385(10)
C(145)-C(146)	1.390(9)
C(151)-C(152)	1.373(10)
C(151)-C(156)	1.39(1)
C(152)-C(153)	1.408(10)
C(153)-C(154)	1.373(11)
C(154)-C(155)	1.395(11)
C(155)-C(156)	1.39(1)
C(213)-C(214)	1.375(10)
C(214)-C(215)	1.385(10)
C(223)-C(224)	1.361(10)
C(224)-C(225)	1.388(10)
C(231)-C(251)	1.521(10)
C(231)-C(241)	1.532(9)

C(241)-C(242)	1.387(9)
C(241)-C(246)	1.407(11)
C(242)-C(243)	1.405(10)
C(243)-C(244)	1.349(11)
C(244)-C(245)	1.395(10)
C(245)-C(246)	1.387(10)
C(251)-C(252)	1.381(10)
C(251)-C(256)	1.403(10)
C(252)-C(253)	1.381(11)
C(253)-C(254)	1.389(12)
C(254)-C(255)	1.379(12)
C(255)-C(256)	1.401(11)
C(313)-C(314)	1.378(9)
C(314)-C(315)	1.399(10)
C(323)-C(324)	1.363(11)
C(324)-C(325)	1.393(9)
C(331)-C(341)	1.521(9)
C(331)-C(351)	1.539(8)
C(341)-C(342)	1.397(10)
C(341)-C(346)	1.398(9)
C(342)-C(343)	1.38(1)
C(343)-C(344)	1.395(11)
C(344)-C(345)	1.380(11)
C(345)-C(346)	1.383(10)
C(351)-C(356)	1.373(10)
C(351)-C(352)	1.383(10)
C(352)-C(353)	1.395(10)
C(353)-C(354)	1.374(11)
C(354)-C(355)	1.378(11)
C(355)-C(356)	1.413(9)
Cl(1)-C(1)	1.765(10)
Cl(2)-C(1)	1.756(10)
Cl(3)-C(2)	1.77(2)
Cl(4)-C(2)	1.81(2)
C(11)-C(12)	1.490(5)
C(12)-O(13)	1.397(5)
O(13)-C(14)	1.418(5)
C(14)-C(15)	1.517(5)
I(4)-I(1)-I(5)	177.48(2)
I(3)-I(2)-I(6)	175.61(2)
N(111)-NI1-N(321)	95.2(2)
N(111)-NI1-N(311)	93.0(2)
N(321)-NI1-N(311)	86.4(2)
N(111)-NI1-N(121)	86.7(2)
N(321)-NI1-N(121)	92.3(2)
N(311)-NI1-N(121)	178.7(2)
N(111)-NI1-N(221)	173.5(2)
N(321)-NI1-N(221)	90.3(2)
N(311)-NI1-N(221)	91.0(2)
N(121)-NI1-N(221)	89.4(2)
N(111)-NI1-N(211)	88.7(2)
N(321)-NI1-N(211)	175.9(2)
N(311)-NI1-N(211)	94.8(2)
N(121)-NI1-N(211)	86.5(2)
N(221)-NI1-N(211)	85.8(2)
C(115)-N(111)-N(112)	105.3(5)
C(115)-N(111)-NI1	123.4(5)
N(112)-N(111)-NI1	128.1(4)
C(113)-N(112)-N(111)	111.0(6)
C(113)-N(112)-C(131)	125.3(6)
N(111)-N(112)-C(131)	122.0(5)

C(125)-N(121)-N(122)	106.0(6)
C(125)-N(121)-NI1	124.3(5)
N(122)-N(121)-NI1	123.5(4)
C(123)-N(122)-N(121)	110.3(6)
C(123)-N(122)-C(131)	124.9(6)
N(121)-N(122)-C(131)	119.2(5)
C(215)-N(211)-N(212)	106.0(6)
C(215)-N(211)-NI1	124.7(5)
N(212)-N(211)-NI1	124.2(4)
C(213)-N(212)-N(211)	109.8(5)
C(213)-N(212)-C(231)	124.3(6)
N(211)-N(212)-C(231)	121.0(5)
C(225)-N(221)-N(222)	105.5(6)
C(225)-N(221)-NI1	124.5(5)
N(222)-N(221)-NI1	125.0(4)
N(221)-N(222)-C(223)	109.8(6)
N(221)-N(222)-C(231)	122.2(5)
C(223)-N(222)-C(231)	124.5(6)
C(315)-N(311)-N(312)	106.4(5)
C(315)-N(311)-NI1	124.8(5)
N(312)-N(311)-NI1	125.1(4)
C(313)-N(312)-N(311)	109.8(5)
C(313)-N(312)-C(331)	124.1(6)
N(311)-N(312)-C(331)	122.2(5)
C(325)-N(321)-N(322)	105.8(5)
C(325)-N(321)-NI1	122.3(5)
N(322)-N(321)-NI1	126.2(4)
C(323)-N(322)-N(321)	110.0(6)
C(323)-N(322)-C(331)	125.9(6)
N(321)-N(322)-C(331)	121.0(5)
N(112)-C(113)-C(114)	107.2(6)
C(113)-C(114)-C(115)	105.8(7)
N(111)-C(115)-C(114)	110.7(7)
N(122)-C(123)-C(124)	108.3(7)
C(123)-C(124)-C(125)	104.5(7)
N(121)-C(125)-C(124)	110.8(6)
N(112)-C(131)-N(122)	109.8(5)
N(112)-C(131)-C(151)	110.6(6)
N(122)-C(131)-C(151)	108.9(5)
N(112)-C(131)-C(141)	106.6(5)
N(122)-C(131)-C(141)	107.9(5)
C(151)-C(131)-C(141)	112.9(6)
C(146)-C(141)-C(142)	118.8(6)
C(146)-C(141)-C(131)	119.9(6)
C(142)-C(141)-C(131)	121.2(6)
C(143)-C(142)-C(141)	120.7(7)
C(144)-C(143)-C(142)	120.3(7)
C(143)-C(144)-C(145)	119.6(7)
C(144)-C(145)-C(146)	120.3(7)
C(141)-C(146)-C(145)	120.3(7)
C(152)-C(151)-C(156)	119.5(7)
C(152)-C(151)-C(131)	121.2(7)
C(156)-C(151)-C(131)	119.0(7)
C(151)-C(152)-C(153)	119.7(7)
C(154)-C(153)-C(152)	120.9(7)
C(153)-C(154)-C(155)	119.4(7)
C(156)-C(155)-C(154)	119.5(7)
C(151)-C(156)-C(155)	120.9(7)
N(212)-C(213)-C(214)	107.6(6)
C(213)-C(214)-C(215)	105.2(6)
N(211)-C(215)-C(214)	111.3(6)
C(224)-C(223)-N(222)	108.0(6)

C(223)-C(224)-C(225)	105.1(6)
N(221)-C(225)-C(224)	111.6(6)
N(222)-C(231)-N(212)	110.4(5)
N(222)-C(231)-C(251)	110.1(6)
N(212)-C(231)-C(251)	109.1(6)
N(222)-C(231)-C(241)	107.3(5)
N(212)-C(231)-C(241)	107.7(5)
C(251)-C(231)-C(241)	112.2(5)
C(242)-C(241)-C(246)	119.4(7)
C(242)-C(241)-C(231)	121.2(7)
C(246)-C(241)-C(231)	119.3(6)
C(241)-C(242)-C(243)	119.6(7)
C(244)-C(243)-C(242)	121.2(7)
C(243)-C(244)-C(245)	119.7(8)
C(246)-C(245)-C(244)	120.7(8)
C(245)-C(246)-C(241)	119.4(7)
C(252)-C(251)-C(256)	118.9(7)
C(252)-C(251)-C(231)	121.3(7)
C(256)-C(251)-C(231)	119.8(7)
C(251)-C(252)-C(253)	121.1(8)
C(252)-C(253)-C(254)	120.0(8)
C(255)-C(254)-C(253)	120.1(8)
C(254)-C(255)-C(256)	119.8(8)
C(255)-C(256)-C(251)	120.0(8)
N(312)-C(313)-C(314)	107.4(6)
C(313)-C(314)-C(315)	104.8(6)
N(311)-C(315)-C(314)	111.5(6)
N(322)-C(323)-C(324)	107.5(6)
C(323)-C(324)-C(325)	106.3(6)
N(321)-C(325)-C(324)	110.3(7)
N(322)-C(331)-N(312)	107.3(5)
N(322)-C(331)-C(341)	108.4(5)
N(312)-C(331)-C(341)	108.5(5)
N(322)-C(331)-C(351)	110.1(5)
N(312)-C(331)-C(351)	109.5(5)
C(341)-C(331)-C(351)	112.9(6)
C(342)-C(341)-C(346)	119.6(7)
C(342)-C(341)-C(331)	121.1(6)
C(346)-C(341)-C(331)	119.3(6)
C(343)-C(342)-C(341)	119.7(7)
C(342)-C(343)-C(344)	120.3(7)
C(345)-C(344)-C(343)	120.1(7)
C(344)-C(345)-C(346)	120.1(7)
C(345)-C(346)-C(341)	120.2(7)
C(356)-C(351)-C(352)	120.4(6)
C(356)-C(351)-C(331)	119.8(6)
C(352)-C(351)-C(331)	119.3(6)
C(351)-C(352)-C(353)	119.6(7)
C(354)-C(353)-C(352)	120.8(7)
C(353)-C(354)-C(355)	119.4(7)
C(354)-C(355)-C(356)	120.4(7)
C(351)-C(356)-C(355)	119.3(7)
CL2-C(1)-CL1	111.7(6)
CL3-C(2)-CL4	113.80(17)
O(13)-C(12)-C(11)	111.0(6)
C(12)-O(13)-C(14)	113.3(6)
O(13)-C(14)-C(15)	108.4(6)

Symmetry transformations used to generate equivalent atoms:

Table IV-19. Torsion angles [deg.] for 'C245 H232 Cl10 I24 N48 Ni4 O3' (5.8)

N(321)	-NI1-	N(111)	-C(115) -100.3(6)
N(311)	-NI1-	N(111)	-C(115) -13.7(6)
N(121)	-NI1-	N(111)	-C(115) 167.6(6)
N(221)	-NI1-	N(111)	-C(115) 114(2)
N(211)	-NI1-	N(111)	-C(115) 81.1(6)
N(321)	-NI1-	N(111)	-N(112) 103.1(5)
N(311)	-NI1-	N(111)	-N(112) -170.2(5)
N(121)	-NI1-	N(111)	-N(112) 11.1(5)
N(221)	-NI1-	N(111)	-N(112) -43(2)
N(211)	-NI1-	N(111)	-N(112) -75.5(5)
C(115)	-N(111)	-N(112)	-C(113) 2.0(8)
NI1	-N(111)	-N(112)	-C(113) 161.8(5)
C(115)	-N(111)	-N(112)	-C(13 167.9(6)
NI1	-N(111)	-N(112)	-C(131) -32.3(8)
N(111)	-NI1-	N(121)	-C(125) -167.5(6)
N(321)	-NI1-	N(121)	-C(125) 97.4(6)
N(311)	-NI1-	N(121)	-C(125) 115(9)
N(221)	-NI1-	N(121)	-C(125) 7.2(6)
N(211)	-NI1-	N(121)	-C(125) -78.7(6)
N(111)	-NI1-	N(121)	-N(122) -19.2(5)
N(321)	-NI1-	N(121)	-N(122) -114.2(5)
N(311)	-NI1-	N(121)	-N(122) -97(9)
N(221)	-NI1-	N(121)	-N(122) 155.6(5)
N(211)	-NI1-	N(121)	-N(122) 69.7(5)
C(125)	-N(121)	-N(122)	-C(123) -2.4(7)
NI1	-N(121)	-N(122)	-C(123) -155.6(5)
C(125)	-N(121)	-N(122)	-C(1) -157.2(6)
NI1	-N(121)	-N(122)	-C(131) 49.6(7)
N(111)	-NI1-	N(211)	-C(215) 3.2(6)
N(321)	-NI1-	N(211)	-C(215) -157(3)
N(311)	-NI1-	N(211)	-C(215) 96.1(6)
N(121)	-NI1-	N(211)	-C(215) -83.6(6)
N(221)	-NI1-	N(211)	-C(215) -173.3(6)
N(111)	-NI1-	N(211)	-N(212) 154.4(5)
N(321)	-NI1-	N(211)	-N(212) -6(4)
N(311)	-NI1-	N(211)	-N(212) -112.7(5)
N(121)	-NI1-	N(211)	-N(212) 67.6(5)
N(221)	-NI1-	N(211)	-N(212) -22.1(5)
C(215)	-N(211)	-N(212)	-C(213) -1.8(8)
NI1	-N(211)	-N(212)	-C(213) -157.4(5)
C(215)	-N(211)	-N(212)	-C(2 -157.9(6)
NI1	-N(211)	-N(212)	-C(231) 46.5(8)
N(111)	-NI1-	N(221)	-C(225) 138.90(19)
N(321)	-NI1-	N(221)	-C(225) -7.0(6)
N(311)	-NI1-	N(221)	-C(225) -93.4(6)
N(121)	-NI1-	N(221)	-C(225) 85.3(6)
N(211)	-NI1-	N(221)	-C(225) 171.8(6)
N(111)	-NI1-	N(221)	-N(222) -12(2)
N(321)	-NI1-	N(221)	-N(222) -158.1(5)
N(311)	-NI1-	N(221)	-N(222) 115.5(5)
N(121)	-NI1-	N(221)	-N(222) -65.7(5)
N(211)	-NI1-	N(221)	-N(222) 20.8(5)
C(225)	-N(221)	-N(222)	-C(223) 0.7(8)
NI1	-N(221)	-N(222)	-C(223) 156.2(5)
C(225)	-N(221)	-N(222)	-C(231) 60.3(6)
NI1	-N(221)	-N(222)	-C(231) -44.2(8)

```
N(111)-NI1-N(311)-C(315)   95.8(6)
N(321)-NI1-N(311)-C(315)-169.2(6)
N(121)-NI1-N(311)-C(315)  174(100)
N(221)-NI1-N(311)-C(315)  -79.0(6)
N(211)-NI1-N(311)-C(315)    6.9(6)
N(111)-NI1-N(311)-N(312)-109.0(5)
N(321)-NI1-N(311)-N(312)  -14.0(5)
N(121)-NI1-N(311)-N(312)  -31(10)
N(221)-NI1-N(311)-N(312)   76.2(5)
N(211)-NI1-N(311)-N(312)  162.1(5)
C(315)-N(311)-N(312)-C(313)-0.5(7)
NI1-N(311)-N(312)-C(313)-159.4(4)
C(315)-N(311)-N(312)-C(3)-159.3(6)
NI1-N(311)-N(312)-C(331)   41.8(8)
N(111)-NI1-N(321)-C(325)-103.0(5)
N(311)-NI1-N(321)-C(325)  164.3(5)
N(121)-NI1-N(321)-C(325)  -16.1(5)
N(221)-NI1-N(321)-C(325)   73.3(5)
N(211)-NI1-N(321)-C(325)   57(3)
N(111)-NI1-N(321)-N(322)  107.5(5)
N(311)-NI1-N(321)-N(322)   14.7(5)
N(121)-NI1-N(321)-N(322)-165.7(5)
N(221)-NI1-N(321)-N(322)  -76.2(5)
N(211)-NI1-N(321)-N(322)  -93(3)
C(325)-N(321)-N(322)-C(323)2.6(7)
NI1-N(321)-N(322)-C(323)  156.1(4)
C(325)-N(321)-N(322)-C(331)63.7(6)
NI1-N(321)-N(322)-C(331)  -42.7(8)
N(111)-N(112)-C(113)-C(114)-1.7(8)
C(131)-N(112)-C(113)-C(1)-167.0(6)
N(112)-C(113)-C(114)-C(115)0.8(8)
N(112)-N(111)-C(115)-C(114)-1.5(8)
NI1-N(111)-C(115)-C(114)-162.5(5)
C(113)-C(114)-C(115)-N(111)0.5(9)
N(121)-N(122)-C(123)-C(124)2.1(8)
C(131)-N(122)-C(123)-C(121)55.2(6)
N(122)-C(123)-C(124)-C(125)-1.0(8)
N(122)-N(121)-C(125)-C(124)1.7(8)
NI1-N(121)-C(125)-C(124)  154.6(5)
C(123)-C(124)-C(125)-N(121)-0.4(8)
C(113)-N(112)-C(131)-N(1)-142.0(7)
N(111)-N(112)-C(131)-N(122)54.2(8)
C(113)-N(112)-C(131)-C(151)97.8(8)
N(111)-N(112)-C(131)-C(15)-66.0(8)
C(113)-N(112)-C(131)-C(14)-25.4(9)
N(111)-N(112)-C(131)-C(14)170.8(6)
C(123)-N(122)-C(131)-N(11)145.3(6)
N(121)-N(122)-C(131)-N(11)-63.8(7)
C(123)-N(122)-C(131)-C(15)-93.4(8)
N(121)-N(122)-C(131)-C(15)157.4(8)
C(123)-N(122)-C(131)-C(14)129.5(9)
N(121)-N(122)-C(131)-C(1)-179.6(6)
N(112)-C(131)-C(141)-C(14)-65.3(8)
N(122)-C(131)-C(141)-C(146)52.6(8)
C(151)-C(131)-C(141)-C(14)173.0(7)
N(112)-C(131)-C(141)-C(14)112.7(7)
N(122)-C(131)-C(141)-C(1)-129.4(7)
C(151)-C(131)-C(141)-C(142)-9.0(9)
C(146)-C(141)-C(142)-C(143)0.50(11)
C(131)-C(141)-C(142)-C(1)-177.5(6)
C(141)-C(142)-C(143)-C(144)-1.00(11)
C(142)-C(143)-C(144)-C(145)1.20(11)
```

C(143)-C(144)-C(145)-C(146)-0.80(12)
C(142)-C(141)-C(146)-C(145)-0.20(11)
C(131)-C(141)-C(146)-C(141)77.9(7)
C(144)-C(145)-C(146)-C(141)0.40(12)
N(112)-C(131)-C(151)-C(15)-24.1(9)
N(122)-C(131)-C(151)-C(1)-144.8(6)
C(141)-C(131)-C(151)-C(152)95.3(8)
N(112)-C(131)-C(151)-C(151)62.1(6)
N(122)-C(131)-C(151)-C(156)41.4(8)
C(141)-C(131)-C(151)-C(15)-78.5(8)
C(156)-C(151)-C(152)-C(153)-1.2(1)
C(131)-C(151)-C(152)-C(1)-175.0(6)
C(151)-C(152)-C(153)-C(154)-0.40(11)
C(152)-C(153)-C(154)-C(155)1.30(11)
C(153)-C(154)-C(155)-C(156)-0.50(11)
C(152)-C(151)-C(156)-C(155)2.00(11)
C(131)-C(151)-C(156)-C(151)75.9(6)
C(154)-C(155)-C(156)-C(151)-1.10(11)
N(211)-N(212)-C(213)-C(214)1.6(9)
C(231)-N(212)-C(213)-C(211)56.7(7)
N(212)-C(213)-C(214)-C(215)-0.7(9)
N(212)-N(211)-C(215)-C(214)1.3(8)
NI1-N(211)-C(215)-C(214) 156.8(5)
C(213)-C(214)-C(215)-N(211)-0.4(9)
N(221)-N(222)-C(223)-C(224)-1.3(8)
C(231)-N(222)-C(223)-C(2)-160.3(7)
N(222)-C(223)-C(224)-C(225)1.3(9)
N(222)-N(221)-C(225)-C(224)0.2(8)
NI1-N(221)-C(225)-C(224)-155.5(5)
C(223)-C(224)-C(225)-N(221)-0.9(9)
N(221)-N(222)-C(231)-N(212)57.8(8)
C(223)-N(222)-C(231)-N(2)-145.7(6)
N(221)-N(222)-C(231)-C(25)-62.7(7)
C(223)-N(222)-C(231)-C(251)93.9(8)
N(221)-N(222)-C(231)-C(241)74.9(6)
C(223)-N(222)-C(231)-C(24)-28.5(9)
C(213)-N(212)-C(231)-N(221)48.5(7)
N(211)-N(212)-C(231)-N(22)-58.9(8)
C(213)-N(212)-C(231)-C(25)-90.4(8)
N(211)-N(212)-C(231)-C(25)162.1(8)
C(213)-N(212)-C(231)-C(24)131.6(9)
N(211)-N(212)-C(231)-C(2)-175.9(6)
N(222)-C(231)-C(241)-C(24)114.1(7)
N(212)-C(231)-C(241)-C(2)-127.0(7)
C(251)-C(231)-C(241)-C(242)-7.0(9)
N(222)-C(231)-C(241)-C(24)-61.9(8)
N(212)-C(231)-C(241)-C(24)657.1(8)
C(251)-C(231)-C(241)-C(24)177.1(6)
C(246)-C(241)-C(242)-C(243)-0.7(1)
C(231)-C(241)-C(242)-C(2)-176.6(6)
C(241)-C(242)-C(243)-C(244)0.60(12)
C(242)-C(243)-C(244)-C(245)-1.30(12)
C(243)-C(244)-C(245)-C(246)2.10(12)
C(244)-C(245)-C(246)-C(241)-2.20(11)
C(242)-C(241)-C(246)-C(245)1.5(1)
C(231)-C(241)-C(246)-C(24)177.5(6)
N(222)-C(231)-C(251)-C(25)154.6(6)
N(212)-C(231)-C(251)-C(252)33.3(9)
C(241)-C(231)-C(251)-C(25)-86.0(8)
N(222)-C(231)-C(251)-C(25)-27.3(9)
N(212)-C(231)-C(251)-C(2)-148.6(6)
C(241)-C(231)-C(251)-C(256)92.2(8)

C(256)-C(251)-C(252)-C(253)1.00(11)
C(231)-C(251)-C(252)-C(251)79.2(6)
C(251)-C(252)-C(253)-C(254)-2.20(11)
C(252)-C(253)-C(254)-C(255)2.50(12)
C(253)-C(254)-C(255)-C(256)-1.60(13)
C(254)-C(255)-C(256)-C(251)0.40(12)
C(252)-C(251)-C(256)-C(255)-0.10(11)
C(231)-C(251)-C(256)-C(2)-178.3(7)
N(311)-N(312)-C(313)-C(314)0.6(7)
C(331)-N(312)-C(313)-C(311)58.9(6)
N(312)-C(313)-C(314)-C(315)-0.4(8)
N(312)-N(311)-C(315)-C(314)0.2(8)
NI1-N(311)-C(315)-C(314) 159.2(5)
C(313)-C(314)-C(315)-N(311)0.2(8)
N(321)-N(322)-C(323)-C(324)-2.5(7)
C(331)-N(322)-C(323)-C(3)-162.5(6)
N(322)-C(323)-C(324)-C(325)1.3(8)
N(322)-N(321)-C(325)-C(324)-1.7(7)
NI1-N(321)-C(325)-C(324)-156.6(5)
C(323)-C(324)-C(325)-N(321)0.3(8)
C(323)-N(322)-C(331)-N(3)-141.4(6)
N(321)-N(322)-C(331)-N(312)60.5(7)
C(323)-N(322)-C(331)-C(34)-24.5(8)
N(321)-N(322)-C(331)-C(341)77.5(5)
C(323)-N(322)-C(331)-C(351)99.4(7)
N(321)-N(322)-C(331)-C(35)-58.6(8)
C(313)-N(312)-C(331)-N(321)43.5(6)
N(311)-N(312)-C(331)-N(32)-60.8(7)
C(313)-N(312)-C(331)-C(341)26.5(8)
N(311)-N(312)-C(331)-C(3)-177.7(5)
C(313)-N(312)-C(331)-C(35)-97.0(7)
N(311)-N(312)-C(331)-C(351)58.7(8)
N(322)-C(331)-C(341)-C(34)122.8(7)
N(312)-C(331)-C(341)-C(3)-121.0(7)
C(351)-C(331)-C(341)-C(342)0.5(9)
N(322)-C(331)-C(341)-C(34)-55.8(8)
N(312)-C(331)-C(341)-C(346)60.4(8)
C(351)-C(331)-C(341)-C(3)-178.0(6)
C(346)-C(341)-C(342)-C(343)1.80(11)
C(331)-C(341)-C(342)-C(3)-176.7(7)
C(341)-C(342)-C(343)-C(344)-0.60(12)
C(342)-C(343)-C(344)-C(345)-0.50(12)
C(343)-C(344)-C(345)-C(346)0.30(12)
C(344)-C(345)-C(346)-C(341)1.00(12)
C(342)-C(341)-C(346)-C(345)-2.10(11)
C(331)-C(341)-C(346)-C(341)76.5(7)
N(322)-C(331)-C(351)-C(35)-32.2(9)
N(312)-C(331)-C(351)-C(3)-150.0(6)
C(341)-C(331)-C(351)-C(356)89.1(8)
N(322)-C(331)-C(351)-C(35)156.0(6)
N(312)-C(331)-C(351)-C(352)38.2(9)
C(341)-C(331)-C(351)-C(35)-82.7(8)
C(356)-C(351)-C(352)-C(353)2.70(11)
C(331)-C(351)-C(352)-C(35)174.5(7)
C(351)-C(352)-C(353)-C(354)-1.90(11)
C(352)-C(353)-C(354)-C(355)0.70(12)
C(353)-C(354)-C(355)-C(356)-0.30(12)
C(352)-C(351)-C(356)-C(355)-2.30(11)
C(331)-C(351)-C(356)-C(3)-174.1(7)
C(354)-C(355)-C(356)-C(351)1.10(12)
C(11)-C(12)-O(13)-C(14) 178.70(11)
C(12)-O(13)-C(14)-C(15) 174.20(11)

Table IV-20. Crystal data and structure refinement for $[(Pz)_6Ni][I]_2$ **(5.9)**.

Identification code	nath16
Empirical formula	C18 H24 I2 N12 Ni
Formula weight	721.00
Temperature	200(2)K
Wavelength	1.54178 Å
Crystal system	Hexagonal
Space group	P-3
Unit cell dimensions	a = 9.84900(10) Å α = 90° b = 9.84900(10) Å β = 90° c = 7.4921(2) Å γ = 120°
Volume	629.388(19)Å^3
Z	1
Density (calculated)	1.902 Mg/m^3
Absorption coefficient	20.634 mm^{-1}
F(000)	350
Crystal size	0.20 x 0.09 x 0.08 mm
Theta range for data collection	5.19 to 68.11°
Index ranges	$-11 \leq h \leq 11$, $-11 \leq k \leq 11$, $-8 \leq \ell \leq 8$
Reflections collected	8510
Independent reflections	775 [R_{int} = 0.028]
Absorption correction	Semi-empirical from equivalents
Max. and min. transmission	0.3700 and 0.2400
Refinement method	Full-matrix least-squares on F^2
Data / restraints / parameters	775 / 0 / 51
Goodness-of-fit on F^2	1.109
Final R indices [I>2sigma(I)]	R_1 = 0.0207, wR_2 = 0.0567
R indices (all data)	R_1 = 0.0208, wR_2 = 0.0567
Largest diff. peak and hole	0.407 and -0.408 e/Å^3

Table IV-21. Atomic coordinates (x 10^4) and equivalent isotropic displacement parameters ($Å^2$ x 10^3) for $[(Pz)_6Ni][I]_2$ (**5.9**).

U_{eq} is defined as one third of the trace of the orthogonalized Uij tensor.

	x	y	z	U_{eq}
I	3333	6667	1346(1)	41(1)
Ni	0	0	0	26(1)
N(1)	2003(2)	1309(2)	1612(3)	30(1)
N(2)	2925(2)	2885(2)	1567(3)	33(1)
C(3)	4081(3)	3401(3)	2763(4)	39(1)
C(4)	3933(3)	2123(3)	3655(4)	38(1)
C(5)	2628(3)	850(3)	2890(3)	36(1)

Table IV-22. Hydrogen coordinates (x 10^4) and isotropic displacement parameters ($Å^2$ x 10^3) for $[(Pz)_6Ni][I]_2$ (**5.9**).

	x	y	z	U_{eq}
H(2)	2780	3500	835	40
H(3)	4864	4462	2959	47
H(4)	4577	2107	4589	46
H(5)	2233	-210	3236	43

Table IV-23. Anisotropic parameters ($Å^2$ x 10^3) for $[(Pz)_6Ni][I]_2$ (**5.9**).

The anisotropic displacement factor exponent takes the form:

$$-2\pi^2 [h^2 a^{*2} U_{11} + ... + 2 h k a^* b^* U_{12}]$$

	U11	U22	U33	U23	U13	U12
I	35(1)	35(1)	52(1)	0	0	18(1)
Ni	24(1)	24(1)	29(1)	0	0	12(1)
N(1)	29(1)	26(1)	34(1)	-2(1)	-2(1)	13(1)
N(2)	28(1)	28(1)	41(1)	0(1)	-3(1)	12(1)
C(3)	27(1)	36(1)	48(1)	-8(1)	-5(1)	11(1)
C(4)	33(1)	46(1)	40(1)	-9(1)	-8(1)	23(1)
C(5)	38(1)	35(1)	38(1)	-2(1)	-5(1)	20(1)

Table IV-24. Bond lengths [Å] and angles [°] for $[(Pz)_6Ni][I]_2$ (**5.9**).

Ni-N(1)'	2.114(2)	N(1)-NI-N(1)#4	90.59(8)
Ni-N(1)#1	2.114(2)	N(1)#1-NI-N(1)#4	89.41(8)
Ni-N(1)#2	2.114(2)	N(1)#2-NI-N(1)#4	89.41(8)
Ni-N(1)#3	2.114(2)	N(1)#3-NI-N(1)#4	90.59(8)
Ni-N(1)#4	2.114(2)	N(1)-NI-N(1)#5	89.41(8)
Ni-N(1)#5	2.114(2)	N(1)#1-NI-N(1)#5	90.59(8)
N(1)-C(5)	1.334(3)	N(1)#2-NI-N(1)#5	90.59(8)
N(1)-N(2)	1.352(3)	N(1)#3-NI-N(1)#5	89.41(8)
N(2)-C(3)	1.334(3)	N(1)#4-NI-N(1)#5	180.00(8)
C(3)-C(4)	1.367(4)	C(5)-N(1)-N(2)	104.35(19)
C(4)-C(5)	1.393(4)	C(5)-N(1)-NI	130.69(17)
N(1)-NI-N(1)#1	180	N(2)-N(1)-NI	124.93(15)
N(1)-NI-N(1)#2	89.41(8)	C(3)-N(2)-N(1)	112.1(2)
N(1)#1-NI-N(1)#2	90.59(8)	N(2)-C(3)-C(4)	107.5(2)
N(1)-NI-N(1)#3	90.59(8)	C(3)-C(4)-C(5)	104.7(2)
N(1)#1-NI-N(1)#3	89.41(8)	N(1)-C(5)-C(4)	111.4(2)
N(1)#2-NI-N(1)#3	180.00(12)		

Symmetry transformations used to generate equivalent atoms:

#1 -x,-y,-z #2 x-y,x,-z #3 -x+y,-x,z
#4 -y,x-y,z #5 y,-x+y,-z

Table IV-25. Torsion angles [°] for $[(Pz)_6Ni][I]_2$ (**5.9**).

N(1)#1-NI-N(1)-C(5)	69(4)	N(1)#5-NI-N(1)-N(2)	103.8(2)
N(1)#2-NI-N(1)-C(5)	-169.1(2)	C(5)-N(1)-N(2)-C(3)	0.0(3)
N(1)#3-NI-N(1)-C(5)	10.9(2)	NI-N(1)-N(2)-C(3)	178.25(17)
N(1)#4-NI-N(1)-C(5)	101.54(18)	N(1)-N(2)-C(3)-C(4)	-0.1(3)
N(1)#5-NI-N(1)-C(5)	-78.46(18)	N(2)-C(3)-C(4)-C(5)	0.2(3)
N(1)#1-NI-N(1)-N(2)	-109(4)	N(2)-N(1)-C(5)-C(4)	0.1(3)
N(1)#2-NI-N(1)-N(2)	13.17(17)	NI-N(1)-C(5)-C(4)	-177.97(18)
N(1)#3-NI-N(1)-N(2)	-166.83(17)	C(3)-C(4)-C(5)-N(1)	-0.2(3)
N(1)#4-NI-N(1)-N(2)	-76.2(2)		

Symmetry transformations used to generate equivalent atoms:

#1 -x,-y,-z #2 x-y,x,-z #3 -x+y,-x,z
#4 -y,x-y,z #5 y,-x+y,-z

Table IV-26. Crystal data and structure refinement for $[(Pz^{Me2})_2NiCl_2(H_2O)_2]$ **(5.10b)**.

Identification code	NATHA2
Empirical formula	C10 H20 Cl2 N4 Ni O2
Formula weight	357.91
Temperature	293(2)K
Wavelength	1.54178 Å
Crystal system	Monoclinic
Space group	$P2_1/c$
Unit cell dimensions	a = 10.794(5) Å α = 90° b = 9.312(3) Å β = 92.26(3)° c = 7.849(2) Å γ = 90°
Volume	788.3(5)Å^3
Z	2
Density (calculated)	1.508 Mg/m^3
Absorption coefficient	4.935 mm^{-1}
F(000)	372
Crystal size	0.40 x 0.27 x 0.11 mm
Theta range for data collection	4.10 to 69.93°
Index ranges	$-13 \leq h \leq 13$, $-11 \leq k \leq 11$, $-13 \leq \ell \leq 13$
Reflections collected	20600
Independent reflections	1494 [R_{int} = 0.091]
Absorption correction	Gaussian
Max. and min. transmission	0.6100 and 0.2400
Refinement method	Full-matrix least-squares on F^2
Data / restraints / parameters	1494 / 5 / 97
Goodness-of-fit on F^2	1.135
Final R indices [I>2sigma(I)]	R_1 = 0.0655, wR_2 = 0.1816
R indices (all data)	R_1 = 0.0665, wR_2 = 0.1833
Extinction coefficient	0.0136(19)
Largest diff. peak and hole	1.121 and -1.606 e/Å^3

Table IV-27. Atomic coordinates (x 10^4) and equivalent isotropic displacement parameters ($Å^2$ x 10^3) for $[(Pz^{Me2})_2NiCl_2(H_2O)_2]$ (**5.10b**).

U_{eq} is defined as one third of the trace of the orthogonalized Uij tensor.

	x	y	z	U_{eq}
Ni	5000	5000	5000	24(1)
Cl	4986(1)	2397(1)	4992(1)	34(1)
O(1)	4181(2)	4960(1)	2517(3)	33(1)
N(1)	6780(2)	5006(2)	4006(3)	30(1)
N(2)	6988(2)	5830(2)	2623(2)	33(1)
C(3)	8157(2)	5736(3)	2124(3)	37(1)
C(4)	8753(3)	4818(3)	3235(4)	40(1)
C(5)	7869(2)	4378(3)	4388(3)	34(1)
C(6)	8577(3)	6548(4)	606(5)	62(1)
C(7)	8065(3)	3359(4)	5837(4)	55(1)

Table IV-28. Hydrogen coordinates (x 10^4) and isotropic displacement parameters ($Å^2$ x 10^3) for $[(Pz^{Me2})_2NiCl_2(H_2O)_2]$ (**5.10b**).

	x	y	z	U_{eq}
H(1A)	4420(30)	4281(14)	1950(30)	49
H(1B)	4370(30)	5664(13)	1960(30)	49
H(2)	6429	6355	2121	40
H(4)	9580	4539	3229	48
H(6A)	8338	6034	-415	92
H(6B)	9462	6649	680	92
H(6C)	8199	7482	579	92
H(7A)	8113	3884	6889	82
H(7B)	8823	2840	5703	82
H(7C)	7385	2695	5851	82

Table IV-29. Anisotropic parameters ($Å^2 \times 10^3$) for $[(Pz^{Me2})_2NiCl_2(H_2O)_2]$ **(5.10b)**.

The anisotropic displacement factor exponent takes the form:

$$-2\pi^2 [h^2 a^{*2} U_{11} + \ldots + 2 h k a^* b^* U_{12}]$$

	U11	U22	U33	U23	U13	U12
Ni	32(1)	23(1)	16(1)	1(1)	4(1)	-1(1)
Cl	54(1)	25(1)	23(1)	-2(1)	5(1)	-3(1)
O(1)	45(1)	26(1)	28(1)	2(1)	11(1)	1(1)
N(1)	35(1)	32(1)	23(1)	5(1)	7(1)	2(1)
N(2)	36(1)	38(1)	25(1)	9(1)	6(1)	3(1)
C(3)	37(1)	43(1)	31(1)	2(1)	10(1)	-4(1)
C(4)	33(2)	45(1)	42(2)	-1(1)	7(1)	3(1)
C(5)	35(1)	36(1)	31(1)	3(1)	1(1)	3(1)
C(6)	56(2)	78(2)	52(2)	23(2)	24(2)	-3(2)
C(7)	46(2)	67(2)	51(2)	27(2)	-1(1)	12(1)

Table IV-30. Bond lengths [Å] and angles [°] for $[(Pz^{Me2})_2NiCl_2(H_2O)_2]$ **(5.10b)**.

Ni-N(1)#1	2.102(3)	N(1)-NI-CL	90.44(4)
Ni-N(1)	2.102(3)	O(1)#1-NI-CL	91.29(3)
Ni-O(1)#1	2.108(2)	O(1)-NI-CL	88.71(3)
Ni-O(1)	2.108(2)	N(1)#1-NI-CL#1	90.44(4)
Ni-Cl	2.4239(10)	N(1)-NI-CL#1	89.56(4)
Ni-Cl#1	2.4239(10)	O(1)#1-NI-CL#1	88.71(3)
N(1)-C(5)	1.336(3)	O(1)-NI-CL#1	91.29(3)
N(1)-N(2)	1.355(3)	CL-NI-CL#1	180
N(2)-C(3)	1.339(3)	C(5)-N(1)-N(2)	104.8(2)
C(3)-C(4)	1.365(4)	C(5)-N(1)-NI	136.41(18)
C(3)-C(6)	1.496(4)	N(2)-N(1)-NI	118.77(16)
C(4)-C(5)	1.402(4)	C(3)-N(2)-N(1)	112.7(2)
C(5)-C(7)	1.490(4)	N(2)-C(3)-C(4)	106.2(2)
N(1)#1-NI-N(1)	180	N(2)-C(3)-C(6)	121.3(3)
N(1)#1-NI-O(1)#1	90.76(9)	C(4)-C(3)-C(6)	132.5(3)
N(1)-NI-O(1)#1	89.24(9)	C(3)-C(4)-C(5)	106.3(2)
N(1)#1-NI-O(1)	89.24(9)	N(1)-C(5)-C(4)	110.0(2)
N(1)-NI-O(1)	90.76(9)	N(1)-C(5)-C(7)	123.2(2)
O(1)#1-NI-O(1)	180	C(4)-C(5)-C(7)	126.8(2)
N(1)#1-NI-CL	89.56(4)		

Symmetry transformations used to generate equivalent atoms:

#1 -x+1,-y+1,-z+1

Table IV-31. Torsion angles [°] for $[(Pz^{Me2})_2NiCl_2(H_2O)_2]$ (**5.10b**).

N(1)#1-NI-N(1)-C(5)	-101(100)	N(1)-N(2)-C(3)-C(4)	-0.5(3)
O(1)#1-NI-N(1)-C(5)	40.7(2)	N(1)-N(2)-C(3)-C(6)	179.3(3)
O(1)-NI-N(1)-C(5)	-139.3(2)	N(2)-C(3)-C(4)-C(5)	0.5(3)
CL-NI-N(1)-C(5)	-50.6(2)	C(6)-C(3)-C(4)-C(5)	-179.2(3)
CL#1-NI-N(1)-C(5)	129.4(2)	N(2)-N(1)-C(5)-C(4)	0.1(3)
N(1)#1-NI-N(1)-N(2)	80(100)	NI-N(1)-C(5)-C(4)	-179.5(2)
O(1)#1-NI-N(1)-N(2)	-138.90(17)	N(2)-N(1)-C(5)-C(7)	-179.6(3)
O(1)-NI-N(1)-N(2)	41.10(17)	NI-N(1)-C(5)-C(7)	0.8(4)
CL-NI-N(1)-N(2)	129.82(17)	C(3)-C(4)-C(5)-N(1)	-0.4(3)
CL#1-NI-N(1)-N(2)	-50.18(17)	C(3)-C(4)-C(5)-C(7)	179.3(3)
C(5)-N(1)-N(2)-C(3)	0.3(3)		
NI-N(1)-N(2)-C(3)	179.96(16)		

Symmetry transformations used to generate equivalent atoms:

#1 -x+1,-y+1,-z+1

Table IV-32. Bond lengths [Å] and angles [°] related to the hydrogen bonding for $[(Pz^{Me2})_2NiCl_2(H_2O)_2]$ (**5.10b**).

D-H	..A	d(D-H)	d(H..A)	d(D..A)	<DHA
O(1)-H(1A)	CL#2	0.82	2.292(5)	3.1039(19)	170(3)
O(1)-H(1B)	CL#3	0.82	2.348(4)	3.1588(19)	170.30(19)
N(2)-H(2)	CL#3	0.86	2.41	3.246(2)	163.1

Symmetry transformations used to generate equivalent atoms:

#1 -x+1,-y+1,-z+1 #2 x,-y+1/2,z-1/2
#3 -x+1,y+1/2,-z+1/2

Table IV-33. Crystal data and structure refinement for $[(Pz^{Me2})_2NiBr_2]$ **(5.11)**.

Identification code	nath32
Empirical formula	C10 H16 Br2 N4 Ni
Formula weight	410.80
Temperature	100(2)K
Wavelength	1.54178 Å
Crystal system	Triclinic
Space group	P-1
Unit cell dimensions	a = 7.9879(2) Å α = 82.9800(10)° b = 8.2289(2) Å β = 75.195(2)° c = 12.3768(3) Å γ = 66.799(2)°
Volume	722.72(3)Å^3
Z	2
Density (calculated)	1.888 Mg/m^3
Absorption coefficient	8.291 mm^{-1}
F(000)	404
Crystal size	0.70 x 0.42 x 0.15 mm
Theta range for data collection	3.69 to 72.70°
Index ranges	$-9 \leq h \leq 8$, $-10 \leq k \leq 10$, $-15 \leq \ell \leq 15$
Reflections collected	8722
Independent reflections	2752 [R_{int} = 0.057]
Absorption correction	Semi-empirical from equivalents
Max. and min. transmission	0.4600 and 0.1400
Refinement method	Full-matrix least-squares on F^2
Data / restraints / parameters	2752 / 0 / 159
Goodness-of-fit on F^2	1.139
Final R indices [I>2sigma(I)]	R_1 = 0.0589, wR_2 = 0.1550
R indices (all data)	R_1 = 0.0602, wR_2 = 0.1567
Extinction coefficient	0.0013(5)
Largest diff. peak and hole	1.696 and -1.564 e/Å^3

Table IV-34. Atomic coordinates (x 10^4) and equivalent isotropic displacement parameters ($Å^2$ x 10^3) for $[(Pz^{Me2})_2NiBr_2]$ (**5.11**).

U_{eq} is defined as one third of the trace of the orthogonalized Uij tensor.

	x	y	z	U_{eq}
Ni	5622(1)	7262(1)	7408(1)	16(1)
Br(1)	7028(1)	8616(1)	5841(1)	22(1)
Br(2)	7205(1)	5000(1)	8601(1)	21(1)
C(1)	2504(6)	6754(5)	5376(3)	19(1)
C(2)	1784(6)	5921(6)	6314(4)	21(1)
C(3)	2719(6)	5907(6)	7134(4)	20(1)
C(4)	2464(7)	5205(7)	8305(4)	27(1)
C(5)	2045(7)	7178(6)	4249(4)	26(1)
C(6)	2423(6)	10016(5)	10275(3)	18(1)
C(7)	1571(6)	11269(6)	9534(4)	21(1)
C(8)	2485(6)	10557(5)	8461(3)	19(1)
C(9)	2133(7)	11332(7)	7358(4)	28(1)
C(10)	2051(7)	9981(6)	11530(4)	26(1)
N(1)	3941(5)	6702(5)	6724(3)	17(1)
N(2)	3791(5)	7197(5)	5646(3)	18(1)
N(3)	3818(5)	8962(5)	8556(3)	17(1)
N(4)	3743(5)	8666(5)	9667(3)	19(1)

Table IV-35. Hydrogen coordinates (x 10^4) and isotropic displacement parameters ($Å^2$ x 10^3) for $[(Pz^{Me2})_2NiBr_2]$ (**5.11**).

	x	y	z	U_{eq}
H(2)	846	5453	6386	25
H(4A)	3370	3989	8334	40
H(4B)	1192	5218	8566	40
H(4C)	2661	5944	8785	40
H(5A)	1179	8411	4221	39
H(5B)	1461	6396	4116	39
H(5C)	3196	7003	3672	39
H(7)	577	12380	9709	26
H(9A)	3130	11743	6963	42
H(9B)	926	12333	7464	42
H(9C)	2109	10434	6916	42
H(10A)	1537	9075	11837	38
H(10B)	1150	11139	11811	38
H(10C)	3222	9705	11760	38
H(2)	4455	7739	5187	22
H(4)	4477	7698	9955	22

Table IV-36. Anisotropic parameters ($Å^2$ x 10^3) for $[(Pz^{Me2})_2NiBr_2]$ (**5.11**).

The anisotropic displacement factor exponent takes the form:

$$-2\pi^2 [h^2 a^{*2} U_{11} + ... + 2 h k a^* b^* U_{12}]$$

	U11	U22	U33	U23	U13	U12
Ni	19(1)	13(1)	13(1)	-3(1)	-6(1)	0(1)
Br(1)	22(1)	26(1)	17(1)	3(1)	-7(1)	-7(1)
Br(2)	22(1)	16(1)	17(1)	-1(1)	-7(1)	3(1)
C(1)	19(2)	15(2)	17(2)	-8(2)	-5(2)	1(2)
C(2)	22(2)	21(2)	22(2)	0(2)	-9(2)	-8(2)
C(3)	22(2)	14(2)	20(2)	-2(2)	-5(2)	-2(2)
C(4)	33(3)	31(2)	19(2)	7(2)	-12(2)	-14(2)
C(5)	29(2)	29(2)	17(2)	-6(2)	-10(2)	-4(2)
C(6)	21(2)	16(2)	18(2)	-4(2)	-4(2)	-6(2)
C(7)	23(2)	14(2)	19(2)	-3(2)	-2(2)	0(2)
C(8)	24(2)	8(2)	18(2)	-2(2)	-4(2)	0(2)
C(9)	31(3)	24(2)	17(2)	-2(2)	-7(2)	3(2)
C(10)	36(3)	23(2)	14(2)	-3(2)	-6(2)	-6(2)
N(1)	21(2)	15(2)	13(2)	-1(1)	-5(1)	-4(1)
N(2)	22(2)	18(2)	15(2)	-2(1)	-8(1)	-4(1)
N(3)	22(2)	14(2)	15(2)	-2(1)	-9(1)	-2(1)
N(4)	25(2)	15(2)	13(2)	-2(1)	-6(1)	-3(1)

Table IV-37. Bond lengths [Å] and angles [°] for $[(Pz^{Me2})_2NiBr_2]$ (**5.11**).

Ni-N(1)	1.974(4)	N(2)-C(1)-C(2)	106.7(4)
Ni-N(3)	1.975(4)	N(2)-C(1)-C(5)	122.2(4)
Ni-Br(1)	2.3682(8)	C(2)-C(1)-C(5)	131.0(4)
Ni-Br(2)	2.3814(7)	C(1)-C(2)-C(3)	106.2(4)
C(1)-N(2)	1.342(6)	N(1)-C(3)-C(2)	109.6(4)
C(1)-C(2)	1.387(6)	N(1)-C(3)-C(4)	121.6(4)
C(1)-C(5)	1.498(6)	C(2)-C(3)-C(4)	128.8(4)
C(2)-C(3)	1.403(6)	N(4)-C(6)-C(7)	106.8(4)
C(3)-N(1)	1.344(6)	N(4)-C(6)-C(10)	122.0(4)
C(3)-C(4)	1.487(6)	C(7)-C(6)-C(10)	131.2(4)
C(6)-N(4)	1.337(5)	C(6)-C(7)-C(8)	105.8(4)
C(6)-C(7)	1.379(6)	N(3)-C(8)-C(7)	109.5(4)
C(6)-C(10)	1.504(6)	N(3)-C(8)-C(9)	121.5(4)
C(7)-C(8)	1.414(6)	C(7)-C(8)-C(9)	129.1(4)
C(8)-N(3)	1.340(5)	C(3)-N(1)-N(2)	105.9(3)
C(8)-C(9)	1.480(6)	C(3)-N(1)-NI	132.2(3)
N(1)-N(2)	1.368(5)	N(2)-N(1)-NI	121.8(3)
N(3)-N(4)	1.358(5)	C(1)-N(2)-N(1)	111.6(4)
N(1)-NI-N(3)	101.71(15)	C(8)-N(3)-N(4)	105.8(3)
N(1)-NI-BR1	99.34(11)	C(8)-N(3)-NI	131.0(3)
N(3)-NI-BR1	113.22(11)	N(4)-N(3)-NI	123.2(3)
N(1)-NI-BR2	115.24(11)	C(6)-N(4)-N(3)	112.2(3)
N(3)-NI-BR2	98.93(10)		
BR1-NI-BR2	126.39(3)		

Table IV-38. Torsion angles [°] for $[(Pz^{Me2})_2NiBr_2]$ (**5.11**).

N(2)-C(1)-C(2)-C(3)	0.0(5)	C(5)-C(1)-N(2)-N(1)	178.9(4)
C(5)-C(1)-C(2)-C(3)	-179.2(4)	C(3)-N(1)-N(2)-C(1)	0.6(5)
C(1)-C(2)-C(3)-N(1)	0.4(5)	NI-N(1)-N(2)-C(1)	-177.0(3)
C(1)-C(2)-C(3)-C(4)	178.8(4)	C(7)-C(8)-N(3)-N(4)	0.3(5)
N(4)-C(6)-C(7)-C(8)	-0.1(5)	C(9)-C(8)-N(3)-N(4)	-179.5(4)
C(10)-C(6)-C(7)-C(8)	-178.5(5)	C(7)-C(8)-N(3)-NI	-179.3(3)
C(6)-C(7)-C(8)-N(3)	-0.2(5)	C(9)-C(8)-N(3)-NI	0.9(7)
C(6)-C(7)-C(8)-C(9)	179.6(5)	N(1)-NI-N(3)-C(8)	-62.0(4)
C(2)-C(3)-N(1)-N(2)	-0.6(5)	BR1-NI-N(3)-C(8)	43.6(4)
C(4)-C(3)-N(1)-N(2)	-179.2(4)	BR2-NI-N(3)-C(8)	179.7(4)
C(2)-C(3)-N(1)-NI	176.7(3)	N(1)-NI-N(3)-N(4)	118.4(3)
C(4)-C(3)-N(1)-NI	-1.9(6)	BR1-NI-N(3)-N(4)	-136.0(3)
N(3)-NI-N(1)-C(3)	-64.1(4)	BR2-NI-N(3)-N(4)	0.1(3)
BR1-NI-N(1)-C(3)	179.6(4)	C(7)-C(6)-N(4)-N(3)	0.3(5)
BR2-NI-N(1)-C(3)	41.7(4)	C(10)-C(6)-N(4)-N(3)	178.9(4)
N(3)-NI-N(1)-N(2)	112.8(3)	C(8)-N(3)-N(4)-C(6)	-0.4(5)
BR1-NI-N(1)-N(2)	-3.5(3)	NI-N(3)-N(4)-C(6)	179.3(3)
BR2-NI-N(1)-N(2)	-141.4(3)		
C(2)-C(1)-N(2)-N(1)	-0.4(5)		

Table IV-39. Crystal data and structure refinement for $[(Pz^{Me2})_2PdCl_2]$ (5.12).

Identification code	NATHA5
Empirical formula	C23 H35 Cl4 N8 Pd2
Formula weight	778.19
Temperature	100(2)K
Wavelength	1.54178 Å
Crystal system	Monoclinic
Space group	$P2_1/c$
Unit cell dimensions	a = 17.5600(3) Å α = 90° b = 12.9457(2) Å β = 102.4970(10)° c = 14.1056(3) Å γ = 90°
Volume	3130.60(10)Å^3
Z	4
Density (calculated)	1.651 Mg/m^3
Absorption coefficient	12.628 mm^{-1}
F(000)	1556
Crystal size	0.49 x 0.41 x 0.10 mm
Theta range for data collection	2.58 to 72.99°
Index ranges	$-21 \le h \le 21$, $-15 \le k \le 16$, $-14 \le \ell \le 16$
Reflections collected	38101
Independent reflections	6154 [R_{int} = 0.092]
Absorption correction	Semi-empirical from equivalents
Max. and min. transmission	0.4500 and 0.1100
Refinement method	Full-matrix least-squares on F^2
Data / restraints / parameters	6154 / 0 / 342
Goodness-of-fit on F^2	1.029
Final R indices [I>2sigma(I)]	R_1 = 0.0462, wR_2 = 0.1147
R indices (all data)	R_1 = 0.0555, wR_2 = 0.1199
Largest diff. peak and hole	1.931 and -1.081 e/Å^3

Table IV-40. Atomic coordinates (x 10^4) and equivalent isotropic displacement parameters ($Å^2$ x 10^3) for $[(Pz^{Me2})_2PdCl_2]$ **(5.12)**.

U_{eq} is defined as one third of the trace of the orthogonalized Uij tensor.

	x	y	z	U_{eq}
Pd(1)	3224(1)	4836(1)	3232(1)	19(1)
Pd(2)	1174(1)	5058(1)	3564(1)	17(1)
Cl(11)	3390(1)	3253(1)	3996(1)	25(1)
Cl(12)	3042(1)	6417(1)	2479(1)	23(1)
Cl(13)	1586(1)	4238(1)	5028(1)	23(1)
Cl(14)	816(1)	5893(1)	2093(1)	22(1)
N(11)	3630(2)	5508(3)	4526(3)	22(1)
N(12)	3272(2)	5364(3)	5276(3)	23(1)
N(21)	2792(2)	4162(3)	1944(3)	22(1)
N(22)	2064(2)	4422(3)	1437(3)	22(1)
N(31)	1413(2)	6422(3)	4236(3)	20(1)
N(32)	1991(2)	7029(3)	4027(3)	21(1)
N(41)	989(2)	3664(3)	2921(3)	20(1)
N(42)	1580(2)	2975(3)	3060(3)	22(1)
C(1)	5232(3)	9307(5)	5728(5)	52(2)
C(2)	4544(4)	9831(5)	5670(5)	54(2)
C(3)	4312(3)	10530(5)	4930(5)	54(2)
C(13)	3637(3)	5886(4)	6060(3)	32(1)
C(14)	4261(3)	6381(4)	5817(4)	40(1)
C(15)	4239(2)	6131(4)	4853(4)	33(1)
C(16)	3354(3)	5855(4)	6991(4)	42(1)
C(17)	4783(3)	6446(5)	4221(4)	43(1)
C(23)	1841(2)	3820(3)	649(3)	25(1)
C(24)	2456(3)	3165(4)	638(3)	29(1)
C(25)	3033(2)	3382(3)	1458(3)	26(1)
C(26)	1062(3)	3928(4)	-7(3)	34(1)
C(27)	3812(3)	2880(4)	1792(4)	40(1)
C(32)	2777(3)	8586(4)	4585(4)	36(1)
C(33)	2161(2)	7809(3)	4653(3)	27(1)
C(34)	1670(2)	7723(3)	5282(3)	26(1)
C(35)	1212(2)	6857(3)	5015(3)	23(1)
C(36)	588(2)	6412(4)	5459(3)	30(1)
C(43)	1375(2)	2110(3)	2547(3)	23(1)
C(44)	616(2)	2243(3)	2066(3)	26(1)
C(45)	390(2)	3218(4)	2307(3)	25(1)
C(46)	-389(2)	3732(4)	1994(3)	29(1)
C(47)	1935(3)	1231(4)	2587(4)	31(1)

Table IV-41. Hydrogen coordinates (x 10^4) and isotropic displacement parameters ($Å^2$ x 10^3) for $[(Pz^{Me2})_2PdCl_2]$ (**5.12**).

	x	y	z	U_{eq}
H(12)	2855	4979	5250	27
H(22)	1778	4919	1604	26
H(32)	2222	6920	3541	25
H(42)	2041	3081	3439	26
H(1)	5395	8821	6235	62
H(2)	4234	9714	6134	65
H(3)	3836	10898	4876	64
H(14)	4633	6809	6226	48
H(16A)	2830	6155	6885	62
H(16B)	3710	6254	7490	62
H(16C)	3338	5138	7207	62
H(17A)	4734	5963	3676	65
H(17B)	5321	6438	4602	65
H(17C)	4651	7145	3971	65
H(24)	2482	2658	160	35
H(26A)	716	4312	325	51
H(26B)	843	3242	-187	51
H(26C)	1114	4303	-594	51
H(27A)	4187	3389	2128	60
H(27B)	3991	2607	1230	60
H(27C)	3767	2313	2238	60
H(32A)	3283	8238	4666	54
H(32B)	2803	9106	5096	54
H(32C)	2650	8924	3948	54
H(34)	1647	8175	5806	31
H(36A)	151	6184	4945	45
H(36B)	406	6938	5858	45
H(36C)	797	5820	5867	45
H(44)	303	1759	1646	31
H(46A)	-376	4409	2307	44
H(46B)	-791	3302	2184	44
H(46C)	-510	3820	1287	44
H(47A)	2254	1341	2105	46
H(47B)	1644	584	2443	46
H(47C)	2273	1193	3237	46

Table IV-42. Anisotropic parameters ($Å^2 \times 10^3$) for $[(Pz^{Me2})_2PdCl_2]$ **(5.12)**.

The anisotropic displacement factor exponent takes the form:

$$-2\pi^2 [h^2 a^{*2} U_{11} + \ldots + 2 h k a^* b^* U_{12}]$$

	U11	U22	U33	U23	U13	U12
Pd(1)	10(1)	22(1)	24(1)	1(1)	2(1)	0(1)
Pd(2)	10(1)	20(1)	22(1)	0(1)	1(1)	0(1)
Cl(11)	15(1)	26(1)	32(1)	5(1)	0(1)	0(1)
Cl(12)	18(1)	24(1)	28(1)	2(1)	3(1)	-1(1)
Cl(13)	17(1)	25(1)	25(1)	3(1)	2(1)	-1(1)
Cl(14)	17(1)	24(1)	25(1)	2(1)	3(1)	3(1)
N(11)	14(2)	28(2)	24(2)	3(2)	-1(1)	-6(1)
N(12)	18(2)	26(2)	23(2)	-2(2)	2(1)	-4(1)
N(21)	16(2)	25(2)	24(2)	-3(1)	3(1)	-1(1)
N(22)	14(2)	26(2)	26(2)	1(2)	3(1)	2(1)
N(31)	14(2)	19(2)	26(2)	-1(1)	3(1)	-1(1)
N(32)	13(2)	23(2)	25(2)	-1(1)	3(1)	-1(1)
N(41)	12(2)	20(2)	28(2)	0(1)	2(1)	-1(1)
N(42)	15(2)	18(2)	30(2)	0(1)	1(1)	-2(1)
C(1)	45(3)	38(3)	65(4)	-2(3)	-1(3)	-7(3)
C(2)	38(3)	62(4)	62(4)	-13(3)	11(3)	-16(3)
C(3)	27(3)	59(4)	71(5)	-16(3)	2(3)	1(3)
C(13)	35(2)	27(2)	29(3)	-2(2)	-2(2)	-2(2)
C(14)	38(3)	36(3)	39(3)	-1(2)	-6(2)	-16(2)
C(15)	19(2)	39(3)	37(3)	9(2)	-4(2)	-12(2)
C(16)	61(3)	31(3)	33(3)	-4(2)	9(3)	-3(2)
C(17)	21(2)	63(4)	42(3)	16(3)	-1(2)	-21(2)
C(23)	22(2)	26(2)	26(2)	-2(2)	5(2)	-4(2)
C(24)	31(2)	26(2)	32(3)	-6(2)	9(2)	1(2)
C(25)	27(2)	24(2)	29(3)	1(2)	12(2)	6(2)
C(26)	26(2)	46(3)	28(3)	-6(2)	0(2)	-8(2)
C(27)	32(3)	45(3)	46(3)	2(2)	15(2)	17(2)
C(32)	32(2)	30(3)	45(3)	-6(2)	8(2)	-10(2)
C(33)	21(2)	23(2)	33(3)	-1(2)	-2(2)	0(2)
C(34)	22(2)	26(2)	25(2)	-6(2)	0(2)	2(2)
C(35)	16(2)	28(2)	23(2)	0(2)	0(2)	6(2)
C(36)	23(2)	40(3)	29(3)	1(2)	9(2)	1(2)
C(43)	25(2)	21(2)	25(2)	1(2)	7(2)	-3(2)
C(44)	22(2)	28(2)	26(2)	-1(2)	2(2)	-9(2)
C(45)	15(2)	35(3)	23(2)	0(2)	4(2)	-6(2)
C(46)	14(2)	36(3)	36(3)	-2(2)	1(2)	-4(2)
C(47)	31(2)	26(2)	35(3)	-2(2)	2(2)	3(2)

Table IV-43. Bond lengths [Å] and angles [°] for $[(Pz^{Me2})_2PdCl_2]$ **(5.12)**.

		N(41)-PD2-CL14	91.63(10)
Pd(1)-N(11)	2.008(4)	CL13-PD2-CL14	177.47(3)
Pd(1)-N(21)	2.011(4)	C(15)-N(11)-N(12)	106.6(4)
Pd(1)-Cl(12)	2.296(1)	C(15)-N(11)-PD1	132.4(3)
Pd(1)-Cl(11)	2.3041(10)	N(12)-N(11)-PD1	121.1(3)
Pd(2)-N(31)	2.005(3)	C(13)-N(12)-N(11)	110.8(4)
Pd(2)-N(41)	2.015(3)	C(25)-N(21)-N(22)	106.4(4)
Pd(2)-Cl(13)	2.2954(10)	C(25)-N(21)-PD1	133.6(3)
Pd(2)-Cl(14)	2.3038(10)	N(22)-N(21)-PD1	119.6(3)
N(11)-C(15)	1.338(5)	C(23)-N(22)-N(21)	111.3(3)
N(11)-N(12)	1.355(5)	C(35)-N(31)-N(32)	105.9(3)
N(12)-C(13)	1.335(6)	C(35)-N(31)-PD2	133.5(3)
N(21)-C(25)	1.339(5)	N(32)-N(31)-PD2	119.6(2)
N(21)-N(22)	1.364(4)	C(33)-N(32)-N(31)	111.2(3)
N(22)-C(23)	1.343(5)	C(45)-N(41)-N(42)	106.3(3)
N(31)-C(35)	1.347(5)	C(45)-N(41)-PD2	134.8(3)
N(31)-N(32)	1.366(4)	N(42)-N(41)-PD2	118.9(2)
N(32)-C(33)	1.332(5)	C(43)-N(42)-N(41)	111.5(3)
N(41)-C(45)	1.340(5)	C(3)#1-C(1)-C(2)	121.4(6)
N(41)-N(42)	1.350(4)	C(1)-C(2)-C(3)	118.8(6)
N(42)-C(43)	1.339(5)	C(1)#1-C(3)-C(2)	119.7(6)
C(1)-C(3)#1	1.367(8)	N(12)-C(13)-C(14)	107.2(4)
C(1)-C(2)	1.373(8)	N(12)-C(13)-C(16)	121.3(4)
C(2)-C(3)	1.375(9)	C(14)-C(13)-C(16)	131.5(5)
C(3)-C(1)#1	1.367(8)	C(13)-C(14)-C(15)	106.2(4)
C(13)-C(14)	1.375(7)	N(11)-C(15)-C(14)	109.2(4)
C(13)-C(16)	1.503(7)	N(11)-C(15)-C(17)	121.6(4)
C(14)-C(15)	1.390(7)	C(14)-C(15)-C(17)	129.2(4)
C(15)-C(17)	1.498(6)	N(22)-C(23)-C(24)	106.1(4)
C(23)-C(24)	1.375(6)	N(22)-C(23)-C(26)	121.7(4)
C(23)-C(26)	1.483(6)	C(24)-C(23)-C(26)	132.2(4)
C(24)-C(25)	1.392(6)	C(23)-C(24)-C(25)	107.4(4)
C(25)-C(27)	1.495(6)	N(21)-C(25)-C(24)	108.8(4)
C(32)-C(33)	1.496(6)	N(21)-C(25)-C(27)	122.4(4)
C(33)-C(34)	1.369(6)	C(24)-C(25)-C(27)	128.8(4)
C(34)-C(35)	1.383(6)	N(32)-C(33)-C(34)	106.7(4)
C(35)-C(36)	1.492(5)	N(32)-C(33)-C(32)	121.9(4)
C(43)-C(44)	1.371(6)	C(34)-C(33)-C(32)	131.5(4)
C(43)-C(47)	1.496(6)	C(33)-C(34)-C(35)	107.4(4)
C(44)-C(45)	1.387(6)	N(31)-C(35)-C(34)	108.8(4)
C(45)-C(46)	1.499(6)	N(31)-C(35)-C(36)	121.8(4)
N(11)-PD1-N(21)	178.61(13)	C(34)-C(35)-C(36)	129.4(4)
N(11)-PD1-CL12	91.21(11)	N(42)-C(43)-C(44)	106.3(4)
N(21)-PD1-CL12	88.92(10)	N(42)-C(43)-C(47)	121.3(4)
N(11)-PD1-CL11	88.62(11)	C(44)-C(43)-C(47)	132.4(4)
N(21)-PD1-CL11	91.23(11)	C(43)-C(44)-C(45)	107.0(4)
CL12-PD1-CL11	179.13(4)	N(41)-C(45)-C(44)	108.9(4)
N(31)-PD2-N(41)	177.07(13)	N(41)-C(45)-C(46)	122.5(4)
N(31)-PD2-CL13	89.39(10)	C(44)-C(45)-C(46)	128.5(4)
N(41)-PD2-CL13	88.84(10)		
N(31)-PD2-CL14	90.04(10)		

Symmetry transformations used to generate equivalent atoms:

#1 -x+1,-y+2,-z+1

Table IV-44. Torsion angles [°] for $[(Pz^{Me2})_2PdCl_2]$ (**5.12**).

N(21)-PD1-N(11)-C(15)	-155(6)	N(12)-N(11)-C(15)-C(14)	-0.1(5)
CL12-PD1-N(11)-C(15)	-59.9(4)	PD1-N(11)-C(15)-C(14)	179.9(3)
CL11-PD1-N(11)-C(15)	121.0(4)	N(12)-N(11)-C(15)-C(17)	179.0(4)
N(21)-PD1-N(11)-N(12)	25(6)	PD1-N(11)-C(15)-C(17)	-1.0(7)
CL12-PD1-N(11)-N(12)	120.2(3)	C(13)-C(14)-C(15)-N(11)	-0.2(6)
CL11-PD1-N(11)-N(12)	-58.9(3)	C(13)-C(14)-C(15)-C(17)	-179.2(5)
C(15)-N(11)-N(12)-C(13)	0.4(5)	N(21)-N(22)-C(23)-C(24)	-1.4(5)
PD1-N(11)-N(12)-C(13)	-179.6(3)	N(21)-N(22)-C(23)-C(26)	178.2(4)
N(11)-PD1-N(21)-C(25)	-133(6)	N(22)-C(23)-C(24)-C(25)	1.7(5)
CL12-PD1-N(21)-C(25)	131.1(4)	C(26)-C(23)-C(24)-C(25)	-177.8(5)
CL11-PD1-N(21)-C(25)	-49.8(4)	N(22)-N(21)-C(25)-C(24)	0.7(5)
N(11)-PD1-N(21)-N(22)	39(6)	PD1-N(21)-C(25)-C(24)	173.4(3)
CL12-PD1-N(21)-N(22)	-56.9(3)	N(22)-N(21)-C(25)-C(27)	-179.8(4)
CL11-PD1-N(21)-N(22)	122.2(3)	PD1-N(21)-C(25)-C(27)	-7.1(7)
C(25)-N(21)-N(22)-C(23)	0.5(5)	C(23)-C(24)-C(25)-N(21)	-1.5(5)
PD1-N(21)-N(22)-C(23)	-173.5(3)	C(23)-C(24)-C(25)-C(27)	179.0(4)
N(41)-PD2-N(31)-C(35)	-105(3)	N(31)-N(32)-C(33)-C(34)	-1.1(5)
CL13-PD2-N(31)-C(35)	-52.1(4)	N(31)-N(32)-C(33)-C(32)	179.8(4)
CL14-PD2-N(31)-C(35)	130.4(4)	N(32)-C(33)-C(34)-C(35)	0.9(5)
N(41)-PD2-N(31)-N(32)	62(3)	C(32)-C(33)-C(34)-C(35)	179.9(5)
CL13-PD2-N(31)-N(32)	114.6(3)	N(32)-N(31)-C(35)-C(34)	-0.3(4)
CL14-PD2-N(31)-N(32)	-63.0(3)	PD2-N(31)-C(35)-C(34)	167.7(3)
C(35)-N(31)-N(32)-C(33)	0.9(5)	N(32)-N(31)-C(35)-C(36)	179.7(4)
PD2-N(31)-N(32)-C(33)	-169.1(3)	PD2-N(31)-C(35)-C(36)	-12.4(6)
N(31)-PD2-N(41)-C(45)	-178(35)	C(33)-C(34)-C(35)-N(31)	-0.4(5)
CL13-PD2-N(41)-C(45)	129.1(4)	C(33)-C(34)-C(35)-C(36)	179.7(4)
CL14-PD2-N(41)-C(45)	-53.4(4)	N(41)-N(42)-C(43)-C(44)	-0.7(5)
N(31)-PD2-N(41)-N(42)	-2(3)	N(41)-N(42)-C(43)-C(47)	-179.9(4)
CL13-PD2-N(41)-N(42)	-54.4(3)	N(42)-C(43)-C(44)-C(45)	0.7(5)
CL14-PD2-N(41)-N(42)	123.1(3)	C(47)-C(43)-C(44)-C(45)	179.7(5)
C(45)-N(41)-N(42)-C(43)	0.5(5)	N(42)-N(41)-C(45)-C(44)	0.0(5)
PD2-N(41)-N(42)-C(43)	-177.0(3)	PD2-N(41)-C(45)-C(44)	176.8(3)
C(3)#1-C(1)-C(2)-C(3)	0.3(1)	N(42)-N(41)-C(45)-C(46)	178.1(4)
C(1)-C(2)-C(3)-C(1)#1	-0.3(1)	PD2-N(41)-C(45)-C(46)	-5.0(7)
N(11)-N(12)-C(13)-C(14)	-0.6(5)	C(43)-C(44)-C(45)-N(41)	-0.4(5)
N(11)-N(12)-C(13)-C(16)	180.0(4)	C(43)-C(44)-C(45)-C(46)	-178.4(4)
N(12)-C(13)-C(14)-C(15)	0.5(6)		
C(16)-C(13)-C(14)-C(15)	179.9(5)		

Symmetry transformations used to generate equivalent atoms:
#1 -x+1,-y+2,-z+1

Table IV-45. Bond lengths [Å] and angles [°] related to the hydrogen bonding for $[(Pz^{Me2})_2PdCl_2]$ (**5.12**).

D-H	..A	d(D-H)	d(H..A)	d(D..A)	<DHA
N(12)-H(12)	CL13	0.88	2.38	3.251(3)	168.3
N(22)-H(22)	CL14	0.88	2.33	3.188(3)	165.6
N(32)-H(32)	CL12	0.88	2.38	3.246(3)	167.6
N(42)-H(42)	CL11	0.88	2.34	3.188(3)	162.1

Symmetry transformations used to generate equivalent atoms:

#1 -x+1,-y+2,-z+1

Table IV-46. Crystal data and structure refinement for (dpdpm)$CuBr_2$ (5.13).

Identification code	nath34
Empirical formula	C19 H16 Br2 Cu N4
Formula weight	523.72
Temperature	150(2)K
Wavelength	1.54178 Å
Crystal system	Triclinic
Space group	P-1
Unit cell dimensions	a = 7.55720(10) Å α = 99.1930(10)° b = 9.1562(2) Å β = 106.7060(10)° c = 14.4575(2) Å γ = 90.2830(10)°
Volume	944.49(3)Å^3
Z	2
Density (calculated)	1.842 g/cm^3
Absorption coefficient	6.666 mm^{-1}
F(000)	514
Crystal size	0.22 x 0.16 x 0.16 mm
Theta range for data collection	3.24 to 68.25°
Index ranges	$-8 \le h \le 8$, $-10 \le k \le 11$, $-17 \le \ell \le 17$
Reflections collected	12265
Independent reflections	3312 [R_{int} = 0.031]
Absorption correction	Semi-empirical from equivalents
Max. and min. transmission	0.5000 and 0.3300
Refinement method	Full-matrix least-squares on F^2
Data / restraints / parameters	3312 / 0 / 235
Goodness-of-fit on F^2	1.042
Final R indices [I>2sigma(I)]	R_1 = 0.0483, wR_2 = 0.1388
R indices (all data)	R_1 = 0.0485, wR_2 = 0.1390
Largest diff. peak and hole	0.876 and -1.588 e/Å^3

Table IV-47. Atomic coordinates (x 10^4) and equivalent isotropic displacement parameters ($Å^2$ x 10^3) for (dpdpm)$CuBr_2$ (**5.13**).

U_{eq} is defined as one third of the trace of the orthogonalized Uij tensor.

	x	y	z	U_{eq}
Cu	3135(1)	5425(1)	8528(1)	14(1)
Br(1)	1878(1)	6607(1)	9713(1)	34(1)
Br(2)	2294(1)	7180(1)	7480(1)	31(1)
N(11)	3012(5)	3372(4)	8833(3)	14(1)
N(12)	3837(5)	2184(4)	8460(2)	13(1)
N(21)	5262(5)	4883(4)	8041(3)	14(1)
N(22)	5718(5)	3486(4)	7742(3)	12(1)
C(13)	3602(6)	986(5)	8863(3)	18(1)
C(14)	2646(7)	1416(6)	9533(3)	24(1)
C(15)	2319(7)	2897(6)	9494(3)	21(1)
C(23)	7287(6)	3555(5)	7467(3)	19(1)
C(24)	7876(6)	5002(5)	7614(4)	21(1)
C(25)	6571(7)	5799(5)	7976(3)	20(1)
C(31)	4384(6)	2217(4)	7561(3)	12(1)
C(41)	5403(6)	823(5)	7327(3)	14(1)
C(42)	7005(6)	510(5)	8027(3)	18(1)
C(43)	8068(7)	-636(5)	7786(4)	20(1)
C(44)	7536(7)	-1486(5)	6844(4)	23(1)
C(45)	5930(7)	-1199(5)	6168(3)	22(1)
C(46)	4866(6)	-39(5)	6402(3)	16(1)
C(51)	2657(6)	2386(5)	6732(3)	13(1)
C(52)	1057(6)	1507(5)	6606(3)	18(1)
C(53)	-485(7)	1553(6)	5814(3)	24(1)
C(54)	-473(7)	2472(6)	5142(3)	26(1)
C(55)	1101(7)	3349(5)	5267(3)	23(1)
C(56)	2670(7)	3308(5)	6052(3)	18(1)

Table IV-48. Hydrogen coordinates (x 10^4) and isotropic displacement parameters ($Å^2$ x 10^3) for (dpdpm)$CuBr_2$ (**5.13**).

	x	y	z	U_{eq}
H(13)	4020	25	8711	21
H(14)	2286	822	9937	28
H(15)	1687	3494	9883	25
H(23)	7871	2733	7214	23
H(24)	8945	5390	7497	26
H(25)	6616	6847	8149	23
H(42)	7363	1083	8666	21
H(43)	9157	-847	8259	24
H(44)	8279	-2256	6672	27
H(45)	5546	-1798	5537	26
H(46)	3772	162	5928	20
H(52)	1029	877	7064	21
H(53)	-1563	947	5732	29
H(54)	-1535	2499	4601	31
H(55)	1111	3988	4811	28
H(56)	3748	3906	6125	21

Table IV-49. Anisotropic parameters ($Å^2 \times 10^3$) for (dpdpm)$CuBr_2$ (**5.13**).

The anisotropic displacement factor exponent takes the form:

$$-2\pi^2 [h^2 a^{*2} U_{11} + \ldots + 2 h k a^* b^* U_{12}]$$

	U11	U22	U33	U23	U13	U12
Cu	14(1)	15(1)	13(1)	2(1)	6(1)	3(1)
Br(1)	33(1)	42(1)	27(1)	-4(1)	14(1)	4(1)
Br(2)	31(1)	28(1)	35(1)	13(1)	10(1)	9(1)
N(11)	13(2)	20(2)	11(2)	1(1)	6(1)	2(1)
N(12)	12(2)	16(2)	10(2)	2(1)	5(1)	2(1)
N(21)	15(2)	13(2)	13(2)	2(1)	4(1)	1(1)
N(22)	9(2)	15(2)	15(2)	4(1)	5(1)	2(1)
C(13)	19(2)	19(2)	17(2)	9(2)	3(2)	1(2)
C(14)	26(3)	30(3)	19(2)	12(2)	9(2)	-1(2)
C(15)	19(2)	32(3)	16(2)	5(2)	11(2)	3(2)
C(23)	14(2)	27(2)	22(2)	9(2)	11(2)	6(2)
C(24)	14(2)	28(2)	27(2)	9(2)	10(2)	-1(2)
C(25)	21(2)	17(2)	20(2)	4(2)	5(2)	-2(2)
C(31)	12(2)	13(2)	11(2)	3(2)	6(2)	1(2)
C(41)	15(2)	13(2)	15(2)	4(2)	7(2)	2(2)
C(42)	18(2)	18(2)	18(2)	5(2)	4(2)	2(2)
C(43)	18(2)	20(2)	25(2)	12(2)	8(2)	6(2)
C(44)	28(3)	17(2)	31(3)	8(2)	20(2)	9(2)
C(45)	29(3)	20(2)	19(2)	1(2)	12(2)	4(2)
C(46)	19(2)	16(2)	16(2)	4(2)	8(2)	3(2)
C(51)	15(2)	15(2)	9(2)	1(2)	3(2)	4(2)
C(52)	16(2)	24(2)	14(2)	2(2)	6(2)	0(2)
C(53)	15(2)	36(3)	19(2)	-1(2)	4(2)	1(2)
C(54)	22(3)	37(3)	14(2)	0(2)	-1(2)	11(2)
C(55)	31(3)	24(2)	13(2)	6(2)	4(2)	11(2)
C(56)	21(2)	16(2)	17(2)	3(2)	7(2)	5(2)

Table IV-50. Bond lengths [Å] and angles [°] for (dpdpm)$CuBr_2$ **(5.13)**.

		C(13)-N(12)-N(11)	110.4(3)
Cu-N(21)	1.967(4)	C(13)-N(12)-C(31)	127.8(4)
Cu-N(11)	2.006(4)	N(11)-N(12)-C(31)	119.7(3)
Cu-Br(1)	2.3167(8)	C(25)-N(21)-N(22)	106.5(4)
Cu-Br(2)	2.3488(8)	C(25)-N(21)-CU	126.9(3)
N(11)-C(15)	1.339(6)	N(22)-N(21)-CU	126.6(3)
N(11)-N(12)	1.369(5)	C(23)-N(22)-N(21)	109.5(4)
N(12)-C(13)	1.354(6)	C(23)-N(22)-C(31)	128.7(4)
N(12)-C(31)	1.478(5)	N(21)-N(22)-C(31)	120.3(3)
N(21)-C(25)	1.328(6)	N(12)-C(13)-C(14)	107.5(4)
N(21)-N(22)	1.362(5)	C(13)-C(14)-C(15)	105.6(4)
N(22)-C(23)	1.359(6)	N(11)-C(15)-C(14)	110.9(4)
N(22)-C(31)	1.475(5)	N(22)-C(23)-C(24)	108.2(4)
C(13)-C(14)	1.378(7)	C(23)-C(24)-C(25)	105.3(4)
C(14)-C(15)	1.386(7)	N(21)-C(25)-C(24)	110.4(4)
C(23)-C(24)	1.360(7)	N(22)-C(31)-N(12)	108.6(3)
C(24)-C(25)	1.399(7)	N(22)-C(31)-C(51)	110.3(3)
C(31)-C(51)	1.525(6)	N(12)-C(31)-C(51)	108.5(3)
C(31)-C(41)	1.535(6)	N(22)-C(31)-C(41)	106.3(3)
C(41)-C(46)	1.387(6)	N(12)-C(31)-C(41)	110.3(3)
C(41)-C(42)	1.401(6)	C(51)-C(31)-C(41)	112.7(3)
C(42)-C(43)	1.386(7)	C(46)-C(41)-C(42)	119.8(4)
C(43)-C(44)	1.401(7)	C(46)-C(41)-C(31)	120.7(4)
C(44)-C(45)	1.378(7)	C(42)-C(41)-C(31)	119.2(4)
C(45)-C(46)	1.393(7)	C(43)-C(42)-C(41)	119.9(4)
C(51)-C(56)	1.396(6)	C(42)-C(43)-C(44)	120.0(4)
C(51)-C(52)	1.400(6)	C(45)-C(44)-C(43)	119.8(4)
C(52)-C(53)	1.385(7)	C(44)-C(45)-C(46)	120.5(4)
C(53)-C(54)	1.385(7)	C(41)-C(46)-C(45)	120.0(4)
C(54)-C(55)	1.384(8)	C(56)-C(51)-C(52)	119.1(4)
C(55)-C(56)	1.391(7)	C(56)-C(51)-C(31)	121.8(4)
N(21)-CU-N(11)	88.71(15)	C(52)-C(51)-C(31)	118.9(4)
N(21)-CU-BR1	151.55(11)	C(53)-C(52)-C(51)	120.2(4)
N(11)-CU-BR1	97.32(10)	C(54)-C(53)-C(52)	120.7(5)
N(21)-CU-BR2	91.71(10)	C(55)-C(54)-C(53)	119.4(4)
N(11)-CU-BR2	152.11(11)	C(54)-C(55)-C(56)	120.8(4)
BR1-CU-BR2	95.49(3)	C(55)-C(56)-C(51)	119.9(4)
C(15)-N(11)-N(12)	105.6(4)		
C(15)-N(11)-CU	129.1(3)		
N(12)-N(11)-CU	125.0(3)		

Symmetry transformations used to generate equivalent atoms:

Table IV-51. Torsion angles [°] for (dpdpm)$CuBr_2$ (**5.13**).

N(21)-CU-N(11)-C(15)	154.9(4)	N(21)-N(22)-C(31)-C(41)	-175.1(3)
BR1-CU-N(11)-C(15)	2.8(4)	C(13)-N(12)-C(31)-N(22)	-138.6(4)
BR2-CU-N(11)-C(15)	-113.8(4)	N(11)-N(12)-C(31)-N(22)	59.7(5)
N(21)-CU-N(11)-N(12)	-17.3(3)	C(13)-N(12)-C(31)-C(51)	101.5(5)
BR1-CU-N(11)-N(12)	-169.4(3)	N(11)-N(12)-C(31)-C(51)	-60.2(5)
BR2-CU-N(11)-N(12)	73.9(4)	C(13)-N(12)-C(31)-C(41)	-22.5(6)
C(15)-N(11)-N(12)-C(13)	1.9(5)	N(11)-N(12)-C(31)-C(41)	175.9(3)
CU-N(11)-N(12)-C(13)	175.7(3)	N(22)-C(31)-C(41)-C(46)	-113.7(4)
C(15)-N(11)-N(12)-C(31)	166.6(4)	N(12)-C(31)-C(41)-C(46)	128.8(4)
CU-N(11)-N(12)-C(31)	-19.7(5)	C(51)-C(31)-C(41)-C(46)	7.3(5)
N(11)-CU-N(21)-C(25)	-156.4(4)	N(22)-C(31)-C(41)-C(42)	59.8(5)
BR1-CU-N(21)-C(25)	-53.4(5)	N(12)-C(31)-C(41)-C(42)	-57.7(5)
BR2-CU-N(21)-C(25)	51.5(4)	C(51)-C(31)-C(41)-C(42)	-179.2(4)
N(11)-CU-N(21)-N(22)	20.8(3)	C(46)-C(41)-C(42)-C(43)	1.5(6)
BR1-CU-N(21)-N(22)	123.8(3)	C(31)-C(41)-C(42)-C(43)	-172.1(4)
BR2-CU-N(21)-N(22)	-131.3(3)	C(41)-C(42)-C(43)-C(44)	-0.3(7)
C(25)-N(21)-N(22)-C(23)	-1.7(5)	C(42)-C(43)-C(44)-C(45)	-1.6(7)
CU-N(21)-N(22)-C(23)	-179.4(3)	C(43)-C(44)-C(45)-C(46)	2.3(7)
C(25)-N(21)-N(22)-C(31)	-169.2(4)	C(42)-C(41)-C(46)-C(45)	-0.8(6)
CU-N(21)-N(22)-C(31)	13.1(5)	C(31)-C(41)-C(46)-C(45)	172.7(4)
N(11)-N(12)-C(13)-C(14)	-1.7(5)	C(44)-C(45)-C(46)-C(41)	-1.1(7)
C(31)-N(12)-C(13)-C(14)	-164.7(4)	N(22)-C(31)-C(51)-C(56)	20.5(5)
N(12)-C(13)-C(14)-C(15)	0.7(5)	N(12)-C(31)-C(51)-C(56)	139.3(4)
N(12)-N(11)-C(15)-C(14)	-1.5(5)	C(41)-C(31)-C(51)-C(56)	-98.2(5)
CU-N(11)-C(15)-C(14)	-174.9(3)	N(22)-C(31)-C(51)-C(52)	-164.5(4)
C(13)-C(14)-C(15)-N(11)	0.5(6)	N(12)-C(31)-C(51)-C(52)	-45.6(5)
N(21)-N(22)-C(23)-C(24)	1.7(5)	C(41)-C(31)-C(51)-C(52)	76.8(5)
C(31)-N(22)-C(23)-C(24)	167.9(4)	C(56)-C(51)-C(52)-C(53)	0.2(7)
N(22)-C(23)-C(24)-C(25)	-1.0(5)	C(31)-C(51)-C(52)-C(53)	-175.0(4)
N(22)-N(21)-C(25)-C(24)	1.1(5)	C(51)-C(52)-C(53)-C(54)	-0.4(7)
CU-N(21)-C(25)-C(24)	178.8(3)	C(52)-C(53)-C(54)-C(55)	0.1(7)
C(23)-C(24)-C(25)-N(21)	-0.1(5)	C(53)-C(54)-C(55)-C(56)	0.6(7)
C(23)-N(22)-C(31)-N(12)	138.6(4)	C(54)-C(55)-C(56)-C(51)	-0.8(7)
N(21)-N(22)-C(31)-N(12)	-56.5(5)	C(52)-C(51)-C(56)-C(55)	0.4(6)
C(23)-N(22)-C(31)-C(51)	-102.5(5)	C(31)-C(51)-C(56)-C(55)	175.4(4)
N(21)-N(22)-C(31)-C(51)	62.4(5)		
C(23)-N(22)-C(31)-C(41)	20.0(6)		

Symmetry transformations used to generate equivalent atoms:

Table IV-52. Crystal data and structure refinement for $[(dpdpm)_2Ni(CH_3CN)_2][(FeBr_3)_2O]$ (**5.14**).

Identification code	nath33
Empirical formula	C42 H38 Br6 Fe2 N10 Ni O
Formula weight	1348.69
Temperature	148(2)K
Wavelength	1.54178 Å
Crystal system	Monoclinic
Space group	C2/c
Unit cell dimensions	a = 23.9391(5) Å α = 90° b = 13.9637(3) Å β = 106.9500(10)° c = 14.9828(3) Å γ = 90°
Volume	4790.86(17)Å^3
Z	4
Density (calculated)	1.870 g/cm^3
Absorption coefficient	11.471 mm^{-1}
F(000)	2632
Crystal size	0.14 x 0.08 x 0.02 mm
Theta range for data collection	3.71 to 68.66°
Index ranges	$-28 \leq h \leq 28$, $-15 \leq k \leq 13$, $-17 \leq \ell \leq 18$
Reflections collected	19766
Independent reflections	4166 [R_{int} = 0.055]
Absorption correction	Semi-empirical from equivalents
Max. and min. transmission	1.0000 and 0.6700
Refinement method	Full-matrix least-squares on F^2
Data / restraints / parameters	4166 / 0 / 282
Goodness-of-fit on F^2	0.979
Final R indices [I>2sigma(I)]	R_1 = 0.0457, wR_2 = 0.1166
R indices (all data)	R_1 = 0.0636, wR_2 = 0.1250
Largest diff. peak and hole	1.248 and -0.914 e/Å^3

Table IV-53. Atomic coordinates (x 10^4) and equivalent isotropic displacement parameters ($Å^2$ x 10^3) for $[(dpdpm)_2Ni(CH_3CN)_2][(FeBr_3)_2O]$ **(5.14)**.

U_{eq} is defined as one third of the trace of the orthogonalized Uij tensor.

	x	y	z	U_{eq}
Br(2)	3512(1)	7639(1)	1942(1)	35(1)
Ni(1)	5000	2655(1)	2500	19(1)
Br(1)	4388(1)	6696(1)	368(1)	50(1)
Br(3)	4387(1)	9367(1)	850(1)	61(1)
Fe	4386(1)	7826(1)	1519(1)	28(1)
N(21)	4397(2)	2660(3)	1182(3)	22(1)
N(11)	5490(2)	3762(3)	2157(3)	19(1)
N(1)	5461(2)	1546(3)	2093(3)	26(1)
N(22)	3889(2)	3186(3)	891(3)	25(1)
C(25)	4464(2)	2266(4)	418(3)	27(1)
N(12)	5989(2)	4159(3)	2733(3)	26(1)
C(14)	6084(3)	5037(4)	2393(4)	36(1)
C(1)	5665(2)	859(4)	1954(4)	26(1)
C(23)	3647(2)	3068(4)	-47(4)	33(1)
C(41)	3098(2)	4247(4)	999(4)	29(1)
C(52)	3114(2)	1947(4)	1517(4)	30(1)
C(51)	3351(2)	2762(4)	2032(4)	26(1)
C(13)	5640(2)	5220(4)	1629(4)	37(1)
C(44)	2245(3)	5450(4)	-69(4)	38(1)
C(45)	2089(2)	4675(4)	379(4)	38(1)
C(15)	5281(2)	4411(4)	1496(4)	29(1)
C(46)	2526(2)	4071(4)	925(4)	31(1)
C(53)	2842(2)	1267(4)	1899(4)	36(1)
C(31)	3593(2)	3571(4)	1560(4)	27(1)
C(55)	3049(3)	2166(4)	3311(4)	38(1)
C(56)	3322(2)	2861(4)	2934(4)	33(1)
C(42)	3252(2)	5014(4)	535(4)	37(1)
C(54)	2802(2)	1373(4)	2796(4)	37(1)
C(43)	2818(3)	5638(4)	5(4)	38(1)
C(24)	4007(3)	2494(4)	-373(4)	33(1)
C(2)	5922(3)	-45(4)	1768(5)	45(2)
O(4)	5000	7733(4)	2500	46(2)

Table IV-54. Hydrogen coordinates (x 10^4) and isotropic displacement parameters ($Å^2$ x 10^3) for $[(dpdpm)_2Ni(CH_3CN)_2][(FeBr_3)_2O]$ **(5.14)**.

	x	y	z	U_{eq}
H(25)	4787	1874	409	32
H(14)	6408	5445	2655	43
H(23)	3289	3338	-411	40
H(52)	3142	1866	902	35
H(13)	5582	5782	1255	44
H(44)	1950	5859	-436	45
H(45)	1689	4551	318	45
H(15)	4933	4335	997	35
H(46)	2423	3542	1243	37
H(53)	2679	717	1545	44
H(55)	3031	2234	3933	45
H(56)	3490	3405	3294	40
H(42)	3650	5121	574	45
H(54)	2607	905	3055	45
H(43)	2922	6180	-296	46
H(24)	3958	2295	-998	39
H(2A)	5614	-527	1558	68
H(2B)	6209	-268	2341	68
H(2C)	6115	55	1282	68

Table IV-55. Anisotropic parameters ($Å^2$ x 10^3) for $[(dpdpm)_2Ni(CH_3CN)_2][(FeBr_3)_2O]$ **(5.14)**.

The anisotropic displacement factor exponent takes the form:

$$-2\pi^2 [h^2 a^{*2} U_{11} + ... + 2 h k a^* b^* U_{12}]$$

	U11	U22	U33	U23	U13	U12
Br(2)	31(1)	35(1)	37(1)	3(1)	8(1)	-3(1)
Ni(1)	19(1)	18(1)	18(1)	0	1(1)	0
Br(1)	42(1)	65(1)	46(1)	-11(1)	14(1)	-6(1)
Br(3)	40(1)	51(1)	82(1)	33(1)	5(1)	-7(1)
Fe	18(1)	33(1)	28(1)	5(1)	-4(1)	-3(1)
N(21)	18(2)	18(2)	24(2)	0(2)	0(2)	0(2)
N(11)	19(2)	19(2)	17(2)	0(2)	1(2)	0(2)
N(1)	22(2)	28(3)	27(2)	-2(2)	6(2)	-2(2)
N(22)	23(2)	22(2)	25(2)	0(2)	-1(2)	-1(2)
C(25)	28(3)	28(3)	25(3)	-1(2)	7(2)	-4(2)
N(12)	21(2)	21(2)	33(3)	-1(2)	4(2)	-1(2)
C(14)	35(3)	24(3)	44(4)	3(2)	7(3)	-6(2)
C(1)	21(3)	23(3)	32(3)	-1(2)	5(2)	0(2)
C(23)	30(3)	39(3)	24(3)	7(2)	-1(3)	-5(2)
C(41)	24(3)	27(3)	31(3)	0(2)	-2(2)	1(2)
C(52)	28(3)	29(3)	27(3)	0(2)	0(2)	-1(2)
C(51)	16(2)	26(3)	33(3)	2(2)	3(2)	2(2)
C(13)	31(3)	28(3)	46(4)	16(3)	2(3)	1(2)
C(44)	39(3)	37(3)	33(3)	5(2)	3(3)	17(3)
C(45)	26(3)	46(4)	38(3)	-4(3)	4(3)	8(3)
C(15)	26(3)	27(3)	30(3)	4(2)	4(3)	0(2)
C(46)	25(3)	32(3)	32(3)	0(2)	4(2)	6(2)
C(53)	29(3)	32(3)	41(3)	1(2)	-1(3)	-8(2)
C(31)	22(3)	28(3)	27(3)	1(2)	2(2)	0(2)
C(55)	38(3)	38(4)	40(3)	2(3)	16(3)	-3(3)
C(56)	35(3)	32(3)	35(3)	-4(2)	13(3)	0(2)
C(42)	27(3)	32(3)	47(4)	6(3)	4(3)	-3(2)
C(54)	30(3)	36(3)	46(4)	7(3)	10(3)	-4(2)
C(43)	40(4)	36(3)	34(3)	7(2)	3(3)	3(2)
C(24)	36(3)	42(4)	18(3)	-1(2)	7(3)	-5(2)
C(2)	39(4)	22(3)	76(5)	-4(3)	19(3)	10(2)
O(4)	31(3)	49(4)	41(4)	0	-13(3)	0

Table IV-56. Bond lengths [Å] and angles [°] for $[(dpdpm)_2Ni(CH_3CN)_2][(FeBr_3)_2O]$ **(5.14)**.

Br(2)-Fe	2.3695(10)	N(1)#1-NI1-N(11)#1	95.40(16)
Ni(1)-N(21)#1	2.079(4)	N(11)-NI1-N(11)#1	84.8(2)
Ni(1)-N(21)	2.079(4)	O(4)-FE-BR1	112.75(15)
Ni(1)-N(1)	2.092(4)	O(4)-FE-BR2	110.94(5)
Ni(1)-N(1)#1	2.092(4)	BR1-FE-BR2	108.35(4)
Ni(1)-N(11)	2.093(4)	O(4)-FE-BR3	108.47(18)
Ni(1)-N(11)#1	2.093(4)	BR1-FE-BR3	107.38(4)
Br(1)-Fe	2.3390(11)	BR2-FE-BR3	108.83(4)
Br(3)-Fe	2.3743(10)	C(25)-N(21)-N(22)	105.5(4)
Fe-O(4)	1.7541(9)	C(25)-N(21)-NI1	126.5(3)
N(21)-C(25)	1.321(6)	N(22)-N(21)-NI1	127.3(3)
N(21)-N(22)	1.379(5)	C(15)-N(11)-N(12)	105.2(4)
N(11)-C(15)	1.328(6)	C(15)-N(11)-NI1	124.8(3)
N(11)-N(12)	1.371(5)	N(12)-N(11)-NI1	126.3(3)
N(1)-C(1)	1.123(6)	C(1)-N(1)-NI1	168.7(4)
N(22)-C(23)	1.365(7)	C(23)-N(22)-N(21)	109.3(4)
N(22)-C(31)	1.486(7)	C(23)-N(22)-C(31)	126.6(4)
C(25)-C(24)	1.395(7)	N(21)-N(22)-C(31)	122.0(4)
N(12)-C(14)	1.372(7)	N(21)-C(25)-C(24)	112.2(5)
N(12)-C(31)#1	1.477(6)	N(11)-N(12)-C(14)	109.7(4)
C(14)-C(13)	1.341(8)	N(11)-N(12)-C(31)#1	120.7(4)
C(1)-C(2)	1.466(7)	C(14)-N(12)-C(31)#1	127.8(4)
C(23)-C(24)	1.367(8)	C(13)-C(14)-N(12)	108.2(5)
C(41)-C(46)	1.365(7)	N(1)-C(1)-C(2)	179.1(5)
C(41)-C(42)	1.384(7)	N(22)-C(23)-C(24)	108.5(5)
C(41)-C(31)	1.556(7)	C(46)-C(41)-C(42)	120.4(5)
C(52)-C(53)	1.368(7)	C(46)-C(41)-C(31)	121.5(5)
C(52)-C(51)	1.399(7)	C(42)-C(41)-C(31)	118.0(5)
C(51)-C(56)	1.380(7)	C(53)-C(52)-C(51)	120.0(5)
C(51)-C(31)	1.532(7)	C(56)-C(51)-C(52)	119.6(5)
C(13)-C(15)	1.398(7)	C(56)-C(51)-C(31)	120.8(5)
C(44)-C(43)	1.369(8)	C(52)-C(51)-C(31)	119.5(5)
C(44)-C(45)	1.382(8)	C(14)-C(13)-C(15)	105.6(5)
C(45)-C(46)	1.406(7)	C(43)-C(44)-C(45)	121.2(5)
C(53)-C(54)	1.382(8)	C(44)-C(45)-C(46)	119.4(5)
C(31)-N(12)#1	1.477(6)	N(11)-C(15)-C(13)	111.3(5)
C(55)-C(54)	1.380(8)	C(41)-C(46)-C(45)	119.9(5)
C(55)-C(56)	1.380(8)	C(52)-C(53)-C(54)	120.6(5)
C(42)-C(43)	1.409(7)	N(12)#1-C(31)-N(22)	109.1(4)
O(4)-Fe#1	1.7541(9)	N(12)#1-C(31)-C(51)	110.3(4)
N(21)#1-NI1-N(21)	179.6(2)	N(22)-C(31)-C(51)	111.3(4)
N(21)#1-NI1-N(1)	90.03(16)	N(12)#1-C(31)-C(41)	107.5(4)
N(21)-NI1-N(1)	90.27(16)	N(22)-C(31)-C(41)	107.0(4)
N(21)#1-NI1-N(1)#1	90.27(16)	C(51)-C(31)-C(41)	111.5(4)
N(21)-NI1-N(1)#1	90.03(16)	C(54)-C(55)-C(56)	120.8(6)
N(1)-NI1-N(1)#1	84.6(2)	C(55)-C(56)-C(51)	119.7(5)
N(21)#1-NI1-N(11)	86.95(15)	C(41)-C(42)-C(43)	120.2(5)
N(21)-NI1-N(11)	92.74(15)	C(55)-C(54)-C(53)	119.4(5)
N(1)-NI1-N(11)	95.40(16)	C(44)-C(43)-C(42)	118.9(5)
N(1)#1-NI1-N(11)	177.22(15)	C(23)-C(24)-C(25)	104.5(5)
N(21)#1-NI1-N(11)#1	92.74(15)	FE-O(4)-FE#1	171.6(4)
N(21)-NI1-N(11)#1	86.95(15)		
N(1)-NI1-N(11)#1	177.22(15)		

Symmetry transformations used to generate equivalent atoms:

#1 -x+1,y,-z+1/2